

Labor division in engineered cross-kingdom consortia: Consolidated bioprocessing of lignocellulosic biomass to carboxylic acids

Thèse N° 9420

Présentée le 26 avril 2019

à la Faculté des sciences de base

Laboratoire des procédés durables et catalytiques

Programme doctoral en chimie et génie chimique

pour l'obtention du grade de Docteur ès Sciences

par

Robert Lawrence SHAHAB

Acceptée sur proposition du jury

Prof. O. Kröcher, président du jury

Prof. J. Luterbacher, Dr M. Studer, directeurs de thèse

Prof. A. Smith, rapporteuse

Dr D. Johnson, rapporteur

Prof. S. Panke, rapporteur

2019

Acknowledgements

As my official thesis directors Prof. Dr. Jeremy Luterbacher and Dr. Michael Studer gave me the opportunity to work in their interdisciplinary research groups at the École Polytechnique Fédérale de Lausanne and the Bern University of Applied Sciences on the very exciting research topic of biochemical conversion of lignocellulosic biomass into platform chemicals. I thank both of you for the time you dedicated to my work, for your support and scientific discussions throughout my thesis. Thank you, that you gave me the freedom to also follow own ideas and that you supported my research stay at the University of Cambridge.

I would like to thank the members of the examination committee Prof. Dr. Alison Smith, Dr. David Johnson, Prof. Dr. Oliver Kröcher and Prof. Dr. Sven Panke for evaluating my thesis and attending the examination.

Thank you, Simone Brethauer-Studer, for your scientific input, in particular regarding our publications. Charilaos Xiros, I would like to thank you for your advices and the scientific discussions. For the good times in the office and the laboratory, I thank Robert Balan, Simon Bowald, Simone Brethauer-Studer, Patrice Bühler, Elisabeth Cazier, David Dempfle, Laszlo Gyenge and Charilaos Xiros. It was a great pleasure for me to work with you.

My special thanks to the people at the Laboratory of Sustainable and Catalytic Processing at EPFL and especially to Bartosz Rozmysłowicz and Jher Hau Yeap for your effort to upgrade the produced carboxylic acids to linear olefins and aromatics. For the reliable administrative support, I would like to thank Anne Lene Odegaard.

My appreciation also goes to Prof. Dr. François Maréchal and Dilan Celebi Ayse for your work on the techno-economical model that describes the entire process of biochemical conversion of lignocellulosic biomass to carboxylic acids and their catalytic upgrading to olefins and aromatics.

Thank you, Manfred Muhr, for your support in constructing and modifying all kinds of components for the laboratory and the bioreactors. In the context of constructions, I would also like to thank Simon Bowald and Robert Balan for the good times in the workshop.

I would like to thank all members of the Plant Metabolism Group in Cambridge, in particular Prof. Dr. Alison Smith, for supervising me and for the scientific discussions we had. I also want to thank you, Matthew Davey and Katrin Geisler, for introducing me to various tools which provided valuable insights into the microalgal-fungal biofilm. My special thanks also to Silvia Vignolini and her Bio-inspired Photonics group. It was great to investigate the radiation properties of the fiber connected to the LEDs to provide a niche for microalgae in our bioreactor.

The work of this PhD thesis was funded by the Swiss National Science Foundation in the framework of the National Research Program70 *Energy Turnaround* (grant number 407040-153868 and 407040-153868/3). The study has been conducted in the framework of the SCCER BIOSWEET, supported by the Swiss Confederation through Innosuisse – Swiss Innovation Agency. My research stay in Cambridge was supported by the Swiss European Mobility Program and the Swiss National Science Foundation (grant number 407040-153868/2). I am grateful for all this financial support.

I would like to warmly thank my parents, my sister, my aunt and my partner for your unlimited support.

Robert Lawrence Shahab, Lausanne 2019

Abstract

Lignocellulose is a renewable source of fixed carbon and a promising substrate for the production of chemicals and fuels in second generation biorefineries. In this thesis, we engineered artificial microbial consortia for consolidated bioprocessing (CBP) of lignocellulose to carboxylic acids and ethanol. Inspired by natural ecosystems following the principle of labor division, we distributed the required metabolic capabilities among different specialized microorganisms. As a vast majority of product-forming microorganisms is non-cellulolytic the fungus *Trichoderma reesei* was employed to produce cellulolytic enzymes.

For the production of lactic acid from steam-pretreated beech wood, the aerobic fungus *T. reesei* was co-cultivated with the non-cellulolytic facultative anaerobic bacterium *Lactobacillus pentosus*. The known instability problem of such a cooperator-cheater community was overcome by enforced niche differentiation. To this end, a novel stirred tank bioreactor was engineered that was equipped with a continuously aerated, oxygen permeable membrane that locally provided oxygen for the aerobic fungus in an otherwise anaerobic bioreactor. The success of this strategy was shown by the formation of a fungal biofilm on the membrane's surface and a lactic acid concentration of 19.8 gL^{-1} (85.2 % of theoretical maximum).

For the production of various carboxylic acids, obligate and strict anaerobic bacteria were added to the community of *T. reesei* and *L. pentosus*. The lactic acid bacterium metabolically funneled the heterogeneous lignocellulosic carbohydrates to lactate as central intermediate in synthetic food chains and with that, compensated for missing metabolic capabilities of the anaerobic secondary fermenters. The feasibility and modularity of the lactate platform was shown by the direct production of acetic, propionic, butyric, valeric and hexanoic acid from beech wood. Integration of the obligate anaerobes *Clostridium tyrobutyricum* or *Veillonella criceti* resulted in 196.5 kg butyric acid or 113.6 kg propionic and 133.3 kg acetic acid, respectively, per ton beech wood. For the production of mixtures of volatile fatty acids (VFAs) with up to six carbon atoms from beech wood the non-cellulolytic strict anaerobe *Megasphaera elsdenii* was integrated into the lactate platform and 220 kg total VFAs per ton beech wood were produced. By adding *C. tyrobutyricum* or *V. criceti* to a three-member microbial community it was shown that the ratio of odd- and even-numbered VFAs can be tuned through intra-consortium competition.

For the production of ethanol from lignocellulose, *T. reesei* and *Saccharomyces cerevisiae* were co-cultivated. They formed a two-layered biofilm on the aerated membrane. The *in situ* degradation of ethanol was dedicated to aerobic metabolism and strategies to tune the oxygen supply were provided.

An advanced bioreactor was engineered and applied that provided multiple niches for the co-cultivation of microorganisms with highly diverse requirements for abiotic parameters (e.g. oxygen, light) to widen the product range. The demonstrated co-cultivation of *T. reesei* and the microalgae *Chlamydomonas reinhardtii* in a two-layered biofilm is an important milestone towards the direct production of lipids from lignocellulose.

The results of this thesis illustrate the potential of community-based CBP of renewable lignocellulosic biomass to fuels and chemicals in second generation biorefineries in tomorrow's bioeconomy.

Keywords: Artificial food chain, biofilm, carboxylic acids, consolidated bioprocessing, cooperator-cheater, lignocellulose, microalgae, niche differentiation, synthetic microbial consortium, *Trichoderma reesei*.

Zusammenfassung

Lignocellulose als erneuerbare Quelle für gebundenen Kohlenstoff ist ein vielversprechendes Substrat für die Produktion von Chemikalien und Treibstoffen in Bioraffinerien der zweiten Generation. In dieser Dissertation wurden künstliche, mikrobielle Konsortien entwickelt, um Lignocellulose mittels konsolidierten Bioprozessen in Carbonsäuren und Ethanol umzuwandeln. Inspiriert von natürlichen Ökosystemen folgend dem Prinzip der Arbeitsteilung wurden metabolische Fähigkeiten auf spezialisierte Mikroorganismen aufgeteilt. Da viele Produktbildner nicht-cellulolytisch sind, wurde der Pilz *Trichoderma reesei* zur Produktion von cellulolytischen Enzymen genutzt.

Zur Milchsäureproduktion aus mit Dampf vorbehandeltem Buchenholz wurde *T. reesei* mit dem nicht-cellulolytischen, fakultativ anaeroben Bakterium *Lactobacillus pentosus* co-kultiviert. Das bekannte Instabilitätsproblem solcher Kooperation-Defektion Gemeinschaften wurde durch erzwungene Nischendifferenzierung überwunden. Dafür wurde ein Rührkessel mit einer Membran ausgestattet, welche dem aeroben Pilz lokal Sauerstoff in einem sonst anaeroben Reaktor bereitstellte. Der pilzliche Biofilm auf der Membran und die Produktion von 19.8 gL^{-1} Milchsäure (85 % des theoretischen Maximums) zeigten den Erfolg dieser Herangehensweise.

Zur Produktion verschiedener Carbonsäuren wurden Anaerobier zu *T. reesei* und *L. pentosus* hinzugefügt. Das Milchsäurebakterium tunnelt heterogene Kohlenhydrate von Lignocellulose metabolisch zu Lactat als zentrales Zwischenprodukt in einer künstlichen Nahrungskette. Damit kompensiert das Bakterium fehlende metabolische Fähigkeiten anaerober, sekundärer Gärer. Die Realisierbarkeit und Modularität der Lactat-Plattform konnte durch Produktion von Essig-, Propion-, Butter-, Valerian- und Capronsäure aus Buchenholz gezeigt werden. Die Integration der obligaten Anaerobier *Clostridium tyrobutyricum* oder *Veillonella criceti* resultierte in 196.5 kg Buttersäure oder 113.6 kg Propion- und 133.3 kg Essigsäure pro Tonne Holz. Für die Produktion von volatilen Fettsäuren (VFAs) mit bis zu sechs Kohlenstoffatomen in einer Kette wurde das nicht-cellulolytische, strikt anaerobe Bakterium *Megasphaera elsdenii* in die Lactat-Plattform integriert (220 kg VFAs pro Tonne Holz). Das Verhältnis von ungeraden zu geraden VFAs konnte durch gezielte Konkurrenz innerhalb der Gemeinschaft durch Integration der obligaten Anaerobier *V. criceti* oder *C. tyrobutyricum* manipuliert werden.

Zur Ethanolproduktion wurden *T. reesei* und *Saccharomyces cerevisiae* co-kultiviert und bildeten einen zweischichtigen Biofilm auf der begasten Membran. Der *in situ* Ethanolabbau wurde einem aeroben Metabolismus zugeschrieben und Strategien zur Regulierung des Sauerstoffeintrags wurden aufgezeigt.

Ein verbesserter Bioreaktor wurde entwickelt und angewendet, welcher mehrere Nischen für die Co-Kultivierung von Mikroorganismen mit höchst unterschiedlichen Ansprüchen an abiotische Faktoren (z.B. Sauerstoffgehalt, Licht) bereitstellt. *T. reesei* und die Mikroalge *Chlamydomonas reinhardtii* formten einen zweischichtigen Biofilm - ein wichtiger Meilenstein Richtung direkter Lipidproduktion aus Lignocellulose.

Die Ergebnisse dieser Dissertation zeigen das Potential von konsolidierten Bioprozessen mittels zusammengestellter, mikrobieller Gemeinschaften zur Produktion von Treibstoffen und Chemikalien aus erneuerbarer, lignocellulosehaltiger Biomasse als Grundstein der Bioökonomie von Morgen.

Schlüsselwörter: Künstliche Nahrungskette, Biofilm, Carbonsäuren, konsolidierter Bioprozess, Kooperation-Defektion, Lignocellulose, Mikroalgen, Nichendifferenzierung, synthetisches mikrobielles Konsortium, *Trichoderma reesei*.

List of figures

1.1	Evolution of the carbon dioxide concentration in the Earth's atmosphere from 1980 to 2018.	2
2.1	Components and structure of lignocellulosic biomass.	9
2.2	Configurations of biologically mediated processes to convert pretreated lignocellulosic biomass to target products.	13
2.3	Schematic overview of the enzymatic hydrolysis of cellulose: Free fungal cellulases and cell-bound bacterial cellulosomes.	15
2.4	Strategies for CBP of lignocellulose to target products.	18
2.5	Ecological interactions in microbial communities.	20
2.6	Heterogeneities in microbial biofilms on an inert surface.	24
3.1	Schematic representation of the consortium composed of <i>T. reesei</i> and <i>L. pentosus</i>	28
3.2	Batch CBP of lignocellulosic biomass to lactic acid using a synthetic microbial consortium of <i>T. reesei</i> and a lactic acid bacterium.	31
3.3	Batch CBP of Avicel and xylose to lactic acid using a synthetic microbial consortium of <i>T. reesei</i> and a lactic acid bacterium.	33
3.4	Fed-batch CBP of heterogeneous substrates containing hexose and pentose to lactic acid using a consortium of <i>T. reesei</i> and <i>L. pentosus</i>	36
4.1	Comparison of the sugar platform and the lactate platform.	42

4.2	CBP of lignocellulosic biomass to butyric and propionic acid by a synthetic microbial consortium.	43
4.3	Photographs of mature fungal biofilms formed on an aerated membrane in a stirred tank bioreactor.	44
4.4	Redox potential and dissolved oxygen concentration during the two-stage inoculation of <i>T. reesei</i> and <i>L. pentosus</i> in the membrane-aerated bioreactor.	45
4.5	CBP of cellulose to butyric acid using a cross-kingdom microbial consortium.	47
4.6	Fermentations of lactate broth with supplementation of sodium acetate or glucose using <i>C. tyrobutyricum</i>	50
4.7	Different production routes from cellulose to butyric acid including theoretical and practical yields using the lactate platform in comparison to the sugar platform.	52
4.8	CBP of microcrystalline cellulose and xylose to propionic and acetic acid using a cross-kingdom microbial consortium.	55
4.9	Mass fluxes of glucan, xylan, acetic acid and lignin for the two-stage steam-pretreatment of beech wood and CBP of pretreated beech wood to butyric acid or propionic and acetic acid, respectively.	57
5.1	CBP for the conversion of lignocellulose into medium-chain volatile fatty acids using <i>T. reesei</i> , <i>L. pentosus</i> and <i>M. elsdenii</i>	65
5.2	CBP for the conversion of lignocellulose to odd- and even-chained volatile fatty acids.	67
5.3	Overview of selected metabolic pathways in the community-based CBP following the artificial food chain from lignocellulose via lactate and acetate as intermediates to medium-chain volatile fatty acids.	69
6.1	Photograph of the scaled-up membrane-aerated stirred tank bioreactor.	73
6.2	Community-based CBP of microcrystalline cellulose for the production of ethanol using the membrane-aerated stirred tank bioreactor.	76
6.3	Variation of the oxygen transfer rate and its effect on the consolidated bioprocessing of microcrystalline cellulose to ethanol.	78

6.4	Comparison of ethanol production using the Crabtree-positive yeast <i>S. cerevisiae</i> VTT C-79095 and the petite yeast <i>S. cerevisiae</i> FYdelta pet191::KanMX4 in SSF and CBP of microcrystalline cellulose.	79
7.1	Schematic representation of advanced membrane-aerated bioreactor.	83
7.2	Schematic representation and photograph of membrane sampling loop.	84
7.3	Piping and instrumentation diagram of UV sampling device for sterile extraction of the fermentation slurry.	85
7.4	Piping and instrumentation diagram of circulation approach.	86
7.5	Measured k_La values in circulation system.	87
7.6	Schematic representations of temperature tolerances of microorganisms and cellulolytic enzymes and formation of a temperature gradient in the membrane-aerated bioreactor.	88
7.7	Tuning the pH in the membrane bioreactor by flushing NH_3 solution or CO_2 through the membrane.	89
7.8	Time-resolved formation of a spatial pH gradient in a solid water/agarose/-sodium chloride/bromothymol blue mixture in a bioreactor exploiting electrolysis of water at two electrodes.	91
7.9	Time-resolved formation of a pH gradient in a biofilm-mimicking agarose coating on the cathode.	93
7.10	Schematic representation of the CBP of lignocellulosic waste materials from agriculture and forestry to lipids using the lactate platform together with microalgae.	95
7.11	External light source with radially emitting light fibers connected to the advanced bioreactor.	96
7.12	Properties of LED light source: Emission spectrum and light intensity at the end of the fiber for various fiber lengths.	97
7.13	Axenic cultivation of <i>C. reinhardtii</i> WT12 using TAP medium in the darkness.	98
7.14	Overview of pathways in a co-culture of <i>T. reesei</i> and <i>C. reinhardtii</i> using cellulose as carbon source and light as energy source.	99
7.15	Chlorophyll fluorescence images of biofilms of <i>T. reesei</i> and <i>C. reinhardtii</i>	100

7.16	Confocal laser scanning microscopy images and photograph of fungal-microalgal biofilm grown on the surface of the membrane in the advanced bioreactor with and without illumination.	101
7.17	Chlorophyll concentration in biofilm samples from cultivations of <i>T. reesei</i> and <i>C. reinhardtii</i> with and without light.	103
B.1	Photographs of the development of a fungal biofilm in the membrane-aerated 500 mL bioreactor and the measured dissolved oxygen concentration as a function of time for various flow rates.	118
B.2	Concentration of cellobiose in the membrane-aerated bioreactor with and without inoculation of <i>L. pentosus</i> using microcrystalline cellulose as substrate.	118
B.3	Axenic cultivation of <i>T. reesei</i> in the membrane-aerated bioreactor on multiple carbon sources.	119
B.4	Axenic cultivation of <i>L. pentosus</i> on glucose and in a SSF process on microcrystalline cellulose.	120
B.5	Consolidated bioprocessing of whole slurry one-stage pretreated beech wood using <i>T. reesei</i> and <i>L. pentosus</i>	120
B.6	Semi-continuous CBP of microcrystalline cellulose to lactic acid using <i>T. reesei</i> and <i>L. pentosus</i>	121
C.1	Overview of metabolic pathways of <i>L. pentosus</i> , <i>L. brevis</i> , <i>V. criceti</i> , <i>C. tyrobutyricum</i> and <i>A. woodii</i>	124
C.2	Schematic representation of the process flow for the subsequent secondary fermentation of lactate to acetate, propionate and butyrate, respectively.	125
C.3	SSF of microcrystalline cellulose and xylose using <i>C. tyrobutyricum</i> in a fed-batch experiment.	126
C.4	Fed-batch experiment for CBP of microcrystalline cellulose and xylose to butyric acid, using <i>T. reesei</i> , <i>L. pentosus</i> , <i>L. brevis</i> and <i>C. tyrobutyricum</i>	127
C.5	Fed-batch experiment for CBP of microcrystalline cellulose and xylose to propionic and acetic acid using <i>T. reesei</i> , <i>L. pentosus</i> and <i>V. criceti</i>	128

C.6	Steam pretreatment of beech wood: Recovery of lignin, acetic acid, xylan and glucan after the first stage at 180 °C and the second stage at 230 °C.	129
C.7	Activity of cellobiohydrolase (CBH), beta-glucosidase (BG), endoglucanase (EG) and xylanase in the supernatant of the fermentation slurry during various stages of the CBP of pretreated beech wood to butyric acid or propionic acid and acetic acid.	130
C.8	CBP for direct production of butyric acid from microcrystalline cellulose and xylose using a co-culture of <i>T. reesei</i> and <i>C. tyrobutyricum</i>	131

List of tables

3.1	Reported and own data on the production of lactic acid from pretreated lignocellulosic material or microcrystalline cellulose either in SSF processes or by CBP.	27
3.2	CBP of different substrates to lactic acid in batch and fed-batch mode by <i>T. reesei</i> and different lactic acid bacteria.	30
4.1	Overview of butyric acid yields with the lactate platform and alternative approaches.	58
6.1	Selected literature on biochemical conversion of lignocellulose to ethanol using CBP.	72
6.2	Volumetric mass transfer coefficients for different properties of the membrane (length, wall thickness) and different oxygen concentrations in air flushed through the membrane.	74
C.1	CBP of different substrates in fed-batch mode using <i>T. reesei</i> , different lactic acid bacteria and <i>C. tyrobutyricum</i>	132
C.2	CBP of different substrates in fed-batch mode using <i>T. reesei</i> , <i>L. pentosus</i> and <i>V. criceti</i>	134
C.3	Cultivations of <i>A. woodii</i> on CBP lactate broths for various media supplements. .	135
C.4	Cultivations of <i>V. criceti</i> on CBP lactate broths for various media supplements. .	136
C.5	Theoretical yields of fermentation via lactate platform compared to alternative direct sugar fermentation routes for selected target products.	137

C.6 Overview of microorganisms and pathways used for the calculation of the theoretical yield of the lactate platform and conventional production routes using glucose as substrate.	138
C.7 Overview of microorganisms and pathways used for the calculation of the theoretical yield of the lactate platform and conventional production routes using xylose as substrate.	141

Table of contents

Acknowledgements	i
Abstract	iii
Zusammenfassung	v
List of figures	vii
List of tables	xiii
1 Introduction	1
1.1 Lignocellulosic biomass as renewable substrate for biorefineries	2
1.2 Thesis objectives	4
2 Fundamentals	7
2.1 Composition and structure of lignocellulosic biomass	7
2.2 Pretreatment - making lignocellulosic biomass accessible for biochemical conversions	9
2.3 Biochemical conversion of pretreated lignocellulosic biomass to target products	12
2.3.1 Production of cellulolytic enzymes and enzymatic hydrolysis	13
2.3.2 Fermentation of hexoses and pentoses	16
2.3.3 Consolidated bioprocessing	17

2.4	Microbial communities	19
2.5	Biofilms	22
3	Lactic acid	25
3.1	Abstract	25
3.2	Introduction	26
3.3	Results and discussion	27
3.3.1	Design and implementation of a microbial consortium for CBP of ligno-cellulose to lactic acid	27
3.3.2	Conversion of cellulose to lactic acid in batch processes	29
3.3.3	Co-fermentation of pentoses and hexoses and <i>in situ</i> acetic acid degradation by the synthetic consortium	32
3.3.4	Conversion of whole-slurry pretreated beech wood in fed-batch experiments	34
3.3.5	Interactions between the members of the consortium	37
3.4	Conclusions	37
4	Butyric acid and propionic acid	39
4.1	Abstract	39
4.2	Introduction	39
4.3	Results	44
4.3.1	Direct production of butyric acid from cellulose and xylose via the lactate platform using a synthetic consortium	44
4.3.2	Strategies to improve butyric acid production	46
4.3.3	CBP of cellulose and xylose to propionic and acetic acid by integration of <i>Veillonella criceti</i> into the lactate platform	54
4.3.4	CBP of pretreated beech wood	54
4.4	Discussion	56

4.5	Conclusions	60
5	Mixed volatile fatty acids	61
5.1	Abstract	61
5.2	Introduction	61
5.3	Results and discussion	63
5.3.1	Co-cultivation of aerobic and strict anaerobic microorganisms	63
5.3.2	Targeted production of odd- and even-numbered medium-chain VFAs	64
5.4	Conclusions	68
6	Ethanol	71
6.1	Introduction	71
6.2	Scaled-up membrane-aerated stirred tank bioreactor	72
6.3	Community-based consolidated bioprocessing of lignocellulose to ethanol	75
6.4	Conclusions	79
7	Towards a wider product range with an advanced membrane-aerated bioreactor	81
7.1	Motivation to engineer an advanced membrane-aerated bioreactor	81
7.2	Overview of setup of advanced membrane-aerated bioreactor	83
7.3	Circulation of fluid for <i>in situ</i> control of oxygen transfer rate and cooling of biofilm	85
7.4	pH gradients	88
7.5	Towards lipids from cellulose: Light for co-cultivation of microalgae and fungus	94
7.5.1	Engineering and realization of artificial light niche	96
7.5.2	Study of fungal-microalgal biofilm	97
7.6	Conclusions	102
8	Summary and conclusions	105

A Materials and methods	109
A.1 Bacterial, fungal and microalgal strains and cultivation methods	109
A.2 Membrane-aerated bioreactors	111
A.3 Steam pretreatment and analysis of beech wood	113
A.4 Enzyme assays	114
A.5 Analytical methods	114
B Supplementary for chapter 3: Lactic acid	117
C Supplementary for chapter 4: Butyric acid and propionic acid	123
D References	145
E List of publications	167
F Curriculum vitae	171

CHAPTER 1

Introduction

To date, humans are highly dependent on fossil resources to satisfy their carbon needs for the production of fuels and chemicals for transportation, industry and housing. In petrochemical refineries fossil crude oil is converted to hundreds of different products using chemical processes developed over the last century. However, the use of fossil resources results in emission of greenhouse gases which accumulate in the atmosphere (Fig. 1.1). These gases are to a great extent responsible for the climate change [1] and its detrimental impact on life on Earth. Combined with their finite nature it is of highest priority to replace fossil resources with renewable resources and replace conventional refineries with biorefineries that allow for the production of bio-based fuels and chemicals which are potentially carbon neutral and renewable.

Electricity can be obtained by conversion of renewable energies using well-developed technologies such as photovoltaics, wind turbines or geothermal power plants. For the production of chemicals carbon is required. On Earth, two natural sources of renewable carbon exist: the atmosphere and biomass. In the Earth's atmosphere on ground level the average carbon dioxide concentration in 2017 was 405 ppm [2,3]. Such highly diluted carbon dioxide streams are challenging for industrial carbon capture processes. Thus, these processes are complex, energy-intensive and even require supplementation of carbon from fossil sources [4]. With an efficiency of 1 to 2 %, plants are able to exploit carbon dioxide available in the atmosphere to grow and thus, to build up biomass.

Biomass as renewable carbon source is practically available and harvesting techniques are well established [5–7]. In contrast to e.g. fossil crude oil whose deposits are limited to few spots world-wide the resource biomass is widely available, including in Europe [8]. Biomass can be processed into chemicals, food, materials and fuels in biorefineries [9]. These elaborated industries cover multiple processing steps which might include physical treatments

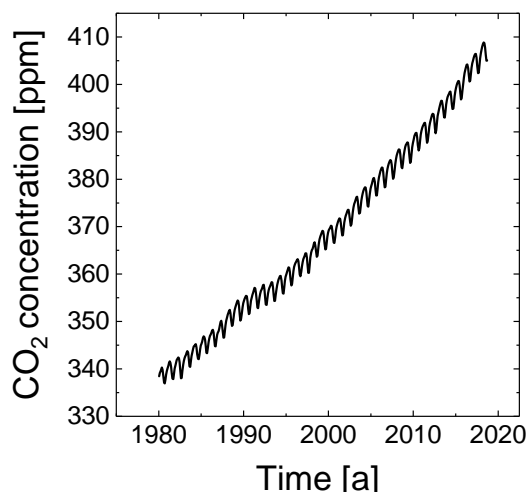


Figure 1.1: Evolution of the carbon dioxide concentration in the Earth's atmosphere from 1980 to 2018. Data taken from [3].

(e.g. milling to reduce the particle size), biochemical process steps (e.g. degradation of the biomass by enzymes and further microbial conversions [10]), chemical/catalytic processes (e.g. hydrogenation/dehydration [11]) and thermochemical steps (e.g. gasification [12] or pyrolysis [13]).

Biorefineries which use easily digestible substrates such as corn, wheat or sugar cane (sugar platform) are called first generation biorefineries. A prominent example is the biochemical conversion of carbohydrates from corn or sugar cane into bioethanol using the yeast *Saccharomyces cerevisiae*. The major challenge of first generation biorefineries is the competition with food and feed industry [14]. Thus, it is highly desirable to find an alternative, sustainable source of biomass.

1.1 Lignocellulosic biomass as renewable substrate for biorefineries

Lignocellulosic biomass is an attractive substrate for biorefineries to produce chemicals and fuels. Taking the example of Switzerland, the sustainable, annual domestic potential for energetic use is 3.3 million tons dry weight (in million tons dry weight: waste wood, 0.7; wood residues, 0.5; forest wood, 1.8; wood from landscape maintenance, 0.3) [15]. Please note that a fraction of this potential is already used for energetic purposes. The primary energy content of 3.3 million tons dry weight woody biomass is 50.2 PJ/a [15] which is approximately 20 times lower compared to the Swiss primary energy consumption in 2017 (1080 PJ) [16]. This

highlights the necessity to use biomass efficiently, thoroughly and targeted and to provide added value [17,18] despite the fact that it is the most abundant source of fixed renewable carbon.

Lignocellulose is composed of cellulose, hemicellulose and lignin that form a highly recalcitrant composite structure. The biological degradation of lignocellulose is therefore more complex than that of sugar-based substrates. Thus, degradation is substantially slower which is an obstacle for the use of lignocellulosic biomass in industrial processes. In addition, only a few microorganisms evolved all metabolic capabilities to depolymerize it. The big advantage of lignocellulose as waste material from agriculture and forestry is that it is neither practical as food nor feed.

Biorefineries that exploit lignocellulosic biomass to produce a variety of fuels and chemicals are called second generation biorefineries. A second generation biorefinery that focuses on biochemical processes follows four main process steps: pretreatment of lignocellulosic biomass to improve the enzymatic digestibility and to reduce the crystallinity of cellulose, production of enzymes such as cellulases and hemicelluloses, enzymatic hydrolysis to hydrolyze the polymeric substrate to fermentable saccharides and lastly, fermentation to the target product. The major obstacle of second generation biorefineries in comparison to first generation biorefineries that rely on the sugar platform is the high conversion cost which is caused by the recalcitrant structure of the substrate used in the former. The cost for the pretreatment process can be as high as 27 % of the total cost [19,20] and thus, it is a significant cost driver. Another major cost factor is attributed to the external production of cellulolytic enzymes which makes up about 10 to 20 % [21,22] to even half of the total costs [23] in case of cellulosic ethanol production.

Several strategies were developed to reduce costs by merging the aforementioned biological process steps. These approaches can be classified according to the degree of consolidation. The combination of the enzymatic hydrolysis and the fermentation of hexoses is called simultaneous saccharification and fermentation (SSF). If pentoses are fermented as well, the process is called simultaneous saccharification and co-fermentation (SSCF). However, both processes, SSF and SSCF, require the addition of external enzymes. Consolidated bioprocessing (CBP) which combines all biological process steps in one process unit allows the *in situ* production of enzymes from the low-cost lignocellulosic substrate. As only one vessel is required for the CBP capital costs are reduced in comparison to strategies with lower level of consolidation. Considering these advantages it becomes clear why CBP attracted considerable attention in the past decade [23,24].

CBP of lignocellulose can be realized with microorganisms that are genetically modified to have the metabolic capabilities to produce on the one hand cellulolytic enzymes and on the

other hand the target product. Inspired by natural ecosystems another approach relies on microbial communities. Following the concept of labor division the metabolic capabilities are distributed among multiple members of the community which together enable the desired biotransformation.

In order to replace fossil-based refineries second generation biorefineries must overcome multiple challenges. They must offer a wide range of possible target products that can be easily adapted to fluctuating demands. Such requirement is a hurdle for the CBP strategy based on the genetically modified superbug because sophisticated cloning is required for the production of each individual target product. A common challenge that evolves when lignocellulosic substrates are used is the inability of many microorganisms to efficiently use pentoses for the product formation. This results in the formation of unwanted side-products and reduced product yields. With an increase in degree of process consolidation it becomes also challenging to provide the abiotic conditions for pH, temperature or dissolved oxygen content that are necessary for optimized sub-processes. Another challenge for second generation biorefineries is the production of chemicals that are highly toxic for microorganisms or enzymes or that cannot be produced straightforwardly via biochemical routes. An attractive interdisciplinary route towards these products would be to combine biochemical conversions of lignocellulose with subsequent catalytic upgrading. This scheme was followed in a joint project of the National Research Program 70 *Energy Turnaround*. A community-based CBP was developed to funnel the heterogeneous substrate lignocellulose to volatile fatty acids as intermediate product for the subsequent catalytic upgrading to olefins as bulk chemical or alkanes and aromatic hydrocarbons as blends for jetfuel.

1.2 Thesis objectives

This thesis reports on labor division in engineered cross-kingdom consortia for the successful production of selected carboxylic acids and ethanol by community-based consolidated bioprocessing of lignocellulosic biomass. The following objectives were defined.

1. **Co-cultivation of an aerobic cellulolytic fungus and a facultative anaerobic bacterium for the direct production of lactic acid from lignocellulosic biomass.** Engineering of a membrane-aerated bioreactor with ecological niches for the fungus *Trichoderma reesei* and the lactic acid bacterium *Lactobacillus pentosus* to stabilize the cooperator-cheater community. Metabolic funneling of hexoses and pentoses from cellulose and hemicellulose, respectively, to the target product lactic acid.

2. **Establishment of the lactate platform as community-based consolidated bioprocessing strategy for the production of volatile fatty acids from lignocellulosic biomass.** Co-cultivation of *Trichoderma reesei*, lactic acid bacteria and the obligate anaerobic bacterium *Clostridium tyrobutyricum* for the production of butyric acid or *Veillonella criceti* for the production of propionic and acetic acid. Engineering of spatial niches to create compartments with suitable dissolved oxygen content and redox potential for aerobes and anaerobes without addition of nitrogen or reducing agents.
3. **Targeted production of odd- and even-numbered medium-chain volatile fatty acids from lignocellulosic biomass using the lactate platform.** Integration of the strict anaerobic bacterium *Megasphaera elsdenii* into the lactate platform for the production of volatile fatty acids with two to six carbon atoms in a chain. Exploitation of intra-consortium competition to tune the share of volatile fatty acids towards even-numbered carbon atoms by integration of *Clostridium tyrobutyricum* and odd-numbered carbon atoms by integration of *Veillonella criceti*.
4. **Scale-up of the consolidated bioprocessing of lignocellulosic biomass to ethanol from 32 mL to 2.7 L.** Co-cultivation of *Trichoderma reesei* and *Saccharomyces cerevisiae* in the scaled-up membrane-aerated bioreactor for the production of ethanol. Variation of oxygen transfer rate to determine the effect on the production of ethanol.
5. **Engineering and application of an advanced membrane-aerated bioreactor towards a wider product range and an increased productivity.** Design of advanced bioreactor with multiple gradients for the abiotic parameters oxygen, temperature, pH and light. Allow the formation of a multispecies biofilm composed of *Trichoderma reesei* and the microalgae *Chlamydomonas reinhardtii* on microcrystalline cellulose.

In chapter 2, the fundamental background for biochemical conversion of lignocellulosic biomass to chemicals is addressed. The recalcitrant structure of lignocellulose is described and methods for its pretreatment are summarized. Strategies for the consolidation of required biochemical process steps are described and ecological interactions in microbial communities are highlighted. Chapter 3 focuses on the direct production of lactic acid from steam-pretreated biomass using a designed synthetic cross-kingdom community. The concept of the lactate platform is established as modular, community-based CBP strategy and applied in chapter 4 for the production of butyric acid or propionic acid and acetic acid. In chapter 5, the production of targeted mixtures of volatile fatty acids from lignocellulosic biomass is demonstrated. The production of ethanol using a scaled-up membrane-aerated bioreactor is addressed in chapter 6. Finally, the features of the developed advanced membrane-aerated bioreactor are described in chapter 7 and their functionality is experimentally verified by e.g. the successful co-cultivation of *Trichoderma reesei* and the microalgae *Chlamydomonas reinhardtii* in a two-layered biofilm.

CHAPTER 2

Fundamentals

In this chapter, the theoretical aspects that are most relevant for the biochemical conversion of lignocellulosic biomass into platform chemicals is provided. Section 2.1 describes the composition and structure of lignocellulosic biomass and the challenges in using it as a substrate in biorefineries. Various pretreatment procedures are described in section 2.2 that are employed to overcome the recalcitrance of lignocellulose and to increase the rate of enzymatic hydrolysis. Section 2.3 describes the biochemical conversion steps of pretreated lignocellulosic biomass to various target products: the production of cellulolytic enzymes, the enzymatic hydrolysis of cellulose and hemicellulose to soluble saccharides and their fermentation to target products. Various levels of process integration together with related challenges are presented. Natural and synthetic microbial communities are addressed in section 2.4 whereby a focus is on intra-consortium ecological dependencies and factors which enhance the stability of the community. In section 2.5 biofilms are discussed as natural strategy of microorganisms to organize themselves in microenvironments with spatial niches.

2.1 Composition and structure of lignocellulosic biomass

The cell wall of higher plants is made of lignocellulose which is mainly composed of the three polymers cellulose (40 to 50 % of the cell wall), hemicellulose (20 to 40 %) and lignin (around 20 to 35 %) (Fig. 2.1). Cellulose is the most abundant organic compound on Earth. It is a linear homopolysaccharide which is composed of β -(1-4)-linked D-glucose units [25]. The repetitive unit is cellobiose. One end of the cellulose chain has a hydroxyl group on the C1 atom which makes this end a reducing end. The other end has a hydroxyl group on the C4 position which makes this end non-reducing. Cellulose chains have the intrinsic tendency to align side by side and to form bundles stabilized via hydrogen bridge bonds which are called elementary

fibrils [25]. Multiple elementary fibrils congregate to microfibrils having a diameter between 2 to 20 nm [25] which in turn tend to arrange themselves in macrofibrils with a diameter between 60 to 400 nm. Neighbouring microfibrils are held together by hydrogen bridge bonds that form between the hydroxyl group of glucose of one of the fibrils and the oxygen atom of the other fibril. Such structure has a high organization degree and it can withstand tensile stress to a certain extent (Fig. 2.1). Aside from these crystalline regions cellulose has amorphous zones with a lower level of order. Enzymes can access amorphous sites easier than crystalline sites and thus, chemical or biological degradation processes preferentially occur in amorphous regions [25].

Hemicellulose is mainly composed of monosaccharides such as glucose, xylose, galactose, arabinose and mannose [26]. The composition of these monosaccharides is specific to each plant species. In hardwood, the dominant hemicellulose is xylan. Hemicellulose in hardwood is based on glucuronoxylan with a xylopyranose backbone [26]. It has a predominantly branched structure which is in contrast to the linear character of cellulose [25]. The branched structure in combination with acetyl or uronic side chains prohibits the formation of crystalline regions which makes hemicellulose easier biologically hydrolyzable than cellulose.

The most common monomeric building blocks of lignins are three monolignols, i.e. *p*-coumaryl alcohol, coniferyl alcohol and synapyl alcohol [26]. For polymerization, the monolignols are oxidized to radicals by enzymes, namely peroxidases or laccases. The free radicals then form dehydrogenative polymers with carbon-carbon and ether linkages. This rather random polymerization process led to the assumption that the structure of lignins does not exhibit any long-range order. However, recent findings point towards certain regularities in the structure of lignins [25]. The heterogenous molecular structure in combination with strong carbon-carbon and ether bonds makes cleavage of lignin challenging.

In lignocellulose, hemicellulose encloses the macrofibrils of cellulose and the two are connected via hydrogen bridge bonds which makes the structure highly flexible (Fig. 2.1). On the other hand, hemicellulose is connected to lignins via covalent ester bonds. Lignins make the structure more rigid and better protected against biological attacks because they serve as a hydrophobic defense barrier. Taken together, this amazing composite system of lignocellulose provides structural stability against tensile and compressive stress and acts as barrier for diseases and insects. In addition, its capillary structure enables the transport of liquids and nutrients from roots to leaves and vice versa.

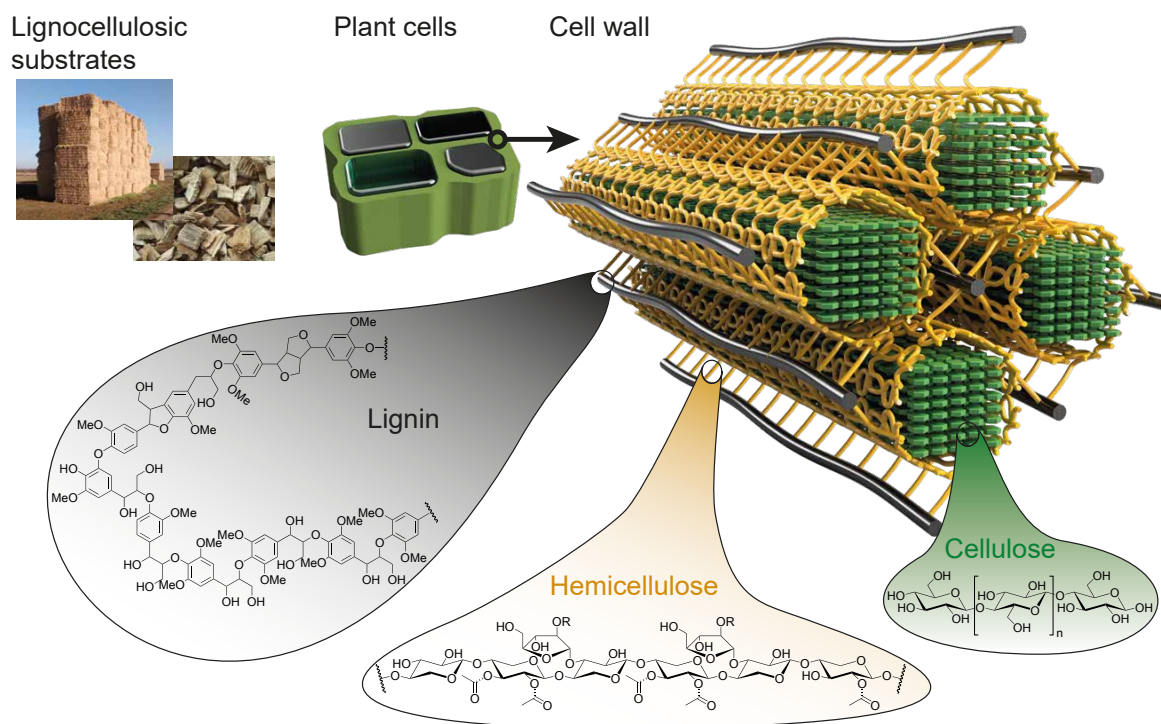


Figure 2.1: **Components and structure of lignocellulosic biomass.** Lignocellulosic biomass is the most abundant raw material on Earth and forms the cell wall of plants. It is composed of cellulose, hemicellulose and lignin forming a recalcitrant structure by cross-linking the polysaccharides (cellulose and hemicellulose) and lignin. The structure of lignin is adapted from [27]. Please note that the structure of the lignocellulosic cell wall is simplified for better visualization and not to scale. For example, in reality the number of elementary fibers which conglomerate to micro- and macrofibrils is significantly higher.

2.2 Pretreatment - making lignocellulosic biomass accessible for biochemical conversions

Lignocellulosic biomass is abundant and renewable which makes it a valuable substrate for biochemical processes for the production of various products. However, the biochemical conversion of lignocellulose is challenging due to its recalcitrant structure as described in section 2.1. As a result, processes on untreated lignocellulose have low productivities and hydrolysis yields below 20 % [28, 29]. In order to make lignocellulose competitive with alternative substrates such as glucose or starch it is essential to increase the hydrolyzability of lignocellulose. To this end, lignocellulose is pretreated to break its geometrical structure to reduce the crystallinity of cellulose, to improve the accessibility for enzymes [30] and to increase the porosity of the feedstock by solubilizing lignin [31]. Pretreatment is of highest

importance in the biorefinery context as it affects all downstream processes such as enzymatic hydrolysis, microbial fermentation, product recovery and handling of waste residues [32].

A wide range of pretreatment methods has been developed over the last decades. Some of the techniques use physical means, others rely on chemical, biological or thermal principles or a combination of those. All of these approaches aim for a high recovery of cellulose and hemicellulose in a biochemically usable form. The recovery of lignins is also highly desirable because they contain polymeric polyphenols. These compounds should be used chemically instead of thermally because of their broad applicability in various industrial processes.

As lignocellulose combines three main compounds with different properties the conditions under which pretreatment is performed have to be chosen carefully. In particular, hemicellulose should be recovered under milder conditions as compared to cellulose. If process conditions are too harsh hemicellulose would depolymerize into pentoses which could further react to furfural. Cellulose would be cleaved to hexoses which would be further converted into hydroxymethylfurfural (HMF), levulinic acid or formic acid. Lignin would release various phenolic compounds [33]. All of these degradation products which would result from inappropriate pretreatment conditions are highly potent inhibitors that hinder desired biochemical conversions. The formation of inhibitory degradation products which alter subsequent process steps should be avoided. In addition, all pretreatment methods should be suitable for high solid loadings to enable high product titers. Furthermore, it is crucial that the total cost of the pretreatment step justifies its application and thus, energy and investment costs should be economically feasible. Typically, 16 to 19 % of the total capital investment costs are attributed to the pretreatment step [34,35].

Physical pretreatment methods aim for the reduction of the particle size to increase the surface to volume ratio of the biomass. To this end, mechanical stress is applied for example by mechanical chipping or grinding of the lignocellulosic biomass. Physical methods can be applied to all kinds of biomass but they are often not sufficient to significantly improve biochemical conversions [32]. Therefore, they are often combined with other subsequent pretreatment methods which need small particles for efficient operation [32].

The pretreatment of lignocellulosic biomass by steam explosion is of commercial relevance [36]. Thereby, the biomass is inserted into a vessel, pressurized and heated using direct injection of saturated steam. The steam penetrates into the fibers and condenses. As a result, acetyl groups in hemicellulose autohydrolyze and form acetic acid which lowers the pH. Acidic conditions catalyze the hydrolysis of hemicellulose and mainly xylooligomers are solubilized in a liquid phase called prehydrolyzate. When the pressure is explosively discharged the water abruptly evaporates. This disrupts the structure of the fibers and reduces the size of the biomass particles [37]. The effect of steam-pretreatment on the biomass is most critically influenced

by the used temperature and process duration. In general, the higher the temperature and the longer the treatment the better the enzymatic hydrolysability of the cellulose fraction. If a temperature below around 180 °C is applied lignin and cellulose are rather unaffected by the treatment and remain solid. In order to reach an optimal hydrolysability of cellulose harsher process conditions, e.g. higher temperatures of up to 230 °C or longer retention times, are required. As hemicellulose is temperature-sensitive the prehydrolyzate should be removed from the reactor vessel before such a harsher treatment is performed. Pretreatment with steam has the advantage that chemicals can be avoided, that the particle size is reduced and that high biomass loadings can be used. The latter is of particular interest to obtain high concentrations of target products after subsequent biochemical conversions. The degradation of hemicellulose with the accompanied formation of inhibitors is problematic and washing steps are usually required.

Chemical pretreatment methods employ alkaline or acidic chemicals to prepare lignocellulose for further biochemical processes. Alkaline chemicals include hydroxyl derivatives of sodium salts or potassium, calcium and ammonium salts. These chemicals degrade the side chains of esters and glycosides which results in cellulose swelling, decrystallization of cellulose and solubilization of hemicellulose. A neutralization step with subsequent washing steps is required to remove the salts which increases process costs. The pretreatment with diluted acidic chemicals is one of the most commonly used chemical methods. The process takes place either at high temperature above 180 °C for 1 to 5 min or at lower temperature below 120 °C for 30 to 90 min [38]. Disadvantages include the need for special equipment which is resistant against corrosion, the formation of a high amount of inhibitory products and the need of washing steps to remove them and the costly recovery of the acid as well as the need for a neutralization step [19].

Optimal hydrolysis rates close to the theoretical yields can be achieved when alkaline pretreatment and steam pretreatment are merged in a process called Ammonia Fiber Explosion (AFEX) [39]. Ammonia is added to the biomass, heated to elevated temperatures up to 180 °C which increases the pressure in the vessel. After a retention time of up to one hour the pressure is explosively discharged which leads to evaporation of ammonia. Aqueous ammonia cleaves the lignin-carbohydrate linkages [39] and modifies the structure of lignins by depolymerization which increases their capacity to capture water [38]. AFEX causes swelling of cellulose and a reduction of the crystallinity. The process is relatively cheap, no washing steps are required, and no inhibitors are formed.

Biological pretreatment methods rely on microorganisms that evolved a sophisticated enzymatic system to degrade lignins. For example, white-rot fungi such as *Ceriporiopsis subvermispora* or *Trametes versicolor* belonging to the divisions of Basidiomycota developed multiple enzymes

such as lignin peroxidases, manganese peroxidases and laccases to solubilize lignins. The degradation of lignins increases the surface area and median pore volume [40] and increases enzyme accessibility to cellulose [41]. It should be noted that the solubilization of lignins is challenging since the extensive size of the polymers requires the use of extracellular ligninolytic systems. The internal carbon-carbon and ether bonds require an oxidative rather than a hydrolytic degradation mechanism. In addition, lignins are highly stereoirregular and a variable mechanism is required for their degradation which is in contrast to the hydrolytic degradation of cellulose [42]. These lignin-degrading enzymes generate free radicals that enable spontaneous cleavage reactions [43]. The lignin content strongly affects the digestibility of lignocellulose. Such a biological pretreatment approach is energy-efficient and environmentally benign, no chemicals are required, and treatment conditions are mild [44]. However, biological pretreatment processes are long due to slow conversion rates and do not allow high process yields. Furthermore, hemicellulose might be lost due to degradation by the fungus.

Balch *et al.* developed a process that combines mechanical milling with biological degradation to enhance the biological solubilization of lignocellulose [45]. A stirred tank bioreactor was equipped with stainless steel balls to continuously mill the biomass to increase the accessibility of lignocellulose for enzymatic attacks. The thermophilic anaerobic bacterium *Clostridium thermocellum* solubilized 88 % of the total carbohydrates of switchgrass in the presence of milling which is nearly twice as much as in the absence of milling (45 %). Despite the efficient degradation of the senescent switchgrass the concentration of ethanol and acetate reached only 0.7 and 1.3 gL⁻¹, respectively [45].

2.3 Biochemical conversion of pretreated lignocellulosic biomass to target products

Pretreatment processes increase the enzymatic digestibility of lignocellulosic biomass as discussed in section 2.2 and make it accessible for biochemical conversions to obtain the target product. Biochemical conversions involve four process steps: the production of cellulolytic enzymes, the enzymatic hydrolysis of polymers to soluble carbohydrates and the fermentation of the hexoses and pentoses to the target product (Fig. 2.2). These steps can be performed independent of each other (called separated hydrolysis and fermentation (SHF)) or they can be combined. The degree of consolidation increases from the three-step process simultaneous saccharification and fermentation (SSF) to the two-step process simultaneous saccharification and co-fermentation (SSCF) and to consolidated bioprocessing (CBP) which combines all four process steps (Fig. 2.2). In the following, each process step is described in detail.

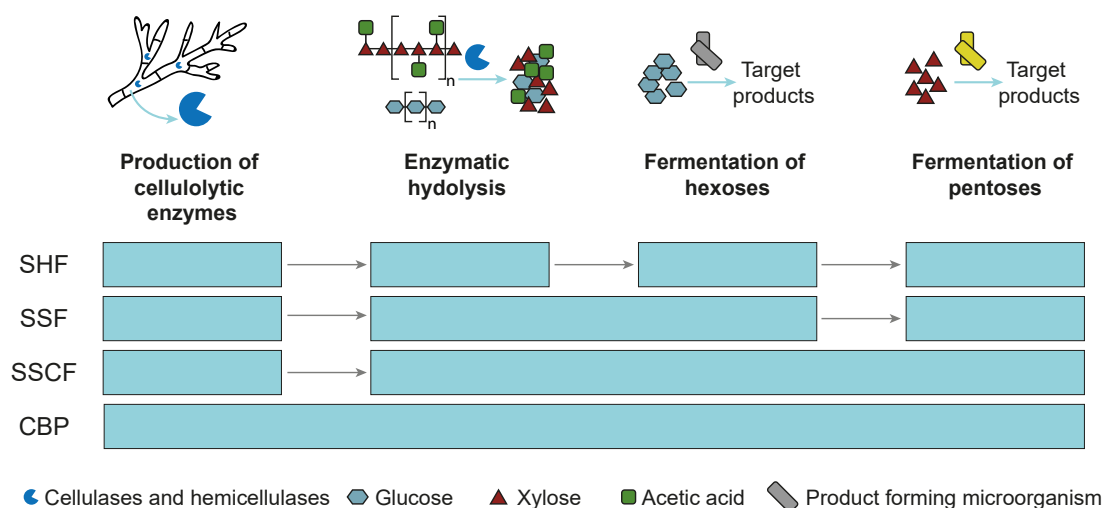


Figure 2.2: **Configurations of biologically mediated processes to convert pretreated lignocellulosic biomass to target products.** Separated hydrolysis and fermentation (SHF), simultaneous saccharification and fermentation (SSF), simultaneous saccharification and co-fermentation (SSCF) and consolidated bioprocessing (CBP).

2.3.1 Production of cellulolytic enzymes and enzymatic hydrolysis

The conversion of pretreated lignocellulosic biomass to target products begins with the production of cellulolytic enzymes which catalyze the hydrolysis of cellulose and hemicellulose to soluble hexoses and pentoses. Multiple enzymes act both complementarily and synergistically enabling the efficient degradation of lignocellulose. Glycosidases that belong to the enzyme class of hydrolases cleave glycosidic linkages in hemicellulose and cellulose. There are mainly three types of hydrolases: cellobiohydrolases, endoglucanases and beta-glucosidases (Fig. 2.3) [46]. Cellobiohydrolases cleave the glucosidic linkages in cellulose at the reducing (CBH type I) and non-reducing (CBH type II) end of the cellulose chain. Cellobiose units are released. Endoglucanases cleave the internal glucosidic bonds favourably in amorphous regions of cellulose [47] at random positions [48]. This step increases the access of cellobiohydrolases to act on the opened chain ends. Beta-glucosidases hydrolyze the final step of cellulose hydrolysis by the conversion of cellobiose to two glucose monomers (Fig. 2.3) [49]. The heteropolymer hemicellulose requires a higher number of enzymes for its hydrolysis compared to cellulose. The xylan backbone is hydrolysed by endoxylanases which catalyze the release of shorter xylooligosaccharides which are further cleaved by the beta-xylosidases into xylose [30]. The substituents which are linked to the xylan backbone include acetyl groups, glucose, arabinose or galactose are released by the action of various types of esterases [50]. This increases the

access of the enzymes to degrade the main xylan backbone [30]. Other enzymes such as peroxidases or laccases modify lignin.

The production of such enzymes relies on only a few microorganisms that have evolved the complete sophisticated enzymatic system required for the degradation of lignocellulose. The microorganisms produce the enzymes intracellularly and may secrete them. For example, fungi produce non-complexed enzymes. In contrast, anaerobic bacteria produce multi-enzyme complexes, which are bound to their outer cell wall (Fig. 2.3). Free cellulases produced by fungi are independent catalytic units, not bound to the fungus and diffuse unrestrictedly in the system (Fig. 2.3A) [51]. An important industrial relevant microorganism for the production of cellulolytic enzymes is the aerobic fungus *Trichoderma reesei*. The mesophilic, filamentous fungus was first isolated during the Second World War and denoted *T. reesei* QM6a [52]. It was discovered that this strain produced extraordinary high amounts of cellulases [53] which motivated the further strain development in multiple mutagenesis programs. The goal was to develop a catabolite derepressed strain with increased production of cellulases [52]. A three-stage process which included a first mutagenesis step with UV light to screen for catabolite derepression, a subsequent N-nitroguanidine mutagenesis step which targeted the increase of the cellulolytic enzyme production and another UV mutagenesis treatment to screen for increased cellulase activity. This process resulted in the hyperproducing strain *T. reesei* RUT-C30 [54–56]. However, *T. reesei* RUT-C30 is deficient in beta-glucosidase production [57]. This lack of beta-glucosidase in the enzyme cocktail leads to the accumulation of cellobiose which inhibits the enzymes cellobiohydrolases and endoglucanases [48,49,58].

Anaerobic bacteria such as *Clostridium thermocellum* and *Clostridium cellulovorans* produce multi-enzyme complexes termed cellulosomes for the decomposition of cellulose and hemicellulose. Cellulosomes combine various catalytic subunits e.g. cellobiohydrolases and endoglucanases [51] and are in most cases directly attached to the cell wall (Fig. 2.3B). The structure of cellulosomes is defined by cohesin containing proteins termed scaffoldins. The enzymatic subunits are bound via dockerin to cohesin molecules of the scaffoldin which serve as backbone of the cellulosome. The bonds are based on non-covalent protein-protein interactions. The scaffolding subunit also contains a cellulose binding module which allows the attachment of the cellulosome to the cellulose chain. The whole complex is bound to the bacterial cell wall by anchoring proteins. Taken together, during the hydrolysis ternary cellulose-enzyme-microbe complexes are formed. In addition, the bacterial cell serves as sink for soluble products such as cellobiose, glucose or xylose formed during the enzymatic hydrolysis which are known to inhibit the enzymatic hydrolysis (Fig. 2.3B).

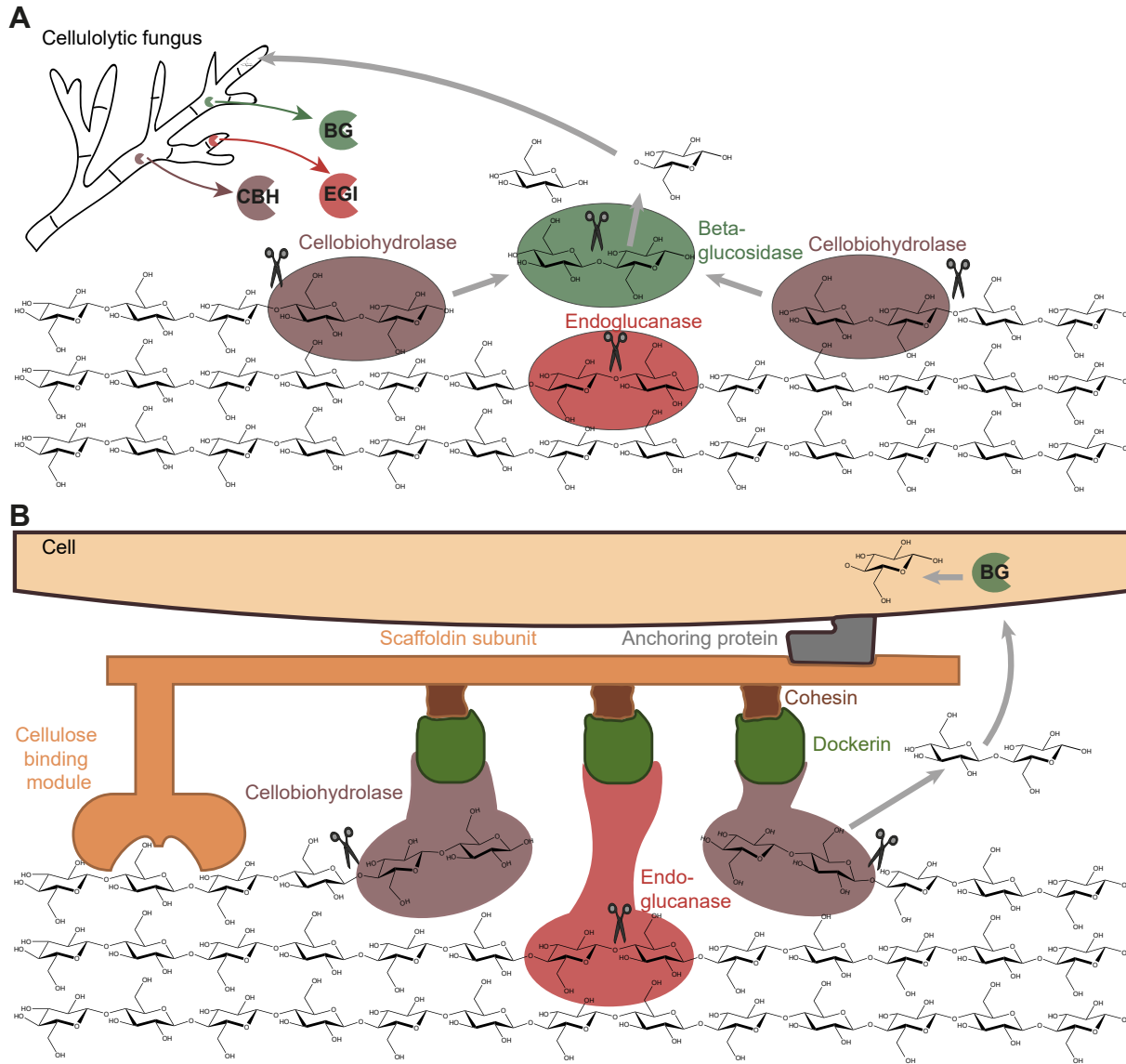


Figure 2.3: Schematic overview of the enzymatic hydrolysis of cellulose: Free fungal cellulases and cell-bound bacterial cellulosomes. (A) A cellulolytic fungus produces and secretes cellobiohydrolases, endoglucanases and beta-glucosidase which move freely. The endoglucanase cleaves the internal β -1-4-glycosidic bonds which makes the open ends of the cellulose chain accessible for cellobiohydrolases. Cellobiohydrolases release soluble short-chain glucooligomers such as cellobiose or cellotriose. Beta-glucosidases hydrolyze cellobiose to glucose monomers which is the carbon source for the fungus. (B) A multi-enzyme complex termed cellulosome bound to the cell wall of an anaerobic cellulolytic bacterium. A scaffoldin subunit serves as backbone of the cellulosome and is attached to an anchoring protein bound to the bacterial cell wall. The cellulose binding module as part of the scaffoldin subunit binds to a cellulose fiber. Multiple cellulolytic enzymes are connected to cohesins present in the scaffoldin subunit via dockerin domains.

In the context of the overall biochemical conversion process it is highly desirable to obtain high final product concentrations to reduce downstream costs for product recovery. This requires elevated solid loadings during the enzymatic hydrolysis [59]. There are two major challenges related to increased solid loadings: the inhibition of cellulolytic enzymes by the end-products and the 'high solid effect'. In the former case, beta-glucosidases are inhibited by glucose while cellulases are inhibited by glucose, cellobiose and monomers released from hydrolysis of hemicellulose such as xylose, mannose and galactose [60]. Accordingly, Lu *et al.* performed experiments which demonstrated the beneficial effect on the hydrolysis rate when lowering the concentration of inhibitory carbohydrates on the surface of cellulose. They used metabolically active, cellulosome producing bacterial cells and compared them to purified cellulosome preparations from *C. thermocellum* [61]. The other challenge termed 'high solid effect' describes the observation that the yield of the enzymatic hydrolysis is reduced with increased solid loading [62]. This phenomenon was explained in literature by a combinatory effect of a mass transfer limitation [63] and reduced availability of water as important reactant of the enzymatic hydrolysis at high concentrations of soluble end-products [59].

2.3.2 Fermentation of hexoses and pentoses

In a fermentation process microorganisms convert energy-rich organic compounds to compounds with less energy to gain energy. Normally, the process happens under anaerobic conditions or in situations when an external electron acceptor for anaerobic respiration is not available. Organic substrates such as carbohydrates or lipids are converted to organic acids, alcohols, carbon dioxide or/and hydrogen in a process called 'primary fermentation'. This step can be the first in an anaerobic food chain. In a 'secondary fermentation' the primary fermentation products are converted into secondary fermentation products such as acetic acid, carbon dioxide or/and hydrogen. Fermentations are classified with respect to the fermented end product which is secreted to the environment. Typical fermentation products include various alcohols (ethanol, butanol, acetone) and acids (lactic acid, propionic acid, butyric acid, caproic acid, succinic acid).

Fermentation is applied in a variety of industrial processes that aim for the production of food (e.g. wine, beer and yogurt) or the production of energy carriers (e.g. biogas and bioethanol). For most of these processes easily digestible substrates such as glucose and starch are used which allow for a high productivity. The fermentation of carbohydrates from hydrolysates of lignocellulosic biomass is more challenging because the substrate contains inhibitors originating from the pretreatment and a heterogeneous mixture of hexoses and pentoses. The complete exploitation of the substrate is desired to achieve a high product yield. However, in particular the fermentation of pentose is critical for many microbial fermenters. As one example, the

ethanol-producing yeast *S. cerevisiae* is a standard strain in industry which is not able to utilize the pentose xylose [64]. Aside from a high product yield from hexoses and pentoses a high tolerance for the target product is desired. This would allow for higher product concentrations without harming the fermenting strain and with that, would lower the downstream processing costs.

2.3.3 Consolidated bioprocessing

As stated above and as depicted in figure 2.2, four process steps are required to biologically convert biomass into target products. In the four-step procedure SHF each step is operated under optimal conditions (e.g. temperature, pH). However, soluble carbohydrates accumulate during the enzymatic hydrolysis due to missing microbial consumers and inhibit cellulolytic enzymes which decreases the enzymatic activity. Lack of consolidation results in relatively high operational and investment costs. In order to omit the inhibition of cellulolytic enzymes by accumulation of soluble carbohydrates and to reduce process costs [65] the enzymatic hydrolysis and the fermentation step are combined in one process step (SSF strategy, Fig. 2.2). A major disadvantage of increased level of consolidation is that the process parameters have to be chosen such that they enable all biochemical subprocesses. For example, the production of ethanol with the yeast *Saccharomyces cerevisiae* is optimum around 30 to 35 °C which is not in line with the optimum temperature of the enzymatic hydrolysis using cellulolytic enzymes from *T. reesei* which is typically at 50 to 55 °C. Although the enzymatic hydrolysis is commonly recognized as major rate limiting process step, the SSF process is performed below the optimum temperature of the enzymatic hydrolysis because *S. cerevisiae* does not withstand temperatures as high as 50 °C. Another drawback is the inhibition of cellulolytic enzymes by various target products such as acetic acid, butyric acid, ethanol or butanol [66].

All four biologically mediated processes are merged in one process step referred to as consolidated bioprocessing (CBP). The highest level of process integration offers the potential to reduce enzyme and capital costs [21,23]. By using the CBP approach to produce ethanol from lignocellulose cost savings of up to 40 % in comparison to the SSF process have been calculated [67]. However, the choice of appropriate process parameters that enable all biologically mediated process steps in one vessel is a great challenge and requires compromises.

Multiple strategies were developed for CBP of lignocellulose to various target products. The most common approach is based on the creation of such a single microbial superbug which is capable to catalyze all biological process steps. The creation of a superbug typically starts with a native cellulolytic microorganism or a native product-forming microorganism whose missing metabolic capabilities are introduced by genetic engineering (Fig. 2.4A). Despite intensive research for decades only very few reports describe commercially attractive product

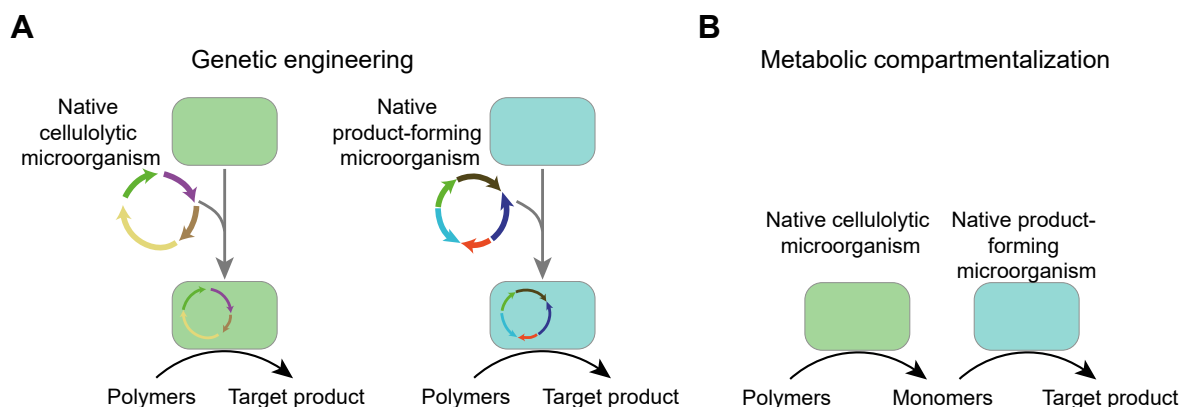


Figure 2.4: **Strategies for CBP of lignocellulose to target products.** (A) Genetic engineering of a superior superbug capable of all biological processes. This strategy can be based on a native cellulolytic or a native product-forming microorganism. In both cases the missing metabolic capabilities are compensated by insertion of genes. (B) Metabolic compartmentalization involving multiple microorganisms. The microbial community has both the native cellulolytic capabilities and the ability to form the target product.

yields, titers or productivities and difficulties in engineering a superior superbug remain [68]. In particular, no CBP strain viable for industrial applications has been created [69]. Axenic cultivations are often used in industrial bioprocesses but are not common in nature. They tend to instability, are dependent on sterilization processes and have a high risk of contamination.

An alternative approach is based on metabolic compartmentalization involving multiple microorganisms whereby each member of the community is specialized in a subtask (principle of labor division) and occupies its ecological niche (Fig. 2.4B). Microbial communities are ubiquitous in natural ecosystems [70] and catalyze complex biotransformations such as the degradation of lignocellulosic biomass [51]. Taken together, the consortium in the CBP approach owns all required metabolic capabilities to decompose the recalcitrant structure of lignocellulosic biomass and to form target products [71].

Natural microbial communities are industrially approved in waste water treatment [72], biogas production [73], production of foods such as cheese, meat products e.g. salami [74], sourdough bread [75] or Kombucha [76]. A remarkable biological multi-component system which combines physical pretreatment in the form of chewing and rumination with biological decomposition of cellulosic biomass evolved in ruminants such as the cow. It is impressive that the cow controls the rate of rumination and the retention time of up to 72 hours in dependence of the hydrolysability and the particle size of the feed material. Ruminants convert the biomass at high solid loadings under non-aseptic conditions, with minimal nutrient requirements and without the need for external heating or pressurization efficiently to high value products [77]. The

system 'cow' runs at a constant temperature of 39 °C, keeps the oxidation-reduction potential stable at -400 mV and efficiently holds the pH without addition of pH control agents at around 7. In addition, anaerobic conditions are obtained by the interaction of facultative anaerobic and strict anaerobic microorganisms [77]. Remarkably, the natural undefined microbial consortium evolved pathways which maximizes the ATP production and microbial growth [78]. These communities produce volatile fatty acids (VFAs) such as acetic acid, propionic acid and butyric acid which serve as energy source for the cow. The evolution evolved the epithelial cells in the rumen wall which allow separation of the VFAs [77] although the maximum VFA concentration is typically 0.1 M [78].

The carboxylate platform as part of the MixAlco process applies an undefined community of different anaerobic partly cellulolytic and/or acid-forming bacteria to produce a mixture of carboxylic acids with up to seven carbon atoms from lignocellulose [79–81]. A major advantage using undefined communities is the elimination of aseptic process conditions [80]. However, the high complexity of natural consortia including the large number of partially uncharacterized species with unknown microbial pathways reduces the level of process control and makes the targeted production of chemicals difficult. Mixed fermentation end-products and relatively low yields are common challenges in natural consortia-based processes.

If the community is artificially constructed with carefully selected, well-characterized, specialized microorganisms the community-based CBP becomes controllable. Such engineering of microbial consortia for consortium-based CBP recently gained attention [10,71]. In literature synthetic CBP targeting various products can be found. Xu and Tschirner [82] showed an improved ethanol production through an anaerobic co-culture of *Clostridium thermocellum* and *Clostridium thermolacticum* which are both cellulolytic and able to produce ethanol from cellulose and microcrystalline cellulose. Zuroff *et al.* [83] demonstrated a consortia-mediated bioprocessing of cellulose to ethanol with a cross-kingdom symbiotic *Clostridium phytofermentans*/yeast co-culture. Brethauer and Studer [10] demonstrated a synthetic microbial community of the fungus *T. reesei* and two yeasts for the direct conversion of lignocellulose to ethanol in a batch reactor. Minty *et al.* [84] established a consortium of the fungus *T. reesei* and a genetically modified bacterium *Escherichia coli* for conversion of microcrystalline cellulose to isobutanol. Wen *et al.* [85] reported an artificial symbiotic system of *Clostridium cellulovorans* and *Clostridium beijerinckii* to produce acetone, butanol and ethanol from alkali extracted deshelled corn cobs.

2.4 Microbial communities

A great number of single step biotransformations was successfully realized in genetically modified microorganisms. The realization of more complex transformations which require

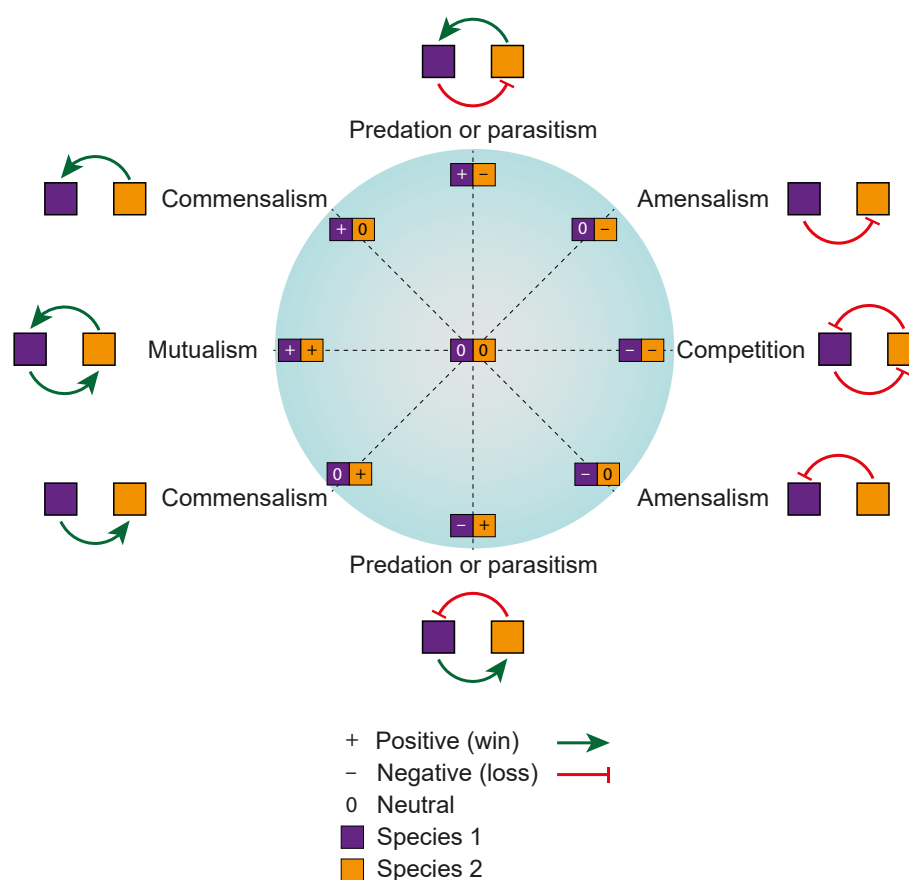


Figure 2.5: **Ecological interactions in microbial communities.** The wheel shows the possible interactions between two members of a microbial community. Each member of the community can be (+) positively, (-) negatively or (0) not affected by the interaction. Adapted from [89] and initially introduced by [90].

a higher number of steps and multiple pathways are more difficult and partly impossible to be performed in a single cell [86]. One possibility to enable such a complex transformation is to split the biological process steps in multiple microorganisms following the principle of division of labor where each member of the community catalyzes only a part of the whole conversion and the intermediate metabolites are exchanged [87]. The microbial community as a whole enables the desired biotransformation. The greater number of microorganisms leads to a larger pool of genes compared to monocultures and a higher diversity of metabolic pathways [88]. The co-cultivation of microorganisms results in multiple possible ecological interactions between the individual organisms. Such interactions might have a positive effect, e.g. in a food chain, where the metabolic end product of one microorganisms is the substrate for another microorganism, a negative effect, e.g. in a competition of both microorganisms for a substrate, or a neutral effect, e.g. if no metabolites are shared among both microorganisms (Fig. 2.5) [89,90].

Natural communities contain up to thousands of species [91] which makes the decoding of the tasks of each member in the community difficult. The microorganisms form multicellular aggregates which create chemical gradients and spatial compartments in natural ecosystems. In order to elucidate and study the tasks and interactions in artificial communities, communities with only two species were constructed [88] to reduce the complexity. Most of such designed systems are characterized by shared medium and homogeneous abiotic factors such as temperature, pH or dissolved oxygen [88]. This might limit the selection of microorganisms and can change their phenotype compared to natural ecosystem.

Multiple microbial communities were developed to enable the efficient co-fermentation of hexoses and pentoses released from lignocellulose. In various bacteria, yeasts and other microorganisms the catabolism of hexoses and pentoses is regulated by carbon catabolite repression. This regulatory phenomenon represses in the presence of a preferred carbon source, e.g. glucose, the expression and activity of catabolic enzymes to use an alternative secondary substrate, e.g. xylose [92]. The co-cultivation of a hexose specialist and a pentose specialist to utilize both monomers simultaneously was performed by multiple research groups [93–96]. For instance, Fu *et al.* co-cultivated the glucose fermenting bacterium *Zymomonas mobilis* and the xylose fermenting yeast *Pichia stipites* for the production of ethanol [93].

Minty *et al.* designed and characterized a synthetic two-member consortium of the cellulase-secreting fungus *T. reesei* and a genetically engineered product-forming *E. coli* to produce isobutanol from cellulosic biomass [84]. The authors state that the designed microbial community is based on cooperator-cheater dependencies [84]¹. The production and secretion of cellulases by *T. reesei* is metabolically costly and the released carbohydrates are not solely consumed by *T. reesei*. The non-cellulolytic bacterium *E. coli* acts as cheater and benefits from the enzymatic hydrolysis by consuming a share of the released carbohydrates [84]. The presented system is fully aerated and allows in contrast to natural ecosystems no spatial niche differentiation which stabilizes natural ecosystems. First, these homogeneous, aerated conditions seem inappropriate to produce anaerobic metabolites. The proposed circumvention could be based on sophisticated cloning to remove all active cytochrome oxidases in the product-forming host as performed by Portnoy *et al.* [99]. The selection of such a knock-out strain deficient in all active cytochrome oxidases showed strongly reduced oxygen uptake rates and as a result the accumulation of anaerobic metabolites under aerobic conditions [99]. Second, following the law of competitive exclusion which states that two species with similar ecological niches

¹The terms *cooperator* and *cheater* are used inconsistently across various biological systems [97]. Following Ghoul *et al.*, in this thesis *cooperation* is a behaviour with a beneficial effect on the recipient and *cheating* is "(...) (i) a trait that is beneficial to a cheat and costly to a cooperator in terms of inclusive fitness (ii) when these benefits and costs arise from the actor directing a cooperative behavior toward the cheat, rather than the intended recipient" [97]. This is also in line with Gore *et al.* [98] and Minty *et al.* [84] who used the terms to describe interactions within microbial communities.

exclude each other [89] such non-compartmentalized communities tend to instability. One possible solution was proposed based on microfluidic devices which provide growth chambers separated by a membrane thereby allowing the interaction between the microorganisms by diffusion of soluble, low-molecular-mass metabolites [100]. Similar approaches based on two compartments separated by a dialysis membrane were published [101–103].

The environmental conditions such as media components and abiotic factors are in all the presented approaches uniform for all microorganisms. This limits the selection of microorganisms since overlapping tolerance ranges of e.g. abiotic factors is mandatory for a successful co-cultivation. A more complex artificial ecological system to mimic natural ecosystems could be based on the integration of compartmentalization. Different local conditions caused by chemical gradients could allow niche formation for each microorganism. It must be assumed that the level of process control increases since in the extreme example each niche is only occupied by one species. Controlling the process conditions in this spatial niche allows for the regulation of the metabolic activity or the growth of the microorganism.

Said and Or proposed a modular process with multiple compartments arranged along a process flow where the microorganisms are ordered for their chronological order in the desired biotransformation [88]. The cells are immobilized in specific compartments by micro- or macromembranes. Each compartment is adapted for the specific abiotic parameters for each microorganism. This concept requires a high instrument-based effort with high costs.

2.5 Biofilms

Biofilms are a natural strategy of microorganisms to self-create a microenvironment and to occupy spatial niches. The formation of biofilms is tracked back to ancient times and they are seen as an essential component of the prokaryotic life cycle [104] which indicates their success. It has been hypothesized that biofilms may be the default mode of growth [105]. In the following paragraphs biofilms are addressed: What is a biofilm? Where, how and why does it form?

A biofilm is a three-dimensional aggregation of microorganisms which are embedded in a matrix of hydrated extracellular polymeric substances (EPS), in particular natural polymers of high molecular weight. The major components of biofilms apart from microorganisms and EPS are water, proteins, lipids and extracellular DNA. The macroscopic appearance of biofilms can be slimy, high-viscous and wet but also smooth, rough, filamentous or fluffy [106].

Biofilms are found ubiquitously in natural habitats e.g. they can be attached to solid surfaces or they can float on liquids. Inorganic substrates e.g. mineral surfaces of rocks on the bottom of streams of flowing waters are colonized by microbes which serves as nourishment for fish.

Biofilms can also form on metal surfaces such as boat hulls. This so-called marine biofouling can negatively impact the hydrodynamic performance of the boat which results in increased fuel consumption. Microorganisms are capable of forming biofilms on ceramic surfaces such as replacement joints, on biological tissues or teeth in the human body. This is a severe problem in medicine because antibiotics and the immune system cannot attack the microorganisms in a biofilm as efficiently as submerged cells which may cause chronic infections [107]. Biofilms are also found on organic substrates such as plant materials.

Both prokaryotic and eukaryotic microorganisms are able to form self-organized biofilms. Planktonic, free-swimming cells can undergo a physiological transition towards the biofilm mode of growth. In the initial attachment phase submerged cells, e.g. bacteria, approach a surface with the help of pili or flagella. Simultaneously the production of adhesives is up-regulated. After the initial attachment of the cells various EPS are produced by the cells which strengthen the bonds between the cells and the substrate [108]. The next stage allows the formation of sophisticated three-dimensional structures followed by a maturation phase. Finally, cells undergo another physiological transition back to planktonic cells which are released to the environment [108]. This allows the formation of new biofilms at other sites [109].

The driving forces for the formation of biofilms are manifold. Natural environments are often deficient in nutrients and can exhibit strong spatial gradients of different abiotic parameters such as light, carbon and oxygen [110]. The firm binding to beneficial habitats enables homeostasis, e.g. if microorganisms bind to a nutrient source in flowing waters they are not washed away and may profit from the nutrient source over a long time. In contrast to submerged cells, cells in the bulk of the biofilm are organized in a sessile and permanent manner [111]. Biofilms may also protect the microorganisms therein from harsh and life-hostile conditions such as biological attacks and toxins. Compared to an axenic single-celled planktonic organism cells growing in a biofilm act physiologically distinct as multicellular organism [104, 110]. Biofilm formation allows the development of high cell densities in a well-defined structure with cell-cell recognition and cell-cell communication [106]. The close proximity of the cells compared to planktonic growth enables the horizontal gene transfer and the exchange of signaling molecules [105, 112]. The biofilm can host a larger subpopulation of persisters which are dormant, non-dividing cells in comparison to submerged growing cells [113]. Their presence is problematic for treatments of infections with antibiotics because persisters tolerate them.

The formation of a biofilm allows the microorganisms to self-create a microenvironment. This environment is characterized by multiple gradients of substrates, metabolic products or metabolic intermediates caused by the metabolic activity of the cells in combination with their diffusion. This allows a higher level of differentiation in the community in contrast to

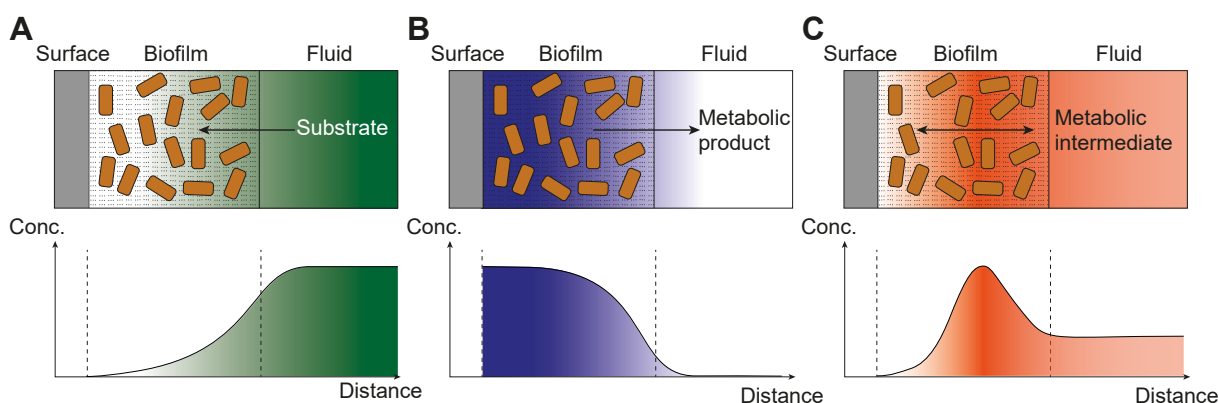


Figure 2.6: **Heterogeneities in microbial biofilms on an inert surface.** The depicted concentration of (A) a substrate which diffuses from the fluid into the biofilm and is consumed by the microorganisms, (B) a metabolic product which is produced in the biofilm and diffuses towards the fluid and (C) a metabolic intermediate which is produced and consumed in the biofilm which can result in a local maximum of the concentration. Inspired by [110].

homogeneous planktonic cultures. If a biofilm grows on an inert surface and if a substrate such as a soluble carbohydrate or a gas is present in the fluid adjacent to the biofilm it diffuses into the biofilm. If the microorganisms in the biofilm consume this substrate, its concentration will drop with increasing depth of the biofilm (Fig. 2.6A). As the biofilm becomes thicker the cells located close to the inert surface will be excluded from the substrate. The secreted metabolic products of the microorganisms such as acids, methane or carbon dioxide diffuse into the fluid and their concentration decreases from the maximum at the inert surface towards the biofilm/fluid interface and reaches its minimum in the fluid (Fig. 2.6B). If a metabolic intermediate is produced and consumed within the biofilm its concentration in the biofilm can form a local maximum which is above the concentration in the bulk fluid (Fig. 2.6C). As a result of such spatial inhomogeneities, multiple physiological states of microorganisms can exist in biofilms [110]. The EPS matrix can also bind and stabilize secreted extracellular enzymes, keep them in close distance to the cells which benefit from the catalytic action of the enzymes. As a result, the biofilm matrix can serve as external digestive system for microorganisms incorporated in the biofilm [106]. The majority of biofilm research was performed on bacterial biofilms in axenic *in vitro* studies [112]. In contrast, natural biofilms are mostly multispecies communities including bacteria, fungi and microalgae which are examined to a lower extent.

Taken together, microbial biofilms are concentrated aggregates of cells surrounded by a hydrated EPS matrix most often adhered to a surface which are characterized by various gradients of e.g. pH, oxygen, nutrients and metabolites which allow the presence of multiple physiological states of one species in close approximation but also strongly favoring biodiversity in mixed communities.

CHAPTER 3

Lactic acid

3.1 Abstract

Consolidated bioprocessing (CBP) of lignocellulosic feedstocks to platform chemicals requires complex metabolic processes, which are commonly executed by single genetically engineered microorganisms. Alternatively, synthetic consortia can be employed to compartmentalize the required metabolic functions among different specialized microorganisms as demonstrated in this chapter for the direct production of lactic acid from lignocellulosic biomass. We composed an artificial cross-kingdom consortium and co-cultivated the aerobic fungus *Trichoderma reesei* for the secretion of cellulolytic enzymes with facultative anaerobic lactic acid bacteria. We engineered ecological niches to enable the formation of a spatially structured biofilm. Up to 34.7 gL⁻¹ lactic acid could be produced from 5 % (w/w) microcrystalline cellulose. Challenges in converting pretreated lignocellulosic biomass include the presence of inhibitors, the formation of acetic acid and carbon catabolite repression. In the CBP consortium hexoses and pentoses were simultaneously consumed and metabolic cross-feeding enabled the *in situ* degradation of acetic acid. As a result, superior product purities were achieved and 19.8 gL⁻¹ (85.2 % of the theoretical maximum) of lactic acid could be produced from non-detoxified steam-pretreated beech wood. These results demonstrate the potential of consortium-based CBP technologies for the production of high value chemicals from pretreated lignocellulosic biomass in a single step.

This chapter is based on published work (reprinted with permission, license no. 4501861424984): R. L. Shahab, J. S. Luterbacher, S. Brethauer, M. H. Studer *Consolidated bioprocessing of lignocellulosic biomass to lactic acid by a synthetic fungal-bacterial consortium*. *Biotechnology and Bioengineering*, 115(5):1207–1215 [2018]. doi: 10.1002/bit.26541.

3.2 Introduction

Lactic acid and its derivatives are versatile sustainable platform molecules for the food and chemical industries [114] and are mainly produced in anaerobic batch fermentations of feedstocks rich in starch or sugar. However, the high costs of these raw materials and their competitive use as food and feed ingredients remain major drawbacks of the fermentative production of lactic acid, which limits the large-scale development of poly-lactic acid as renewable alternative to fossil-based plastics. Alternatively, lignocellulosic biomass - the most abundant form of fixed renewable carbon on earth - is a promising feedstock for producing sustainable chemicals at low cost [21].

Generally, the biotechnological processing of lignocellulose can be divided in four main steps: pretreatment to enhance enzymatic digestibility, production of saccharifying enzymes (cellulases and hemicellulases), enzymatic hydrolysis to depolymerize cellulose and hemicellulose to fermentable saccharides and fermentation of soluble saccharides to the target product [10,84]. Central barriers of the industrial-scale conversion of lignocellulosic biomass to biochemicals are the high capital costs due to the complex process and the high cost of cellulolytic enzymes [115,116]. The simplification of the process by integrating all biochemical process steps into one single unit operation, an approach termed consolidated bioprocessing (CBP), has attracted considerable attention for the production of biochemicals, due to its anticipated favorable economic performance [23,116]. The engineering and the optimization of multiple capabilities, e.g. the production of cellulolytic enzymes, the co-fermentation of hexoses and pentoses and the tolerance to inhibitory degradation products derived from biomass pretreatment, in one single strain has proven to be challenging [69,71,84]. Thus, consortium-based bioprocesses, where different specialized microorganisms can efficiently combine various pathways and processes required for the degradation of complex substrates, are developed and investigated as an alternative approach for CBP [71].

Successful consortium-based conversions of cellulosic feedstocks to a variety of different compounds including ethanol [10,82,83], isobutanol [84] or acetone, butanol and ethanol [85] have been reported. However, improved strategies to control intercellular interactions and to enable stable microbial communities are required [86,117,118]. Furthermore, any biological production of lactic acid from lignocellulosic biomass is especially challenging as recently described due to three major limitations specifically associated with its fermentation from heterogeneous saccharides (e.g. glucose, xylose): (i) The heterofermentation of xylose via the phosphoketolase (PK) pathway leads to the accumulation of high amounts of by-products such as acetic acid which increases the downstream cost and reduces the profitability. (ii) Carbon catabolite repression (CCR) of the non-favorable sugars such as xylose lowers the productivity of the process. (iii) Lactic acid bacteria are sensitive to inhibitory compounds released during

Table 3.1: Reported and own data on the production of lactic acid from pretreated lignocellulosic material or microcrystalline cellulose either in SSF processes or by CBP.

Microorganisms	Feedstock	Process	$C_{LA,max}$ [gL ⁻¹]	Productivity [gL ⁻¹ h ⁻¹]	References
<i>L. rhamnosus</i> + <i>L. brevis</i>	Corn stover	SSF	20.95	0.58	[120]
<i>B. coagulans</i>	Solka Floc crystalline cellulose	SSF	80	0.30	[121]
<i>L. rhamnosus</i>	Cellulosic biosludge	SSF	39.4	0.82	[122]
<i>B. coagulans</i>	Sugarcane bagasse	SSF	58.7	1.33	[123]
<i>B. coagulans</i>	Wheat straw	SSF	40.7	0.74	[124]
<i>T. reesei</i> RUT-C30 + <i>L. pentosus</i>	Microcrystalline cellulose	CBP	34.7	0.16	This chapter
<i>T. reesei</i> RUT-C30 + <i>L. pentosus</i>	Beech wood	CBP	19.8	0.10	This chapter

pretreatment of the biomass [119]. Table 3.1 summarizes recently published results for the production of lactic acid from lignocellulosic biomass. To the best of our knowledge, only simultaneous saccharification and fermentation (SSF) processes which require the addition of costly, externally produced cellulolytic enzymes were developed, but no consolidated bioprocesses targeting lactic acid were reported.

In this chapter, we designed and characterized artificial cross-kingdom microbial consortia of *Trichoderma reesei* and different lactic acid bacteria for the production of lactic acid from lignocellulosic biomass. We demonstrate their ability to directly convert non-detoxified pretreated biomass containing pentoses and hexoses to lactic acid without carbon catabolite repression and to concomitantly remove the unwanted side product acetic acid.

3.3 Results and discussion

3.3.1 Design and implementation of a microbial consortium for CBP of lignocellulose to lactic acid

Consortium-based CBP of lignocellulosic biomass to lactic acid requires at least one microorganism for the production of cellulolytic enzymes and one strain that converts the sugars released

3.3.2 Conversion of cellulose to lactic acid in batch processes

In order to prove the functionality of the synthetic consortia, we first studied the conversion of different amounts and types of carbon sources (microcrystalline cellulose (Avicel) and steam-pretreated beech wood) to lactic acid by a co-culture of *T. reesei* and *L. pentosus*. A sequential inoculation scheme with a two-day delay between the inoculation of the fungus and the bacterium was applied to enable the formation of a fungal biofilm and to ensure anaerobic conditions in the bulk phase at the time of inoculation with the product forming strain. In effect, the dissolved oxygen concentration dropped below the detection limit 12 hours after fungal inoculation indicating that growth of *T. reesei* was oxygen limited and not nutrient limited (further details, chapter 4 and Fig. 4.4). With microcrystalline cellulose as the substrate, the maximum lactic acid yield increased from 0.45 g g⁻¹ (45.9 % of the theoretical maximum) at 1.75 % (w/w) Avicel to 0.62 g g⁻¹ (62.4 % at 5.00 % (w/w) Avicel) (Tab. 3.2). The latter corresponds to a maximum lactic acid concentration of 34.7±0.2 g L⁻¹ (Fig. 3.2) and a productivity of 0.16 g L⁻¹h⁻¹. Due to the chosen sequential inoculation scheme, *T. reesei* had during the first two days exclusive access to the substrate. The increasing lactic acid yield suggested that the amount of the carbon source that was consumed for fungal growth remained constant and was independent of the solid loading, i.e. the fraction of carbon source that remained for the conversion to lactic acid increased with increasing carbon loading. Next, we switched to one-stage steam-pretreated washed beech wood (containing mainly cellulose and lignin) as a substrate and investigated three different solid loadings (1.93, 2.21 and 3.86 % (w/w)). Due to stirring limitations in the reactor, higher solid loadings could not be tested. Up to 15.1 g L⁻¹ lactic acid (65.6 % yield) were produced after 134 hours without any detectable amounts of acetic acid as a side product. The highest yield of 78.1 % lactic acid (10.3 g L⁻¹) was reached with an initial solid loading of 2.21 % (w/w) (Fig. 3.2C, Tab. 3.2).

The activity of cellobiohydrolase (CBH), beta-glucosidase (BG) and endoglucanase (EG) in the supernatant of the fermentation slurry during various stages of the fermentation is shown for 1.75 % (w/w) Avicel in figure 3.2B and different pretreated beech wood loadings in figure 3.2D. The enzymatic activity of CBH and EG on Avicel increased over two days after inoculation of *L. pentosus* and reached 289 mIU mL⁻¹ and 9.48 IU mL⁻¹, respectively. In comparison to the CBP on Avicel the enzymatic activities in the supernatant using pretreated beech wood were lower and reached a maximum CBH activity of 127 mIU mL⁻¹ (Fig. 3.2D). Although the initial lactic acid accumulation was similar for all tested beech wood loadings which indicates comparative enzymatic hydrolysis rates in the sugar-limited system the CBH activity was reduced with increasing solid loading. This was presumably caused by a higher non-productive binding of CBH with increasing lignin content in the reactor [127] and might explain the lower yield in comparison to 2.21 % (w/w).

Table 3.2: CBP of different substrates to lactic acid in batch and fed-batch mode by *T. reesei* and different lactic acid bacteria.

Experiment	Microorganisms	Solid [% (w/w)]	Xylose [g L ⁻¹]	$C_{LA,max}$ [g L ⁻¹]	Time ¹ [h]	γ_{P/S^2} [g g ⁻¹]	γ_{LA}^3 [%]	C_{AA}^1 [g L ⁻¹]
Avicel (batch)	<i>T. reesei</i> , <i>L. pentosus</i>	1.75	-	8.9±0.3	109.8	0.46	45.9	-
		3.50	-	23.0±0.2	145.0	0.59	59.1	0.1±0.1
		5.00	-	34.7±0.2	215.4	0.62	62.4	0.1±0.1
Avicel + xylose (batch)	<i>T. reesei</i> , <i>L. pentosus</i>	1.75	9.32	11.3±0.3	116.5	0.39	45.0	0.4±0.3
	<i>T. reesei</i> , <i>L. brevis</i>	1.75	9.32	9.3±0.1	184.8	0.32	60.4	4.4±0.3
Washed steam-pretreated beech wood solids (batch)	<i>T. reesei</i> , <i>L. pentosus</i>	1.93	-	8.6	60.7	0.75	74.6	0.5
		2.21	-	10.3	91.9	0.78	78.1	-
		3.86	-	15.1	133.8	0.66	65.6	-
Avicel (batch) + xylose (fed-batch, 100 h)	<i>T. reesei</i> , <i>L. pentosus</i>	1.75	9.32	14.5±0.7	146.7	0.50	57.9	0.8±0.2
		5.00	26.63	54.6±2.1	398.9	0.66	76.3	4.2±0.9
1-stage pretreated beech wood solids + prehydrolyzate	<i>T. reesei</i> , <i>L. pentosus</i>	3.86	-	15.7±0.2	250.3	0.68	68.1	0.1±0.1
		3.86	5.01 ⁴	19.8±0.7	200.5	0.78	85.2	0.5±0.1

¹ At maximum lactic acid concentration² Yield coefficient expressed as mass of product formed per mass of fermentable carbohydrates at maximum lactic acid concentration. Glucan and xylan concentrations were calculated to corresponding glucose and xylose concentrations using a conversion factor of 1.11 and 1.136, respectively.³ The theoretical yields for *L. pentosus* are based on pentose assimilation through the PK pathway and hexose assimilation through the Embden-Meyerhof-Parnas pathway. The theoretical yields for *L. brevis* are based on the assimilation of both hexoses and pentoses through the PK pathway.⁴ Recalculated from xylooligosaccharides and xylose fed with the prehydrolyzate.

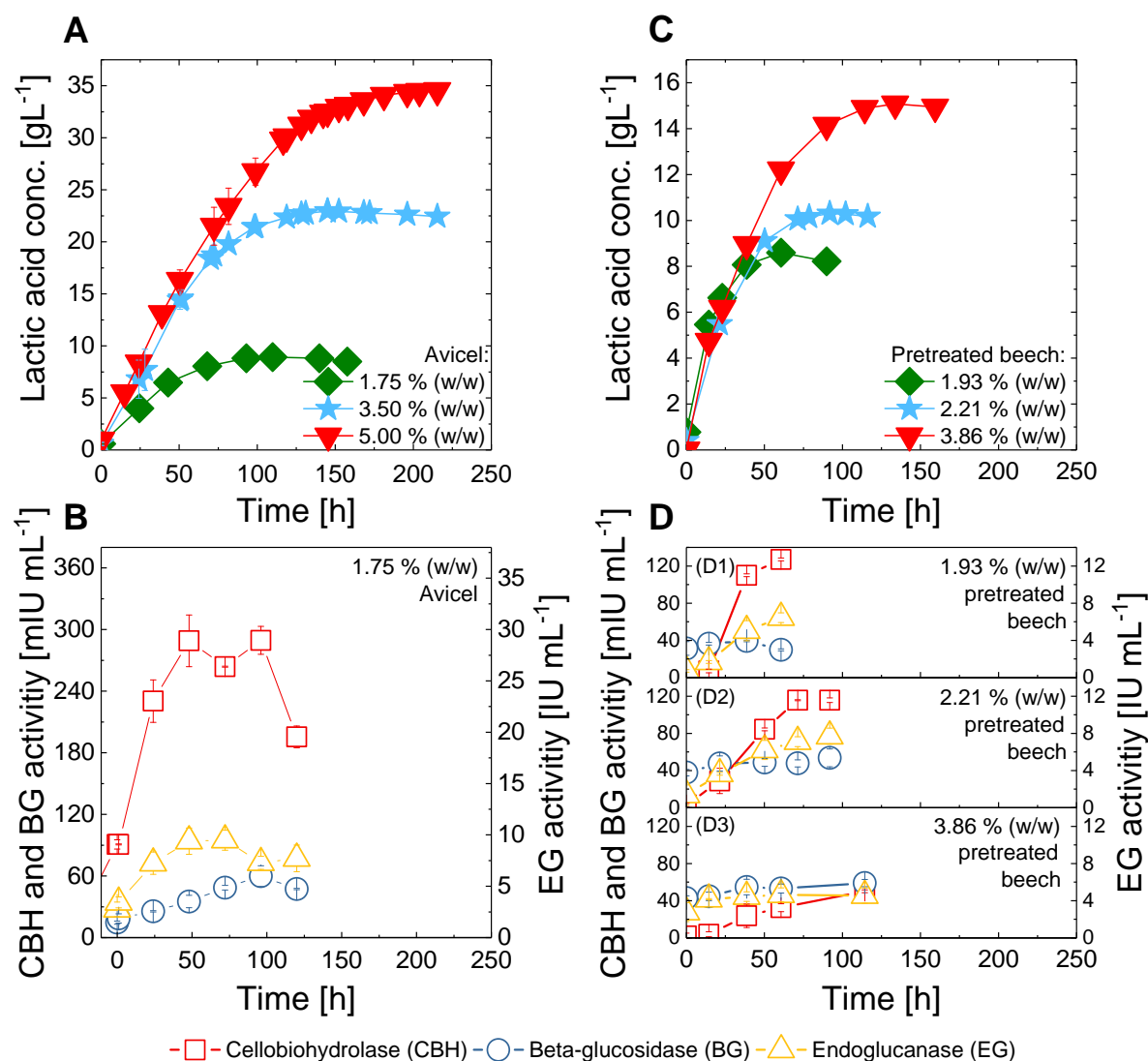


Figure 3.2: **Batch CBP of lignocellulosic biomass to lactic acid using a synthetic microbial consortium of *T. reesei* and a lactic acid bacterium.** Conversion of (A) microcrystalline cellulose (Avicel) and (C) one-stage steam-pretreated washed beech wood to lactic acid using *L. pentosus* as the fermenting strain. Error bars represent the standard deviation from two independent batch experiments. (B,D) Corresponding activities of cellobiohydrolase (CBH), beta-glucosidase (BG) and endoglucanase (EG) in the supernatant of the fermentation slurry during various stages of the fermentation: (B) Avicel (as shown in (A)) or (D) different solid loadings of pretreated beech wood (as shown in (C)). Error bars represent the standard deviation from duplicates.

We also studied the reuse of the immobilized fungal cells in a semi continuous experiment and exchanged every 72 hours one quarter of the fermentation slurry (Fig. B.6). Although

we measured a decrease of CBH and EG activity during the course of the experiment, the immobilization of the fungal biomass in the biofilm prevented its washout. An increase of CBH and EG after the dilution indicates the possible reuse and stability of the fungal biofilm.

3.3.3 Co-fermentation of pentoses and hexoses and *in situ* acetic acid degradation by the synthetic consortium

The co-fermentation of hexoses and pentoses is a prerequisite for the cost-effective conversion process of heterogeneous lignocellulosic feedstocks containing both types of sugars in polymeric form. Generally, several LAB can consume pentoses that are converted by heterofermentation via the Phosphoketolase (PK) pathway to lactic acid, acetic acid and ethanol with a theoretical lactic acid yield of 0.6 g g^{-1} xylose [128]. Furthermore, it is known that *L. pentosus* controls the utilization of carbohydrates by carbon catabolite repression (CCR) [129]. Glucose represses the *xylAB* operon encoding D-xylose isomerase and D-xylulose kinase which are both required for xylose fermentation [130]. To study the co-fermentation abilities of the consortium and the possible presence of CCR, mixtures of Avicel and xylose were used as the carbon source. A co-culture of *T. reesei* and *L. pentosus* - a facultative heterofermentative strain - on 1.75 % (w/w) Avicel and 9.32 g L^{-1} xylose resulted in $11.3 \pm 0.3 \text{ g L}^{-1}$ lactic acid (45.0 % yield) and $0.4 \pm 0.3 \text{ g L}^{-1}$ acetic acid after 117 hours. Xylose was consumed from the beginning of the fermentation, while more acetic acid was accumulating compared to when only Avicel was fermented. This indicated that Avicel and xylose were simultaneously co-degraded without active CCR. Generally, the amounts of acetic acid measured in the co-cultures were very low, up to ten times lower than the values detected in monoseptic cultures of only *L. pentosus* (Tab. 3.2, Fig. B.4) were detected. Furthermore, acetic acid degradation was observed in some experiments (see for example Fig. 3.3A, where only up to 1.0 g L^{-1} acetic acid accumulated temporarily). Thus, we investigated the apparent *in situ* acetic acid degradation of the consortia in more detail. Degradation experiments confirmed the ability of *T. reesei* to co-degrade acetic acid, glucose and xylose (Fig. B.3). However, acetic acid mineralization to presumably carbon dioxide was not associated with growth [131] and above 0.3 g L^{-1} , acetic acid inhibited the metabolic activity of *T. reesei*. In order to test the limits of the *in situ* acetic acid degradation, *L. pentosus* was replaced with *L. brevis* - an obligate heterofermentative strain that utilizes pentoses and hexoses exclusively via the PK pathways - which leads to a higher production of acetic acid. Under these conditions, 9.3 g L^{-1} lactic acid (60.4 % yield) and $4.4 \pm 0.3 \text{ g L}^{-1}$ acetic acid were measured after 185 hours (Fig. 3.3B, Tab. 3.2). The high accumulation of acetic acid indicated that the purification potential of *T. reesei* was exceeded in this case. As the degradation of acetic acid required oxygen, the oxygen transfer rate presumably determined the limits of the *in situ* purification rate. This assumption was confirmed by a mono-culture of *T. reesei* in the

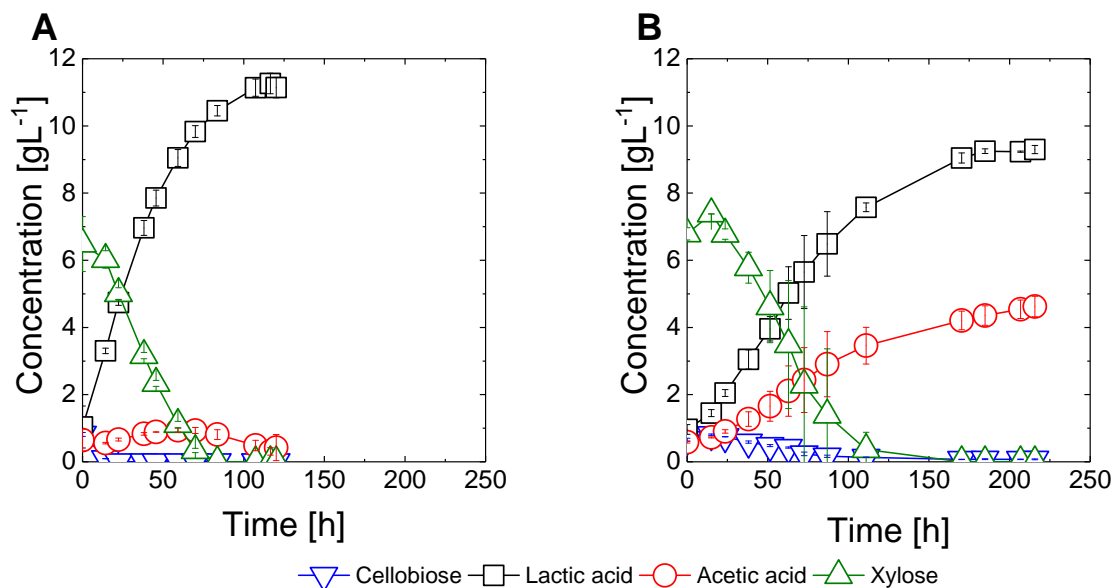


Figure 3.3: **Batch CBP of Avicel and xylose to lactic acid using a synthetic microbial consortium of *T. reesei* and a lactic acid bacterium.** 1.75 % (w/w) Avicel and 9.32 gL⁻¹ xylose were co-fermented by *T. reesei* and (A) *L. pentosus* or (B) *L. brevis*. Error bars represent the standard deviation from two independent batch experiments.

biofilm-membrane reactor with acetic acid as the sole carbon source, which showed a constant acetic acid degradation rate of 0.01 gL⁻¹h⁻¹ (data not shown).

In order to simulate the continuous release of xylose from the enzymatic hydrolysis of soluble xylooligosaccharides, we also performed fed-batch experiments with Avicel and xylose as model substrates. While 1.75 % (w/w) Avicel was added all at once, xylose was fed linearly with a constant feeding rate to the reactor to an accumulated theoretical concentration of 9.32 gL⁻¹. This led to a lactic acid concentration of 14.5±0.7 gL⁻¹ after 146 hours (Fig. 3.4A, Tab. 3.2). The highest xylose concentration of 1.1 gL⁻¹ was measured after 103 hours and dropped below the detection limit after 139 hours. The amount of xylose measured at any sampling point in the fed-batch experiments was below the theoretical amount calculated from the feeding rate. The highest acetic acid concentration of 1.1 gL⁻¹ was measured after 126 hours fermentation time and dropped below the detection limit after 215 hours, due to *in situ* acetic acid degradation by *T. reesei*.

The lactic acid yield in the fed-batch experiments was 28 % higher than in the batch experiment at identical substrate levels (Fig. 3.3A, Tab. 3.2). This could be explained by the exclusive access of *T. reesei* to xylose prior to inoculation of LAB in the batch experiment. Feeding is known to influence the microbial interactions and can increase the stability of the microbial

community [132]. We reduced the interactions between the species by feeding xylose as an additional alternative carbon source. While *L. pentosus* – as non-cellulolytic bacterium – was previously on Avicel as sole carbon source dependent on the secretome of *T. reesei*, the additional xylose feed reduced this level of dependency because *L. pentosus* was able to metabolize xylose directly. Therefore *L. pentosus* was only extrinsically limited by the feed and not exclusively dependent on the secretome of *T. reesei*, which might explain the higher lactic acid yields in fed-batch mode. In order to converge to industrially achievable lactic acid concentrations, the substrate loading was increased to 5.00 % (w/w) Avicel and a feed of accumulated 26.7 gL^{-1} xylose over a period of 200 hours. Under these conditions, a concentration of $54.6 \pm 2.1 \text{ gL}^{-1}$ lactic acid was measured after 398 hours (Fig. 3.4B, Tab. 3.2).

3.3.4 Conversion of whole-slurry pretreated beech wood in fed-batch experiments

Finally, we aimed to directly convert whole-slurry steam-pretreated beech wood (i.e. the unprocessed liquid and the solid phase after pretreatment) to lactic acid. In the pretreatment process, a liquid phase - called prehydrolyzate - is formed by condensation of steam, which contains soluble xylooligosaccharides, acetic acid derived from deacetylation of the hemicellulose and other inhibitory substances such as formic acid, phenolics, furfural and hydroxymethylfurfural [133,134]. The composition of the prehydrolyzate depends on the pretreatment conditions. When beech wood was steam-pretreated at $230 \text{ }^{\circ}\text{C}$ for 15 min (the conditions that allowed maximal glucose release by enzymatic hydrolysis with commercial cellulase cocktails, but led to complete degradation of xylan (data not shown)), the resulting slurry could not directly be converted to lactic acid by the consortium, due to the high concentration inhibitors such as acetic acid (Fig. B.5), which inhibited *T. reesei*. Thus, in order to enable growth on the inhibitory substrates and to benefit from the *in situ* detoxification potential of *T. reesei* at moderate acetic acid concentrations, we chose to feed the prehydrolyzate to the membrane biofilm reactor, which initially only contained the pretreated beech wood solids. Since acetic acid degradation occurs at a constant rate due to being limited by the oxygen transfer rate, we chose a constant feeding profile. Under these conditions, whole-slurry pretreated beech wood could successfully be converted to lactic acid resulting in a concentration of $15.7 \pm 0.2 \text{ gL}^{-1}$ after 250 hours (Fig. 3.4C, Tab. 3.2). This amount corresponded to a similar lactic acid yield compared to the experiment where only pretreated solids were used.

In order to investigate the co-fermentation abilities of the consortium in the presence of inhibitors, we used two-stage pretreated beech wood as the substrate. Here, beech wood was first pretreated under moderate conditions ($180 \text{ }^{\circ}\text{C}$, 25 min) that were optimized for maximal hemicellulose recovery in the liquid phase. After removal of the liquid phase, a second pretreatment of the remaining solids was performed under harsher conditions that allowed

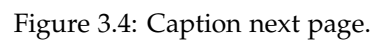


Figure 3.4: **Fed-batch CBP of heterogeneous substrates containing hexose and pentose to lactic acid using a consortium of *T. reesei* and *L. pentosus*.** (A) Co-fermentation of 1.75 % (w/w) Avicel added at $t=0$ and xylose fed over a period of 100 hours to a total concentration of 9.32 gL^{-1} . (B) Co-fermentation of 5.0 % (w/w) Avicel added at $t=0$ and xylose fed over a period of 200 hours to a total concentration of 26.63 gL^{-1} . (C) Conversion of 3.86 % (w/w) one-stage steam-pretreated beech wood solids with a feed of the prehydrolyzate over a period of 100 hours. The dashed red line shows the amount of acetic acid added through the prehydrolyzate feed. (D) Co-fermentation of 3.86 % (w/w) two-stage steam-pretreated beech wood solids added at $t=0$ and xylooligomer containing first stage prehydrolyzate fed over a period of 100 hours. The dashed green lines show the amount of xylose (A,B) or xylose recalculated from xylooligomers (D), respectively, added through the substrate feed. Error bars represent standard deviation from two independent fed-batch experiments. (E) Activity of cellobiohydrolase (CBH), beta-glucosidase (BG), endoglucanase (EG) and xylanase in the supernatant of the fermentation slurry during various stages of the fermentation shown in figure 3.4D. Error bars represent the standard deviation from duplicates.

maximal glucose release by subsequent enzymatic hydrolysis. Fed-batch experiments on two-stage pretreated beech wood were performed with a linear feed of the 180°C prehydrolyzate which contained, among others, 25.8 gL^{-1} of soluble xylooligosaccharides. The feeding of soluble xylooligosaccharides, instead of monomeric saccharides such as xylose, changed the metabolic dependencies in the consortium.

Although putative orthologs of the xylosidase *xynB2* of *L. brevis* were found in the genome of *L. pentosus*, which has a high catalytic efficiency for xylobiose, LAB depend on the secretome of *T. reesei* for both longer xylooligomers and cellulose conversion [135]. The feeding of the prehydrolyzate seems to be beneficial for fungal enzyme production as it resulted in an increase of the CBH and EG activities by a factor of two (Fig. 3.4E) compared to the experiment where only pretreated solids were used (Fig. 3.2D). Despite the heterogeneous and metabolically challenging mixture only $0.5 \pm 0.1 \text{ gL}^{-1}$ acetic acid accumulated and $19.8 \pm 0.7 \text{ gL}^{-1}$ lactic acid was produced after 200 hours (Fig. 3.2D, Tab. 3.2). This corresponds to a productivity of $0.1 \text{ gL}^{-1}\text{h}^{-1}$ (Tab. 3.1) and a yield of 85.2 %, which is the highest yield achieved with the synthetic microbial consortium. Future work will include the optimization of the *in situ* enzyme production in order to increase lactic acid productivity to a level comparable to state of the art SSF approaches (Tab. 3.1).

Taken together, the fed batch experiments showed the potential of the synthetic consortium to utilize unprocessed inhibitory process streams that are detoxified *in situ* without any detectable carbon loss. In contrast, significant carbon loss has been reported, when separate biological detoxification was performed [136].

3.3.5 Interactions between the members of the consortium

The results presented show that the synthetic consortium of *T. reesei* RUT-C30 and *L. pentosus* (DSM-20314) is highly functional. The stable coexistence of the two strains over 250 hours is mainly based on competitive cheater-cooperator interactions. Secretion of cellulases by *T. reesei* is a cooperative feature because it is metabolically costly and the sugars released by enzymatic hydrolysis are available as public goods for both strains. *L. pentosus* consumes the released soluble saccharides as a cheater without contributing energy to enzyme production. However, *T. reesei* also benefits from the presence of *L. pentosus*. *T. reesei* is deficient in beta-glucosidase production [57], which leads to an accumulation of cellobiose - a potent inhibitor of endoglucanase and of cellobiohydrolases I and II [48]. For example, in a monoseptic cultivation of *T. reesei* growing on microcrystalline cellulose, a cellobiose concentration above 0.7 gL^{-1} was measured after 48 hours throughout the experiment (Fig. B.2) which is in the inhibitory concentration range of several cellulases, including CBHI [48,137]. Upon inoculation with *L. pentosus*, the cellobiose concentration dropped below the detection limit (Fig. B.2), because the LAB were able to metabolize the disaccharide [138]. Thus, *L. pentosus* reduces the negative product inhibition on the cellulolytic system and facilitates the faster release of glucose. Furthermore, *L. pentosus* produces acetic acid as a by-product, which can be consumed by *T. reesei* by metabolic cross feeding (commensalism). These beneficial effects of LAB for the fungus lead to microbial mutualism. Simultaneously, an inhibitory effect of acetic acid on the metabolic activity of *T. reesei* was observed (amensalism). It has been suggested that such unilateral interactions greatly enhance community stability [139].

3.4 Conclusions

We successfully established a consolidated bioprocess for the direct production of lactic acid from lignocellulosic biomass using a synthetic consortium of *T. reesei* and a lactic acid bacterium growing in a membrane-aerated biofilm reactor. In particular, we demonstrated the ability of the consortium to co-ferment hexoses and pentoses from non-detoxified whole-slurry pretreated beech wood without carbon catabolite repression. Furthermore, superior product purities were achieved by *in situ* acetic acid degradation by *T. reesei*. We applied metabolic compartmentalization and spatial structuring to stabilize the cooperator-cheater community. Our results establish the potential of engineering microbial consortia for the CBP of lignocellulosic biomass to high value biochemicals.

CHAPTER 4

Butyric acid and propionic acid

4.1 Abstract

We engineered artificial ecosystems to metabolically funnel heterogeneous lignocellulosic carbohydrates to lactate as central intermediate in synthetic food chains producing carboxylic acids. This lactate platform is based on defined microbial cooperator-cheater consortia, with up to four microorganisms, stabilized and controlled by enforced niche differentiation. A spatial niche enabled *in situ* cellulolytic enzyme production using the aerobic fungus *Trichoderma reesei* next to an obligate anaerobe. Lactic acid bacteria (LAB) compensated for the missing metabolic capabilities of anaerobic secondary fermenters. Intra-consortium competition directed the metabolic flux to LAB which increased product selectivity. The feasibility and modularity of the lactate platform was exemplified by integrating *Clostridium tyrobutyricum* or *Veillonella criceti* to produce 196.5 kg butyric acid or 113.6 kg propionic and 133.3 kg acetic acid, respectively per ton beech wood. With the lactate platform, the theoretical yield of butyric acid increased to 131 % of its equivalent theoretical yield for direct carbohydrate conversion.

This chapter is based on a manuscript under review in Nature Biotechnology: R. L. Shahab, S. Brethauer, M. Davey, J. S. Luterbacher, A. Smith, S. Vignolini, M. H. Studer *The lactate platform – a consortium based consolidated bioprocessing strategy for the yield-optimized production of volatile fatty acids from lignocellulose*.

4.2 Introduction

Lignocellulosic biomass is the most abundant source of fixed, renewable carbon and is a promising alternative to fossil petroleum. Biorefining of this heterogeneous, recalcitrant

feedstock aims to produce a range of chemicals, materials, fuels and power to maximize the value derived from the feedstock and minimize waste streams. Volatile fatty acids (VFAs) such as propionic and butyric acid are important target products which are currently produced from fossil resources and have been suggested as potential bio-derived platform molecules [140]. However, the combination of the heterogeneous carbohydrate composition of lignocellulose and the limited metabolic flexibility of many VFA producers leads to low product yields and undesired by-product formation (Fig. 4.1A). In order to provide a more homogeneous carbon source for the VFA producers, the heterogeneous mixture of carbohydrates in the biomass can be metabolically funneled to a central platform molecule in a primary fermentation followed by a secondary conversion to the desired product (Fig. 4.1B).

Ideally, the primary and secondary fermentation, as well as the depolymerization of the carbohydrates by cellulolytic enzymes, can be performed in one processing step which is termed consolidated bioprocessing (CBP). The engineering of such complex reaction cascades into one microbial host can create a substantial metabolic burden that limits the overall productivity of the system [141]. Consequently, low carbon fluxes remain a major challenge [46,142] for CBP approaches based on genetically engineered microorganisms, which are often characterized by metabolic imbalances [143–145]. This limitation could be overcome by metabolic division of labor [141] which is also observed in natural consortia, where complex reaction cascades are common and biochemically difficult tasks are catalyzed by multiple species according to the principle of metabolic compartmentalization [86]. Each member of the community occupies its ecological niche and is specialized in a subtask or metabolizes different beneficial exchange molecules such as vitamins, amino acids, etc. However, the high complexity of natural consortia makes the targeted engineering of the desired trait difficult and limits their industrial application for the production of biochemicals. Alternatively, less complex and more defined synthetic consortia can be engineered [146] and have been applied for CBP of lignocellulose to produce isobutanol [84], ethanol [82,83], or acetone, butanol and ethanol [85]. A major challenge of such bottom-up consortia is their stability and control [71,86,132,147], which fundamentally require overlapping tolerance ranges of several abiotic process parameters such as pH, temperature and oxygen concentration. Thus, the majority of co-culture studies reported to date were carried out using only two species [146] with similar abiotic requirements. However, few examples of artificial consortia with more than two populations have been reported. Artificial tricultures were used to convert glucose to electrical power [148] or to demonstrate the importance of defined spatial structures for the stable co-existence of soil bacteria [100]. Larger artificial consortia containing more than three species were either mimicking existing natural consortia useful for e.g. bioremediation [149–154] or medical purposes [155].

If cooperator-cheater dependencies are present in such communities, e.g. if one strain secretes cellulolytic enzymes to provide carbohydrates as a public good [118], a sufficient niche differen-

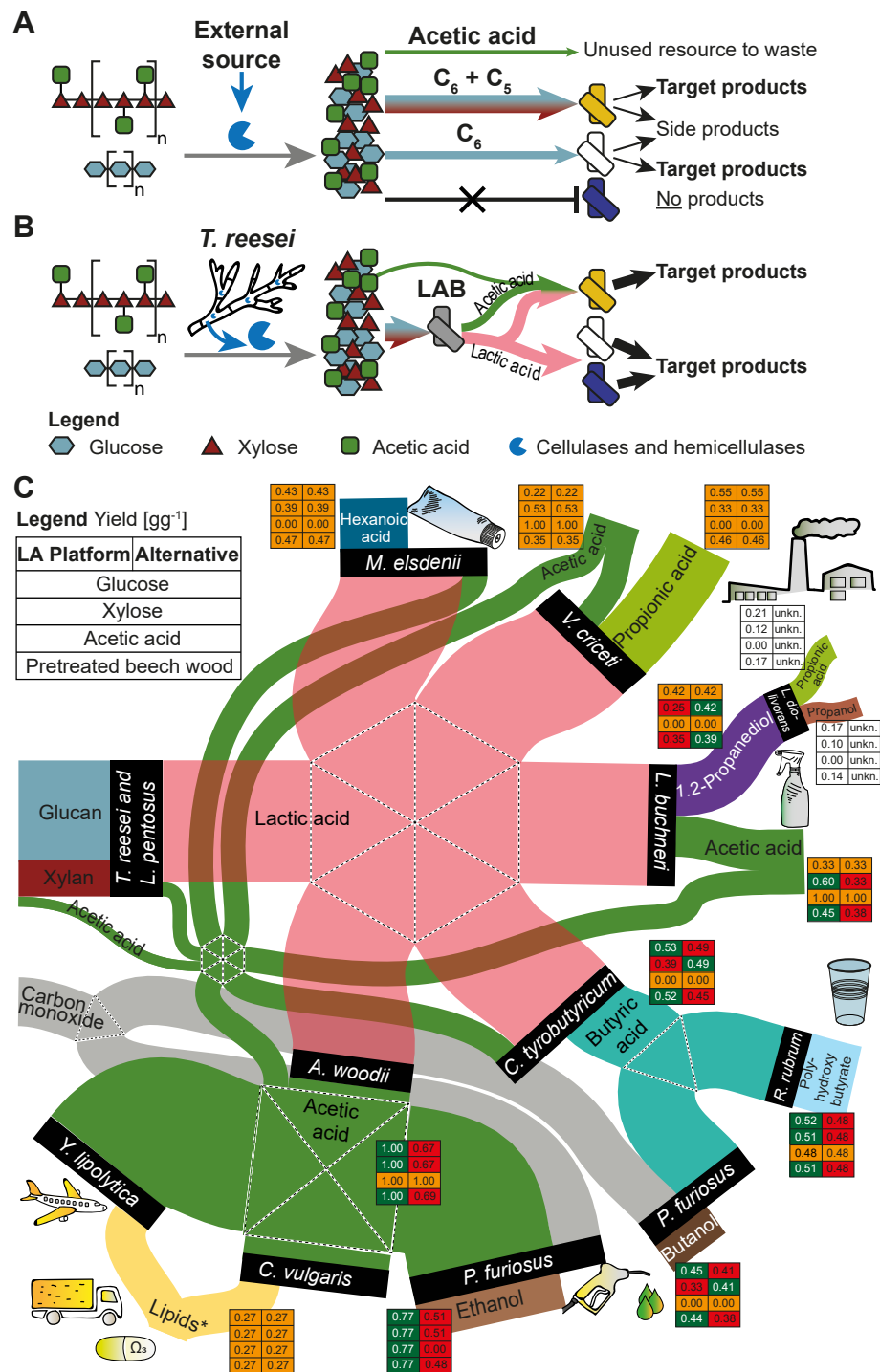


Figure 4.1: Caption next page.

Figure 4.1: **Comparison of the sugar platform and the lactate platform.** (A) Schematic illustration of the common sugar platform. The polymeric compounds glucan and xylan are hydrolyzed by cellulases and hemicellulases added from an external source to yield a heterogeneous mixture of glucose and xylose together with acetic acid which is released from the xylopuranose backbone of xylan. Many natural product-forming microorganisms lack the metabolic flexibility to efficiently and selectively convert this heterogeneous carbohydrate mixture to the target products, and usually acetic acid is not utilized as carbon source. Increased by-product formation and reduced product yield and concentration are the major challenges. (B) Schematic illustration of the lactate platform. *T. reesei* is introduced as *in situ* producer of cellulolytic enzymes. The heterogeneous mixture of carbohydrates is metabolically funneled to lactic acid, which is further converted to the target products. This reduces the required metabolic flexibility of the target product-forming microorganisms. Furthermore, some product forming strains are able to co-consume lactic and acetic acid which results in lower by-product formation. (C) CBP of pretreated beech wood via the lactate platform to selected target products. The thickness of the lines corresponds to calculated theoretical mass fluxes based on pathways shown in table C.6 and C.7. Side products such as water, carbon dioxide and hydrogen are not illustrated. The tables next to the products display the theoretical yields for bioconversion of glucose, xylose, acetic acid or 2-stage pretreated beech wood (glucose+xylose+acetic acid) via the lactate platform compared to alternative direct fermentations (Tab. C.5, C.6 and C.7).

tiation has to be guaranteed to create a stable community. This differentiation must exist despite mutual resource utilization and a sufficiently high net benefit for the cooperator [98]. The latter is supported in biofilms by low diffusion and decay rates of the cooperative enzymes that are secreted, flat colony structures [118, 156] and spatial heterogeneities in the form of nutrient microgradients [118, 157]. Oxygen gradients stabilize communities by promoting community diversification to the detriment of pure growth competition [10, 158, 159]. Additionally, spatial structuring in biofilms stabilizes natural cooperator-cheater communities [157] and positively influences the local productivity and fitness of cooperators.

In this study, we introduce a CBP strategy for the direct production of different VFAs from lignocellulose. Our approach enables an enhanced metabolic flux to the target product by distributing the pathway among different microorganisms of an adaptable artificial ecosystem. By funneling the heterogeneous sugar mixture derived from lignocellulosic biomass to lactic acid as the central intermediate, which can be further converted to the desired product by several VFA producers, their missing metabolic flexibility to utilize different carbohydrates can be compensated (Fig. 4.1B). Furthermore, many VFA producing strains have the ability or even depend on the co-consumption of lactic and acetic acid thereby making the latter compound, which is a generally unused fraction of lignocellulosic biomass, available for product formation. As the acid producing strains are non-cellulolytic, the lactate platform consists (1) of the aerobic fungus *T. reesei* for the cooperative secretion of cellulolytic enzymes, which provide soluble sugars, and (2) of facultative anaerobic lactic acid bacteria (LAB) that are able to convert

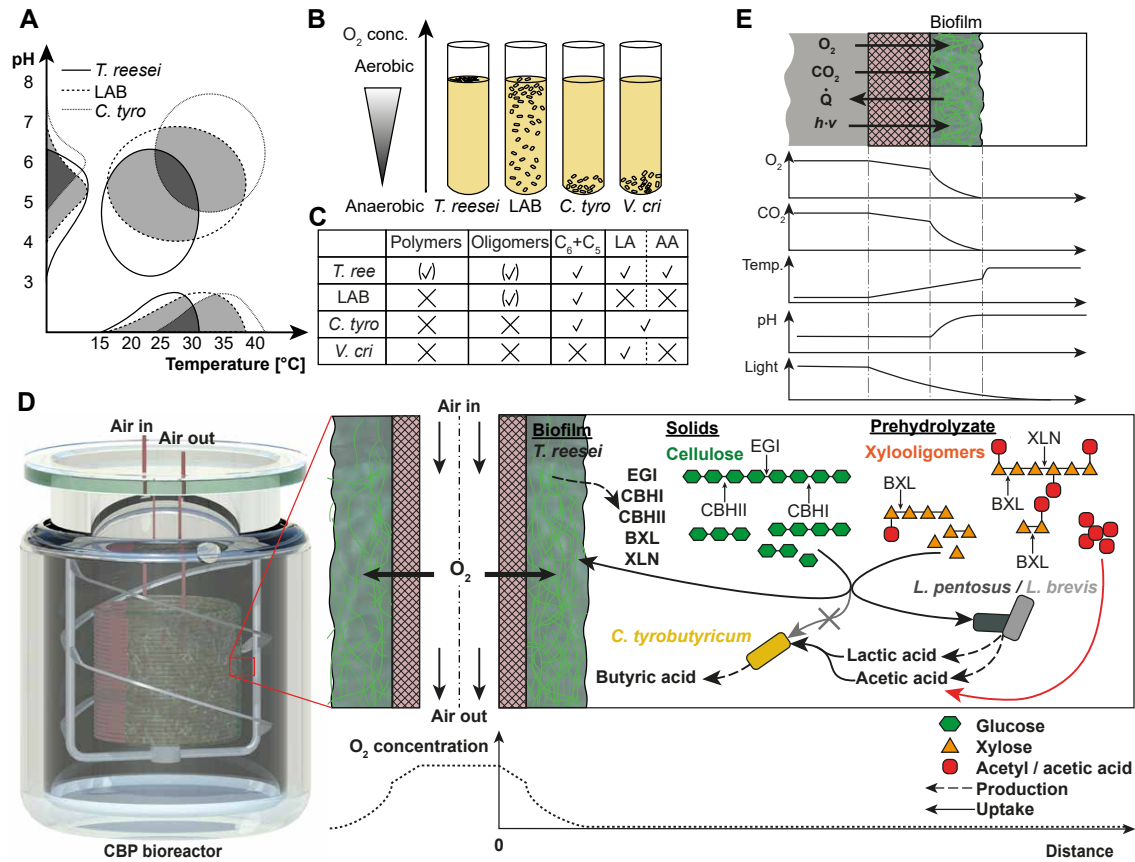


Figure 4.2: CBP of lignocellulosic biomass to butyric and propionic acid by a synthetic microbial consortium. (A) Approximate tolerance ranges for external pH and temperature of *T. reesei*, LAB and *C. tyrobutyricum*. The dark grey area shows the overlap of the tolerance ranges. (B) Requirements of *T. reesei*, LAB, *C. tyrobutyricum* and *V. criceti* for the dissolved oxygen concentration. (C) Capability of the involved strains to metabolize polymers (cellulose and hemicellulose), oligomers (gluco- and xylooligosaccharides), C5/C6 sugars, lactate (LA) and acetate (AA): extracellular degradation (check in brackets), intracellular utilization (check) and no utilization (cross). (D) Schematic representation of the membrane-aerated reactor for CBP of lignocellulosic biomass to butyric acid. An oxygen permeable tubular polydimethylsiloxane membrane is installed in the stirred tank reactor and continuously flushed with air. *T. reesei* forms an aerobic biofilm on top of the membrane and secretes cellulases and hemicellulases (EGI: endoglucanase I, CBHI: cellobiohydrolase I, CBHII: cellobiohydrolase II, BXL: beta-xylosidase, XLN: beta-endoxylanase). The enzymatic hydrolysis takes place in the fermentation slurry under anaerobic conditions created by the metabolic activity of the microbial consortium. *L. pentosus* (and *L. brevis*) metabolically funnel the released saccharides to lactic and acetic acid. Lactic and acetic acid (partly from deacetylation of the xylopuranose backbone) are selectively converted by *C. tyrobutyricum* to butyric acid. The dissolved oxygen concentration is depicted below the diagram. (E) Reactor cross-section with different gradients of abiotic factors as measures to stabilize communities composed of microorganisms that have non-overlapping tolerance ranges for abiotic parameters.

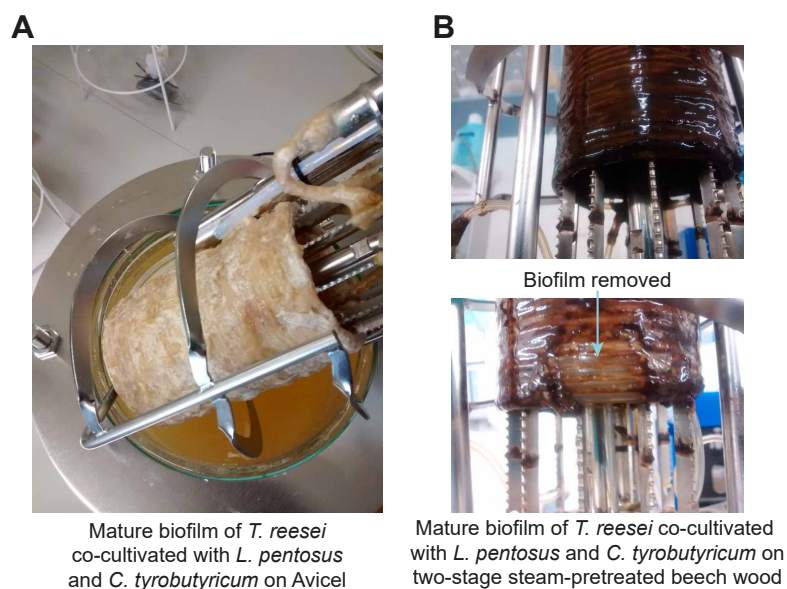


Figure 4.3: **Photographs of mature fungal biofilms formed on an aerated membrane in a stirred tank bioreactor.** The community of *T. reesei*, *L. pentosus* and *C. tyrobutyricum* was grown on **(A)** Avicel or **(B)** steam-pretreated beech wood.

all types of the solubilized sugars to lactic acid. In contrast to other abiotic factors such as temperature or pH (Fig. 4.2A), the oxygen requirements of *T. reesei* and *C. tyrobutyricum* do not overlap at all (Fig. 4.2B). Oxygen is essential for the aerobic fungus, but it is highly toxic for the VFA-producing anaerobic bacteria. By employing a membrane-aerated biofilm reactor in combination with the facultative anaerobic LAB, an oxygen gradient is generated that allows fulfilling the redox potential requirements of all strains (Fig. 4.2D). Specifically, the feasibility and the modularity of the lactate platform was exemplified by using either *Clostridium tyrobutyricum* to produce butyric acid, or *Veillonella criceti* for the production of propionic and acetic acid.

4.3 Results

4.3.1 Direct production of butyric acid from cellulose and xylose via the lactate platform using a synthetic consortium

In order to prove the feasibility of the lactate platform concept, we first aimed to produce butyric acid from a mixture of cellulose (17.5 gL^{-1}) and xylose (9.32 gL^{-1}) as a model substrate for lignocellulose. The synthetic consortium consisted of *T. reesei* for cellulolytic enzyme secretion, *L. pentosus* for lactic acid production and *C. tyrobutyricum* for the production of the

target product butyric acid. *L. pentosus* converts glucose to lactic acid via the homofermentative pathway while xylose is metabolized heterofermentatively to lactic and acetic acid (Fig. C.1). We followed a three-step inoculation scheme: First, the reactor was inoculated with *T. reesei* to allow the formation of a fungal biofilm on top of the membrane (Fig. 4.3). After 48 hours, *L. pentosus* was inoculated followed by the subsequent inoculation of *C. tyrobutyricum* after waiting another 48 hours. While all cellulose was added to the reactor at the time of the fungal inoculation, xylose was fed to the reactor over a time span of 75 hours after inoculation with *L. pentosus*. The metabolic activity of *T. reesei* reduced the dissolved oxygen content below the detection limit within eight to twelve hours after fungal inoculation and lowered the redox potential to values between +20 and -20 mV (Fig. 4.4). The inoculation of *L. pentosus* (beginning of phase I in Fig. 4.5A) led to an accumulation of lactic acid with a simultaneous drop of the redox potential to less than -300 mV which is suitable for the cultivation of obligate anaerobes. After inoculation of *C. tyrobutyricum* (beginning of phase II in Fig. 4.5A), the redox potential decreased further to values below -450 mV, probably due to hydrogen by-product formation by *C. tyrobutyricum*. Butyric acid production began after 100 hours and was accompanied by a decrease of lactic and acetic acid. A maximum concentration of 4.1 gL^{-1} (0.14 g butyric acid per g total fermentable sugars, 93.1 % selectivity) was reached at the end of phase II

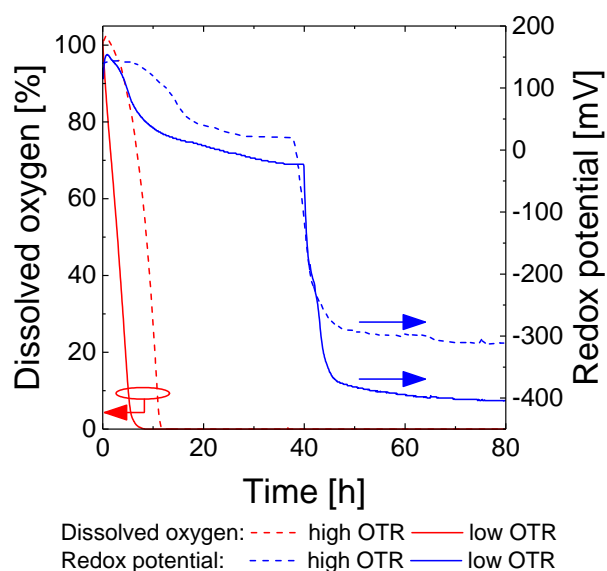


Figure 4.4: **Redox potential and dissolved oxygen concentration during the two-stage inoculation of *T. reesei* and *L. pentosus* in the membrane-aerated bioreactor.** *T. reesei* was inoculated at time zero. The dissolved oxygen concentration dropped below the detection limit after eight hours in the low oxygen transfer rate (OTR) approach (0.34 h^{-1}) and after 12 hours in the high OTR approach (3.24 h^{-1}). Due to the metabolic activity of *T. reesei*, the redox potential was lowered to approximately +40 mV (high OTR) and -20 mV (low OTR). After approximately 40 hours, *L. pentosus* was inoculated and the redox potential dropped below -300 mV (high OTR) and -400 mV (low OTR) approach.

(Tab. C.1). At the beginning of phase III, acetic acid was depleted and lactic acid utilization by *C. tyrobutyricum* stopped because lactic acid cannot serve as a sole carbon source but must be co-consumed with either glucose or acetic acid (Fig. 4.6A-E) [160]. Because of the reduced metabolic activities of the consortium members due to substrate depletion, the redox potential in phase III increased as oxygen was still fed to the reactor via the membrane. The successful production of butyric acid proved the validity of the lactate platform where a cross-kingdom consortium of aerobic and anaerobic microorganisms was employed.

4.3.2 Strategies to improve butyric acid production

In order to allow the complete conversion of lactic acid to butyric acid, the amount of acetic acid had to be increased. We investigated four strategies to improve the lactic to acetic acid ratio: (i) adding acetic acid, (ii) converting a fraction of lactic acid to acetic acid with a homoacetogenic strain, (iii) expanding the microbial consortium with an obligate heterofermentative lactic acid bacterium to enhance the metabolic flux from carbohydrates to acetic acid via the phosphoketolase (PK) pathway and (iv) reducing the oxygen transfer rate (*OTR*) to decrease the acetic acid consumption of *T. reesei*. These strategies are discussed in detail below.

Supplementation of acetic acid

In contrast to the model substrate (cellulose and xylose), lignocellulosic biomass contains acetic acid which is bound to the xylopuranose backbone and is solubilized during pretreatment [26,136]. Prior to using real biomass hydrolysates as an acetic acid source, we tested the external supplementation of pure acetate. In comparison to the base case (Fig. 4.5A), the additional feed of 2 gL⁻¹ acetic acid resulted in an increased acetate and xylose concentration at the end of phase I (Fig. 4.5B) and enabled the complete utilization of the lactic acid to produce a concentration of 10.7 gL⁻¹ butyric acid (0.37 gg⁻¹, 77.6 % selectivity, Tab. C.1).

Integration of the homoacetogen *Acetobacterium woodii* for carbon optimized acetate production

In order to avoid the addition of externally produced acetic acid, we used the homoacetogen *Acetobacterium woodii* to convert part of the lactate to acetate. To this end, we first produced a lactate broth using a co-culture of *T. reesei* and *L. pentosus*, then we converted a fraction of the lactate to acetate using *A. woodii* and finally we blended the two streams to the target lactic to acetic acid ratio to produce butyrate (Fig. 4.7B). With this subsequent fermentation strategy, 12.2 gL⁻¹ butyric acid (0.41 gg⁻¹, 97.6 % selectivity) was produced (Fig. C.2). The next step

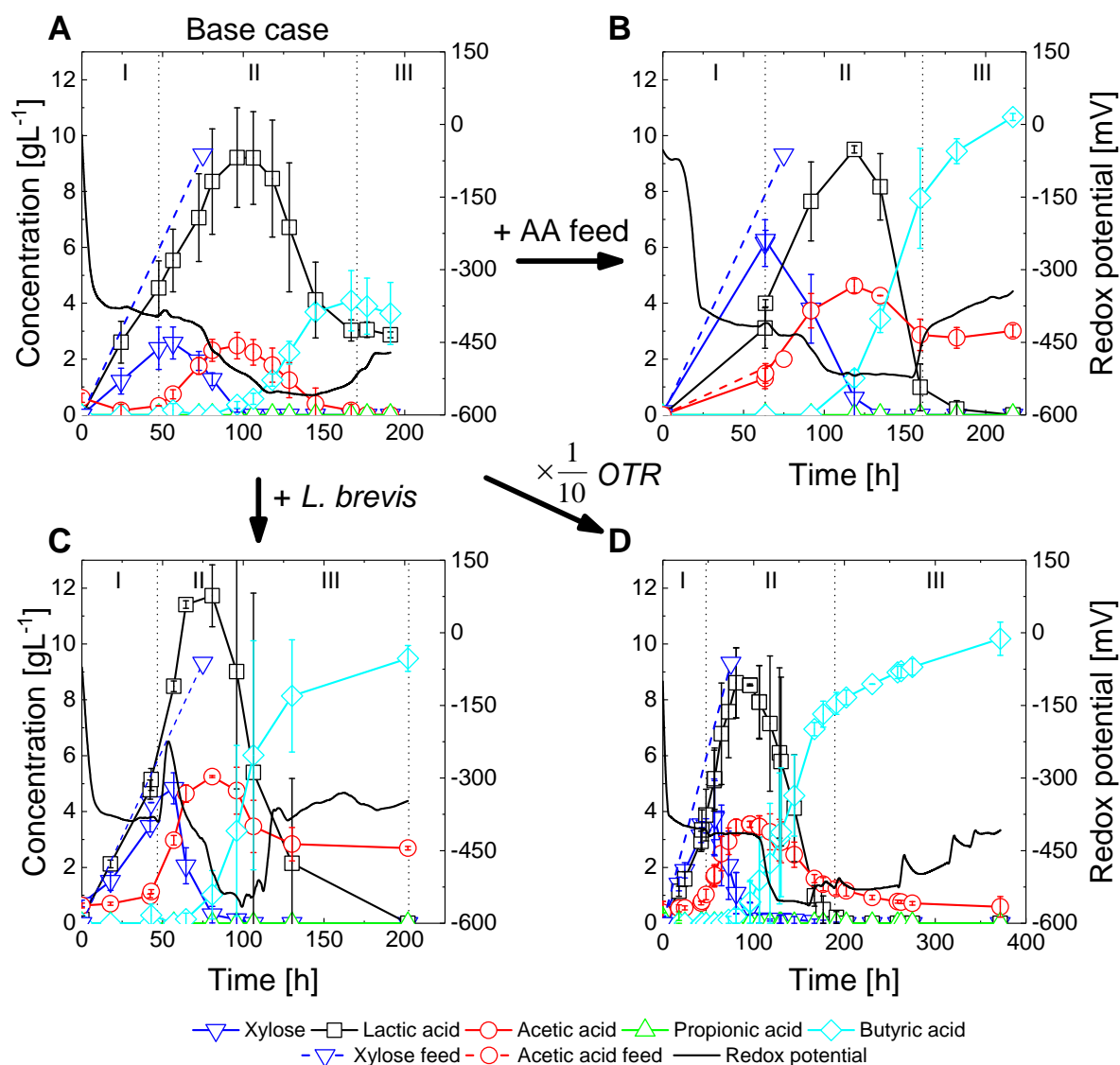


Figure 4.5: **CBP of cellulose to butyric acid using a cross-kingdom microbial consortium.** A three-step inoculation scheme was followed: For the first two days, only *T. reesei* grew in the reactors. Then, *L. pentosus* and if mentioned *L. brevis* were inoculated at the beginning of phase I, followed by the addition of *C. tyrobutyricum* at the beginning of phase II. **(A)** In the base case, 17.5 gL^{-1} Avicel and 9.32 gL^{-1} xylose (fed over a time period of 75 hours, dashed blue line) were converted to butyric acid at a high OTR of 3.24 h^{-1} . Differences from the base case: **(B)** Addition of acetic acid feed to 2.00 gL^{-1} over a time period of 75 hours (dashed red), **(C)** addition of *L. brevis* to the consortium, **(D)** reduction of OTR to 0.34 h^{-1} (mono-lumen tubing $1.58 \text{ mm} \times 3.18 \text{ mm} \times 0.80 \text{ mm}$). Error bars represent the standard deviation from two independent experiments.

would be to integrate *A. woodii* into the CBP consortium (Fig. 4.7A). However, *A. woodii* requires a carbonated medium realized by e.g. a carbon dioxide overpressure. As the current reactor setup does not withstand overpressure, these experiments remain to be accomplished.

Enhanced acetic acid production by integration of the obligate heterofermentative strain *Lactobacillus brevis*

As an alternative to the addition or external production of acetic acid, we aimed to enhance the metabolic flux from carbohydrates to acetic acid by extending the microbial consortium with the obligate heterofermentative strain *Lactobacillus brevis* which produces lactic and acetic acid from both hexoses and pentoses (Fig. C.1). In comparison with the base case consortium containing only *L. pentosus* as the lactic acid producer (Fig. 4.5A), the extended microbial consortium produced a higher amount of acetic acid in phase I and II (Fig. 4.5C). This enabled the complete re-utilization of lactic acid leading to 9.5 gL⁻¹ butyric acid being accumulated (0.33 gg⁻¹, 77.9 % selectivity, Tab. C.1). However, in comparison to the base case the selectivity for butyric acid was smaller, as too much acetic acid was produced.

Reduced oxygen transfer rate to decrease acetic acid consumption by *T. reesei*

As shown in chapter 3 *T. reesei* is able to aerobically degrade acetic acid. While this is helpful to detoxify pretreatment hydrolysates, it is a disadvantage if acetic acid is the limiting co-substrate. As the degradation rate is limited by the amount of oxygen entering the reactor, we decreased the oxygen transfer rate (*OTR*) by a factor of about ten using a siloxane membrane with a thicker wall. With this measure, a higher concentration of acetic acid accumulated in phase II compared to the base case (Fig. 4.5A and D) and lactic acid could be completely converted to 10.2 gL⁻¹ butyric acid after 372 hours (0.35 gg⁻¹, 96.7 % selectivity, Tab. C.1).

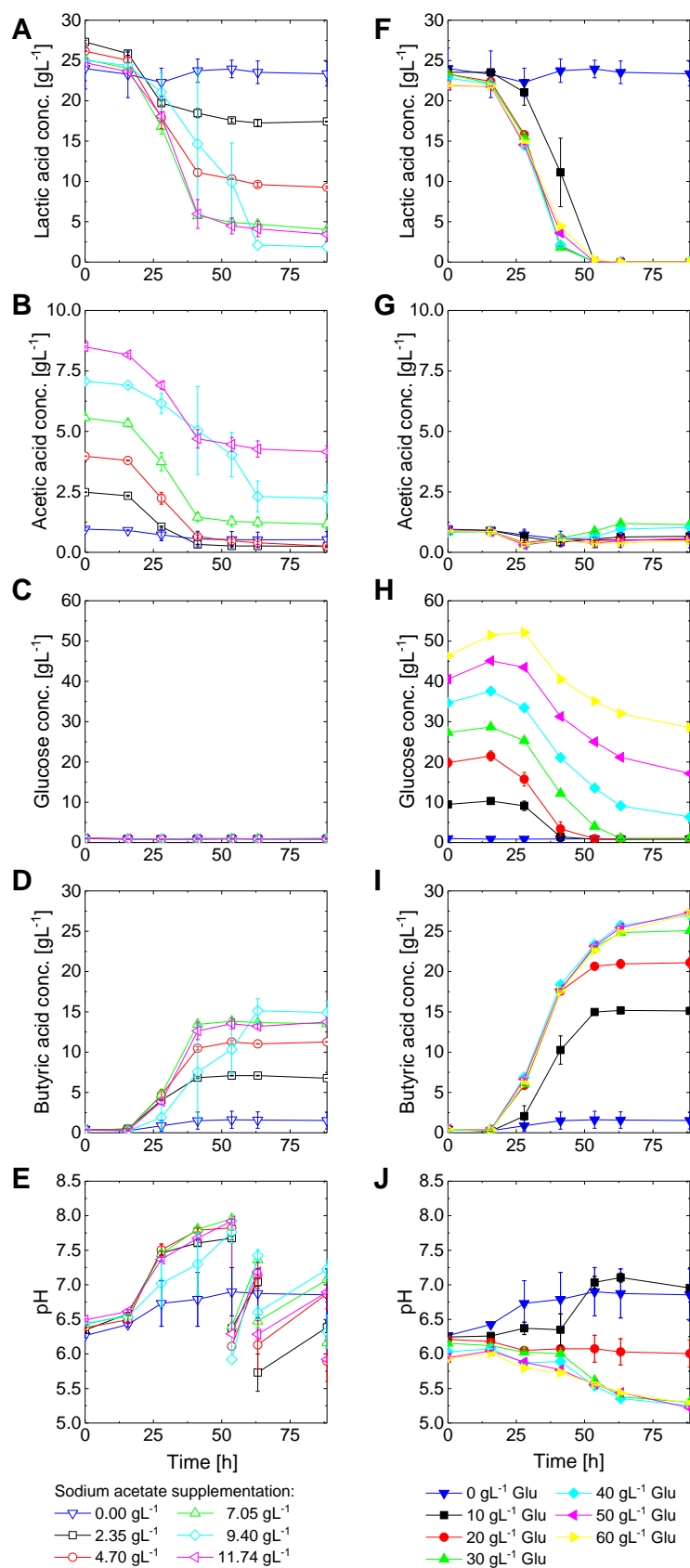


Figure 4.6: Caption next page.

Figure 4.6: Fermentations of lactate broth with supplementation of sodium acetate or glucose using *C. tyrobutyricum*. (A-E) The lactate broth was obtained using the consolidated bioprocess (CBP) with 35 gL^{-1} microcrystalline cellulose and 18.64 gL^{-1} xylose as substrates. *C. tyrobutyricum* is unable to use lactic acid as its sole carbon source and is therefore unable to grow in the lactate broth without supplementation. Since *C. tyrobutyricum* co-utilizes lactic acid and acetic acid, the lactate broth was supplemented with different concentrations of sodium acetate (i) to test if *C. tyrobutyricum* required additional nutritional supplementation and (ii) to determine the required lactic to acetic acid ratio to completely utilize both carbon sources **(A-E)**. The addition of only sodium acetate already enabled its co-utilization with lactate and the production of butyrate **(A-E)**, so no further complex medium supplementation was tested. *C. tyrobutyricum* stopped consuming lactic acid when the acetic acid was exhausted. In order to determine the required lactic to acetic acid ratio, the lactic acid consumed by subtracting the final lactic acid concentration from the initial one was calculated, and divided by the concentration of acetic acid obtained by subtracting the final acetic acid concentration from the initial one. A lactic to acetic acid ratio of $4.50 \pm 0.07 \text{ gg}^{-1}$ or $3.01 \pm 0.05 \text{ molmol}^{-1}$ was determined, averaged from experiments shown in **(A-E)**, which is similar to literature data [161]. Due to the re-utilization of lactic and acetic acid and the formation of butyric acid by *C. tyrobutyricum*, the molar concentration of acids was halved. The pH increased and the addition of hydrochloric acid at 53.7 and 63.2 hours was necessary to lower it again. **(F-J)** In order to avoid the external addition of sodium acetate, the ability of *C. tyrobutyricum* to co-utilize lactate and glucose was studied. By adding glucose in increments of 10 gL^{-1} , up to a maximum of 60 gL^{-1} **(F-J)**, we showed that 10 gL^{-1} were required for complete utilization of the lactate without accumulation of acetic acid ($0.42 \text{ g glucose/g consumed lactic acid}$). The utilization of lactic acid suggests the ability of *C. tyrobutyricum* to convert glucose to acetic acid with its subsequent co-consumption with lactic acid to butyric acid. Since the most energy efficient electron bifurcation pathway does not result in sufficiently high amounts of acetic acid, we suggest that a self-regulated metabolic shift towards a less energy efficient pathway for production of acetic acid is occurring (Fig. C.1). While the pH increased slightly with 10 gL^{-1} glucose, it remained constant at 20 gL^{-1} , which indicates a dynamic equilibrium of the molarity of the acids. Higher levels of glucose supplementation resulted in a drop of the pH after the concentration of lactic acid fell below the detection limit. The remaining glucose was mainly converted to butyric acid. The pH was not adjusted externally during the experiments shown in **(F-J)**.

Comparison of different options for butyric acid production

In order to evaluate different options for producing butyric acid from lignocellulosic biomass and model substrates, we analyzed the theoretical yields and the necessary amount of pH control and reducing reagents. *C. tyrobutyricum* can convert glucose, xylose or lactic and acetic acid to butyric acid according to the stoichiometric equations summarized in figure C.1. To calculate the theoretical yields of the lactate platform we assumed that all hexoses are fermented by lactic acid bacteria through the Embden-Meyerhof-Parnas pathway to lactic acid, while xylose is metabolized through the PK pathway to lactic and acetic acid (Fig. C.1). These products as well as the acetic acid present in the feedstock are then converted by *C. tyrobutyricum* to butyric acid. As only very little information could be found for the latter pathway, we experimentally determined the required ratio of lactic to acetic acid. We found that 3 moles lactic acid and 1 mol of acetic acid are converted to 2 moles of butyric acid (Fig. 4.6A-E). With this information, we calculated the theoretical yields of the direct sugar conversion route and the lactate platform route for feedstocks consisting of varying fractions of glucan, xylan and acetic acid. While the theoretical butyric acid yield for the direct sugar conversion varies only slightly between 0.486 and 0.493 gg^{-1} fermentable carbohydrates, it ranges from 0 gg^{-1} (for pure glucan) up to 0.635 gg^{-1} (81 % glucan, 19 % acetic acid) for the lactate platform (Fig. 4.7F, left). If for the latter case also acetic acid is accounted as a carbon source, the theoretical butyric acid yield of the lactate platform is 0.52 gg^{-1} substrate which is 7 % higher than the theoretical yield of the direct sugar conversion. For a feedstock composition corresponding to that of pretreated beech wood (68.5 % glucan, 24.3 % xylan, 7.2 % acetic acid), the theoretical yield of butyric acid produced via the lactate platform is 0.525 gg^{-1} fermentable carbohydrates, which is 7.5 % higher than the theoretical yield of 0.488 gg^{-1} for the direct fermentation of the carbohydrates by *C. tyrobutyricum*. To underpin this theoretical framework with experimental data, we determined the butyric acid yield of the lactate platform using the optimal mixture of glucose and acetic acid. To this end, glucose was first metabolized to lactic acid using *L. pentosus*, followed by the addition of *C. tyrobutyricum* and acetic acid in the second phase of the fermentation. A butyric acid yield of 0.53 gL^{-1} glucose could be achieved, which corresponds to 109.4 \pm 2.7 % of the theoretical yield for the direct glucose conversion by *C. tyrobutyricum* (Fig. 4.7G-H).

We also compared the microbial strategies presented above with the sugar platform to improve the butyric acid yield if acetate is the limiting factor, e.g. if the feedstock contains only glucan. The direct fermentation of cellulose and xylose by *C. tyrobutyricum* in a simultaneous saccharification and fermentation (SSF) approach resulted in the formation of acetic acid as an undesired side product with a molar butyric to acetic acid ratio of 3:1 (Fig. C.3). This can be explained by the higher ATP gain for *C. tyrobutyricum* using electron bifurcation (Fig. C.1). Overall the carbon efficiency of the direct sugar conversion expressed as the ratio of carbon

present in the target product to total carbon present in the feedstock was 57 % (Fig. 4.7E). If the CBP consortium of the lactate platform is extended with an obligate heterofermentative LAB, such as *L. brevis*, which also converts glucose via the PK pathway to lactic acid and acetic acid (Fig. C.1), no acetic acid is formed as a side product by *C. tyrobutyricum*. The carbon efficiency in this pathway is 66 % (Fig. 4.7E), which is higher than for the direct sugar conversion although some carbon is lost in the heterofermentative conversion of glucose. To further improve the carbon efficiency, we proposed to convert part of the lactic acid to acetic acid with the homoacetogen *A. woodii* (Fig. 4.7A and B), which employs a pathway where no

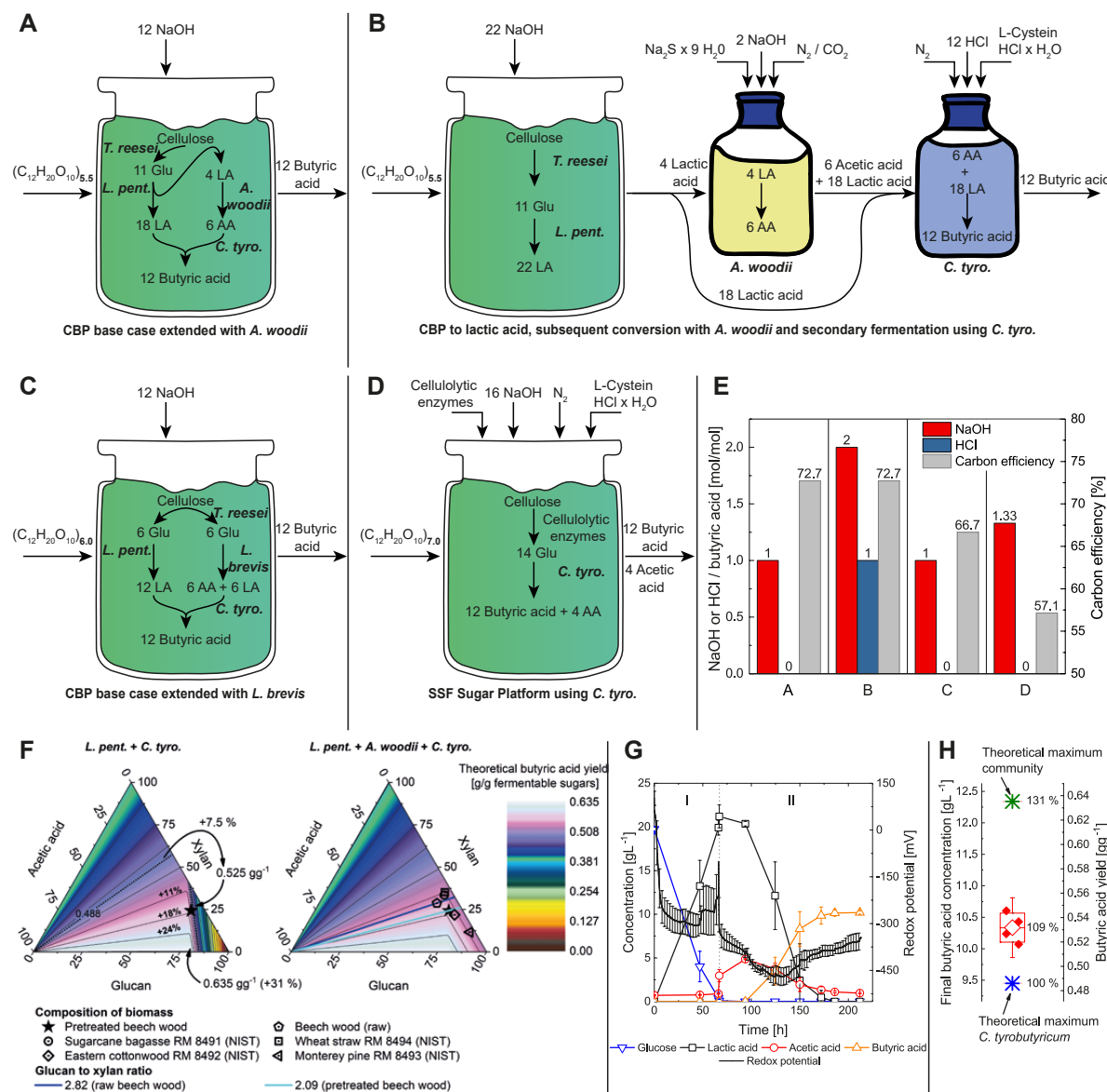


Figure 4.7: Caption next page.

Figure 4.7: **Different production routes from cellulose to butyric acid including theoretical and practical yields using the lactate platform in comparison to the sugar platform.** Schematic representation of metabolic fluxes in different production routes for butyric acid: **(A)** CBP base case extended with *A. woodii*, **(B)** subsequent production of butyric acid from cellulose using *T. reesei*, *L. pentosus*, *A. woodii* and *C. tyrobutyricum*, **(C)** CBP base case extended with *L. brevis* and **(D)** simultaneous saccharification and fermentation (SSF) sugar platform using *C. tyrobutyricum*. **(E)** Comparison of acid and base consumption (expressed in mol per mol of produced butyric acid) and carbon efficiency (expressed as ratio of carbon present in target product to total carbon present in the carbohydrates of the feedstock) for production routes **(A-D)**. **(F)** Ternary plots of modelled theoretical butyric acid yield (g butyric acid per g fermentable sugars) for feedstocks containing different fractions of glucan, xylan and acetic acid. **(F, left)** *L. pentosus* assimilate hexose through the Embden-Meyerhof-Parnas pathway and xylose through the PK pathway to lactic and acetic acid. *C. tyrobutyricum* forms 2 moles of butyric acid using 3 moles of lactic acid and 1 mol of acetic acid. *C. tyrobutyricum* can convert sugars directly to butyric acid with a theoretical yield of 0.486 gg^{-1} for glucose and 0.493 gg^{-1} for xylose. The glucan to xylan ratio of pretreated beech wood was 2.82 resulting in a maximal yield of 0.488 gg^{-1} . The application of the lactate platform concept increased the theoretical yield by 7.5 % to 0.525 gg^{-1} fermentable carbohydrates. The maximum yield of 0.635 gg^{-1} was found for a glucan/xylan/acetic acid ratio of 81/0/19, which corresponds to an increase of 31 %. When not only the carbohydrates, but also acetic acid is counted as carbon source for the lactate platform, the theoretical yield of the latter case is 0.52 gg^{-1} and 107 % of the theoretical yield for direct sugar conversion. If the feedstock contains low fractions of acetic acid and xylan (e.g. Monterey pine) acetic acid limits butyric acid production. The extension of the consortium composed of *L. pentosus* and *C. tyrobutyricum* with *A. woodii* **(F, right)** increases the theoretical yield by conversion of lactic to acetic acid by *A. woodii*. Calculations are based on the assumption that *A. woodii* converts lactic to acetic acid until the required LA:AA ratio is reached. **(G)** Fermentation of 19.425 gL^{-1} glucose by *L. pentosus* in Mandel's medium. After complete consumption of glucose at the beginning of phase II, 4.375 gL^{-1} acetic acid and 0.5 gL^{-1} L-cysteine $\text{HCl} \cdot \text{H}_2\text{O}$ were added and the reactor was inoculated with *C. tyrobutyricum*. The glucose/acetic acid ratio corresponded to the optimal theoretical yield for the lactate platform. Nitrogen was not added at any time. **(H)** The final butyric acid concentration reached $10.3 \pm 0.2 \text{ gL}^{-1}$ as shown in **(G)**, which is 1.094 ± 0.027 times the theoretical butyric acid yield of *C. tyrobutyricum* from glucose and $83.7 \pm 1.9 \%$ of the theoretical yield of the lactate platform. The experiment was done in quadruplicate. Error bars represent the standard deviation of the mean in **(G)**. The box represents the standard deviation of the mean and error bars the 99 % confidence interval in **(H)**. Abbreviations: LA = Lactic acid, AA = acetic acid, Glu = glucose, $(\text{C}_{12}\text{H}_{20}\text{O}_{10})_n = n$ cellobiose repeating units that are β -1,4-glycosidically linked.

carbon is lost (Fig. C.1). Thus, it is the most efficient way (carbon efficiency of 72 %) to produce butyric acid from cellulose (Fig. 4.7E). Using this approach, the theoretical yields for mixed feedstocks low in xylan or acetic acid can be improved considerably as presented in figure 4.7F, right.

Increasing the butyric acid titer

In order to increase butyric acid concentrations using the consortium extended with *L. brevis*, we doubled the substrate loading. Under these conditions, 14.7 gL⁻¹ butyric acid (0.26 gg⁻¹, 83.6 % selectivity) were produced (Fig. C.4, Tab. C.1). The lower yield observed with increased substrate loading could be caused by the inhibitory effect of butyric acid on the microbial community and the cellulolytic enzymes [66].

4.3.3 CBP of cellulose and xylose to propionic and acetic acid by integration of *Veillonella criceti* into the lactate platform

To demonstrate the modularity of the lactate platform we replaced *C. tyrobutyricum* with *V. criceti* to produce propionic and acetic acid. *V. criceti* is an obligate anaerobic bacterium which is unable to utilize carbohydrates but converts lactic acid to propionic and acetic acid (Fig. 4.8A). Thus, the lactate platform approach compensates for the missing metabolic flexibility of the strain. CBP of 1.75 % (w/w) microcrystalline cellulose and 9.32 gL⁻¹ xylose (fed over a period of 75 hours) yielded 8.9 gL⁻¹ total carboxylic acids (Fig. C.5, Tab. C.2). When doubling both carbon sources 13.7 gL⁻¹ acetic acid and 9.3 gL⁻¹ propionic acid were produced (Fig. 4.8B, Tab. C.2).

4.3.4 CBP of pretreated beech wood

Finally, we targeted the direct conversion of beech wood to butyric acid or propionic and acetic acid. We applied a two-stage steam pretreatment procedure developed in our laboratory to recover temperature sensitive xylooligomers and acetic acid in a moderately inhibitory process stream. Beech wood was first pretreated at 180 °C for 25 minutes. Acetic acid bound as an acetyl side chain to the xylopyranose backbone in hardwood [26] was solubilized during the treatment when steam condensation formed a prehydrolyzate, which can be withdrawn from the reactor under pressure. The prehydrolyzate contained 46 % of the xylan in the form of xylooligomers, 5 % xylan degraded to formic acid and furfural, 41 % of the acetic acid and some solubilized phenolic compounds from lignin. The remaining solids were pretreated again under harsher conditions (230 °C, 14.1 minutes) in order to increase the enzymatic digestibility of the glucan fraction. The solids, that were separated from the prehydrolyzate by filtration, contained 88 % of the original glucan, 9 % of the original xylan, 15 % of the original acetate and 78 % of the total lignin (Fig. 4.9A and C.6). For CBP of beech wood, we added 3 % (w/w) pretreated solids at the beginning of the fermentation and started the first stage prehydrolyzate feed with the inoculation of *L. pentosus*. A consortium composed of

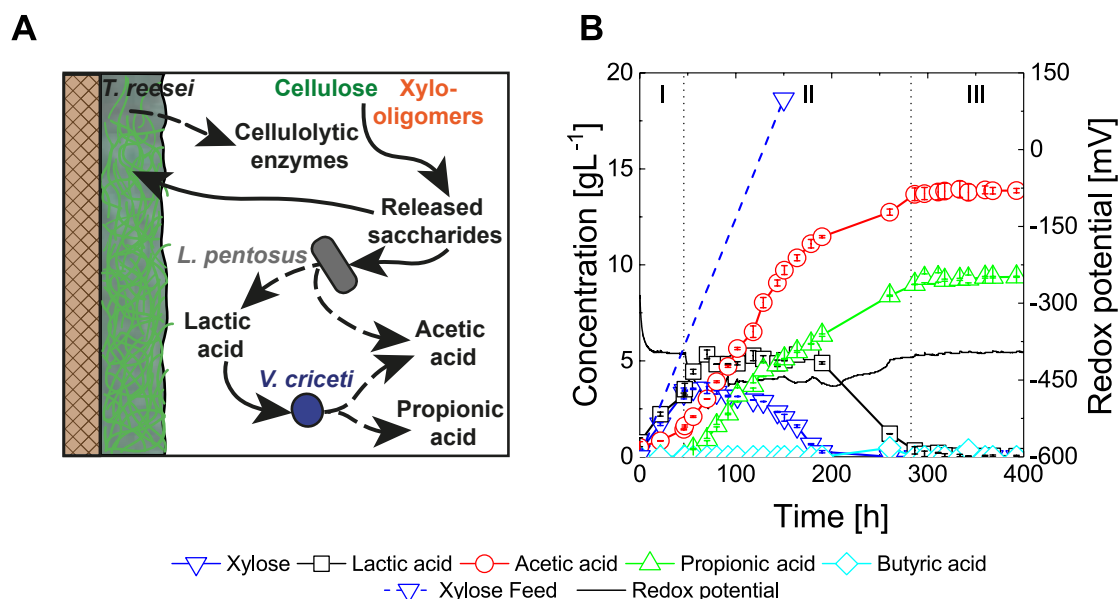


Figure 4.8: **CBP of microcrystalline cellulose and xylose to propionic and acetic acid using a cross-kingdom microbial consortium.** (A) Schematic representation of the synthetic microbial consortium for the production of propionic and acetic acid with the lactate platform. A three-step inoculation scheme was followed: For the first two days, only *T. reesei* grew in the reactors. Then, *L. pentosus* was inoculated at the beginning of phase I, followed by the addition of *V. criceti* at the beginning of phase II. (B) CBP of 35 gL⁻¹ Avicel and 18.64 gL⁻¹ xylose (fed over a time period of 150 hours) to propionic and acetic acid. The experiments were performed with a low OTR of 0.34 h⁻¹ (mono-lumen tubing 1.58 mm×3.18 mm×0.80 mm). Error bars represent the standard deviation from two independent experiments.

T. reesei, *L. pentosus* and *C. tyrobutyricum* produced 9.5 gL⁻¹ butyric acid (0.38 gg⁻¹, 91.5 % selectivity, Fig. 4.9B, Tab. C.1), which corresponded to an overall yield of 196.5 kg butyric acid per ton of dry raw beech wood (217.1 kg total VFAs/t) (Fig. 4.9A). A consortium composed of *T. reesei*, *L. pentosus* and *V. criceti* produced 6.7 gL⁻¹ acetic acid and 5.6 gL⁻¹ propionic acid (0.49 gg⁻¹, Fig. 4.9C, Tab. C.2) from pretreated beech wood. This corresponds to 133.3 kg acetic acid and 113.6 kg propionic acid per ton of raw biomass (Fig. 4.9A). In these batches, we also determined the activity of hydrolytic enzymes. We confirmed that *T. reesei* was active also after inoculation of LAB and product forming strains as was indicated by the increasing activities of cellobiohydrolases, endoglucanases, beta-glucosidases and xylanases in the supernatants (Fig. C.7).

4.4 Discussion

In this study, we merged synthetic microbial ecology with process engineering to realize and control artificial food chains distributed over up to four highly diverse microorganisms. Our goal was to provide a platform that minimizes the required metabolic capabilities of product forming microorganisms to facilitate their integration into an artificial ecosystem utilizing all biomass fractions. To this end, we developed the lactate platform concept to metabolically funnel the heterogeneous lignocellulosic carbohydrates to lactate as the central intermediate by employing LAB. The non-cellulolytic nature of LAB necessitated the integration of a cellulolytic strain. We chose the aerobic fungus *T. reesei* as it is one of the most common

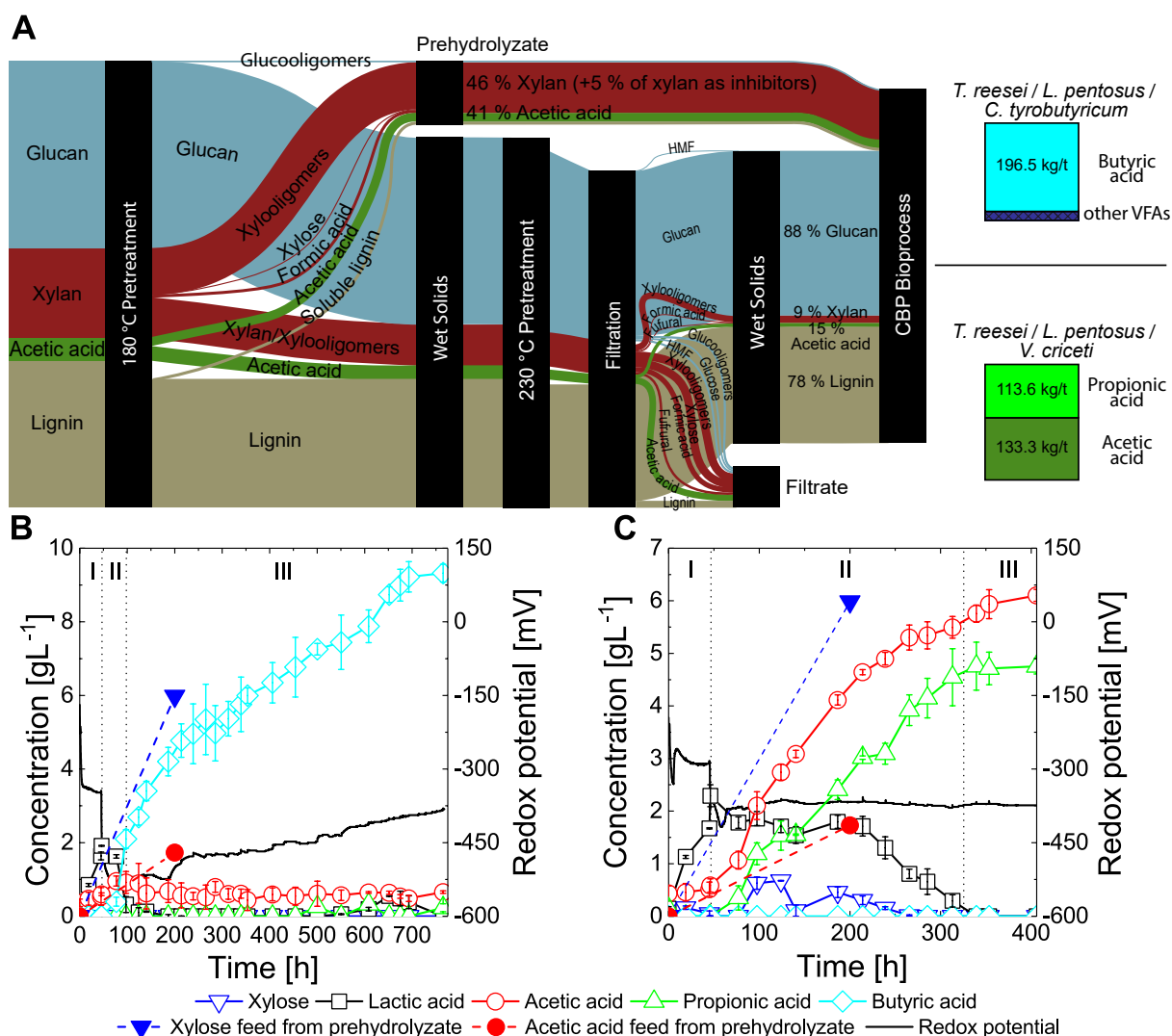


Figure 4.9: Caption next page.

Figure 4.9: **Mass fluxes of glucan, xylan, acetic acid and lignin for the two-stage steam-pretreatment of beech wood and CBP of pretreated beech wood to butyric acid or propionic and acetic acid, respectively.** (A) A two-stage pretreatment procedure was applied to (i) partially recover dissolved acetic acid and xylan (as xylooligomers) in a prehydrolyzate and (ii) alter the structure of the solids to allow maximum glucose yields during enzymatic hydrolysis. First, beech wood was steam-pretreated at 180 °C for 24.8 minutes. Steam condensation formed a prehydrolyzate which contained 46 % of the raw xylan as xylooligomers, 5 % of the xylan as formic acid, and 41 % of acetate. The prehydrolyzate was separated under pressure through a nozzle. Subsequently, the pressure was slowly released and the recovered solids were treated at 230 °C for 14.1 minutes, followed by an abrupt pressure release to disrupt the structure of the biomass. A filtration step separated the inhibitory filtrate from the wet solids which contained 88 % of the raw glucan, 9 % of the xylan, 15 % of the acetic acid and 78 % of the lignin. The solids and the prehydrolyzate were utilized in the CBP processes with *T. reesei*, *L. pentosus* and *C. tyrobutyricum*, yielding 196.5 kg butyric acid per ton of raw beech wood (217.2 kg total VFA/t), *T. reesei*, *L. pentosus* and *V. criceti*, yielding 113.6 kg propionic acid per ton and 133.3 kg acetic acid per ton. Further details of recovery percentages can be found in (Fig. C.6). (B-C) CBP of 3 % (w/w) two-stage steam-pretreated beech wood solids with a feed of the corresponding prehydrolyzate over a period of 200 hours to (B) butyric acid and (C) propionic and acetic acid. The dashed blue line shows the amount of xylose in the form of xylooligomers and the dashed red line the amount of acetic acid added with the prehydrolyzate. A low OTR (0.34 h^{-1}) was applied (mono-lumen tubing $1.58 \text{ mm} \times 3.18 \text{ mm} \times 0.80 \text{ mm}$). Error bars represent the standard deviation from two independent experiments.

hosts for industrial enzyme production. Inspired by natural ecosystems, we stabilized the composed cooperator-cheater communities by using sufficient niche differentiation despite partly mutual resource utilization. In order to allow the integration of the anaerobic product forming strains besides *T. reesei*, we developed a membrane-aerated biofilm reactor to create stable spatial niches for aerobes and anaerobes. However, in this system a mono-culture of the fungus lowered the redox potential to only -20 mV (Fig. 4.4) which is not suitable for obligate anaerobes. Consequently, the co-cultivation of the aerobe *T. reesei* and the obligate anaerobe *C. tyrobutyricum* failed (Fig. C.8). In contrast, the LAB *L. pentosus* lowers the redox potential to -300 mV (Fig. 4.4) by reducing molecular oxygen to either hydrogen peroxide or water for the regeneration of NAD^+ by NADH oxidases (Fig. C.1) [162]. Overall, the lactate platform facilitates the creation of an ecological niche for anaerobes without addition of reducing agents or purging with nitrogen.

Aside from spatial niches we stabilized our consortium using metabolic niche differentiation. For example, *V. criceti* is unable to utilize lignocellulosic sugars [103,170] and thus did not compete with *L. pentosus* (Fig. 4.2C). Contrarily, *C. tyrobutyricum* is able to consume monomeric sugars and thus can compete with LAB for the available carbohydrates. However, the particular ability of *L. pentosus* to use oligomers intracellularly favored the metabolic flux to lactic and acetic acid (Fig. 4.2C) [171]. Low concentrations of monomeric sugars were present (below

Table 4.1: Overview of butyric acid yields with the lactate platform and alternative approaches.

Microorganisms	Feedstock	Process	Conc. [g _L ⁻¹]	Selectivity [%]	Yield ¹ [g _g ⁻¹]	References
Mixed natural anaerobic consortium	NaOH pretreated rice straw	CBP	15.1	60.9	0.19	[163]
<i>C. thermocellum</i> + <i>C. thermobutyricum</i>	NaOH pretreated rice straw	CBP	33.9	78.0	0.19	[164]
<i>Thermobifida fusca</i>	Cellulose	CBP	2.1	n.d.	0.19	[165]
LA platform ² + <i>C. tyrobutyricum</i>	Steam-pretreated beech wood	CBP	9.5	91.5	0.38	This chapter
LA platform ² + <i>A. woodii</i> + <i>C. tyrobutyricum</i>	Cellulose	CBP + subseq. batches ³	12.2	97.6	0.41	This chapter
GM0 <i>C. tyrobutyricum</i> ⁴	Glucose	Fed-batch	46.8	93	0.39	[166]
GM0 <i>E. coli</i>	Glucose, acetate	Fed-batch	10.0	99	0.50 ⁶	[167]
<i>C. tyrobutyricum</i>	Corn straw hydrolysate	Batch	29.6	84	0.32	[168]
<i>Clostridium</i> sp S1 ⁵	Softwood hydrolysate	Batch	21.2	96	0.45 ⁷	[169]
Sequential LA platform ² + <i>C. tyrobutyricum</i>	Glucose, acetate	Seq. batch	10.3	92	0.53 ⁸	This chapter

¹ Yield in g_g⁻¹ (fermentable sugars added to the fermentation).
² Lactate platform with *L. pentosus*.
³ CBP to lactate, subsequent batch fermentations to acetate and butyrate.
⁴ Engineered to improve product selectivity.
⁵ Isolated strain able to consume acetate.
Yield in g_g⁻¹ (glucose and acetic acid): ⁶ 0.36, ⁷ 0.42, ⁸ 0.43.

0.05 gL⁻¹ in our experiments) and it is assumed that *C. tyrobutyricum* grew on lactic and acetic acid forming butyric acid (Fig. C.1). When acetic acid was exhausted, we observed that *C. tyrobutyricum* could not deplete lactic acid (Fig. 4.5A) although we proved that *C. tyrobutyricum* is able to utilize lactic acid when glucose is present (Fig. 4.6F-J). This is an indication that glucose or its oligomers are indeed consumed by LAB and are not available for *C. tyrobutyricum*. The low sugar flux to *C. tyrobutyricum* in the lactate platform is very favorable because, as a result, product selectivity and theoretical yield are enhanced. Under the assumption of an exclusive sugar flux to LAB, the theoretical butyric acid yield based on fermentable carbohydrates – depending on the feedstock composition – was up to 1.31 times the theoretical yield of the sugar platform. In practice, we reached a 1.09 times higher yield in a subsequent fermentation of glucose and acetate by *L. pentosus* and *C. tyrobutyricum* compared to the theoretical yield of the sugar platform (Fig. 4.7G and H). The achieved yield (0.53 gg⁻¹ glucose or 0.43 gg⁻¹ carbon source, respectively) also outperforms published data for fermentations of the same substrates employing natural or genetically engineered fermentation strains (Tab. 4.1). Yields for butyric acid production by CBP of lignocellulosic feedstocks are generally lower than the yields achieved on monomeric substrates, as the hydrolysis yields of recalcitrant polymeric carbohydrates are generally below the optimum. Also in this processing mode, the lactate platform outperforms alternative fermentation systems: the butyric acid yields were approximately twice as high as the reported yields of a natural consortium [163], an anaerobic co-culture [164] or a natural single cellulolytic strain [165]. They were even comparable to yields achieved on lignocellulosic hydrolysates [168,169] although we did not add external enzymes (Fig. 4.1B and Tab. 4.1).

The theoretical yields that can be achieved with the lactate platform triculture employing *T. reesei*, *L. pentosus* and *C. tyrobutyricum* depend on the feedstock composition. For feedstocks low in xylan or acetate, butyric acid yields are lower than in the sugar platform because the lactic acid conversion is incomplete due to missing acetate. For these cases, we presented and compared several strategies to tune the lactic to acetic acid ratio (Fig. 4.5 and 4.7). The utilization of *A. woodii* for acetic acid production in a subsequent three-step lactate platform process showed the highest carbon efficiency but also required the highest amount of pH control agents (Fig. 4.7B). However, if the homoacetogen would be integrated in the consortium (Fig. 4.7A), the amount of pH control agents could be reduced considerably while maintaining the excellent carbon efficiency (Fig. 4.7E). On the other hand, the latter approach requires a pressure reactor and the addition of vitamins and trace elements (Tab. C.3). Thus, the CBP lactate platform including *L. brevis* is likely the most sustainable route if acetate is limiting, as the yield is only slightly lower, but no costly medium additives are required, and the same amount of base is needed (Fig. 4.7C and E).

The modularity of the lactate platform was exemplarily demonstrated by the successful production of propionic acid. To the best of our knowledge, this is the first report of targeted production of this acid using CBP. Besides propionic and butyric acid, we identified several other bulk or fine chemicals including acetic and hexanoic acid, different alcohols (ethanol, propanol, butanol, 1,2-propanediol), polyhydroxybutyrate and lipids which can be produced through this platform (Fig. 4.1C). An analysis of the required pathways revealed, that for the production of acetic acid, polyhydroxybutyrate, ethanol and butanol, the lactate platform boosts the carbon flux from lignocellulose to the target product compared to the alternative direct sugar fermentation routes (Fig. 4.1C, Tab. C.5, C.6 and C.7). Furthermore, metabolic funneling through lactate and acetate might especially facilitate the production of lipids from lignocellulosic feedstocks using microalgae which are usually deficient in effective utilization of carbohydrates. However, the switch to another target product requires the exchange of the lactic acid fermenting strain(s) and with that, different abiotic requirements such as pH, temperature or presence co-substrates will likely have to be fulfilled. For some products the artificial food chain must be extended, i.e. consortia containing at least four different microorganisms are necessary.

Based on the presented promising results with the application of cell immobilization and oxygen gradients to create and control stable consortia, the creation of additional spatial and/or metabolic niches is thus desirable to fully harness the potential of the lactate platform. To this end, the membrane reactor could be adapted in several ways (Fig. 4.2E). For instance, temperature gradients could be created by installing local heat sinks or sources in the reactor or pH gradients could be formed by introducing carbon dioxide or ammonia through a membrane to the reactor. In the same way, co-substrates such as hydrogen or carbon monoxide could be fed to the consortium. Such a hydrogen niche could be used to reduce the carbon loss through carbon dioxide formation by converting it *in situ* to acetic acid which would improve the carbon efficiency of a range of aerobic and anaerobic bioprocesses.

4.5 Conclusions

Taken together, we are the first reporting the engineering of stable cross-kingdom cooperator-cheater communities of up to four aerobic and obligate anaerobic microorganisms for metabolic funneling of heterogeneous lignocellulosic carbohydrates to lactate as the central intermediate in the synthetic food chains producing butyric or propionic and acetic acid. The lactate platform boosts the theoretical carbon flux to several additionally possible target products and it is adaptable to the varying compositions in lignocellulosic feedstocks making it a promising concept to further pursue on the way to a more sustainable chemical industry.

CHAPTER 5

Mixed volatile fatty acids

5.1 Abstract

We employed synthetic microbial communities with up to four microorganisms to produce targeted mixtures of volatile fatty acids (VFAs) from steam-pretreated beech wood. A specifically designed membrane-aerated bioreactor was used to co-cultivate the strict anaerobic, non-cellulolytic, VFA-producing bacterium *Megasphaera elsdenii* next to the aerobic, cellulolytic fungus *Trichoderma reesei*. The metabolic activity of the facultative anaerobic lactic acid bacterium *Lactobacillus pentosus* allowed the formation of an ecological niche for *M. elsdenii* and the production of lactic acid as central intermediate for the chain elongation. We tuned the ratio of produced odd- and even-numbered VFAs by adding the obligate anaerobes *Veillonella criceti* or *Clostridium tyrobutyricum* to alter intra-consortium competition. The obtained yield of up to 0.455 g total VFAs per g total fermentable sugars or 0.24 g VFAs per g raw beech wood as well as the modularity of the microbial community demonstrates the potential of consortium-based CBP for the production of various valuable biochemicals from lignocellulosic feedstocks.

This chapter is based on a manuscript under review in Nature Biotechnology: R. L. Shahab, S. Brethauer, M. Davey, J. S. Luterbacher, A. Smith, S. Vignolini, M. H. Studer *The lactate platform – a consortium based consolidated bioprocessing strategy for the yield-optimized production of volatile fatty acids from lignocellulose*.

5.2 Introduction

Medium-chain carboxylic acids find various applications as platform chemicals in food industry and as fuel precursors in the aviation sector [172]. To date the commercial production of

these chemicals is restricted to petrochemical routes. A sustainable route could be based on biochemical pathways such as the reversed beta-oxidation which offers a metabolic platform for the synthesis of fatty acids with varying functionalities [173]. Only a few strict anaerobic microorganisms are capable to follow this chain elongation pathway. *Clostridium kluyveri* [174,175] and *Eubacterium pyruvativorans* [176] ferments ethanol and acetate to VFAs such as butyrate and caproate. *Megasphaera elsdenii* is capable to metabolize monomeric carbohydrates and organic acids [177,178] to a mixture of odd- and even-numbered VFAs. The control of the chain lengths is to date a major challenge [179]. In particular, the biochemical production of odd-numbered VFAs is valuable because they occur less frequent in natural pathways and are industrially usefully as plasticizers, herbicides or scents [180].

Toward a bio-based economy the production of medium-chain carboxylic acids from lignocellulose would be highly favorable because it is a renewable low-cost source of fixed carbon. However, *C. kluyveri*, *E. pyruvativorans* and *M. elsdenii* are non-cellulolytic and multiple process steps are required to make the polymeric substrate accessible for them. The steps include an initial pretreatment to increase the enzymatic hydrolyzability of the recalcitrant substrate and multiple biochemical conversions. Cellulolytic and hemicellulolytic enzymes are produced and hydrolyze cellulose and hemicellulose to monomeric carbohydrates which are converted to volatile fatty acids in a one or two step fermentation. Consolidated bioprocessing (CBP) merges all biochemical processes a single process. This approach offers strongly reduced costs as compared to other techniques that require external cellulolytic enzymes [23].

CBP can be based on a single microorganism that has been genetically modified to possess all required metabolic capabilities. An alternative approach relies on a microbial community based on the principle of labor division which attracted the increased attention of researchers worldwide [10,70,87,141,158]. It was shown that undefined communities can be used for the production of medium-chain VFAs e.g. based on the carboxylate platform [140,181]. Undefined communities benefit from stability [182] and reduced costs (e.g. no sterilization needed). However, the control of complex natural consortia remains a major challenge.

Another approach relies on defined communities. The long-term co-cultivation of multiple, selected microorganisms and the prediction of the targeted metabolic output of such communities require a high level of process control and knowledge on the ecological dependencies [71,86,132,147,183]. However, similar to natural ecosystems different microorganisms with highly diverse abiotic requirements can be stabilized by sufficiently high niche differentiation. As shown in chapter 3, a community composed of the aerobic fungus *T. reesei* and the facultative anaerobic bacterium *L. pentosus* funnels the metabolic flux of the heterogeneous carbohydrate mixture of lignocellulose to lactate. This can compensate missing metabolic capabilities of subsequent microorganisms in an artificial food chain. We extended the synthetic ecosystem

with obligate anaerobes and were able to broaden the product palette to acetic, propionic and butyric acid, see chapter 4. In this chapter, we aim for the production of medium-chain VFAs from lignocellulosic biomass using the chain elongation pathway. We selected *M. elsdenii* as it is the only bacterium known to utilize lactate as substrate for chain elongation. The successful co-cultivation of up to four microorganisms including a strict anaerobe and an aerobe in a CBP is demonstrated whereby the share of VFA end-products can be controlled through intra-consortium competition.

5.3 Results and discussion

5.3.1 Co-cultivation of aerobic and strict anaerobic microorganisms

We have designed a microbial community composed of three microorganisms to establish an artificial food chain based on lignocellulosic biomass to produce mixtures of medium-chain VFAs. The aerobic fungus *T. reesei* produces cellulases and hemicellulases. The enzymatic hydrolysis releases heterogeneous mixtures of soluble carbohydrates. The facultative anaerobic bacterium *L. pentosus* metabolically funnels the carbohydrates to lactic and acetic acid which serve as feedstock for the subsequent biochemical conversion [158]. The strict anaerobic bacterium *M. elsdenii* converts lactic and acetic acid to a mixture of medium-chain VFAs.

The stable co-cultivation of microorganisms with different abiotic requirements is challenging. In order to enable growth of the aerobic fungus *T. reesei* and the strict anaerobic bacterium *M. elsdenii* together in one bioreactor an oxygen gradient across a polydimethylsiloxane membrane was established to allow niche differentiation (Fig. 5.1A). The fungus forms a spatially confined aerated biofilm on the surface of the membrane while *M. elsdenii* grows under anaerobic conditions in the fermentation slurry.

We tested the co-cultivation of *T. reesei*, *L. pentosus*, *M. elsdenii* in our bioreactor by subsequent inoculation (Fig. 5.1B). Microcrystalline cellulose (Avicel) and xylose were used as model substrates for lignocellulosic biomass. The presence of *T. reesei* and *L. pentosus* ($t=0$ h to $t=48$ h) resulted in the accumulation of 3.4 gL^{-1} lactic acid. As previously shown the dissolved oxygen concentration in the slurry drops below the detection limit of the oxygen sensor of 4 ppb after biofilm formation (Fig. 4.4). Anaerobic metabolism usually takes place at redox potential of -250 to -300 mV [184,185]. In our membrane aerated reactor a drop of the redox potential to -430 mV was observed which indicates anaerobic conditions without the need for application of costly nitrogen and reducing agents. After inoculation with *M. elsdenii* the lactic acid concentration was reduced to below the detection limit of 0.05 gL^{-1} and we recorded the simultaneous accumulation of 4.3 gL^{-1} acetic acid, 1.2 gL^{-1} propionic acid, 5.0 gL^{-1} butyric acid, 1.5 gL^{-1}

valeric and 1.3 gL^{-1} caproic acid. The presence of medium-chain VFAs in the bioreactor prove the metabolic activity of *M. elsdenii* and we conclude that we have successfully co-cultivated an aerobic and strict-anaerobic microorganism in a CBP. This demonstrates the functionality of the artificial ecosystem composed of *T. reesei* and *L. pentosus* to compensate the limited capabilities of *M. elsdenii* to metabolize carbon from xylose [186] and cellulose. However, after inoculation of *M. elsdenii* the redox potential rapidly increased (around 1.5 mV h^{-1} from $t=50 \text{ h}$ to $t=200 \text{ h}$) indicating that the metabolic activity of *T. reesei* and *L. pentosus* is not sufficient to maintain a sufficiently low redox potential. The obtained VFA yields were around $0.46 \pm 0.07 \text{ g VFA per g fermentable sugars}$ (Fig. 5.1B).

In order to enable long-term conditions suitable for anaerobic metabolism we reduced the oxygen transfer into the reactor by using a membrane with thicker walls. For the experiments pretreated beech wood was used as substrate. A two-stage procedure was applied to increase the enzymatic digestibility of the wood. Temperature sensitive hemicellulose was recovered in a liquid phase called prehydrolyzate in a first process step at $180 \text{ }^{\circ}\text{C}$ for 25 minutes. The remaining solid fraction was treated at $230 \text{ }^{\circ}\text{C}$ for 14 minutes to maximize glucose release in the subsequent enzymatic hydrolysis. The solids were introduced at once at the beginning of the experiment and the corresponding prehydrolyzate was fed with a constant rate within 200 hours. Within 1080 hours our designed community composed of *T. reesei*, *L. pentosus*, *M. elsdenii* produced 6.8 gL^{-1} of acetic acid, 4.2 gL^{-1} of butyric acid, 2.4 gL^{-1} of caproic acid and small amounts of propionic and valeric acid (each around 1 gL^{-1}) (Fig. 5.1C). The process yielded $0.42 \text{ g total VFAs per g total fermentable sugars}$ and $0.22 \text{ g total VFAs per g of raw beech wood}$. Even after more than 600 hours after inoculation of *M. elsdenii* the accumulation of metabolic end-products of the anaerobic pathways such as caproic acid were recorded indicating that the reduced oxygen transfer rate prolonged the metabolic activity of the strict anaerobic strain (Fig. 5.1C). This is in line with the measured smaller slope of the redox potential (around 0.23 mV h^{-1} from $t=400 \text{ h}$ to $t=1094 \text{ h}$) in comparison to the approach with the thinner membrane. Throughout the experiment, enzymatic activities of cellobiohydrolases, beta-glucosidases, endo-glucanases and xylanases were detected (Fig. 5.1D).

5.3.2 Targeted production of odd- and even-numbered medium-chain VFAs

M. elsdenii produced a mixture of odd- and even-numbered medium-chain VFAs in a consortium-based CBP with lignocellulose as substrate as shown above (Fig. 5.1C). Our aim is to control the share of produced odd- or even-numbered VFAs.

We extended the community composed of *T. reesei*, *L. pentosus* and *M. elsdenii* with the obligate anaerobic bacterium *V. criceti* (Fig. 5.2A). Two-stage pretreated beech wood was used as substrate and *V. criceti* and *M. elsdenii* were added together to *T. reesei* and *L. pentosus*. After

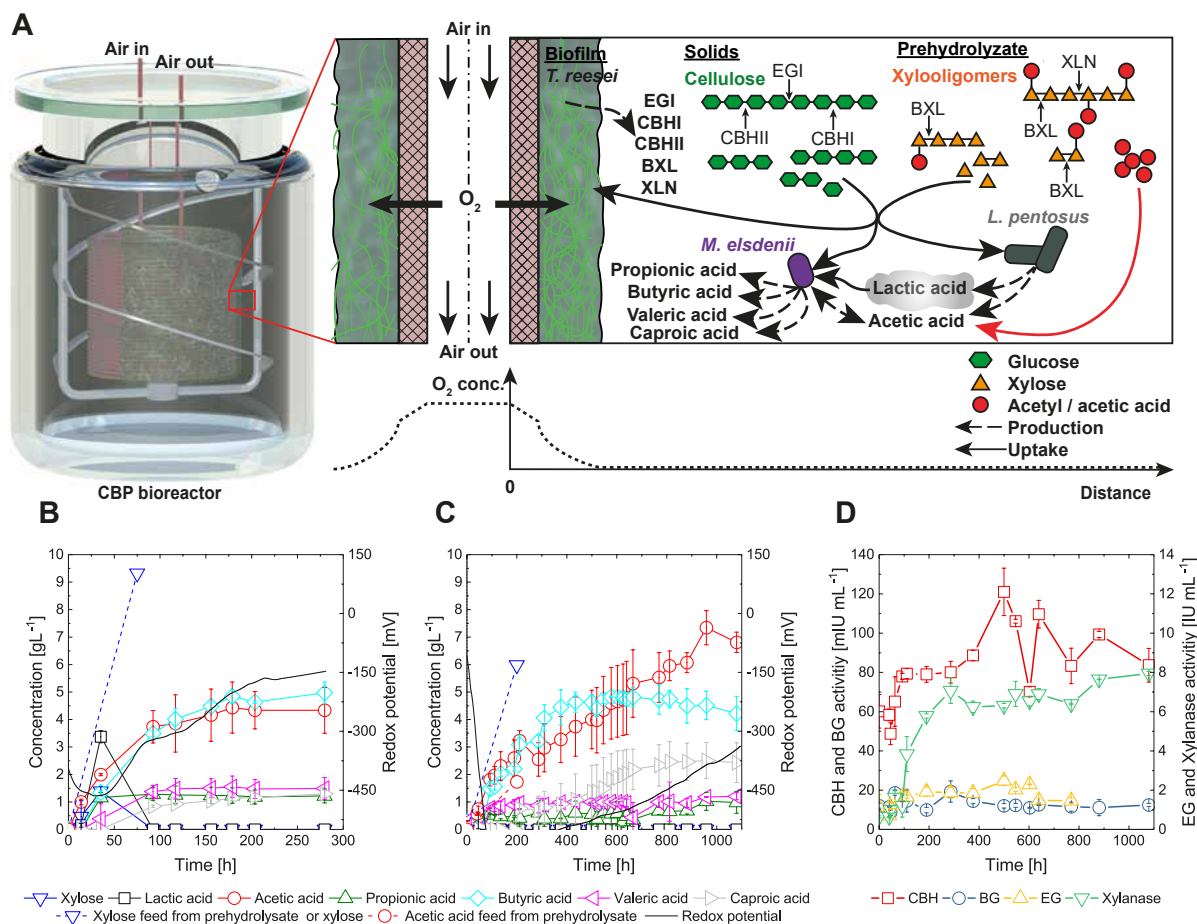


Figure 5.1: CBP for the conversion of lignocellulose into medium-chain volatile fatty acids using *T. reesei*, *L. pentosus* and *M. elsdenii*. (A) Illustration of membrane bioreactor and schematic visualization of the membrane/fermentation slurry interface and fermentation slurry. The aerobic fungus *T. reesei* forms a biofilm on the surface of an oxygen permeable, dense membrane and secretes cellobiohydrolases (CBHI and II), endoglucanases (EGI), beta-xylosidase (BXL) and beta-endoxylanase (XLN) to the fermentation slurry. The enzymatic hydrolysis releases a mixture of soluble carbohydrates which are metabolized by *L. pentosus* to lactic and acetic acid. *M. elsdenii* uses the metabolic end-products of *L. pentosus* and carbohydrates to produce various medium-chain VFAs. The dissolved oxygen profile is indicated below the sketch. Time-resolved redox potential and concentration of dissolved medium-chain VFAs, lactic acid and xylose produced from (B) 1.75 % (w/w) microcrystalline cellulose (Avicel) and 9.32 gL⁻¹ xylose fed over a period of 75 hours and (C) 3.86 % (w/w) two-stage steam-pretreated beech wood (solid) and xylooligomers containing first stage prehydrolyzate (liquid) fed over a period of 200 hours. The amount of xylose calculated from xylooligomers (dashed blue line) and amount of acetic acid (dashed red line), added through the prehydrolyzate feed. The experiments were performed with an OTR of 0.34 h⁻¹ (mono-lumen tubing 1.58 mm×3.18 mm×0.80 mm). (D) Activity of CBH, BG, EG and xylanase in the supernatant of the fermentation slurry at various stages of the fermentation. Error bars represent the standard deviation from duplicates.

958 hours the microbial community produced 2.6 gL^{-1} of acetic acid, 0.8 gL^{-1} of propionic acid, 6.7 gL^{-1} butyric acid, 3.5 gL^{-1} valeric acid and 2.1 gL^{-1} of caproic acid (Fig. 5.2B). The integration of the *V. criceti* to the community resulted in a higher valeric acid concentration (almost factor 3) as compared to the CBP based on the community without *V. criceti*. The process yield is with 0.42 g total VFAs per g total fermentable sugars and 0.22 g total VFAs per g of raw beech wood similar to the community without *V. criceti*. When we added the anaerobe *C. tyrobutyricum* instead of *V. criceti* to the community (Fig. 5.2C), we measured a different ratio of medium-chain VFAs, i.e. 4.6 gL^{-1} of acetic acid, 1.0 gL^{-1} of propionic acid, 7.4 gL^{-1} butyric acid, 1.4 gL^{-1} valeric acid and 2.5 gL^{-1} of caproic acid (Fig. 5.2D). The yield of the community extended with *C. tyrobutyricum* increased to 0.455 g total VFAs per g total fermentable sugars and 0.24 g VFAs per g raw beech wood.

M. elsdenii is capable to elongate acetate and butyrate with acetyl-CoA to medium-chain VFAs with four, six or more even-numbered carbon atoms via the reverse beta-oxidation (Fig. 5.3) [46, 187]. Furthermore, *M. elsdenii* uses the acrylate pathway which provides intracellular propionyl-CoA from lactate (Fig. 5.3). Propionyl-CoA serves as precursor for the chain elongation of e.g. acetic acid to odd-numbered VFAs such as valeric acid.

The metabolism of organic acids in *M. elsdenii* depends on the concentration of lactic acid in the surrounding [188]. The excess of lactic acid results in the accumulation of acetate and propionate in the growth medium. Lactic acid limited conditions result in a mixture of acetate and butyrate [188]. In our CBP the measured lactic acid concentration was below the detection limit of 0.05 gL^{-1} after inoculation of *M. elsdenii* (Fig. 5.1B, 5.2B). This indicated lactic acid limited growth of *M. elsdenii* and is in line with the observation of a low share of odd-numbered VFAs (Fig. 5.1B).

V. criceti follows the Methyl-Malonyl-CoA pathway to metabolize lactate to propionic and acetic acid (Fig. 5.3). Therefore, by addition of *V. criceti* to the community *M. elsdenii* and *V. criceti* compete for lactic acid and the amount of formed propionic and acetic acid is increased. *M. elsdenii* can take up extracellular propionic acid which is activated intracellularly to propionyl-CoA by a propionyl-CoA transferase (PCT) (Fig. 5.2). Due to the broad substrate spectrum of the PCT the functional group CoA can be swapped between acetyl-CoA and short-chain VFAs [186, 189, 190]. This is essential for the chain elongation process. In our experiments the concentration of propionic and acetic acid remained constant between 100 and 800 hours after inoculation. This indicates that *M. elsdenii* consumes both acids instantaneously which is in line with the observed increase of the butyric, valeric acid and caproic acid concentrations (Fig. 5.2A and B versus Fig. 5.1C). Our results demonstrate that a defined natural microbial community by itself can produce propionate from lignocellulose as intermediate for the chain elongation in *M. elsdenii*. So far, the synthesis of odd-chain alcohols and VFAs relied on the

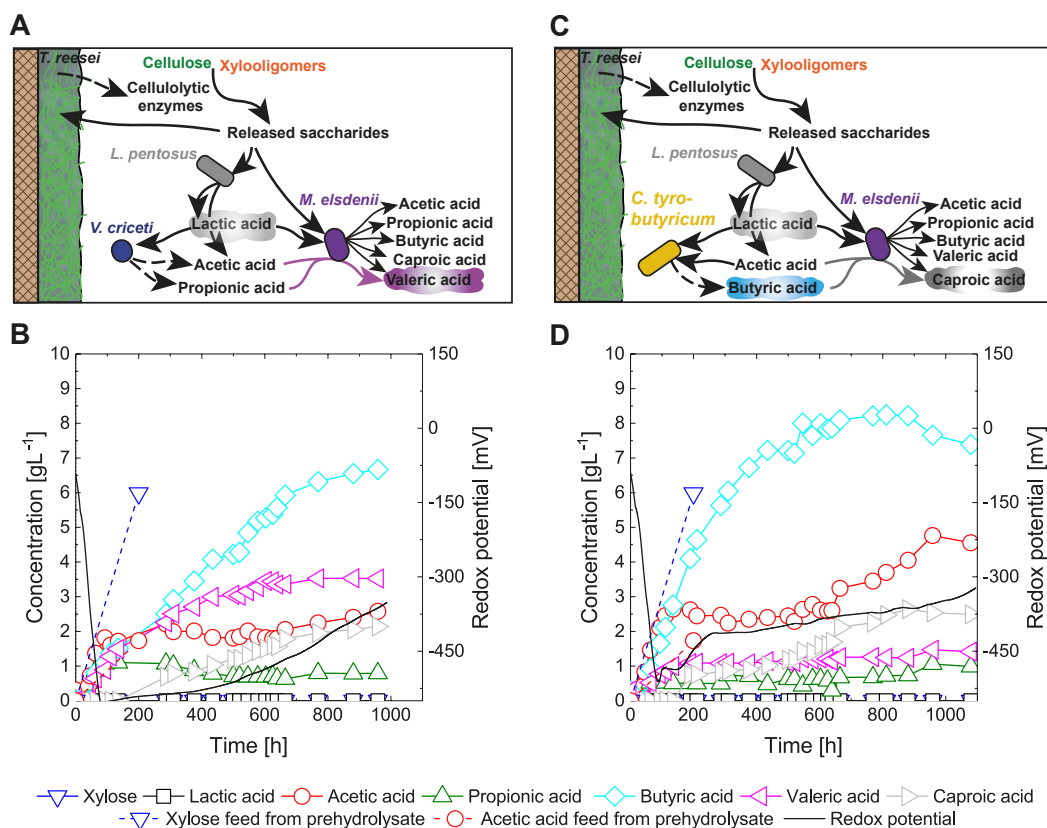


Figure 5.2: **CBP for the conversion of lignocellulose to odd- and even-chained volatile fatty acids.** Community of *T. reesei*, *L. pentosus*, *M. elsdenii* and (A,B) *V. criceti* or (C,D) *C. tyrobutyricum*. (A,C) Schematic visualization of the artificial food chains. (B,D) Time-resolved redox potential and concentration of dissolved medium-chain VFAs, lactic acid and xylose produced from 3.86 % (w/w) two-stage steam-pretreated beech wood (solid) and xylooligomers containing first stage prehydrolyzate (liquid) fed over a period of 200 hours. The amount of xylose calculated from xylooligomers (dashed blue line) and amount of acetic acid (dashed red line), added through the prehydrolyzate feed. The experiments were performed with an OTR of 0.34 h^{-1} (mono-lumen tubing $1.58 \text{ mm} \times 3.18 \text{ mm} \times 0.80 \text{ mm}$).

supplementation of propionate [172] or glucose [180,191] and genetic modification of *E. coli*. The substrates are either costly or in competition with food and feed markets.

C. tyrobutyricum can convert lactic and acetic acid in a molar ratio of 3:1 to butyric acid as sole VFA. As a result, *M. elsdenii* and *C. tyrobutyricum* compete for lactic and acetic acid and the amount of formed butyric acid is increased in comparison to the community without *C. tyrobutyricum*. The metabolism of *M. elsdenii* would allow the reverse beta-oxidation of butyric acid (electron acceptor) taken from the environment to hexanoic acid if an electron donor such as lactate is available (Fig. 5.3) measured a higher butyric acid concentration (factor 1.75) and lower acetic acid concentration (factor 0.66) with *C. tyrobutyricum* in comparison to without *C. tyrobutyricum* (Fig. 5.2C and D versus Fig. 5.1C). On the other hand, the caproic

acid concentration was unchanged which indicates the lack of electron donors for *M. elsdenii* which prevented the continuation of chain elongation [192]. In our experiments *M. elsdenii* produced 2.5 gL^{-1} of caproic acid which is above the concentration which is usually reached under axenic conditions ($< 1.0 \text{ gL}^{-1}$) [186,187].

5.4 Conclusions

In this chapter, we designed artificial microbial communities for the production of targeted mixtures of VFAs from steam-pretreated beech wood. We showed that in a specifically designed membrane-aerated bioreactor the metabolic activity of the aerobic fungus *T. reesei* and the facultative anaerobic bacterium *L. pentosus* enabled the formation of an ecological niche for the strict anaerobic bacterium *M. elsdenii*. The developed community enabled the use of pentoses and hexoses from the heterogenous mixed lignocellulosic substrate for chain elongation by metabolic funneling by the lactic acid bacterium. In order to control the share of odd- and even-numbered VFAs in the product mixture intra-consortium competition was applied and the community extended with the obligate anaerobes *V. criceti* or *C. tyrobutyricum*. Our results demonstrate the strong potential of a CBP based on a defined microbial community for the production of industrially relevant biochemicals from sustainable low-cost carbon sources and paves the way towards a bio-based economy.

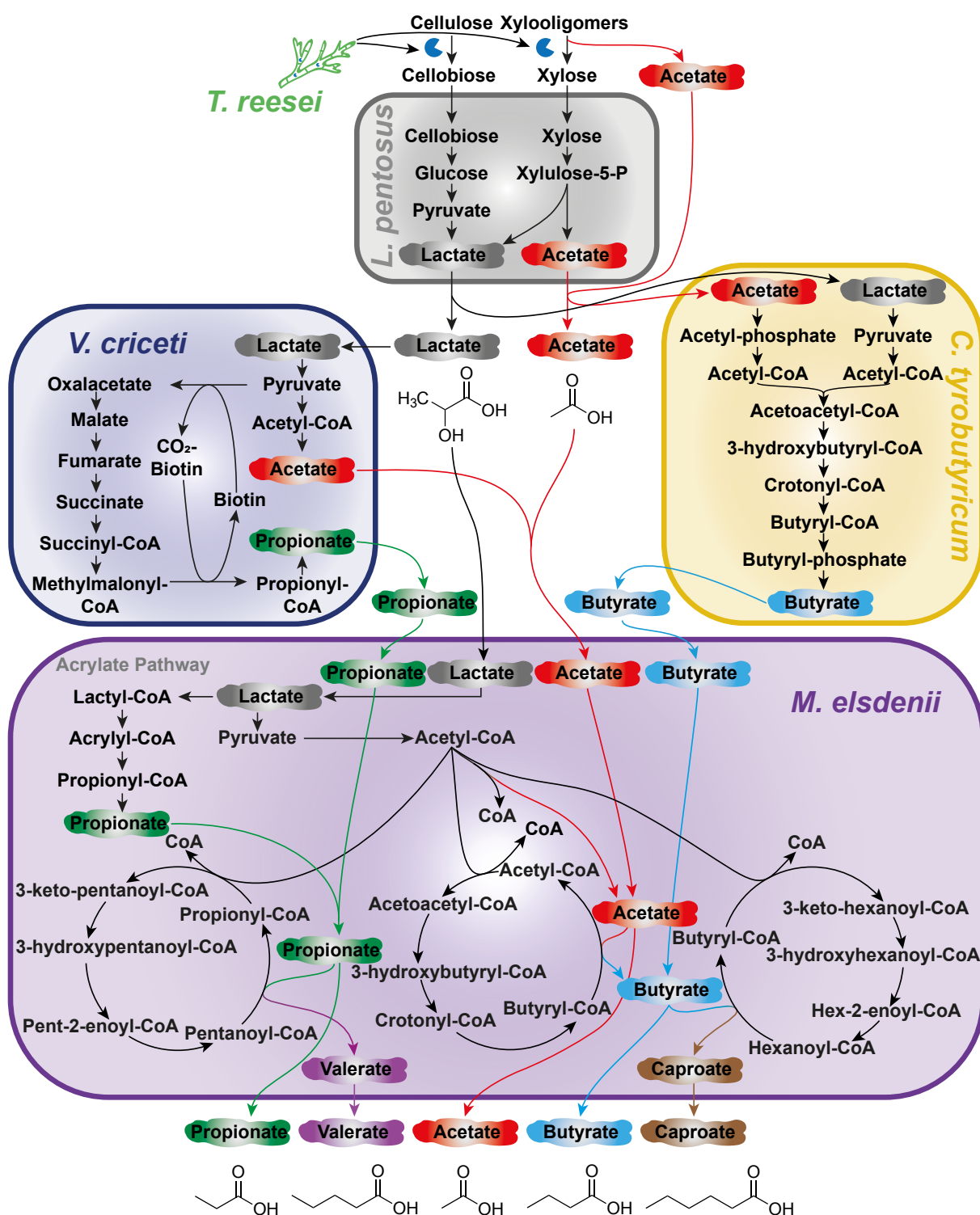


Figure 5.3: Overview of selected metabolic pathways in the community-based CBP following the artificial food chain from lignocellulose via lactate and acetate as intermediates to medium-chain volatile fatty acids. Colored areas represent microbial cells of *L. pentosus* (grey), *V. criceti* (blue), *C. tyrobutyricum* (yellow) and *M. elsdenii* (purple).

CHAPTER 6

Ethanol

6.1 Introduction

Ethanol is a chemical compound which finds wide-spread applications. Aside from its use as a fine-chemical ethanol became a prominent biofuel [193]. On the roadmap to a carbon-neutral transportation sector the production of bioethanol from sustainable carbon sources is highly desired. To date, bioethanol is mainly produced from plants with a high sugar or starch content such as sugar cane, corn, wheat and sugar beets. However, to avoid competition with food and feed industry, it is of highest interest to replace these substrates with lignocellulosic waste materials from agriculture and forestry.

In recent years, much progress was made to establish biochemical production routes for the conversion of lignocellulose to ethanol. The most commonly applied ethanol-producing microorganism is the baker's yeast *Saccharomyces cerevisiae*. Using industrially proven strains of *S. cerevisiae* and easily digestible carbohydrates as substrate ethanol yields close to the theoretical maximum can be achieved. Unfortunately, *S. cerevisiae* is non-cellulolytic and much effort has been undertaken to introduce cellulolytic and hemicellulolytic capabilities into the yeast [193]. Table 6.1 shows selected literature on the CBP of cellulose and lignocellulose to ethanol. So far, CBP based on genetically modified *S. cerevisiae* face multiple challenges such as low levels of enzyme production, incomplete conversion of the substrate, in particular pentoses, and low ethanol titers [69]. Aside from yeasts, anaerobic bacteria or filamentous fungi can produce ethanol under anaerobic conditions. Some of them are even cellulolytic. The fungus *Fusarium oxysporum* is a prominent example and 0.43 g ethanol were achieved per g fermentable carbohydrates [194]. This is comparable to yields observed with *S. cerevisiae*. In contrast to the classical CBP approach based on a single, genetically engineered superbug, microbial communities may be employed for the production of ethanol [10].

Table 6.1: Selected literature on biochemical conversion of lignocellulose to ethanol using CBP.

Microorganism(s)	Substrate, conc. [gL ⁻¹]	Product, conc. [gL ⁻¹]	References
<i>Clostridium thermocellum</i> M1570 and <i>Thermoanaerobacterium saccharolyticum</i> ALK2	Cellulose, 92	Ethanol, 38	[195]
<i>Fusarium oxysporum</i> F3	Cellulose, 50	Ethanol, 14.5	[194]
<i>Clostridium thermocellum</i> LL1210	Cellulose, 60	Ethanol, 22.4	[196]
<i>Trichoderma reesei</i> , <i>Saccharomyces cerevisiae</i> , <i>Scheffersomyces stipites</i>	Dilute acid pretreated wheat straw, ¹	Ethanol, 9.8	[10]
<i>Trichoderma reesei</i> , <i>Saccharomyces cerevisiae</i>	Microcrystalline cellulose, 35	Ethanol, 12	This chapter

¹ Initially containing 17.5 gL⁻¹ cellulose.

Brethauer and Studer developed a consortium-based CBP of undetoxified whole slurry dilute acid pretreated wheat straw to produce ethanol [10]. A yield of 67 % of the theoretical maximum was achieved. *Trichoderma reesei* was employed as producer of cellulolytic enzymes. The yeasts *S. cerevisiae* and *Pichia stipites* were inserted as ethanol-producing strains, whereby the latter is mainly responsible for the utilization of pentoses. The three microorganisms were cultivated in a flat-sheet, 32 mL membrane bioreactor [10].

In this chapter, it is demonstrated that the CBP of lignocellulose to ethanol using a microbial community of *T. reesei* and *S. cerevisiae* is also successful when a scaled-up stirred tank membrane-aerated bioreactor is used. The *in situ* degradation of ethanol by aerobic respiration was identified as a challenge and possible approaches are discussed to circumvent such unwanted effects.

6.2 Scaled-up membrane-aerated stirred tank bioreactor

The bioreactors that are used for the community-based CBP of lignocellulose are based on commercially available Labfors 5 bioreactors (Infors, Bottmingen, Switzerland). A stirred tank reactor was selected as it is the most prominent reactor type in industrial applications. The supply of oxygen through a flat-sheet membrane located at one side of the reactor as used in [10] would not be an appropriate geometry for the scaled-up 2.7 liter stirred tank reactors.

Instead of the flat membrane, a tubular membrane made of polydimethylsiloxane (PDMS) was used which was helically coiled around a metal structure (Fig. 6.1). One end of the membrane is connected to a mass flow controller which is connected to a source of compressed air while the other end is open to the environment ('open end approach'). The oxygen permeable membrane is continuously flushed with air to locally introduce oxygen to the fermentation slurry. The reactor is equipped with a helical stirrer suitable to stir media with high-solid loadings (Fig. 6.1). In order to control the biochemical processes probes are installed that monitor pH and the dissolved oxygen content in the fermentation slurry.

The online monitoring of the dissolved oxygen concentration in the liquid phase of the reactor can be used for the determination of the volumetric mass transfer coefficient (k_La). The k_La is the proportionality constant that relates the oxygen transfer rate (OTR) to the difference between the maximum concentration of dissolved oxygen ($C_{O_2}^*$) in a given media and the actual concentration of oxygen (C_{O_2}) in this media at a given temperature.

$$OTR = k_La \cdot (C_{O_2}^* - C_{O_2}) \quad (6.1)$$

Three characteristics of the membrane, i.e. its chemical properties, length and wall thickness, affect the k_La and with that, the OTR . At constant partial pressure of oxygen in the membrane, the k_La is lower when the membrane is made thicker or shorter (Tab. 6.2). Another parameter

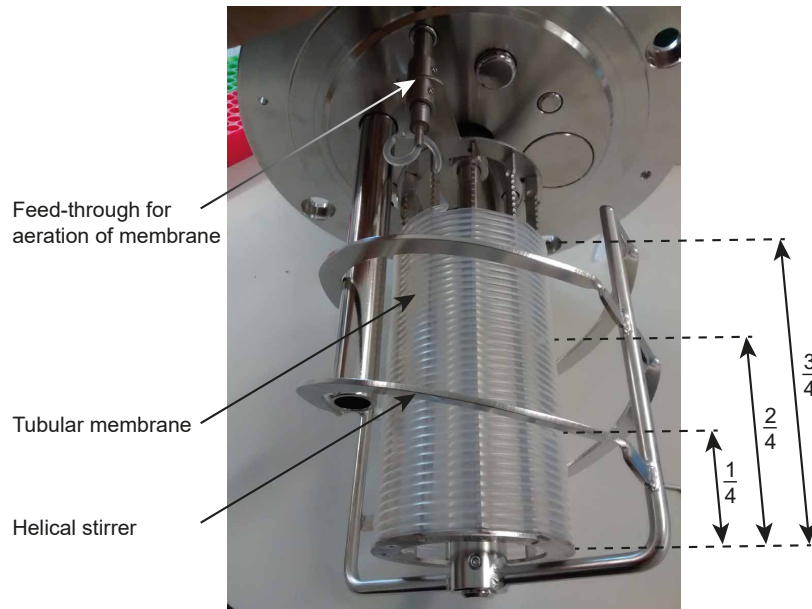


Figure 6.1: **Photograph of the scaled-up membrane-aerated stirred tank bioreactor.** The length of the tubular membrane can be varied as one method to influence the supply of oxygen to the reactor. $\frac{1}{4}$, $\frac{2}{4}$ and $\frac{3}{4}$ correspond to a membrane length of 2.71 m, 5.42 m and 8.13 m, respectively.

Table 6.2: **Volumetric mass transfer coefficients for different properties of the membrane (length, wall thickness) and different oxygen concentrations in air flushed through the membrane.** The reactor was filled to a working volume of 2.7 liter with water and with 0.02 % (w/v) sodium azide to prevent microbial growth. The liquid was stirred at 50 rpm. The maximal oxygen solubility in water was taken from literature ($C_{O_2}^* = 7.53 \text{ mgL}^{-1}$ at 30°C) [197]. The mono-lumen tubing had an outer diameter of 3.18 mm. The fluid was flushed with 140 mLmin^{-1} per liter reactor volume through the membrane. Error bars represent the standard deviation of $n=3$ to $n=7$ independent replicates.

Length, wall thickness of membrane	Oxygen concentration in membrane	$k_L a$ [h^{-1}]	Nomenclature
8.13 m, 0.61 mm	21.0 vol. %	1.08 ± 0.01	$\frac{3}{4}$, thin, 21 % O_2
5.42 m, 0.61 mm	21.0 vol. %	0.46 ± 0.01	$\frac{2}{4}$, thin, 21 % O_2
2.71 m, 0.61 mm	21.0 vol. %	0.28 ± 0.01	$\frac{1}{4}$, thin, 21 % O_2
8.13 m, 0.81 mm	21.0 vol. %	0.57 ± 0.01	$\frac{3}{4}$, thick, 21 % O_2
5.42 m, 0.81 mm	21.0 vol. %	0.34 ± 0.01	$\frac{2}{4}$, thick, 21 % O_2
2.71 m, 0.81 mm	21.0 vol. %	0.20 ± 0.01	$\frac{1}{4}$, thick, 21 % O_2
8.13 m, 0.61 mm	5.3 vol. %	0.28 ± 0.05	$\frac{3}{4}$, thin, 5.3 % O_2
8.13 m, 0.61 mm	10.5 vol. %	0.51 ± 0.08	$\frac{3}{4}$, thin, 10.5 % O_2
5.42 m, 0.61 mm ¹	21.0 vol. %	1.25 ± 0.35	Backpressure
7.02 m, 0.28 mm ²	21.0 vol. %	3.37 ± 0.05	500 mL reactor

¹ Artificial backpressure of 1.1 bar realized with a pressure holding valve mounted to the end of the membrane.

² 500 mL membrane-aerated bioreactor, length of membrane: 7.02 m, outer diameter of 1.19 mm.

which affects the $k_L a$ is the partial pressure of oxygen in the membrane. The increase of the partial pressure of oxygen results in an increased $k_L a$ (Tab. 6.2). The partial pressure can be influenced either by changing the concentration of oxygen in the fluid flushed through the membrane or by increasing the pressure in the membrane. The former can be achieved by addition of oxygen or by dilution with e.g. nitrogen. The $k_L a$ was increased from 0.46 h^{-1} ($\frac{2}{4}$, thin, without backpressure) to 1.25 h^{-1} ($\frac{2}{4}$, thin, with backpressure of about 1.1 bar) by increasing the pressure in the membrane artificially using a pressure holding valve. In order to ensure the same oxygen transfer rate over the length of the membrane the pressure drop over the length of the membrane must be negligible. This requirement is fulfilled in the 2.7 liter bioreactor when a flow rate of approximately 140 mLmin^{-1} per liter reactor volume is used (data not shown).

6.3 Community-based consolidated bioprocessing of lignocellulose to ethanol

For the direct production of ethanol from microcrystalline cellulose as model substrate or from steam-pretreated beech wood via consolidated bioprocessing a two-member community was employed. The aerobic fungus *T. reesei* RUT-C30 was used as producer of cellulolytic enzymes and the facultative anaerobic yeast *S. cerevisiae* VTT C-79095 was used as ethanol-producer. *T. reesei* is deficient in beta-glucosidase production [57]. As demonstrated in the appendix, figure B.2, 0.6 gL⁻¹ of cellobiose accumulated when *T. reesei* grew under axenic conditions in a membrane-aerated reactor. *S. cerevisiae* is unable to use cellobiose, a known inhibitor for cellulolytic enzymes. In order to avoid accumulation of cellobiose 30 CBU of beta-glucoside per g cellulose was added from an external source.

As demonstrated in figure 6.2, the bioreactor is suitable for the co-cultivation of the aerobic fungus *T. reesei* next to the facultative anaerobic yeast *S. cerevisiae*. If the membrane was flushed with air and 17.5 gL⁻¹ microcrystalline cellulose (Avicel) was used as substrate, a concentration of about 5.3 gL⁻¹ ethanol, i.e. 53 % of the theoretical yield, was produced 500 hours after inoculation. If the concentration of the substrate was increased to 35 gL⁻¹, a concentration of up to about 12 gL⁻¹ was achieved 500 hours after inoculation (61 % of the theoretical yield). Ethanol produced in the reactor partially diffused through the membrane and left the reactor via the gas flushed through the membrane. An at-line gas chromatograph allowed the quantification of ethanol that left the system. All ethanol concentrations displayed in this chapter refer to a total concentration in the liquid phase which includes the concentration in the fermentation slurry and the amount of ethanol that left through the membrane [10]. The concentrations of cellobiose and glucose as products of the enzymatic hydrolysis of cellulose were below the detection limit of 0.05 gL⁻¹ throughout the experiment.

The model substrate Avicel was replaced by steam-pretreated beech wood. In both cases an accumulation of ethanol was observed (Fig. 6.2A). After approximately 200 hours, a concentration of about 4.0 gL⁻¹ was demonstrated. Note that the beech wood employed in this experiment was pretreated under sub-optimal conditions, i.e. 1-stage at 230 °C, pretreatment time of 4.7 min. Thus, the result on lignocellulose serves the purpose of proving a concept.

The fungus and the yeast formed a two-layered biofilm on the surface of the aerated membrane with the fungus being in direct contact to the membrane (Fig. 6.2B). The formation of such a biofilm is in line with observations in [10]. The question arises why the yeast forms such high-cell densities close to the local source of oxygen in an otherwise anaerobic environment?

It is known from literature that *S. cerevisiae* is capable to perform both, aerobic respiration and anaerobic fermentation. When the yeast aerobically respire, it regenerates about eight times more ATP and builds up significantly more biomass compared to when it ferments [198]. In such aerobic situations, *S. cerevisiae* can degrade ethanol to water and carbon dioxide. In case of fermentation, the major metabolic end-product is ethanol. One phenomenon in the catabolism of the yeast, called the Crabtree effect [199], is remarkable: *S. cerevisiae* ferments carbon sources in the presence of oxygen if the glucose concentration is above a certain threshold (around 0.15 gL^{-1}) [200,201]. This is because glucose represses the expression of respiratory genes [202].

The measured dissolved oxygen concentration in the fermentation slurry revealed anaerobic conditions despite of continuous supply of oxygen through the membrane. On the other hand, the concentration of glucose was below 0.05 gL^{-1} in the reactor. The accumulation of yeast

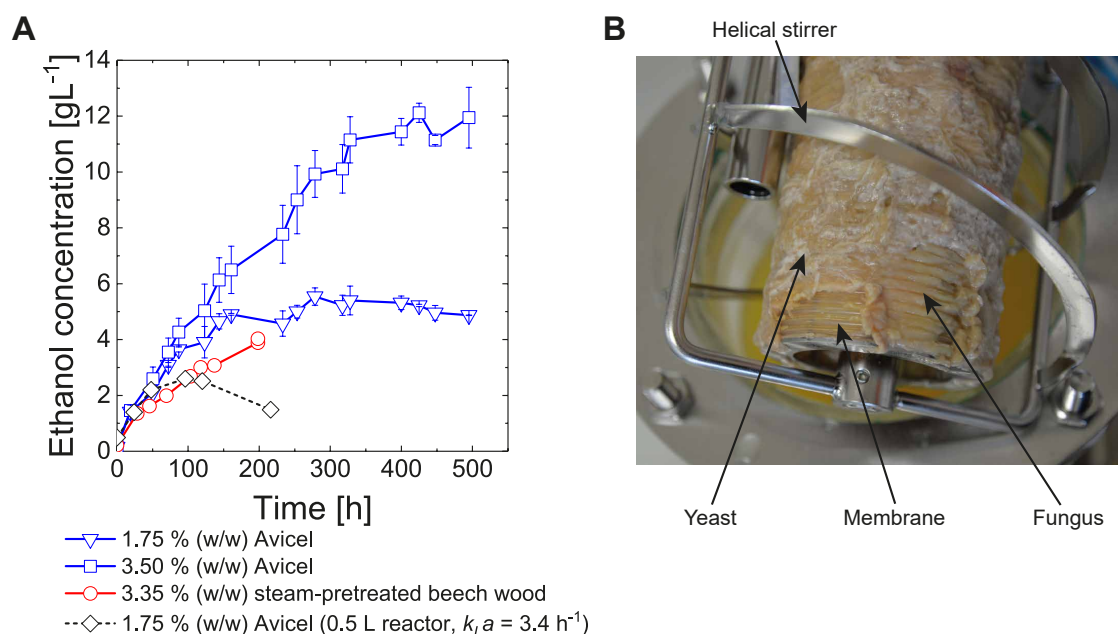


Figure 6.2: Community-based CBP of microcrystalline cellulose for the production of ethanol using the membrane-aerated stirred tank bioreactor. (A) Ethanol concentration as a function of time for different substrate loadings of microcrystalline cellulose and 1-stage, steam-pretreated beech wood. Beech wood was pretreated under non-optimal conditions (230°C , pretreatment time of 4.7 min). The solids were washed and inserted with a solid loading of 3.35 % beech wood which corresponds to a cellulose loading of 1.75 % (w/w). The fungus *T. reesei* was inoculated two days before the yeast was inoculated. If not otherwise stated the 2.7 liter membrane-aerated bioreactor was used with the conditions $\frac{2}{4}$, thick, 21 % O_2 (Tab. 6.2) (solid lines). The 0.5 liter membrane-aerated bioreactor was equipped with an around three times thinner membrane (Tab. 6.2) (dashed line). Error bars represent the standard deviation of two independent experiments. **(B)** Photograph of the two-layered fungal-yeast biofilm which covered the oxygen permeable membrane in the 2.7 liter bioreactor.

cells in a biofilm on top of the fungal biofilm (Fig. 6.2B) could point towards aerobic respiration of *S. cerevisiae* and with that, degradation of ethanol. The *in situ* degradation of ethanol would lower the yields. Thus, towards industrial application our CBP has to be developed further with respect to technological and biological aspects. In the following, a first attempt is made by studying the degradation of ethanol in detail.

A first indication that ethanol can be degraded *in situ* by microbial aerobic respiration was made when a 0.5 liter bioreactor with a 0.28 mm thin, 7.02 m long membrane was used to provide a niche for oxygen. With a k_La of 3.4 h^{-1} the *OTR* is about ten times higher as compared to the 2.7 liter setup. A maximum of only 2 gL^{-1} ethanol accumulated and a decrease in the ethanol concentration was observed after 100 hours (Fig 6.2A).

In further experiments with *T. reesei* and *S. cerevisiae* the oxygen transfer rate across the membrane into the reactor was varied and the concentration of ethanol was recorded (Fig. 6.3A). Results indicate that a lower concentration of oxygen in the fluid flushed through the membrane leads to a higher total concentration of ethanol. With 21.0 vol. % oxygen (highest concentration tested), the maximum concentration of ethanol seems to be reached about 150 hours after inoculation while with lower concentrations of oxygen the concentration of ethanol still increases slightly (Fig. 6.3A). It seems that the rate of production increases with increasing *OTR* which could be explained by a higher activity of the cellulolytic enzymes. In order to verify this assumption the enzymatic activity must be measured in a future experiment. When the oxygen transfer rate was varied by changing the thickness of the membrane wall, it was demonstrated that with thicker membrane, a slightly higher ethanol concentration of maximum 6.3 gL^{-1} was reached compared to a thinner membrane (maximum at 6.0 gL^{-1}). It is assumed that ethanol is degraded throughout both experiments whereby the rate of degradation is higher in the case of the thin membrane. In both cases, a decrease of the total ethanol concentration was observed starting about 200 hours after inoculation (Fig. 6.3B). These results underline the hypothesis that aerobic *in situ* degradation of ethanol occurs. Please note that the results shown in figure 6.3B represent single runs only, except for $\frac{3}{4}$, thin, 21.0 % O_2 .

In order to study the degradation of ethanol by the yeast, simultaneous saccharification and fermentation (SSF) experiments were performed. The production of ethanol from microcrystalline cellulose by either the petite yeast *S. cerevisiae* FYdelta pet191::KanMX4¹ (incapable for aerobic respiration and thus, no degradation of ethanol is expected) or the Crabtree-positive yeast *S. cerevisiae* VTT C-79095 (capable of aerobic metabolism) was examined. In order to test the influence of the oxygen transfer rate on the accumulation of ethanol, experiments with and without aeration using the membrane were performed.

¹Generously provided by Professor Stephen G. Oliver, University of Cambridge [203].

With both yeasts, ethanol accumulated (Fig. 6.4A). However, there is a clear difference in the ethanol concentration. The petite yeast produced similar amounts of ethanol under aerobic and anaerobic conditions. If the Crabtree-positive yeast was cultivated in an anaerobic environment the concentration of ethanol was in a similar range as with the petite yeast. However, under aerobic conditions the ethanol concentration was reduced. These results underpin the assumption that *in situ* degradation of ethanol can be attributed to aerobic metabolism of the Crabtree-positive yeast. As shown in figure 6.4A, degradation of ethanol (difference between the ethanol concentration obtained with the petite yeast and the concentration obtained with the Crabtree-positive yeast) under aerobic conditions happens during the entire experiment with an average rate of ethanol degradation of $0.012 \pm 0.001 \text{ gL}^{-1}\text{h}^{-1}$. According to figure 6.4A, 3.31 g of ethanol was degraded 310 hours after inoculation. Considering the chemical reaction of aerobic ethanol degradation $\text{C}_2\text{H}_5\text{OH} + 3 \text{O}_2 \rightarrow 2 \text{CO}_2 + 3 \text{H}_2\text{O}$, it becomes clear that 2.084 g of oxygen is required to degrade one gram of ethanol and with that, 6.9 g of oxygen is required to degrade 3.31 g of ethanol. In this case, a k_La of about 3 h^{-1} would be required, but the measured k_La for the employed membrane is lower (0.46 h^{-1} , Tab. 6.2). This discrepancy could be partly attributed to parasitic oxygen input from sampling and the sterile filter located on

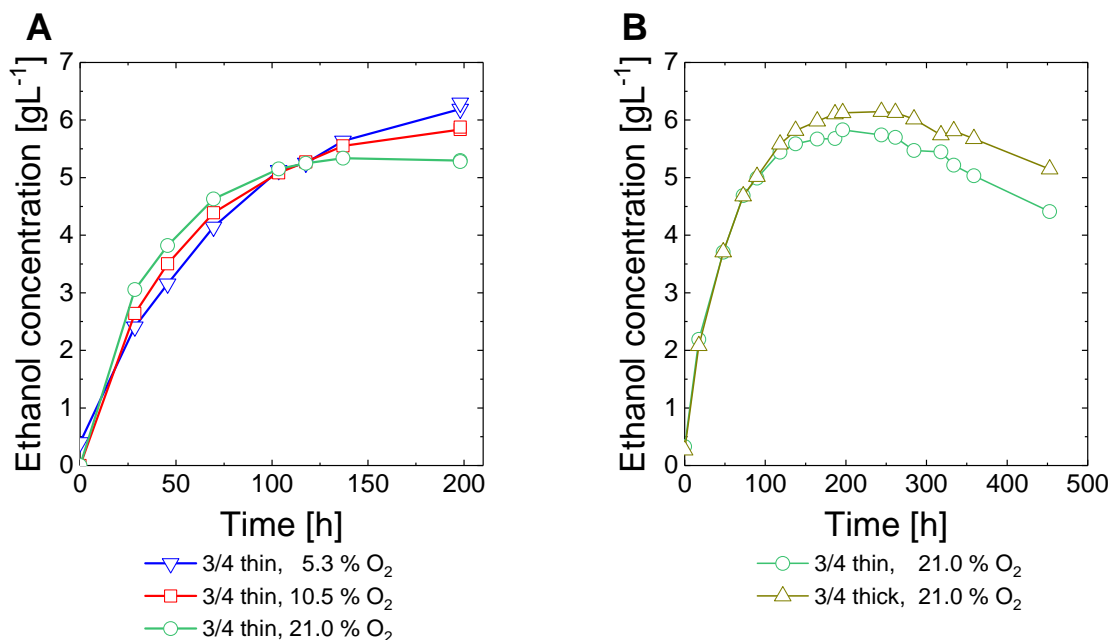


Figure 6.3: **Variation of the oxygen transfer rate and its effect on the consolidated bioprocessing of microcrystalline cellulose to ethanol.** (A) *T. reesei* and *S. cerevisiae* were cultivated in the membrane-aerated bioreactor with a working volume of 2.7 liter. Measured ethanol concentration over time for (A) different oxygen concentrations in the fluid flushed through the membrane using the $\frac{3}{4}$, thin membrane and (B) two different thicknesses of the membrane wall (Tab. 6.2).

top of the lid. As such reasoning does not explain such large difference, further investigations must be conducted in the future to clarify this point. Comparing the ethanol production in a CBP using *T. reesei* in a co-culture with either the Crabtree-positive yeast or the petite yeast an obvious degradation of ethanol was observed only in case of the Crabtree-positive yeast (Fig. 6.4B). This is in line with the results shown in figure 6.3B.

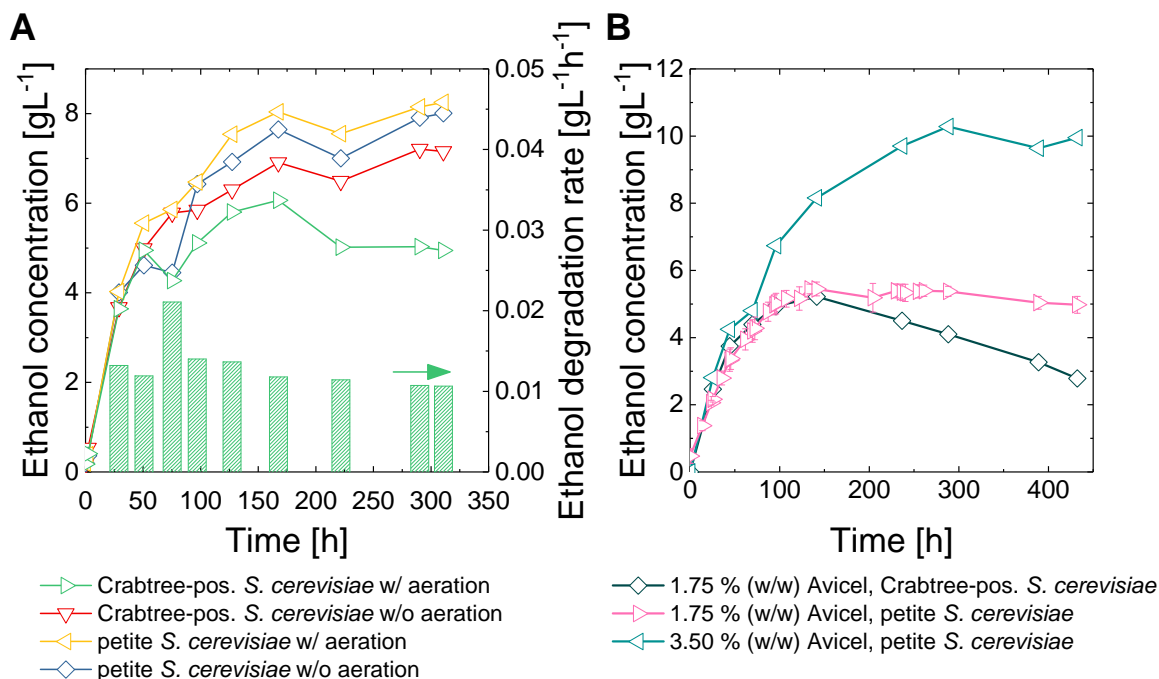


Figure 6.4: **Comparison of ethanol production using the Crabtree-positive yeast *S. cerevisiae* VTT C-79095 and the petite yeast *S. cerevisiae* FYdelta pet191::KanMX4 in SSF and CBP of microcrystalline cellulose. (A)** SSF process on 1.75 % (w/w) microcrystalline cellulose with 15 FPU per g of cellulose Accellerase © 1500 kindly provided from DuPont (Wilmington, United States of America). The Crabtree-positive *S. cerevisiae* yeast and the petite yeast were cultivated under aerobic and anaerobic conditions using the $\frac{2}{4}$, thin, 21 % O₂ setup. The shown degradation rate of ethanol was calculated for aerobic conditions by subtracting the ethanol concentration obtained with the petite yeast from the concentration obtained with the Crabtree-positive yeast. **(B)** Consolidated bioprocess of two different concentrations of microcrystalline cellulose to ethanol using *T. reesei* and either the Crabtree-positive yeast *S. cerevisiae* or the petite yeast.

6.4 Conclusions

The results discussed in this chapter demonstrate that ethanol can be produced from lignocellulose using community-based consolidated bioprocessing in 2.7 liter stirred tank membrane-aerated bioreactors. The use of reactors that are commonly used in industrial processes is

beneficial for further scale-up. However, the observed *in situ* degradation of ethanol is one major challenge aside from productivity and product concentration on the way to industrial applications. It was shown that the degradation process could be attributed to aerobic metabolism of the yeast *S. cerevisiae*. Several strategies were demonstrated to alter the volumetric mass transfer coefficient (k_La) and with that, the oxygen transfer rate across the membrane into the reactor. Preliminary experiments point towards a higher ethanol concentration with decreasing k_La when employing the Crabtree-positive yeast, achieved either with increased wall thickness of the membrane or lower concentration of oxygen in the fluid flushed through the membrane. It was demonstrated that another option to omit degradation by the yeast is to employ a petite yeast, which is not capable of aerobic degradation of ethanol. When it can be verified in future experiments that a higher rate of hydrolysis can be achieved by increasing the oxygen transfer rate, it is suggested to use the petite yeast in a high *OTR* approach to overcome low productivities and to improve ethanol concentrations.

In order to omit addition of costly beta-glucosidase it is suggested that *S. cerevisiae* is replaced with a yeast that is able to utilize cellobiose. Another option would be to add another fungus such as *Aspergillus phoenicis* to compensate the lack of beta-glucosidases in the enzymatic cocktail produced by *T. reesei* RUT-C30 [204].

CHAPTER 7

Towards a wider product range with an advanced membrane-aerated bioreactor

In this chapter a novel membrane-aerated bioreactor is motivated that tackles limitations of the reactors used in all experiments described in previous chapters for the production of carboxylic acids and ethanol. The advanced reactor setup is described and the feasibility of add-ons is demonstrated in preliminary experiments. The advanced bioreactor is applied to co-cultivate the fungus *T. reesei* and the microalgae *Chlamydomonas reinhardtii*. On the long term, this could pave the way for lipid production from lignocellulosic biomass via a cost-efficient community-based CBP.

Parts of this chapter are included in a patent application: R. L. Shahab, M. H. Studer *A method for the microbial production of short chain fatty acids and lipids* (DE 10 2018 206 987.5).

7.1 Motivation to engineer an advanced membrane-aerated bioreactor

In the beginning of this PhD a commercially available stirred tank bioreactor was purchased and equipped with a membrane. This reactor was employed to produce various carboxylic acids and ethanol in a CBP of lignocellulosic biomass using defined microbial communities (chapter 3-6). It is highly desirable to widen the product range which requires engineering of the microbial community. In order to co-cultivate multiple microorganisms with non-overlapping requirements for abiotic parameters in one vessel and to avoid the law of competitive exclusion sufficient spatial or metabolic niche differentiation must be provided. In nature, thousands of microorganisms co-exist and form complex ecosystems. These ecosystems are characterized by a variety of gradients of different abiotic parameters which enable the growth of different

microorganisms in spatial closeness. The reactor used so far enabled the co-cultivation of aerobes and strict anaerobes in one vessel by providing a local source of oxygen via the aerated membrane. The novel reactor concept is based on inhomogeneities which is in contrast to the common trend of homogeneous conditions in stirred tank reactors used in other processes. Relevant abiotic parameters for niche differentiation are nutrients (e.g. oxygen), temperature, pH and light. Gradients of those would allow the cultivation of e.g. thermophilic microorganisms next to psychrophilic microorganisms or alkaliphilic microorganisms next to acidophilic microorganisms.

A temperature gradient does not only provide a niche for microorganisms with non-overlapping temperature tolerances but could also be beneficial to tackle the identified challenge of a low productivity and long process times of up to 1000 hours which is a key challenge on the way towards industrial applications (e.g. Fig. 5.1 or 5.2). The rate limiting step in the consortium-based CBP was identified to be the enzymatic hydrolysis as after the inoculation of *L. pentosus* in all experiments the concentration of glucose and cellobiose was below the detection limit of 0.05 gL^{-1} (e.g. Fig. B.2). The activity of the secreted enzymes by *T. reesei* is highest at about 50°C . The growth rate of the mesophilic fungus *T. reesei* peaks at a temperature of about 30°C . Since the fungus does not tolerate 50°C , the consolidated bioprocess using *T. reesei* is performed under conditions which are suboptimal for the enzymatic hydrolysis. A temperature gradient could allow to overcome this hurdle.

With the reactor design used so far, it was required to harvest the entire reactor to analyze the biofilm which formed on the surface of the aerated membrane (Fig. 4.3). The procedure is not only time-consuming but also limits insights into the development of the biofilm over time. It would be desirable to take multiple samples of the biofilm from one reactor throughout the course of one experiment. The novel reactor should be based on standardized components such as fittings, ports and magnetic couplings to facilitate and reduce maintenance and to provide flexibility with respect to design configurations. Furthermore, commercially available sterile sampling devices are not compatible with high solid loadings because the particles tend to clog the widely used unidirectional valves, which allow fluids to flow through only in one direction. The novel reactor should allow sampling at high solid loadings. Finally, in case of a power outage, the system should be able to automatically reboot and in contrast to the various commercially available bioreactor systems to continue to control the bioprocess.

As shown in chapters 4 and 6, the oxygen transfer rate (*OTR*) greatly affects the formation of butyric acid or ethanol in the CBP of lignocellulose (Fig. 4.5 or 6.3). According to the first Fick's law diffusion is proportional to a concentration gradient with the diffusion coefficient as proportionality constant. Diffusion of oxygen across the polydimethylsiloxane membrane flushed with air depends on the membrane thickness and length. The drawback is that these

properties are selected at the beginning of each experiment and are fixed hereafter. This prevents *in situ* control of the *OTR*.

A major limitation of the bioreactor used so far is that air is flushed through the membrane once and released to the environment. Furthermore, in order to enable a constant *OTR* over the entire length of the membrane, a high gas flow rate of 140 to 160 mLmin⁻¹ per liter liquid phase was chosen in previous experiments (Fig. B.1). This is costly, because compressed air is a major cost driver in aerobic processes. It would be desirable to reuse the gaseous fluid and provide online control of the *OTR*.

7.2 Overview of setup of advanced membrane-aerated bioreactor

In the framework of this PhD work a membrane-aerated bioreactor was designed and constructed that solves limitations of the reactors used in chapter 3 to 6. The entire setup is displayed in figure 7.1.

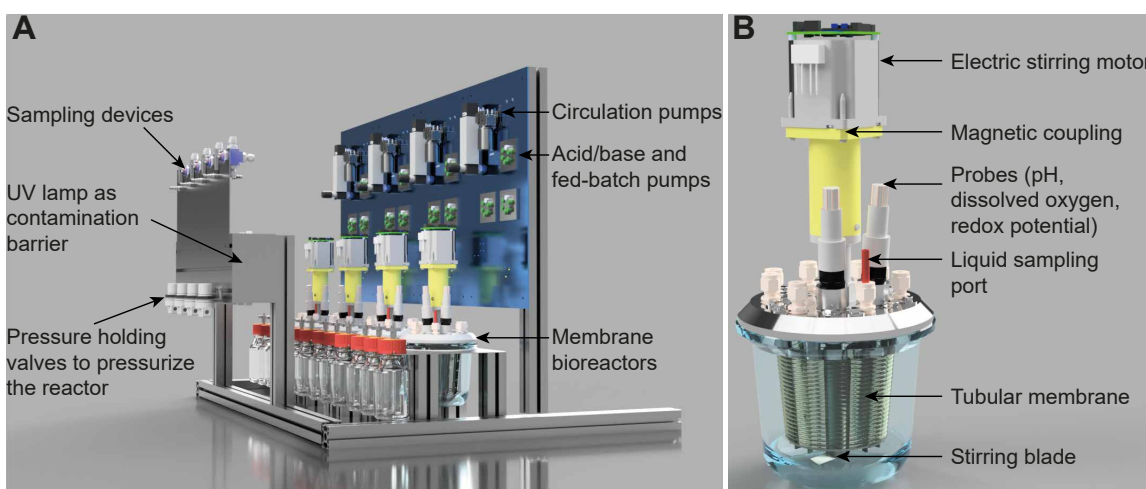


Figure 7.1: **Schematic representation of advanced membrane-aerated bioreactor.** (A) Overview of bioreactor rack with periphery. Tubes are not displayed for visibility. (B) Single bioreactor with labeled components. The shown configuration is to a great extent modular. For example the stirrer can be exchanged with a helical stirrer for high solid loadings.

In total, four identical bioreactors were fabricated to enable several experiments in parallel. The basic design of the engineered bioreactor follows the design of standard bioreactors for sterile cultivations. The working volume of each glass vessel is one liter. The tubular membrane is helically coiled onto a metal structure and flushed with an oxygen-containing fluid. Multiple membrane sampling loops are installed in the lid which are connected in series with the main

membrane mounted to the metal structure in the center (Fig. 7.2). These loops can be removed under sterile conditions in a laminar flow cabinet to allow for a time-resolved characterization of the biofilm. Each reactor is equipped with a stirrer that is moved by an electric motor located above the lid. Aside from the port for the stirrer, the lid is equipped with other uniform ports for probes for measurement of pH, redox potential and dissolved oxygen concentration. Acid-, base- and fed-batch pumps are mounted onto the back plate of the setup and controlled. The pumps are used to control pH and nutrient supply in the reactor and are controlled with a computer. All components are chosen such that they withstand the autoclave temperature of 121 °C.

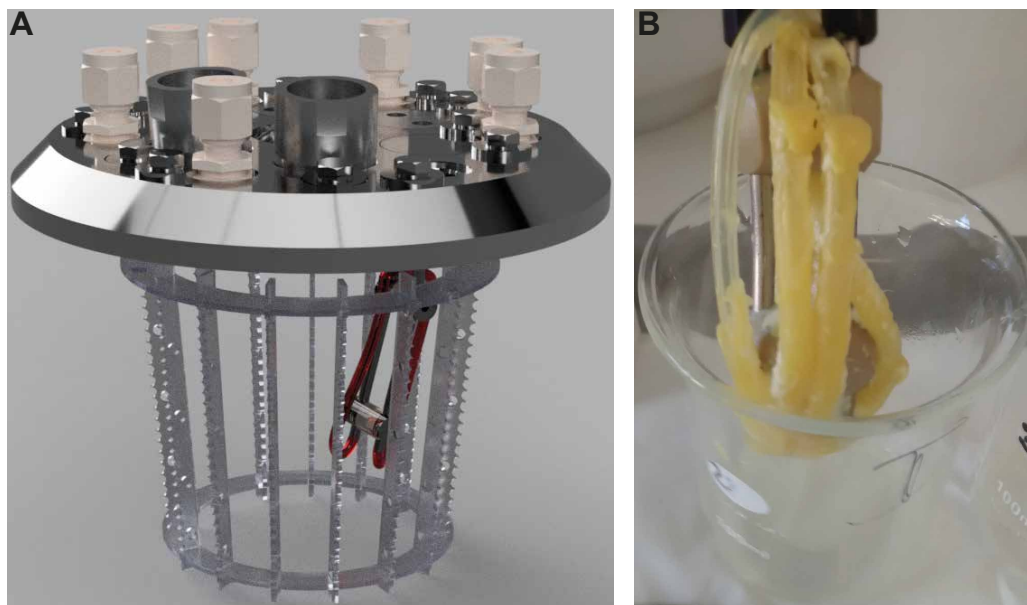


Figure 7.2: **Schematic representation and photograph of membrane sampling loop.** (A) Schematic representation of reactor lid with integrated membrane sampling loop (red). (B) Photograph of sampling loop covered with mature biofilm of *T. reesei* 23 days after inoculation grown on microcrystalline cellulose and Mandel's medium.

In order to collect samples from the fermentation slurry a UV sampling device was designed (Fig. 7.3). A UV lamp emitting at 200 to 300 nm acts as barrier for microbial contaminations of the fermentation broth. The tubing inside the lamp is made of UV transparent quartz glass. The device also contains a dip tube, a three-way plug valve, a sterile filter and a sampling loop. This setup allows sampling of solutions that contain biomass particles with a size in the millimeter range without blockage of sampling tubes. The sampling procedure is as follows: The sampling loop is filled with two to four milliliter of fermentation slurry. The three-way plug valve is turned and sterile gases are used to push the liquid in the tubing between the valve and the reactor back into the reactor. The valve is turned again and the sampled slurry

in the loop is extracted by passing the UV barrier. The slurry which is simultaneously pulled again into the tubing before the valve is pushed back with gas a second time. Then the UV-lamp is turned back on.

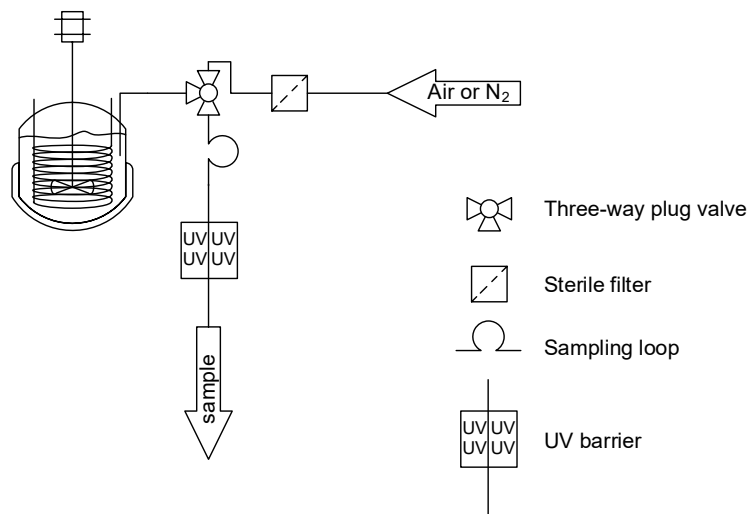


Figure 7.3: Piping and instrumentation diagram of UV sampling device for sterile extraction of the fermentation slurry. All components are autoclavable. Figure can also be found in [205].

7.3 Circulation of fluid for *in situ* control of oxygen transfer rate and cooling of biofilm

In the advanced bioreactor, the gaseous fluid which is flushed through the membrane is circulated in a closed system with a pump (Fig. 7.4). Oxygen is lost through diffusion into the reactor where it is consumed by the fungus acting as oxygen sink. An expansion vessel (oxygen-impermeable bag (Convar Europe, Rochester, United Kingdom)) is integrated into the circuit to buffer volume changes of the gas. The oxygen level in the expansion vessel is monitored with an oxygen meter. Oxygen from an external source (air or gas bottle) can be added on demand which is regulated by an electromagnetic valve. By circulation of the gaseous fluid, costs for compressed air and other gases can be reduced compared to the 'open end approach' without circulation. The oxygen concentration in the fluid can be adjusted online which affects the *OTR* and with that, the metabolic activity of oxygen-consuming microorganisms in the reactor can be controlled.

To demonstrate the feasibility of the circulation approach for online control of the *OTR* a test setup was built according to figure 7.4A. In order to quantify the diffusion of oxygen across the membrane into the reactor (from gas phase into liquid phase) the volumetric mass transfer

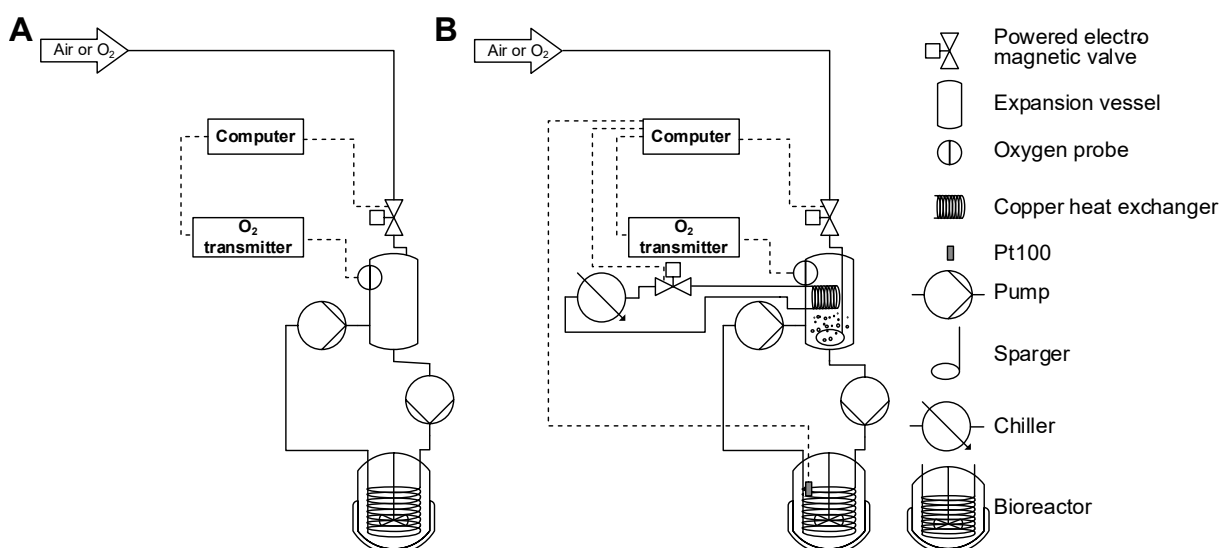


Figure 7.4: **Piping and instrumentation diagram of circulation approach.** Circulation of fluids in the advanced bioreactor for (A) *in situ* control of oxygen transfer rate and (B) additional cooling of biofilm. Parts of this figure can also be found in [205].

coefficient ($k_L a$) was determined for different conditions. When the circulation pump was used to purge the thick membrane (length $\frac{3}{4}$) with air the $k_L a$ was similar ($0.53 \pm 0.01 \text{ h}^{-1}$) as compared to the setup without circulation pump and with compressed air (Tab. 6.2, $\frac{3}{4}$, thick, 21 % O₂) which shows that the influence of the pump on the $k_L a$ is neglectable. As can be seen in figure 7.5, circulating a gas with increased oxygen concentration increases the $k_L a$ (31.5 vol. %: $0.68 \pm 0.02 \text{ h}^{-1}$, 42 vol. %: $0.95 \pm 0.02 \text{ h}^{-1}$). A similar effect can be achieved when a backpressure is applied to the open end of the membrane to increase the partial pressure of oxygen (Tab. 6.2). In another version of the circulation system the expansion bag is replaced by a pressure resistant vessel which allows to pressurize the entire circulation loop. This is in particular essential if the bioreactor is set under pressure as discussed below.

The circulation approach offers another possibility: it can be used to cool the biofilm when heat is locally discharged from the reactor or to heat the biofilm when heat is locally charged to the biofilm in both cases using the fluid flushed through the membrane (Fig. 7.4B). Such an add-on would allow the co-cultivation of psychrophilic and mesophilic microorganisms as exemplified in figure 7.6A. For the implementation, the gaseous fluid (e.g. air) should be replaced by a liquid (e.g. water) because the specific heat capacity of air is more than four times lower than that of water [206]. The liquid must be selected such that it provides oxygen for *T. reesei*, i.e. oxygen must be soluble in the liquid to some extent. To insert oxygen into the liquid a sparger is installed in the expansion vessel (Fig. 7.4B). In order to control the temperature in the biofilm, a heat exchanger is placed in the expansions vessel to cool the circulating fluid. Pt100 devices are installed at different depths of the biofilm and a computer-controlled electromagnetic

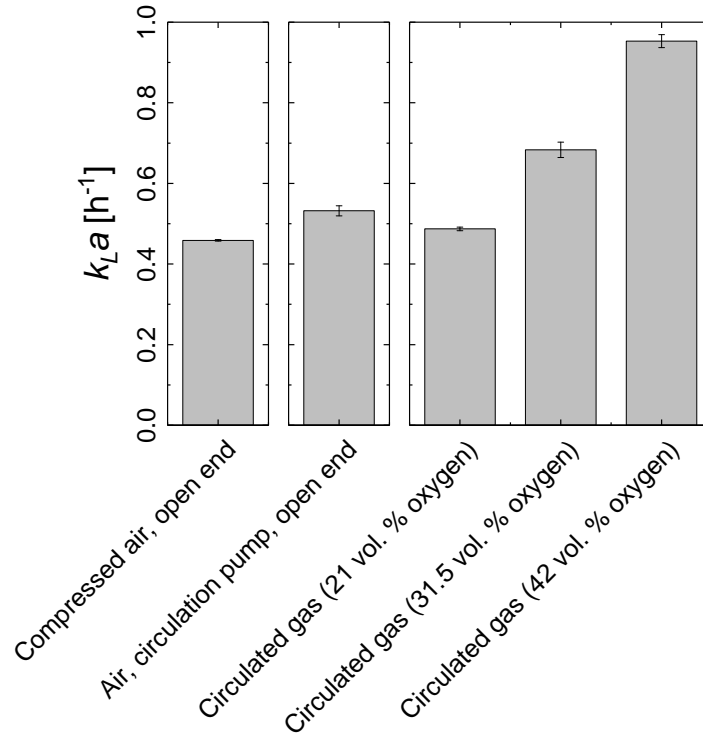


Figure 7.5: **Measured $k_L a$ values in circulation system.** The $k_L a$ value can be influenced by the oxygen concentration in the membrane in the circulation approach. Two values correspond to the 'open end' approach discussed in section 6.2. The reactor was filled to the working volume with water. Sodium azide (0.02 % (w/w)) was added to prevent microbial growth. The helical stirrer was used at 50 rpm. The temperature was set to 30 °C and the maximal oxygen solubility in water was assumed to be 7.53 mgL^{-1} [197]. The flow rate was 140 mLmin^{-1} per liter liquid phase. Mono-lumen tubing 1.98 mm×3.18 mm×0.61 mm with a length of approximately 5.4 meters was used. Error bars represent the standard deviation of $n=3$ to $n=7$ independent replicates.

valve opens on demand to discharge heat to the secondary cooling circuit. The temperature gradient realized by cooling of the membrane provides a local niche for e.g. psychrophilic and mesophilic microorganisms. When the biofilm is cooled locally, the fermentation broth can be heated to e.g. 50 °C for improved rate of enzymatic hydrolysis without harming e.g. the mesophilic fungus *T. reesei*. To this end, heat jackets are wrapped around the reactor vessels. The temperature in the fermentation slurry is monitored with Pt100 devices and adjusted to reach the desired set point. If, for example, the thermophilic genetic modified microorganism *P. furiosus* [207] is inserted into the lactate platform developed in this thesis, the CBP of lignocellulose and carbon monoxide via butyric acid to butanol would be possible. Another promising community that would profit from the temperature gradient is composed of *T. reesei*, a thermophilic homoacetogen and a psychrophilic, acetic acid consuming microalgae or

bacterium. As last example, in order to enhance the productivity for the production of ethanol from ligocellulosic biomass the temperature-sensitive yeast *S. cerevisiae* could be replaced with the thermotolerant yeast *Kluyveromyces marxianus* [208].

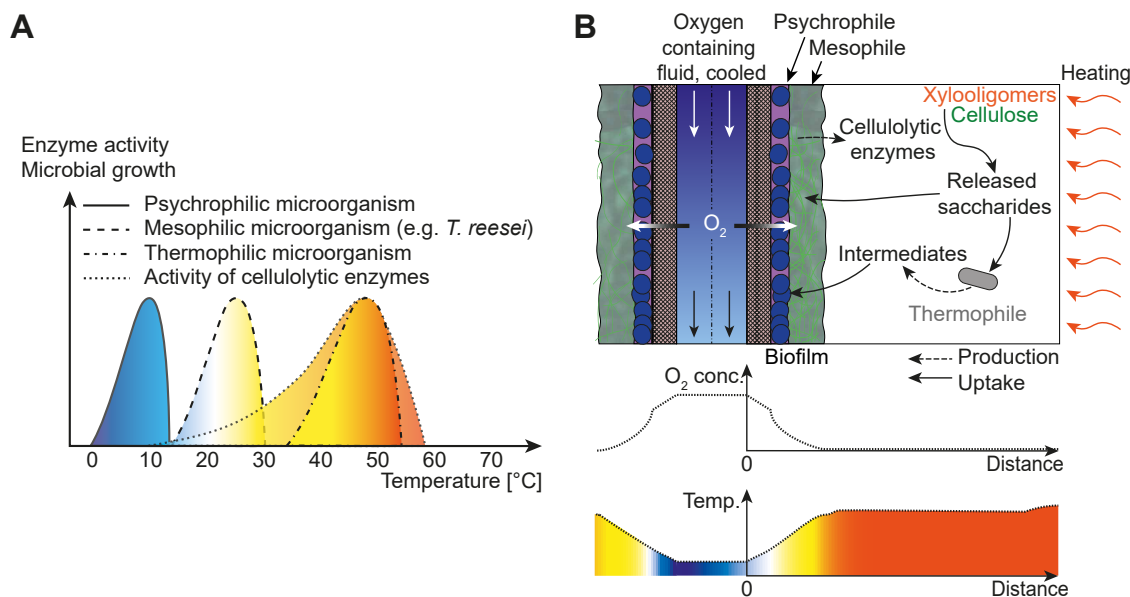


Figure 7.6: **Schematic representations of temperature tolerances of microorganisms and cellulolytic enzymes and formation of a temperature gradient in the membrane-aerated bioreactor.** (A) Approximated microbial growth curves of psychrophilic, mesophilic and thermophilic microorganisms and the activity of cellulolytic and hemicellulolytic enzymes as function of the temperature. (B) Formation of an oxygen and temperature gradient by flushing the membrane with an oxygen containing, cooled fluid and creation of spatial niches for psychrophilic, mesophilic and thermophilic microorganisms.

7.4 pH gradients

In order to integrate alkaliphiles such as *Bacillus* strains and/or acidophiles next to neutrophiles in a community-based CBP of lignocellulose it is necessary to create pH niches. As demonstrated in the following the membrane-aerated bioreactor offers the possibility to alter the pH locally. One strategy is based on purging a fluid through the membrane which contains molecules which can pass the membrane and affect the pH of aqueous solutions in the reactor. Another approach is based on electrolysis of water.

In order to show the feasibility of the former approach two experiments were performed in a stirred tank reactor with an uncovered membrane to locally increase and decrease the pH, respectively. The pH can be increased by circulating an ammonia solution through the membrane using the circulation setup. Using a 10 % (w/w) NH₃ solution the pH in the liquid

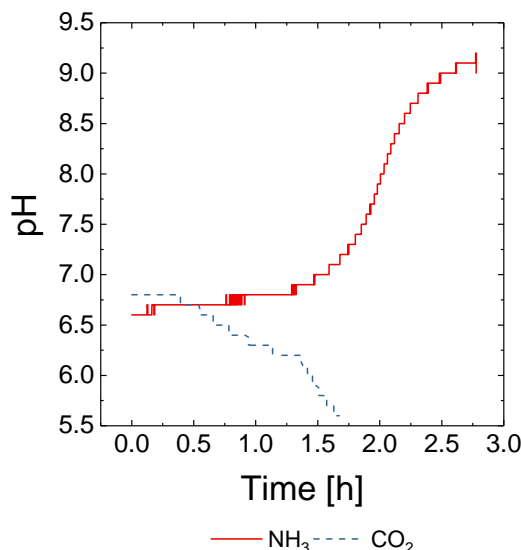


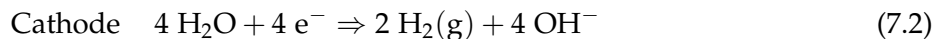
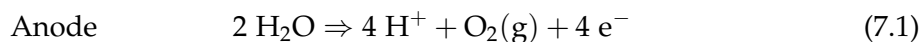
Figure 7.7: **Tuning the pH in the membrane bioreactor by flushing NH_3 solution or CO_2 through the membrane.** Time-resolved pH in 200 mL aqueous solution stirred at 300 rpm with a magnetic stir bar at room temperature. Three meters of the tubular polydimethylsiloxane membrane (inner diameter 1.58 mm, outer diameter 3.18 mm, wall thickness 0.81 mm) were located in the liquid. A 10 % (w/w) NH_3 solution was continuously flushed through the membrane at 368 mLmin^{-1} to achieve alkaline conditions (red, solid) or the membrane was pressurized with carbon dioxide to 1.2 bar to achieve acidic conditions (blue, dashed).

phase of the reactor increased steadily from slightly acidic (pH 6.8) to alkaline (pH 9.0) in approximately 2.5 hours which indicates that NH_3 molecules passed the membrane (Fig. 7.7). NH_3 molecules acquire hydrogen ions from water and produce ammonium ions (NH_4^+) and a hydroxide ion (OH^-). As a result, the pH increases.

In order to lower the pH in the reactor the membrane was pressurized with carbon dioxide to 1.2 bar in a dead-end approach (one end of the membrane closed). The pH decreased from slightly acidic (pH 6.8) to acidic (pH 5.5) after about 1.5 hours (Fig. 7.7). This indicates that CO_2 molecules passed the membrane and formed carbonic acid in the aqueous solution.

Another option to alter the pH locally in the reactor is based on the principle of electrolysis of water. Electric energy can be used to split water whereby the following reactions take place at the electrodes. Two water molecules react at the anode and form four protons, one oxygen molecule and four electrons (Eq. (7.1)). At the cathode four water molecules react with four electrons and form two hydrogen molecules and four hydroxide ions (Eq. (7.2)). The

formed protons and hydroxide ions affect the pH in the vicinity of the anode and the cathode, respectively.



A test setup was built to demonstrate the feasibility to use electricity to create a spatial pH gradient in the bioreactor. To this end, a test vessel which is identical to the one used in the advanced bioreactor was equipped with two electrodes. The aqueous 15 gL^{-1} agarose solution was used to mimic the biofilm as both have a high content of water and are highly viscous. In order to increase the electric conductivity 1 gL^{-1} sodium chloride was added to deionized water. Such a salt concentration is typical for standard cultivation media. The pH indicator bromothymol blue was added to visualize pH changes (Fig. 7.8). The pH was set to either pH 4.0 (Fig. 7.8A) or pH 9.0 (Fig. 7.8C). When a constant voltage of 3 V was applied across the electrodes bubbles appeared at the electrodes which indicated the process of the electrolysis. As expected, the pH at the anode decreased while it increased at the cathode in both experiments (Fig. 7.8). With time, circular areas around the electrodes indicate the expansion of the formed hydroxide ions and hydrogen ions, respectively. A wide range of pH was realized ranging from highly acidic (below pH 4) to highly alkaline (above pH 12).

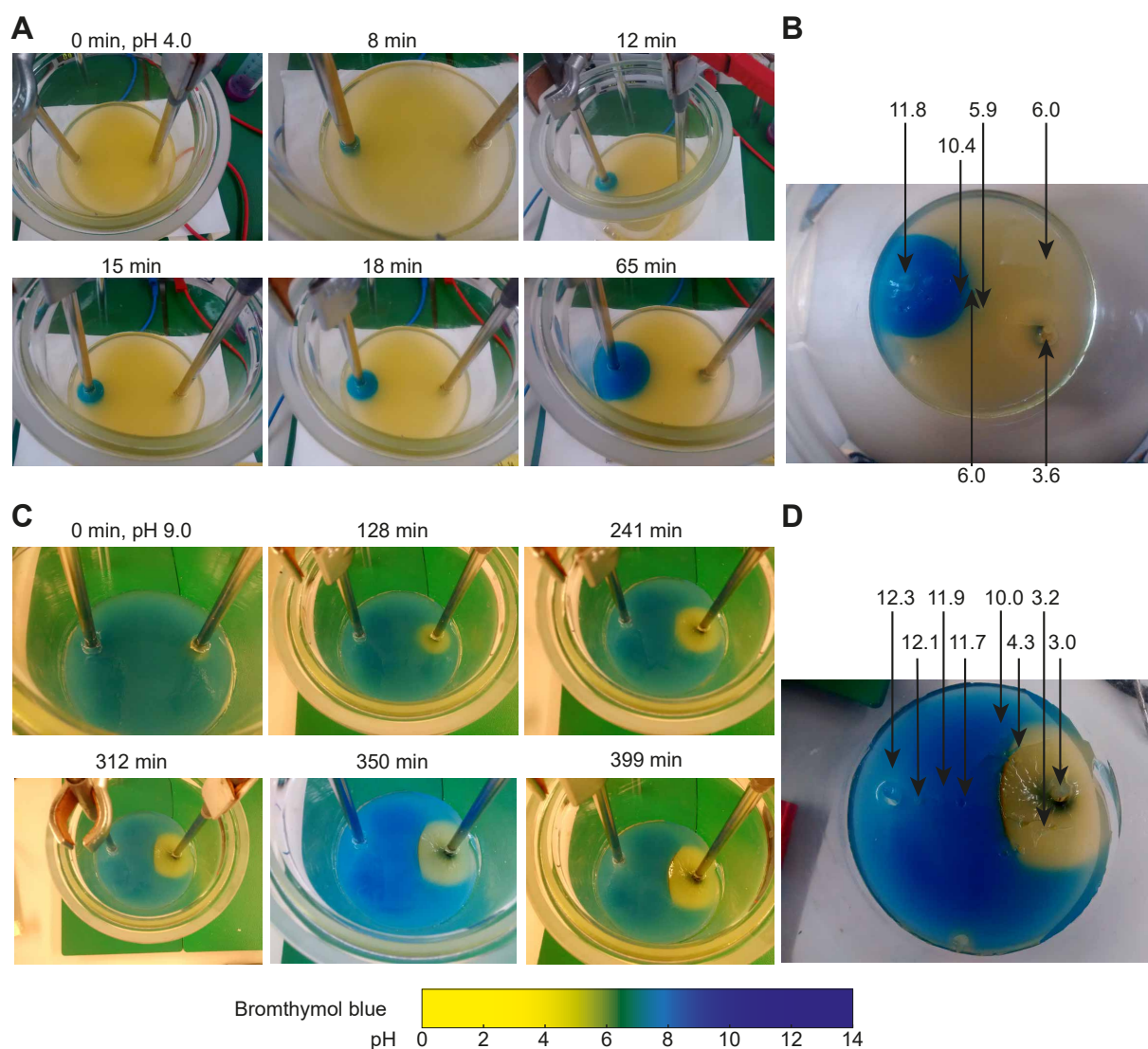


Figure 7.8: Time-resolved formation of a spatial pH gradient in a solid water/agarose/sodium chloride mixture in a bioreactor exploiting electrolysis of water at two electrodes. Two experiments with different starting pH of 4.0 (**A,B**) and 9.0 (**C,D**) were performed. Electrodes made of V4A stainless steel tubes (outer diameter: 8 mm, inner diameter: 6 mm) are installed in the bioreactor 8 cm apart from each other. A constant voltage of 3.0 V is applied across the electrodes and the current is limited to 0.1 A. After (**B**) 65 minutes and (**D**) 399 minutes of applied voltage the pH was measured at various spots. Bromothymol blue was used as pH indicator. Agarose 15 gL^{-1} , sodium chloride 1 gL^{-1} .

After forming successfully a pH gradient in the whole reactor the next test experiment targeted the formation of a pH gradient locally in a biofilm-mimicking agarose gel (15 gL^{-1} agarose) which covered the cathode. The test vessel was filled with bromothymol blue stained water with 1 gL^{-1} sodium chloride (without agarose) and the pH was set to 4.1. Two electrodes were located in the fermenter, but only the cathode was covered with the biofilm-mimicking mixture

(Fig. 7.9). The uncovered anode was located 8 cm apart from the cathode in the bioreactor. A magnetic stirrer was used to continuously stir at 300 rpm. As can be seen in figure 7.9 the biofilm-mimicking bromothymol blue located in the agarose matrix covering the cathode experienced a color change indicating a gradual change in pH starting at 4.1 and increasing to 11.0 with time. The change of the pH in the liquid is neglectable. As the same amount of H^+ and OH^- was formed at anode and cathode (Eq. (7.1) and (7.2)), respectively, but the volume of the 'biofilm' (about 50 mL) was much smaller than the volume of the liquid (about 1 L), the change in pH is stronger in the 'biofilm' than in the stirred liquid. The next step would be to enable online control of the pH in the biofilm by embedding microsensors for pH measurements in the biofilm and to process the signal to regulate the voltage across the electrodes. Furthermore, both electrodes could be covered with a biofilm to provide two niches with extreme pH values at the electrodes and an intermediate pH value in the stirred liquid between the electrodes.

Summarizing, both approaches to locally alter the pH in the bioreactor, either by flushing the membrane with fluids such as CO_2 or NH_3 solution or by using electricity to split water, appear to be promising strategies to create local pH niches and with that, to widen the microbial community and extend the product range.

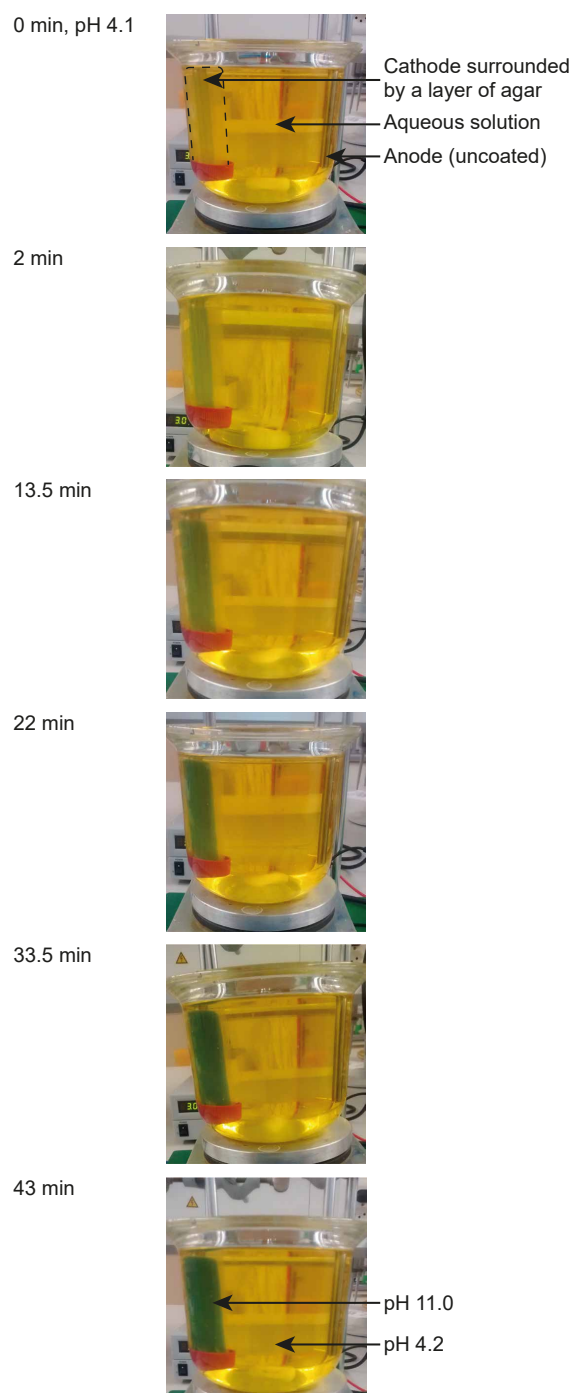


Figure 7.9: **Time-resolved formation of a pH gradient in a biofilm-mimicking agarose coating on the cathode.** The cathode was covered with an agar layer made of bromothymol blue stained water/agarose/sodium chloride mixture, the anode was uncovered. Both electrodes are located in a water/sodium chloride solution stained with bromothymol blue with an initial pH of 4.1. The electrodes are made of V4A stainless steel tubes (outer diameter: 8 mm, inner diameter: 6 mm) which are installed 8 cm apart from each other. A constant voltage of 3.0 V is applied across the electrodes and the current is limited to 0.1 A. The reactor was stirred at 300 rpm using a magnetic stirrer. 15 gL^{-1} agarose, 1.0 gL^{-1} sodium chloride. The pH-dependent color schema of bromothymol blue can be seen in figure 7.8.

7.5 Towards lipids from cellulose: Light for co-cultivation of microalgae and fungus

Microalgae can produce lipids in form of triacylglycerides (TAG) which have various applications e.g. as source of polyunsaturated fatty acids for human nutrition and feed for aquacultures or as precursors for the production of biodiesel. Most microalgae grow autotrophically, which means that light provides the required energy to fix carbon from carbon dioxide. However, in scaled-up photo-bioreactors it is challenging to efficiently illuminate microalgae and to prevent self-shading which results in low cell densities and reduced volumetric productivities [209]. It is valuable that microalgae can also grow on organic carbon sources such as acetic acid or carbohydrates in the absence of light when oxygen is present (heterotrophic growth). When microalgae grow on light and carbohydrates or acetic acid the mode of growth is called mixotrophic. Heterotrophic and, in particular, mixotrophic metabolism allows for higher growth rates, higher biomass density and higher lipid content compared to autotrophic growth [210]. Furthermore, the fitness of microalgae that grow heterotrophically in darkness is lower than that of microalgae that grow mixotrophically because light, in particular wavelengths between 420 to 470 nm (blue) and 660 to 680 nm (red), induces cell division and gene expression among others [211,212].

It would be highly desirable to cultivate microalgae mixotrophically on renewable lignocellulosic waste materials from agriculture and forestry. However, the use of lignocellulose as substrate for microalgal growth is challenging as a majority of microalgae is non-cellulolytic. One possibility to address this challenge is to incorporate microalgae into the lactate platform to allow the production of microalgal metabolites from lignocellulose using the community-based CBP approach (Fig. 7.10). A promising implementation would be as follows. In line with the principle of labor division a fungus produces cellulolytic enzymes for the community which catalyzes the enzymatic hydrolysis of cellulose and hemicellulose to monomeric hexoses and pentoses. These monomers are used by lactic acid bacteria to produce lactic acid (chapter 3). Homoacetogens such as *A. woodii* or *M. thermoacetica* (section 7.3) convert lactic acid to acetic acid which is an excellent and wide-spread substrate for the heterotrophic growth of microalgae.

In order to co-cultivate microalgae together with a fungus and bacteria niches must be engineered in the reactor. In order to profit from mixotrophic growth the niche for the microalgae must provide oxygen and organic carbon (e.g. acetic acid) as well as light and carbon dioxide. In the membrane-aerated bioreactor oxygen is supplied locally through the membrane. The measured dissolved oxygen content in the liquid phase is below the detection limit of 4 ppb when the membrane is covered with the biofilm formed by *T. reesei* (Fig. 4.4 and section 5.3.1).

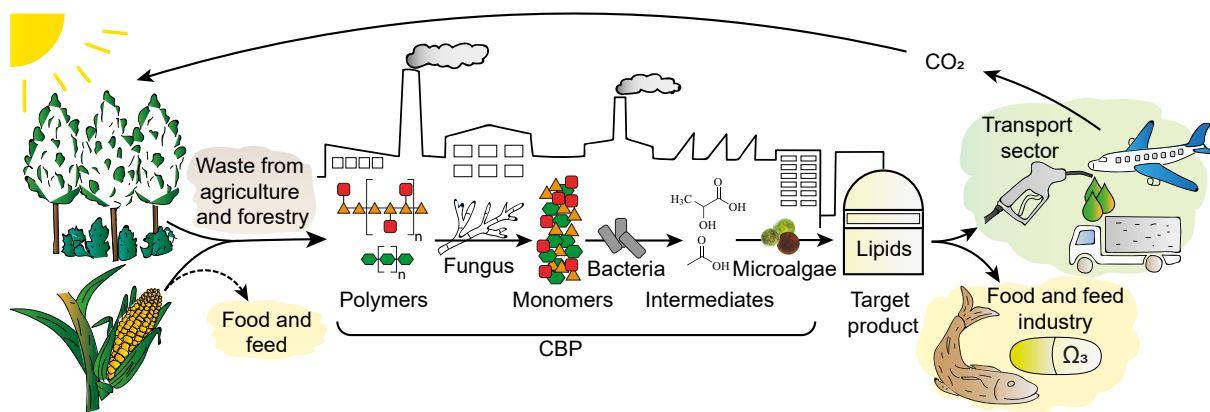


Figure 7.10: Schematic representation of the CBP of lignocellulosic waste materials from agriculture and forestry to lipids using the lactate platform together with microalgae.

Thus, light must be provided in physical closeness to the membrane. In contrast to the communities studied so far, the fungus has a competitor for oxygen, i.e. the microalgae. Thus, the formation of a mixed fungal-microalgal biofilm is essential to achieve the desired community-based CBP. Literature on biofilms based on cellulolytic fungi and microalgae is rare which motivates the investigation of the properties of the biofilm formed in the advanced bioreactor. An interesting question is whether the biofilm is a single, homogeneous layer or a two-layered structure as observed for fungal-yeast CBP for the production of ethanol (Fig. 6.2B).

The products formed by microalgae are located intracellularly which requires the harvest of the cells to obtain the target product. If microalgae grow submerged the harvest is a major challenge and results in high capital costs and operational energy costs for pumps and centrifuges [213]. For autotrophically grown microalgae, 21 % of the total costs are dedicated to capital costs for the harvest of the biomass [214]. Alternative harvesting techniques such as cross-flow membrane filtration and flocculation are currently under development. Biofilms also allow for the efficient harvest of the microalgal biomass as they contain high cell densities with solid contents of up to 10 to 20 % [215]. Thus, it would be highly beneficial if the microalgae in the community-based CBP would adhere to the surface of a membrane and form a biofilm.

In the framework of this thesis the co-cultivation of the fungus *T. reesei* and the microalgae *C. reinhardtii* wild-type 12 (WT12) is studied as a first step towards the production of lipids from lignocellulose. It is described how an artificial light niche for the microalgae is realized in the advanced bioreactor (subsection 7.5.1). The engineered setup is then employed to cultivate *C. reinhardtii* in a single culture and, later, in a co-culture together with *T. reesei* (subsection 7.5.2).

7.5.1 Engineering and realization of artificial light niche

The advanced bioreactor described in section 7.2 is equipped with a light source to provide a niche for microalgae. As light source, 3000 K high power LEDs were chosen with an emission spectrum suitable for photosynthesis (Fig. 7.12A). The spectrum peaks at 442.5 nm (blue) and 615 nm (red) whereby the power density is higher in the red region. Flexible fibers with an outer diameter of 1.5 mm are used to direct the light of the LED into the reactor's interior (Fig. 7.11). The physical properties of the fiber allow radial light emission by internal scattering. An exponential decay of light was measured over the length of the fiber (200 to 2000 mm) (Fig. 7.12B). Approximately 80 % of the light coupled into the fiber is emitted through radial emission at a fiber length of about one meter. In order to increase the amount of light emitted in the reactor even more both ends of the fiber instead of only one are connected to one LED. The number of photons in the 400 to 700 nm range emitted from the fiber (called photosynthetically active radiation (PAR)) was quantified using a Sky light meter with a SKL 215 PAR 'Quantum' sensor (Skye Instruments, Llandrindod Wells, United Kingdom). While about $5 \mu\text{molm}^{-2}\text{s}^{-1}$ was measured in the upper part closer to the lid, at the bottom about $1 \mu\text{molm}^{-2}\text{s}^{-1}$ was measured. These values are small in comparison to 80 to 90 $\mu\text{molm}^{-2}\text{s}^{-1}$ which are typically used for autotrophic or mixotrophic growth of microalgae. The heat produced by the LEDs is discharged with a heat sink with enforced convection on which the LEDs are glued (Fig. 7.11).

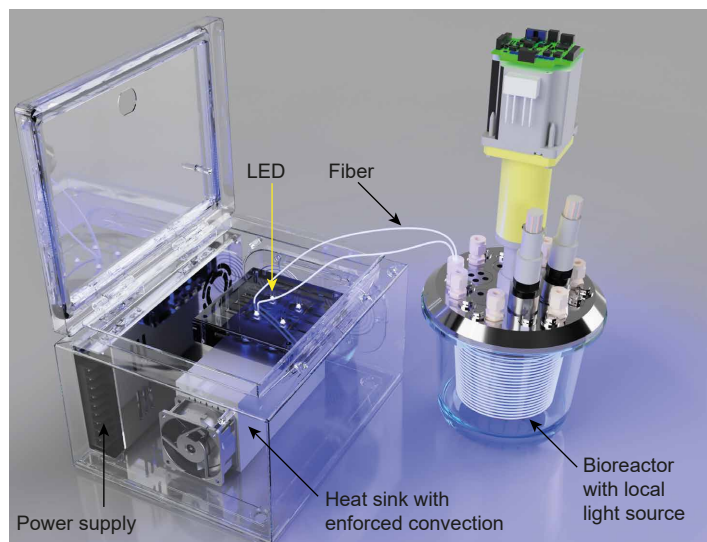


Figure 7.11: **External light source with radially emitting light fibers connected to the advanced bioreactor.** LEDs are glued on top of a heat sink with enforced convection. The light is coupled into both ends of a side-emitting light fiber which is helically coiled around the membrane holding structure in the interior of the reactor.

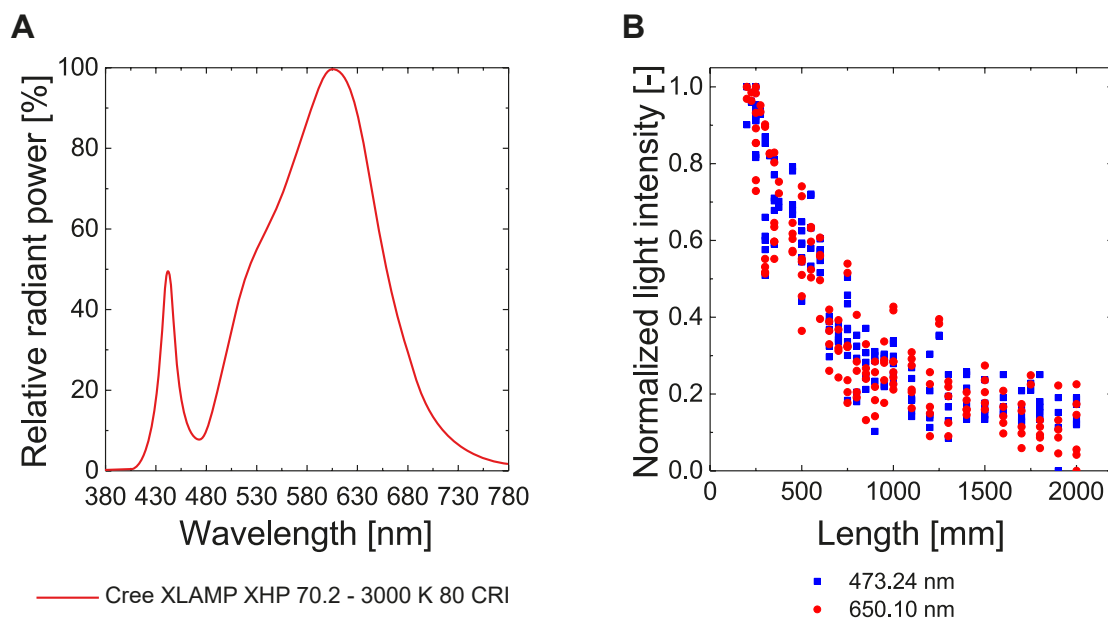


Figure 7.12: **Properties of LED light source: Emission spectrum and light intensity at the end of the fiber for various fiber lengths.** (A) Emission spectrum of Cree XLAMP XHP 70.2 - 3000 K 80 CRI used as light source to illuminate the advanced bioreactor. Data taken from [216]. (B) Light intensity measured at one end of the fiber while the other was connect to the LED. The measurement was repeated for different fiber lengths between 200 and 2000 mm. As an example, at about 1000 mm fiber length around 20 % of light coupled into the fiber was emitted at the open end of the fiber. The remaining 80 % were emitted over the length of the fiber.

7.5.2 Study of fungal-microbial biofilm

Prior to the study of the microalgal-fungal co-culture, the axenic growth of *C. reinhardtii* WT12 was studied in the advanced bioreactor. It was analyzed if *C. reinhardtii* forms a biofilm on the aerated-membrane and if it benefits from mixotrophic growth conditions (unshaded bioreactors) in comparison to heterotrophic growth conditions (shaded bioreactors). The results show that *C. reinhardtii* WT12 did not form a biofilm but instead, it grew submerged on acetate. In darkness a maximum optical density at 600 nm (OD_{600}) of 0.30 was obtained which is lower than in the unshaded reactor where a maximum OD_{600} of about 0.55 was measured (Fig. 7.13A). These results indicate that the aeration through the membrane enables growth of *C. reinhardtii* and that the microorganism tolerates the shear forces from stirring. With and without shading a slight accumulation of cells was visible in the spacing between the tubular shaped membrane, 262 hours after inoculation (Fig. 7.13B). However, in contrast to the fungus *T. reesei* the microalgae *C. reinhardtii* did not form a biofilm on the surface of the membrane

which indicates that *C. reinhardtii* does not produce extracellular polymeric substances (EPS) under these conditions which would allow adhesion to the membrane.

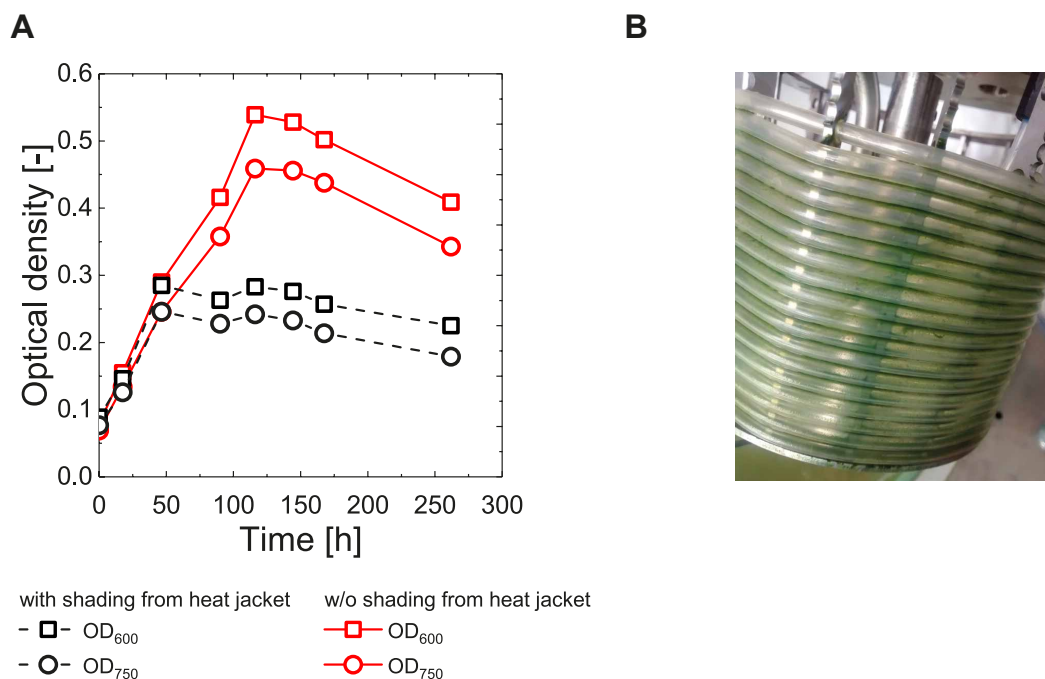


Figure 7.13: Axenic cultivation of *C. reinhardtii* WT12 using TAP medium in the darkness. *C. reinhardtii* grows submerged but forms no biofilm on membrane. Optical density measured at 600 and 750 nm. Photograph of *C. reinhardtii* WT12 after 267 hours after inoculation.

The observation that *C. reinhardtii* grows submerged but not in a biofilm under the studied conditions raises the question whether *C. reinhardtii* has access to oxygen when *T. reesei* covers the aerated membrane because the fungus consumes the oxygen which enters the reactor through the membrane. If *C. reinhardtii* is not able to penetrate the fungal biofilm, it cannot grow hetero- or mixotrophically and one could not profit from the benefits of these modes of growth over autotrophic growth as listed above.

In order to co-cultivate *T. reesei* and *C. reinhardtii* a suitable substrate would be microcrystalline cellulose (Fig. 7.14). *T. reesei* is capable to produce cellulolytic enzymes and to consume glucose as end-product of the enzymatic hydrolysis of cellulose. In contrast to a vast majority of microalgae *C. reinhardtii* is able to consume cellobiose and the species *C. reinhardtii* cc124 and cw10 were identified as producers of endoglucanases [217]. However, the activity of endoglucanases is approximately 200 times lower as compared to the activity measured for *T. reesei* [217]. *C. reinhardtii* is incapable to use glucose in the darkness [218] due to lack of glucose transporters in the plasma membrane [219]. As *T. reesei* secretes only a limited amount of

beta-glucosidases (BG) [57] it is expected that a share of cellobiose is available for *C. reinhardtii*. In order to boost growth of *C. reinhardtii* light is locally provided in the reactor as described in section 7.5.1 which would allow *C. reinhardtii* to use carbon dioxide autotrophically. This potentially also increases the carbon efficiency of the entire bioprocess.

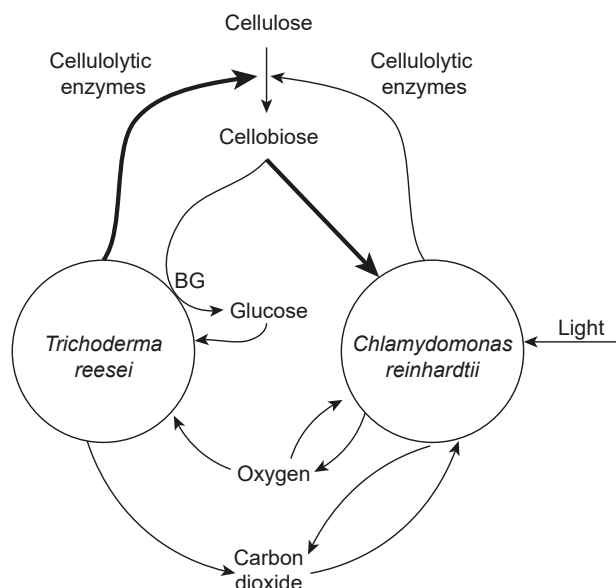


Figure 7.14: **Overview of pathways in a co-culture of *T. reesei* and *C. reinhardtii* using cellulose as carbon source and light as energy source.** The thickness of the arrows indicates increased production of cellulolytic enzymes by *T. reesei* compared to *C. reinhardtii* and increased cellobiose consumption of *C. reinhardtii* compared to *T. reesei*, respectively. Beta-glucosidase (BG).

In order to study the co-cultivation of *T. reesei* and *C. reinhardtii* in the advanced membrane-aerated bioreactor both microorganisms were inoculated simultaneously using 17.5 gL^{-1} microcrystalline cellulose as substrate. In one experiment the reactor was in darkness while it was illuminated with the LED setup in another experiment. In both cases the formation of a biofilm on the surface of the aerated-membrane was observed. The evolution of this biofilm was analyzed using the developed membrane-sampling loops (Fig. 7.2).

A chlorophyll fluorescence imager was used to measure the F_v to F_m ratio which is an indicator for the maximum quantum yield of the photosystem II. A confocal laser scanning microscope (CLSM) was employed to study the presence and spatial distribution of microalgae and fungal hyphae in the biofilm. The microscope detects the autofluorescence of chlorophyll produced by microalgae which appear red in the images. Fluorescein diacetate was used for live staining. Fluorescein was detected between 510 and 520 nm and appear green in the images. The content of chlorophyll a and b in the biofilms was determined as an indirect measure of the amount of microalgae.

In order to analyze whether *C. reinhardtii* can exist in the membrane-aerated bioreactor next to *T. reesei* three biofilms were studied using a chlorophyll fluorescence imager (Fig. 7.15): Two biofilms were based on co-cultures of *T. reesei* and *C. reinhardtii*, whereby one was without and one with illumination. The third biofilm was based on an axenic cultivation of *T. reesei* as a control. No counts were detected for any Fv to Fm ratios for the axenic fungal biofilm (Fig. 7.15A). This demonstrates the absence of microalgae which was expected. Both biofilms of the co-cultivation of *T. reesei* and *C. reinhardtii* without and with light showed counts whereby in both cases the maximum number of counts was at Fv to Fm ratios of around 0.3 (Fig. 7.15B and C). These values are lower compared to Fv to Fm ratios obtained with plant materials such as leaves (up to 0.83 [220]). It could be that the microalgae in the biofilm were buried under a layer of EPS which would have masked the cells and would have lowered their photochemical activity. The results indicate fluorescence activity and therefore the presence of microalgae in the biofilm. Please note, that the results do not provide quantitative information about the number of microalgae in the biofilms.

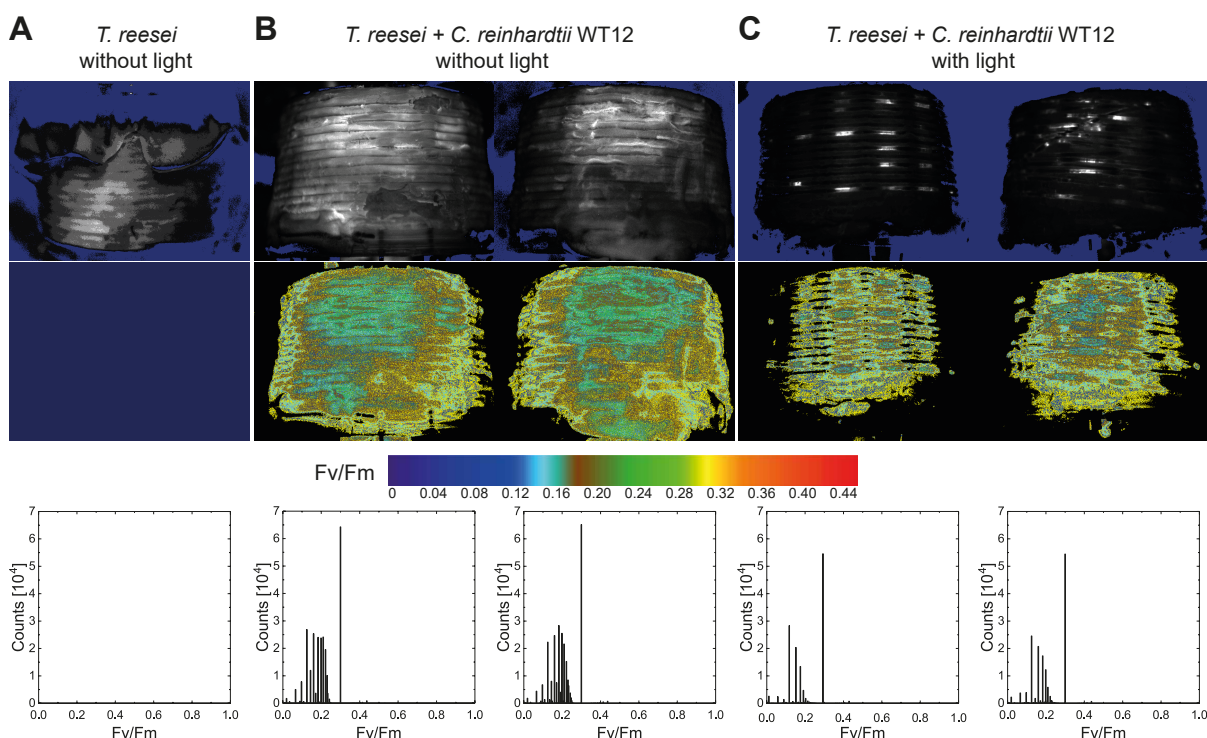


Figure 7.15: Chlorophyll fluorescence images of biofilms of *T. reesei* and *C. reinhardtii*. (A) Biofilm of *T. reesei* grown in darkness. Biofilm of *T. reesei* and *C. reinhardtii* grown (B) in darkness and (C) under illumination. Biofilms were dark-adapted for 15 min to measure the maximum of photosystem II. The saturation pulse was $6172 \mu\text{molm}^{-2}\text{s}^{-1}$. Please note that the horizontal diameter of the metal structure which holds the membrane is about 9 cm.

CLSM images of biofilm samples from the co-cultivation of *T. reesei* and *C. reinhardtii* without illumination confirmed the presence of both species five days after inoculation (Fig. 7.16A). It is observed, that the signal in the channel that detects the autofluorescence of chlorophyll decreases with time and two weeks after inoculation almost no autofluorescence of chlorophyll was detected (data not shown). A possible explanation would be that the microalgae cannot grow due to oxygen limitations. The comparison of CLSM images of biofilm samples taken five days after inoculation from the reactor without and with illumination indicates that more microalgae are present in the illuminated biofilm (Fig. 7.16A versus B). This result shows that the addition of light supports the growth of *C. reinhardtii* despite the relatively low PAR below

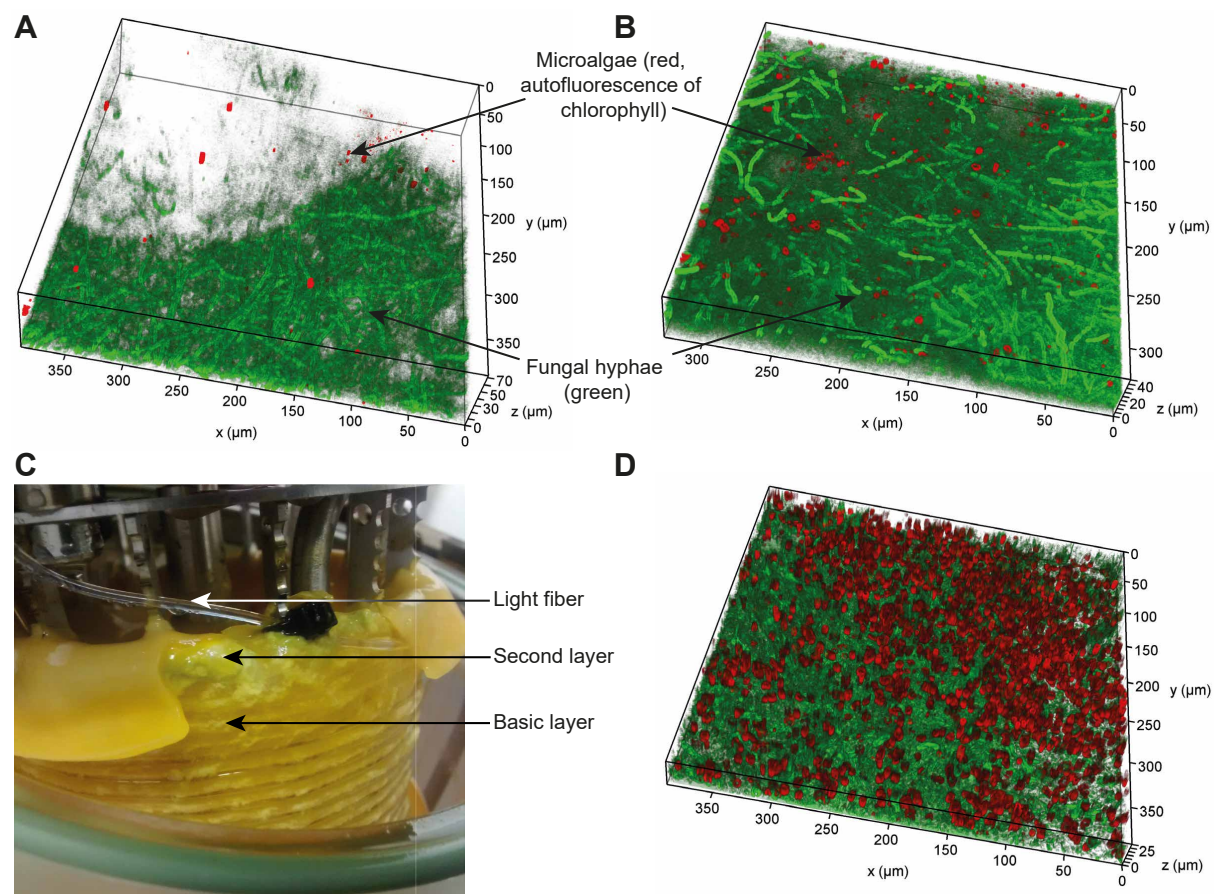


Figure 7.16: Confocal laser scanning microscopy images and photograph of fungal-microalgal biofilm grown on the surface of the membrane in the advanced bioreactor with and without illumination. (A,B) CLSM z-stack images about five days after inoculation of *T. reesei* and *C. reinhardtii*: (A) without illumination, (B) with illumination. (C,D) Microalgal-fungal biofilm about one week after inoculation. (C) Photograph of the biofilm attached to the membrane which is helically coiled around the membrane-holding structure next to the light fiber. A slightly green second layer in the upper part of the biofilm is on top of a basic layer. (D) CLSM z-stack of biofilm shown in (C). Higher z-values indicate an increased distance from the surface of the membrane (source of oxygen).

$5 \mu\text{mol m}^{-2}\text{s}^{-1}$. It might be that the illuminated microalgae is able to conduct photosynthesis which would provide oxygen. Taking into account that the enzymatic hydrolysis provides carbohydrates such as cellobiose it is assumed that the microalgae can grow either hetero- or mixotrophically. In the liquid phase of the reactor, the dissolved oxygen concentration was below the detection limit. Seven days after inoculation the macroscopic appearance of the biofilm with light is similar to the biofilm of *T. reesei* under axenic conditions except of a slightly green second layer on top of a basic layer (Fig. 7.16C). A corresponding CLSM image indicates that the top layer is mainly composed of microalgae whereby the basic layer is primarily composed of fungal hyphae (Fig. 7.16D). Measurements of the concentration of chlorophyll a and b confirm the conclusion that the top layer contains more chlorophyll, i.e. more microalgae, as compared to the basic layer (Fig. 7.17).

Xavier *et al.* performed simulations of the co-cultivation of two bacteria which differ in their ability to produce EPS and discuss the effect of an oxygen gradient [159]. Their results show that the EPS producer and the non-EPS producer can co-exist. In the absence of an oxygen gradient the non-EPS producer dominates over the microorganism that can produce EPS. In the presence of an oxygen gradient the EPS producer dominates. This is in line with the experimental results presented above for the biofilm composed of the EPS producer *T. reesei* and *C. reinhardtii* which is assumed to be not capable to produce EPS.

7.6 Conclusions

An advanced membrane-aerated bioreactor was designed to enable co-cultivation of microorganisms with highly diverse requirements for abiotic parameters and with that to widen the range of products accomplishable with community-based CBP. To this end, artificial habitats were engineered with controlled oxygen, pH, temperature and light conditions to mimic complex natural ecosystems that are built on inhomogeneities. Preliminary results demonstrate that a pH gradient can be realized either by electrolysis of water or by purging ammonia solution or carbon dioxide through the membrane. The option to cool the biofilm paves the way towards increased rates of enzymatic hydrolysis in CBP of lignocellulose. This would allow higher productivities of the entire CBP which would be an important step towards an industrial application. We conclude that the concepts which are implemented in the advanced membrane-aerated bioreactor are suitable to cultivate modular consortia which include e.g. psychrophiles next to thermophiles or acidophiles next to alkaliphiles.

By applying the advanced reactor we demonstrated the successful creation of an ecological niche for *C. reinhardtii* next to *T. reesei* despite potential competition for space, oxygen and organic carbon. The observed formation of a two-layered biofilm is very promising for the

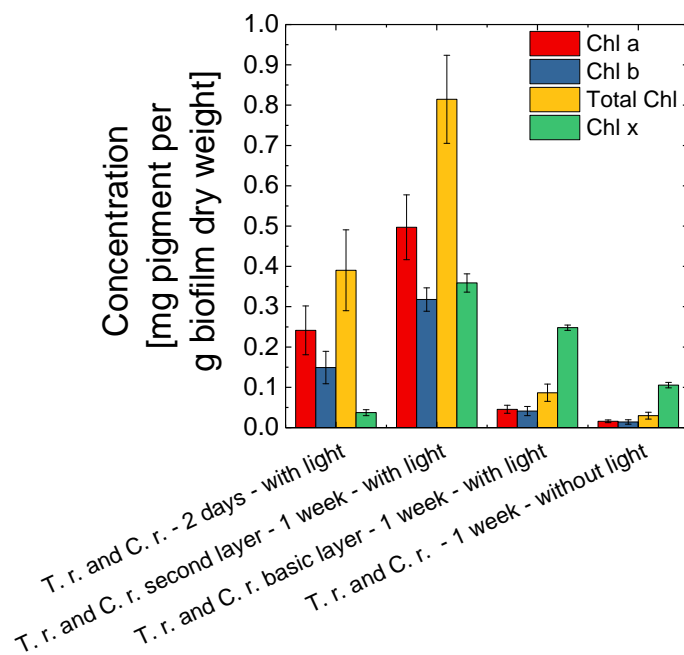


Figure 7.17: **Chlorophyll concentration in biofilm samples from cultivations of *T. reesei* and *C. reinhardtii* with and without light.** Pigments from biofilm samples are extracted using the solvent dimethylformamide. A spectrophotometric determination is performed at 480, 647 and 664.5 nm. Chlorophyll a (Chl a), chlorophyll b (Chl b) and total chlorophyll (Total Chl) are calculated using the equations from Inskeep and Bloom [221]. The total amount of carotenoids (Chl x) is calculated using the equation from Wellburn [222].

efficient harvest of microalgal biomass. After the demonstration that *C. reinhardtii* finds an ecological niche to grow in the biofilm next to the fungus *T. reesei* an interesting next target would be to apply the lactate platform and produce acetic acid, propionic acid or butyric acid (with e.g. the secondary fermenters *C. tyrobutyricum* or *V. criceti*, chapter 4) which are all accepted carbon sources for heterotrophic growth of *C. reinhardtii* [223]. Another option would be to use a homoacetogen for the production of only acetic acid from lactic acid with a high carbon efficiency. Acetic acid is a widely accepted substrate for a variety of different microalgae that can produce e.g. omega-3 fatty acids. Overall, with the presented approach the product range of the community-based CBP could be extended to lipids and other high-valuable products from lignocellulose using microalgae.

CHAPTER 8

Summary and conclusions

Lignocellulosic biomass is the most abundant source of fixed, renewable carbon. Despite its highly recalcitrant nature it is a promising feedstock for the production of platform chemicals in a second generation biorefinery. In this PhD thesis it was experimentally demonstrated that defined microbial communities can be engineered to enable the consolidated bioprocessing (CBP) of steam-pretreated lignocellulosic biomass into a wide range of products including carboxylic acids and ethanol. Following the principle of labor division, each member of the community fulfills a specific task in a given biochemical process. The modularity of the synthetic community allows the variation of the product-forming microorganisms to direct the bioprocess towards the desired target product. Up to four different microorganisms with in part non-overlapping tolerance ranges for e.g. oxygen were successfully co-cultivated in a bioreactor that was carefully engineered to allow sufficient niche differentiation.

For the direct production of lactic acid from lignocellulosic biomass a consolidated bioprocessing based on a synthetic cross-kingdom community was developed as presented in chapter 3. Lactic acid producing bacteria are non-cellulolytic. Thus, the aerobic fungus *Trichoderma reesei* was added for the *in situ* production of cellulolytic enzymes which is a cooperative feature. In contrast to the cooperator *T. reesei*, lactic acid bacteria act as cheater as they benefit from the carbohydrates released by the enzymatic hydrolysis without ‘paying’ the metabolic cost. Communities that rely on such cooperator-cheater dependencies tend to instability. The community was stabilized by spatial compartmentalization. The 500 mL stirred tank bioreactor used in this thesis was equipped with an aerated-membrane which locally supplied oxygen. This spatial niche allowed *T. reesei* to form a biofilm on the surface of the membrane. The community of *T. reesei* and *Lactobacillus pentosus* produced 19.8 gL^{-1} lactic acid from steam-pretreated beech wood without carbon catabolite repression. Despite the heterogeneous substrate a high purity

of lactic acid was observed which was dedicated to the *in situ* degradation of side products by *T. reesei*.

After biofilm formation the dissolved oxygen concentration in the fermentation slurry was below 4 ppb despite continuous aeration via the membrane. The metabolic activity of *T. reesei* and *L. pentosus* lowered the redox potential to a value below -300 mV. It is concluded that the two-member community is able to create a spatial niche where anaerobes can exist without the need for sparging with nitrogen or addition of costly reducing agents. The possibility to integrate anaerobes into the membrane-aerated bioreactor significantly widens the range of products that can be obtained with the community-based CBP.

Anaerobic, product-forming microorganisms are often characterized by limited metabolic flexibilities. This leads to low product yields due to side-product formation and low carbon efficiencies due to incomplete usage of the substrate lignocellulose, in particular xylose and acetic acid. In this thesis the lactate platform was established to circumvent these problems. The heterogeneous lignocellulosic carbohydrates are metabolically funneled to lactate as the central intermediate in artificial food chains. The production of various chemicals from steam-pretreated beech wood via the lactate platform was evaluated in terms of product yields and compared to corresponding sugar-based fermentation routes. The results reveal that pathways via lactate are known for a variety of industrially relevant chemicals and that the lactate platform route can outcompete conventional pathways.

The lactate platform was exemplified by co-cultivation of *T. reesei* and *L. pentosus* together with the obligate anaerobes *Clostridium tyrobutyricum* or *Veillonella criceti* in a scaled-up 2.7 liter membrane-aerated bioreactor as described in chapter 4. These secondary fermenters utilize lactic acid (and acetic acid) to produce 196.5 kg butyric acid or 113.6 kg propionic acid and 133.3 kg acetic acid, respectively, per ton of beech wood. The fact that *C. tyrobutyricum* can co-ferment lactic acid together with acetic acid exclusively to butyric acid resulted in an increased theoretical butyric acid yield of up to 1.31 times of its equivalent theoretical yield for direct carbohydrate conversion. On the roadmap towards production of jetfuels and olefins from lignocellulose butyric acid can be used as substrate. In the framework of the National Research Program 70 *Energy Turnaround* the developed microbial community of *T. reesei*, *L. pentosus* and *C. tyrobutyricum* was employed to provide butyric acid which was subsequently catalytically upgraded to linear olefins [11] or aromatic hydrocarbons.

The number of carbon atoms in the end products of the catalytic upgrading process is affected by the chain length of the carboxylic acids used as substrate. To this end, the production of volatile fatty acids (VFA) with up to six carbon atoms from lignocellulose was targeted in this thesis (chapter 5). The strict anaerobe *Megasphaera elsdenii* which is capable to elongate carboxylic acids using the reverse beta-oxidation pathway was added to the lactate platform

and successfully co-cultivated with the aerobic fungus in one vessel. It was demonstrated that the ratio of odd- and even-numbered VFAs can be tuned by intra-consortium competition in the community-based CBP. A four-member community composed of *T. reesei*, *L. pentosus*, *M. elsdenii* and *V. criceti* was established. The competition between *M. elsdenii* and *V. criceti* for lactic acid increased the share of odd-numbered valeric acid in comparison to the product mixture obtained with the three-member community without *V. criceti*. This is remarkable as none of the used substrates was a molecule with three-carbon atoms such as propionic acid. In contrast, when *V. criceti* was replaced with *C. tyrobutyricum* the share of the even-numbered VFA butyric acid was increased while the share of acetic acid was decreased. This was attributed to the competition between *M. elsdenii* and *C. tyrobutyricum* for lactic acid and acetic acid.

The 2.7 liter membrane-aerated bioreactor is suitable to produce ethanol from microcrystalline cellulose using a two-member community of *T. reesei* and the yeast *S. cerevisiae*. However, our results indicate that the yeast aerobically degrades ethanol which results in reduced ethanol yields. In order to circumvent this problem the oxygen transfer rate can be varied as demonstrated by changing the properties of the membrane and the concentration of oxygen in the fluid purged through the membrane.

In the course of the thesis several limitations of the developed membrane-aerated bioreactor were identified. An advanced bioreactor was designed and built to tackle these problems. The advanced bioreactor is equipped with several niches for abiotic parameters (oxygen, temperature, pH, light). It was demonstrated that pH gradients form by flushing the membrane with gaseous carbon dioxide or liquidous ammonia. Another route is based on the electrolysis of water. Independent of the initial pH in the medium 3.0 V applied across two electrodes resulted in a wide spread of pH ranging from about 3 to 12. A local light niche was implemented based on LEDs and radially emitting light fibers to enhance the growth of microalgae in the reactor. It was shown that microalgae profit from the light and co-exist in a two-layered biofilm next to the fungus *T. reesei* despite of potential competition for space, oxygen and organic carbon. The formation of a biofilm containing microalgae facilitates the harvest of microalgal products such as lipids or pigments which are located in the cells. Another feature of the advanced bioreactor is that it exhibits membrane loops that can be independently removed from the bioreactor throughout one experiment.

Today, biotechnological whole-cell processes are to a great extent dominated by monocultures grown in homogeneous reactors. However, the increasing number of publications addressing microbial co-cultures highlights the paradigm shift from axenic to mixed cultures. Thus, it would be of highest interest to further study complex co-cultures in defined environments using the advanced bioreactor of inhomogeneities developed in this thesis.

The productivity of the CBP is a key parameter towards industrial application. It would be interesting to quantify the productivity of bioprocesses with temperature gradients as it is expected that these are significantly higher as compared to the ones at mesophilic conditions where the enzymatic hydrolysis limits the overall process. Another promising idea is to benefit from synergistic interactions of the free cellulolytic enzymes produced by an aerobic fungus and cellulosomes attached to an anaerobic bacterium. It is expected that their integration into the lactate platform is rather uncomplicated because a suitable niche for the growth of a strict anaerobe was demonstrated.

More technical directions relate to the extraction of toxic target products such as butyric acid from the bioreactor with the circulation system. This is expected to increase the product yield because high concentrations of inhibitory products in the reactor are prevented. The implementation of the membrane into a stirred tank bioreactor which is a standard reactor design in industry was a first step towards industrialization. Now it is required to scale-up the reactor volume progressively. We hope that the reader is convinced that the consortium-based consolidated bioprocessing of lignocellulose has the potential to contribute to a sustainable chemical industry in a future bioeconomy.

APPENDIX A

Materials and methods

A.1 Bacterial, fungal and microalgal strains and cultivation methods

L. pentosus (DSM-20314), *L. brevis* (DSM-20054), *C. tyrobutyricum* (DSM-2637), *V. criceti* (DSM-20734) and *A. woodii* (DSM-1030) were purchased from Leibniz Institute DSMZ-German Collection of Microorganisms and Cell Cultures (Braunschweig, Germany).

One mL of glycerol stock was inoculated to MRS medium for precultures of *Lactobacillus* in 500 mL Erlenmeyer flasks and incubated for 48 hours at 150 rpm at 33 °C. The MRS medium contained (in gL⁻¹): peptone from casein, 10; meat extract, 10; yeast extract, 5; glucose, 20; Tween 80, 1; K₂HPO₄, 2; sodium acetate, 5; ammonium citrate, 2 and MgSO₄ · 7 H₂O, 0.2. The pH was adjusted to 6.2-6.5 with hydrochloric acid.

C. tyrobutyricum precultures were cultivated in a reinforced clostridial medium (RCM). Composition of the RCM medium (in gL⁻¹): yeast extract, 13; peptone, 10; glucose, 5; soluble starch, 1; sodium chloride, 5; sodium acetate, 3; L-cysteine-HCl, 0.5; agar, 0.5.

V. criceti precultures were cultivated in medium containing (in gL⁻¹): trypticase (BBL), 5; yeast extract, 3.0; Na-(DL)-lactate, 7.5; Na-thioglycolate, 0.75; Tween 80, 1.0; Glucose, 1.0; Na-resazurin solution (0.1 % (w/v)), 0.5 mL. The medium for *C. tyrobutyricum* and *V. criceti* was boiled under continuous flushing with nitrogen and the pH was adjusted to 6.8 before it was aliquoted to 100 mL serum bottles (50 mL in each) and autoclaved at 121 °C for 20 minutes.

A. woodii precultures were cultured in DSMZ-medium 135: 1.0 g NH₄Cl, 0.33 g KH₂PO₄, 0.45 g K₂HPO₄, 0.1 g MgSO₄ · 7 H₂O, 20 mL *Acetobacterium* trace element solution (DSMZ-medium 141), 2.0 g yeast extract, 0.5 mL Na-resazurin solution (0.1 % (w/v)) and 1000 mL water were boiled and cooled to room temperature under a 80 % N₂ and 20 % CO₂ gas mixture. Solid

sodium bicarbonate (10 g) was added and the pH was equilibrated by aeration with the gas mixture until a value of 7.4 was reached. The medium was aliquoted into serum bottles (60 mL in each) under anaerobic conditions and autoclaved at 121 °C for 20 minutes. Before inoculation, the pH was adjusted to 8.2 by addition of a sterile anoxic stock solution of potassium carbonate (5 % (w/v)) prepared under a 80 % nitrogen and 20 % carbon dioxide gas mixture (0.25 mL per 10 mL medium) and the following stock solutions were added: fructose (10 gL⁻¹ final concentration, sterile filtrated), L-cysteine-HCl · H₂O (0.5 gL⁻¹, anoxic and autoclaved), and Na₂S · 9 H₂O (0.5 gL⁻¹, anoxic and autoclaved). Composition of the *Acetobacterium* trace element solution (in gL⁻¹): nitrilotriacetic acid, 1.5; MgSO₄ · 7 H₂O, 3.0; MnSO₄ · H₂O, 0.5; NaCl, 1.0; FeSO₄ · 7 H₂O, 0.1; CoSO₄ · 7 H₂O, 0.18; CaCl₂ · 2 H₂O, 0.1; ZnSO₄ · 7 H₂O, 0.18; CuSO₄ · 5 H₂O, 0.01; KAl(SO₄)₂ · 12 H₂O, 0.02; H₃BO₃, 0.01; Na₂MoO₄ · 2 H₂O, 0.01; NiCl₂ · 6 H₂O, 0.03; Na₂SeO₃ · 5 H₂O, 0.0003 and Na₂WO₄ · 2 H₂O, 0.0004. Nitrilotriacetic acid was dissolved in distilled water, the pH adjusted to 6.5 with KOH, the minerals added and the final pH adjusted to 7.0 with KOH. The composition of the vitamin solution was as follows (in mgL⁻¹): biotin, 2.0; folic acid, 2.0; pyridoxine-HCl, 10.0; thiamine-HCl · 2 H₂O, 5.0; riboflavin, 5.0; nicotinic acid, 5.0; D-Ca-pantothenate, 5.0; vitamin B₁₂, 0.1; p-aminobenzoic acid, 5.0 and lipoic acid 5.0. All serum bottles were inoculated from a two-day liquid culture stored at 4 °C and incubated on an orbital shaker at 140 rpm at 37 °C (expect *A. woodii* at 30 °C).

T. reesei RUT-C30 (ATCC 56765) was purchased from VTT, Finland. Spores from a seven-day old potato dextrose agar slant culture were incubated at 28 °C and stored at 4 °C. For precultures Mandel's medium containing 7.5 gL⁻¹ microcrystalline cellulose (Avicel PH-101, Sigma Aldrich, Buchs, Switzerland) was inoculated with spores from the agar slant in an Erlenmeyer flask for four days at 28 °C and 150 rpm. Mandel's medium contained the following ingredients (in gL⁻¹): KH₂PO₄, 2; (NH₄)₂SO₄, 1.4; MgSO₄ · 7 H₂O, 0.3; CaCl₂ · 6 H₂O, 0.4; urea, 0.3; peptone, 0.75; yeast extract, 0.25 and trace element stock, 1 mL⁻¹. The trace element stock contained (in gL⁻¹): FeSO₄ · 7 H₂O, 5; MnSO₄ · H₂O, 1.6; ZnSO₄ · 7 H₂O, 1.4; CoCl₂ · 6 H₂O, 3.7 and 10 mL⁻¹ concentrated hydrochloric acid and was sterile filtered. To avoid precipitation, 100x CaCl₂ and 100x MgSO₄ solutions were autoclaved separately before merging with the remaining ingredients.

Saccharomyces cerevisiae VTT C-79095 was purchased from VTT, Finland. The petite yeast *Saccharomyces cerevisiae* FYdelta pet191::KanMX4 was generously provided by Professor Stephen G. Oliver, University of Cambridge [203]. Precultures of both *S. cerevisiae* strains were cultivated in YPD medium containing (in gL⁻¹): yeast extract, 10; peptone, 20 and dextrose, 10. Erlenmeyer flasks were incubated overnight at 28 °C and 200 rpm. Kryostocks were prepared by mixing overnight cultures with glycerol to a final concentration of glycerol of 20 % (v/v).

C. reinhardtii wild-type strain (WT12) was generously provided from Prof. Alison Smith (University of Cambridge). Stocks of *C. reinhardtii* were stored at room temperature in TAP medium. TAP medium contained per liter: TRIS, 2.42 g, TAP salt stock, 25 mL; phosphate solution, 0.375 mL, six Kropat's trace element stock solutions, 1 mL each and glacial acetic acid, 1 mL. The medium was autoclaved for 20 minutes at 121 °C. TAP salt stock solution contained (in gL⁻¹): NH₄Cl, 15.0; MgSO₄ · 7 H₂O, 4.0; CaCl₂ · 2 H₂O, 2.0. The phosphate solution contained 28.8 g K₂HPO₄ and 14.4 g KH₂PO₄ and water was added to a volume of 100 mL. Kropat's trace element stock solutions contained: 1) 25 mM EDTA-Na₂; 2) 28.5 μM (NH₄)₆Mo₇O₂₄; 3) 2 mM CuCl₂ · 2 H₂O and 2 mM EDTA; 4) 2.5 mM ZnSO₄ · 7 H₂O and 2.75 mM EDTA; 5) 6 mM MnCl₂ · 4 H₂O and 6 mM EDTA; 6) 20 mM FeCl₃ · 6 H₂O, 22 mM EDTA and 22 mM Na₂CO₃. For liquid precultures of *C. reinhardtii* Erlenmeyer flasks were filled with fresh TAP medium and inoculated with 5 % (v/v) stock solution and incubated at 25 °C with a 18 hour light to 6 hour dark cycle with 120 molm⁻²s⁻¹ for five days under shaking at 120 rpm.

A.2 Membrane-aerated bioreactors

Throughout the thesis three different membrane-aerated bioreactors were used for community-based CBP of lignocellulose to carboxylic acids and ethanol. Two of them were based on commercially available reactors modified with a custom-made metal structure to support the membrane. The advanced reactor was developed from scratch. Their specifications are provided in the following.

The membrane bioreactors were based on Multifors 2 and Labfors 5 bioreactors (Infors HT, Bottmingen/Basel, Switzerland) with 0.5 and 2.7 liter working volume, respectively. The 0.5 liter reactor (Fig. B.1A) was used in chapters 3 and 4 and the 2.7 liter reactor (Fig. 6.1) was used in chapters 4, 5 and 6. Both reactors were modified with a tubular polydimethylsiloxane (PDMS) membrane. The membrane area to volume ratio was 0.3 cm²mL⁻¹ at 0.5 liter scale. A mono-lumen tubing 0.64 mm × 1.19 mm × 0.28 mm (Dow Corning, Midland, United States of America) gave a k_{La} value of 3.24 h⁻¹ in the Multifors reactors. The membrane area to volume ratio was 0.3 cm²mL⁻¹ in the Labfors. A mono-lumen tubing 1.58 mm × 3.18 mm × 0.80 mm (Dow Corning, Midland, United States of America) gave a k_{La} value of 0.34 h⁻¹ in the 2.7 liter reactor if not otherwise stated. The membrane was continuously flushed with air at 140 mLmin⁻¹ per liter liquid phase. The temperature in the liquid phase of the reactor was set to 30 °C and the pH to 6.0 using 4 N phosphoric acid and 4 M sodium hydroxide. The redox potential and the pH were measured using EasyFerm Plus ORP Arc and EasyFerm Plus PHI Arc probes (Hamilton, Bonaduz, Switzerland). Liquid samples were collected using a UV lamp as the contamination barrier (Fig. 7.3). Neither mixtures of external cellulolytic

enzymes nor purging with nitrogen was applied. The reactor was autoclaved for 20 minutes at 121 °C with microcrystalline cellulose or steam-pretreated beech wood. The remaining medium components were added when the reactor was inoculated with 5 % (v/v) *T. reesei*. After 48 hours, the lactic acid bacteria (LAB) were inoculated to an optical density measured at 600 nm (OD_{600}) of 0.5 by centrifuging the cells at 3000 rpm for 10 minutes and suspending them in fresh Mandel's medium. This time was defined as time zero. 48 hours after inoculation of the LAB, the anaerobic bacteria *C. tyrobutyricum*, *V. criceti* or *M. elsdenii* were inoculated to 5 % (v/v) from a two-day old pre-culture. For fed-batch experiments, the feed solution was sterile filtered and fed at a constant feeding rate. For co-culture experiments Mandel's medium was used.

For the production of ethanol 2.7 liter Labfors 5 bioreactors were prepared as described above. 48 hours after inoculation of the fungus the yeast was inoculated to an optical density at 600 nm (OD_{600}) of 0.5. Beta-glucosidase was added together with the yeast. The enzyme loading was 30 CBU per g of cellulose. The outlet of the membrane was connected to a custom-made in-line sampling tray which allowed the automated sampling of a gas chromatograph.

The advanced membrane-aerated bioreactor which was used in chapter 7 was based on a 1 liter glass vessel enclosed with a custom-made reactor lid (Fig. 7.1). In the center of the lid the autoclavable magnetic coupling MRK 60 Ncm (Premex Reactor, Lengnau, Switzerland) was installed. The reactor was equipped with an electric stepper motor QSH6018-45-28-110 (1.10 Nm, 2.8 A) (Tri-Matic, Hünenberg, Germany). The motor was controlled by the stepper motor driver TMCM-6110 via RS-485 using the software TMCL-IDE 3.0 (V3.0.21.0) (Tri-Matic, Hünenberg, Germany). A pitched blade stirrer with fixed pitch of 45 ° was mounted to the bottom end of the stirring shaft. The reactor was equipped with metal structure to support a tubular membrane with an outer diameter of 3.18 mm as used for the modified Labfors 5 bioreactors described above. The membrane was continuously flushed using NFB30 twin head pumps (PML013335-NFB30 IP 30 24 V, KNF, Baltherswil, Switzerland). The four connections of the pump were connected in a suction-pressure configuration to the membrane in- and outlet and in case of the circulation approach to the expansion vessel. In one configuration the expansion vessel was an oxygen-impermeable bag with custom-made in- and outlets for the pump, the oxygen inlet and the oxygen probe. The oxygen probe was a SP-PSt3-YAU-D10-YOP spot glued to a quartz glass (Fig. 7.4). The optical fiber POF-L2.5-2SMA was attached to the glass plate using a stick-on adapter. The other side of the optical fiber was connected to the EOM-tO2-mini-180-T4D-v3 electro-optical module for oxygen measurements (Presens, Regensburg, Germany). The oxygen inlet was controlled by a direct-acting 2/2 way plunger valve type 0255 (Bürkert, Ingelfingen, Germany) operated at 24 V. In another configuration of the expansion vessel a GL45 pressure plus 1 liter bottle (Duran, Wertheim, Germany) was used. A pressure holding valve (AP100-F01B-X201, SMC Switzerland, Weisslingen, Switzerland)

was connected to both the expansion vessel and the reactor. The probes for dissolved oxygen and pH were the same as used for the Infors reactors described above. Peristaltic pumps with 24 V operating voltage (Kamoer, Shanghai, China) were used for fed-batch experiments and for the regulation of pH by addition of 4 N phosphoric acid and 4 M sodium hydroxide. The temperature in the stirred liquid phase of the bioreactor was tapped from the pH probe. Heating of the bioreactor was realized by an electric heat jacket which was wrapped around the glass vessel. The heating power was limited using a phase control dimmer and the on-off state was controlled by a relay. The reactor was equipped with up to four fully encapsulated, waterproof, autoclavable Pt100 sensors which allowed temperature measurements in the biofilm at defined distances from the surface of the membrane. The Pt100 probes were soldered to autoclavable FGG.0B.304.CLAD22 plugs and connected to the control unit via EGG.0B.304.CLL sockets (Lemo, Écublens, Switzerland). The measured signal of the Pt100 sensors was used to control an electromagnetic valve (Sirai L121B02, ZA19AF1m G1/4, 2/2 way plunger valve, ASCO Numatics Sirai Srl, Bussero, Italy) to allow cool water to flow through a copper tube inserted in the expansion vessel. This setup allowed the cooling of the biofilm if e.g. water was used as circulated fluid. The system was powered by 24 V power supplies. Labview was used for all control loops and recorded relevant process parameters. The reactor was autoclaved for 20 minutes at 121 °C with water and if stated in the caption of a given figure with microcrystalline cellulose. The remaining medium components were added when the reactor was inoculated with 5 % (v/v) *T. reesei* and/or 5 % (v/v) *Chlamydomonas reinhardtii*. For co-culture experiments Mandel's medium was used.

A.3 Steam pretreatment and analysis of beech wood

Beech wood chips (*Fagus sylvatica*) from a local forest were air-dried (dry matter 94 %) and milled to <1.5 mm. The raw biomass was composed of (% (w/w)) glucan 39.95±1.25, xylan 19.0±0.5, acetic acid 7.3±0.2, acid-insoluble lignin 25.6±0.7, acid-soluble lignin 5.3±0.1, ash 0.5 and extractives 0.9. A two-stage steam pretreatment was applied with a custom-built steam gun (Industrieanlagen Planungsgesellschaft m.b.H., Austria) to target the partial recovery of soluble xylooligosaccharides from hemicellulose in the prehydrolyzate and simultaneously maximize the glucose yield in the enzymatic hydrolysis of the solids. Beech wood was heated to 180 °C by the injection of saturated steam and pretreated for a residence time of 24.8 minutes. At constant pressure and temperature, the liquid phase was removed through a circular nozzle located slightly above the lower ball valve. Subsequently, the pressure was slowly released to 2.0 bar, which is below the known pressure needed to see an effect of the explosion [37]. At 2.0 bar, the lower ball valve opened, and the solids were removed from the reactor. The solids composed of (% (w/w)) 49.0±0.62 glucan, 7.55±0.1 xylan, 4.2±0.1 acetic acid, 29.9±0.73 acid-insoluble lignin

and 3.68 ± 0.37 acid-soluble lignin. The recovered solids were treated a second time at $230\text{ }^{\circ}\text{C}$ for 14.1 minutes and the pressure was abruptly released. The solids contained (in % (w/w)) 55.0 ± 1.4 glucan, 2.1 ± 0.1 xylan, 1.2 ± 0.2 acetic acid, 35.4 ± 0.8 acid-insoluble lignin and 2.5 ± 0.1 acid-insoluble. The 180 ° liquid fraction contained (in g L^{-1}): acetic acid, 2.13; formic acid, 0.4; xylose, 1.1; xylooligosaccharides calculated as xylan, 22.35. During acid-hydrolysis, an additional 5.57 g L^{-1} acetic acid was released from deacetylation of xylooligomers.

A.4 Enzyme assays

Endoglucanase (EG), beta-glucosidase (BG), cellobiohydrolases (CBH) and xylanase activity assays were performed at pH 5.0 in the presence of 50 mM citrate buffer, 0.02 % (w/v) sodium azide at $50\text{ }^{\circ}\text{C}$ in duplicates. The enzymatic activity was expressed in International Units (IU). One IU is defined as the amount of enzyme that catalyzes the conversion of one micro-mole of substrate per minute. EG, BG and CBH assays were performed accordingly to [204]. Ultra-low viscosity carboxymethylcellulose (2 % (w/w)) was used as substrate for EG assays, Avicel (2 % (w/w)) for CBH and 4-Nitrophenyl α -D-glucopyranoside (1 mM) for BG. Birch wood xylan (1 % (w/w)) was used as substrate for xylanase activity measurements (12.5 μL sample in 125 μL total reaction volume). Reducing sugars were quantified using the 3,5-Dinitrosalicylic acid (DNS) method [224].

A.5 Analytical methods

Acetic acid, lactic acid, propionic acid, butyric acid, formic acid, glucose, cellobiose, xylose, ethanol hydroxymethylfurfural and furfural were quantified by high performance liquid chromatography (Waters 2695 Separation Module, Waters Corporation, Milford, United States of America), using an Aminex HPX-87H column (Bio-Rad, Hercules, United States of America) at $65\text{ }^{\circ}\text{C}$ with 5 mM H_2SO_4 as the mobile phase a flow at 0.6 mL min^{-1} , a refractive index detector (Waters 410) at $40\text{ }^{\circ}\text{C}$ and a photo diode array detector (Waters 2998) at 210 nm. The detection limit was 0.05 g L^{-1} . Structural carbohydrates and lignin were measured according to standard methods [225].

Ethanol in the off-gas of the membrane was quantified using a gas chromatograph (7890A with C506 Controller, Agilent Technologies, Santa Clara, United States of America) equipped with a MultiPurpose sampler (Gerstel, Mülheim an der Ruhr, Germany). Polyether ether ketone (PEEK) tubing (outer diameter 1.59 cm, inner diameter 1.00 mm, BGB Analytics, Boeckten, Switzerland) was used to connect the outlet of the membrane to the gas chromatograph. The

tubing was heated to 35 °C to prevent condensation of water. A self-regulating electric heating line (HW-R, 9 W/m, purchased from Peter Heizungen, Reinach, Switzerland) as well as Pt100 probes were connected to an electronic microstat (eTRON M, JUMO, Fulda, Germany). 470 ppm ethanol gas (PanGas, Dagmersellen, Switzerland) was used to calibrate the gas chromatograph.

A spectrophotometer (Thermo Spectronic UV-1 (Thermo Fisher Scientific, Waltham, United States of America)) was used to measure the optical density at 480, 647 and 664.5 nm to quantify chlorophyll a, chlorophyll b, total chlorophyll and total carotenoids. Prior to the measurement the pigments were extracted using dimethylformamide (DMF). The preparation of the samples is as follows. Samples with a specific volume or mass were centrifuged in a 1.5 mL Eppendorf vial. In a fume hood 1 mL DMF was added to the pellet and the vials were agitated using a vortex at room temperature for 15 minutes. The vials were centrifuged at 10.000 rpm on a benchtop centrifuge. Ideally, the pellet should be white or colorless and the DMF light green. When the pellet was still green another vortex step for 5 to 10 minutes with recentrifugation was performed. The supernatant was transferred to another vial to measure the optical density. If the measured optical density was not in the linear absorbance range of the spectrophotometer a dilution with DMF was performed. The measurements were performed in DMF resistant cuvettes. The chlorophyll a, chlorophyll b and total chlorophyll were calculated using the equations from Inskeep and Bloom [221] and the amount of carotenoids using the equation from Wellburn [222].

The chlorophyll fluorescence (CF) imager (Technologica, Colchester, United Kingdom) was used for Fv to Fm measurements. The resolution of the camera was 696 pixels×519 pixels. Biofilms were dark-adapted for 15 minutes to measure the maximum of photosystem II. The saturation pulse was $6172 \mu\text{mol m}^{-2}\text{s}^{-1}$.

A confocal laser scanning microscope from Leica SP8 (Leica Microsystems, Germany) was used to analyze stained biofilm samples. The setup was equipped with a white light laser set to 30 % laser power to excite the sample. The scan speed was 400 Hz and the objective HC PL APO CS2 40x/1.30 oil with a magnification of 40 was installed. Autofluorescence from photosynthetic pigments was detected in the red channel (excitation at 650 nm and emission at 680 to 700 nm). Fluorescein diacetate was used as viability stain. Fluorescein was detected in the green channel (excitation 495 nm and emission at 514 to 521 nm). The fluorescence projections of the biofilm were generated using the Leica LAS software.

APPENDIX B

Supplementary for chapter 3: Lactic acid

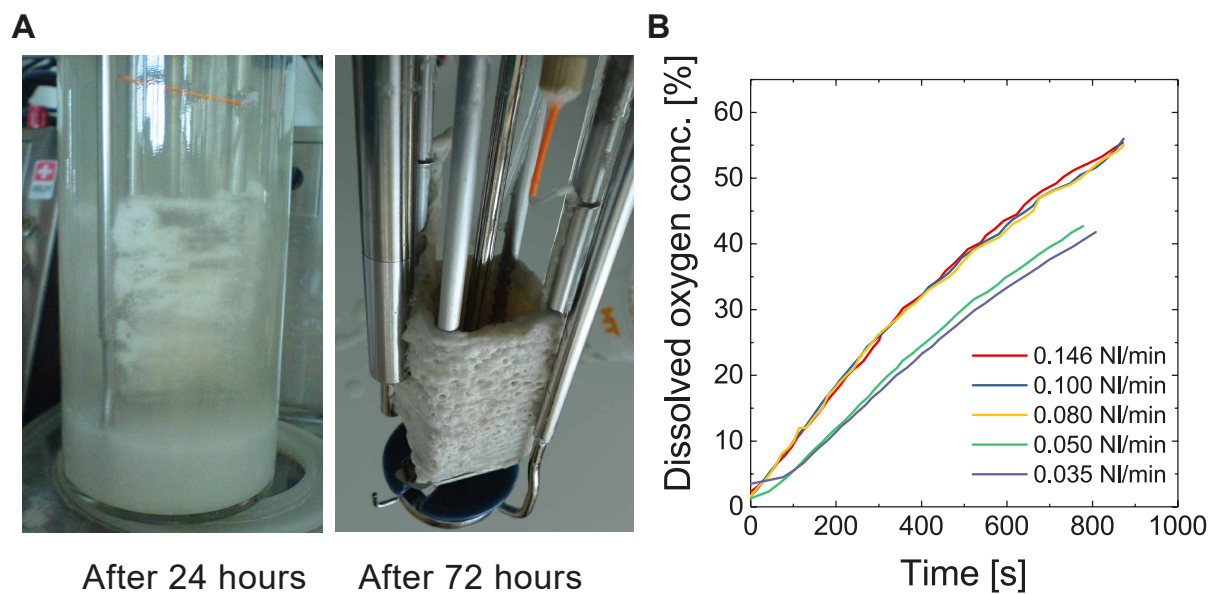


Figure B.1: Caption next page.

Figure B.1: **Photographs of the development of a fungal biofilm in the membrane-aerated 500 mL bioreactor and the measured dissolved oxygen concentration as a function of time for various flow rates. (A)** Pictures of the biofilm of *T. reesei* grown on microcrystalline cellulose 24 and 72 hours after inoculation. The membrane was partially covered after 24 hours (left), completely after 48 hours (not shown) as well as 72 hours (right) with the fungal biofilm. Membrane fouling is not observed in the consolidated bioprocess since a non-porous membrane was used. We were able to use the same membrane per reactor for all experiments shown in this chapter. **(B)** Measured dissolved oxygen concentration as a function of time in the membrane bioreactor without microorganisms. Dissolved oxygen was removed prior to each measurement by flushing the reactor with nitrogen. The effect of different air flow rates (0.035 to 0.146 NL/min) on the dissolved oxygen concentration was studied. The temperature was set to 30 °C. The dissolved oxygen probe was calibrated to 100 % air saturation. As can be seen the dissolved oxygen concentration is independent of the air flow rate for rates equal to or above 0.08 NL/min. This means that no oxygen gradient over the length of the membrane is present. Thus, for all experiments in the 0.5 L scale an air flow rate of 0.08 NL/min was selected.

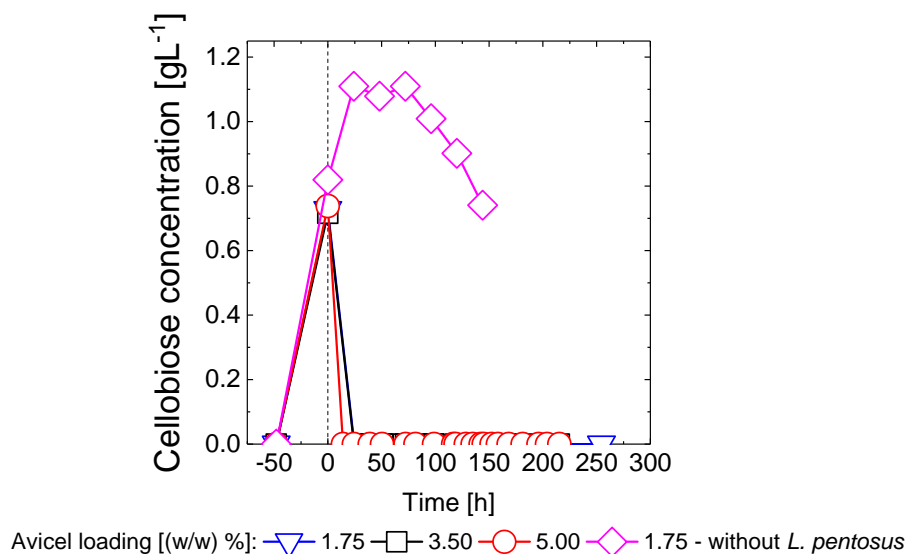


Figure B.2: **Concentration of cellobiose in the membrane-aerated bioreactor with and without inoculation of *L. pentosus* using microcrystalline cellulose as substrate.** Cellobiose concentration during consolidated bioprocessing of 1.75 % (w/w) (triangle), 3.50 % (w/w) (square) and 5.00 % (w/w) (circle) Avicel to lactic acid by *T. reesei* and *L. pentosus*. A two-stage inoculation scheme was applied. *L. pentosus* was inoculated two days after *T. reesei* at time zero. After inoculation of *L. pentosus* the concentration of glucose (not shown) was below the detection limit of 0.05 gL⁻¹. For comparison, also the cellobiose concentration during an experiment without *L. pentosus* inoculation is shown.

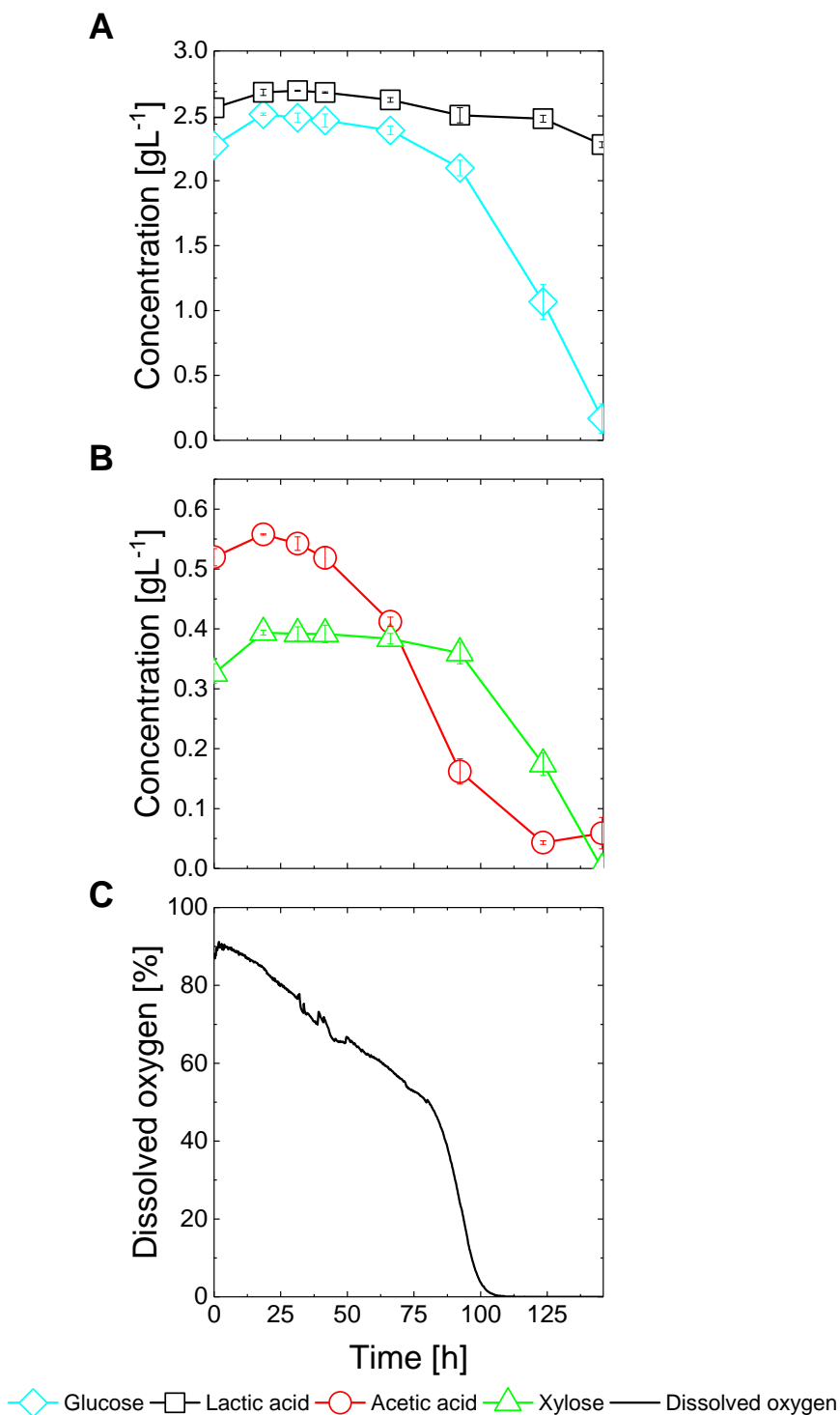


Figure B.3: **Axenic cultivation of *T. reesei* in the membrane-aerated bioreactor on multiple carbon sources.** Batch process on 2.5 gL^{-1} glucose, 2.5 gL^{-1} lactic acid, 0.55 gL^{-1} acetic acid and 0.4 gL^{-1} xylose. *T. reesei* slowly consumes acetic acid. The slower decrease of the dissolved oxygen concentration in comparison to the case without acetic acid (low OTR approach in Fig. 4.4) indicates that the fungal metabolism is inhibited. The change of the slope of the dissolved oxygen concentration at about 80 hours indicates the point at which the acetic acid concentration dropped below the inhibitory threshold of approximately 0.3 gL^{-1} and allowed for simultaneous consumption of glucose, xylose and acetic acid. Error bars represent standard deviation from two independent experiments.

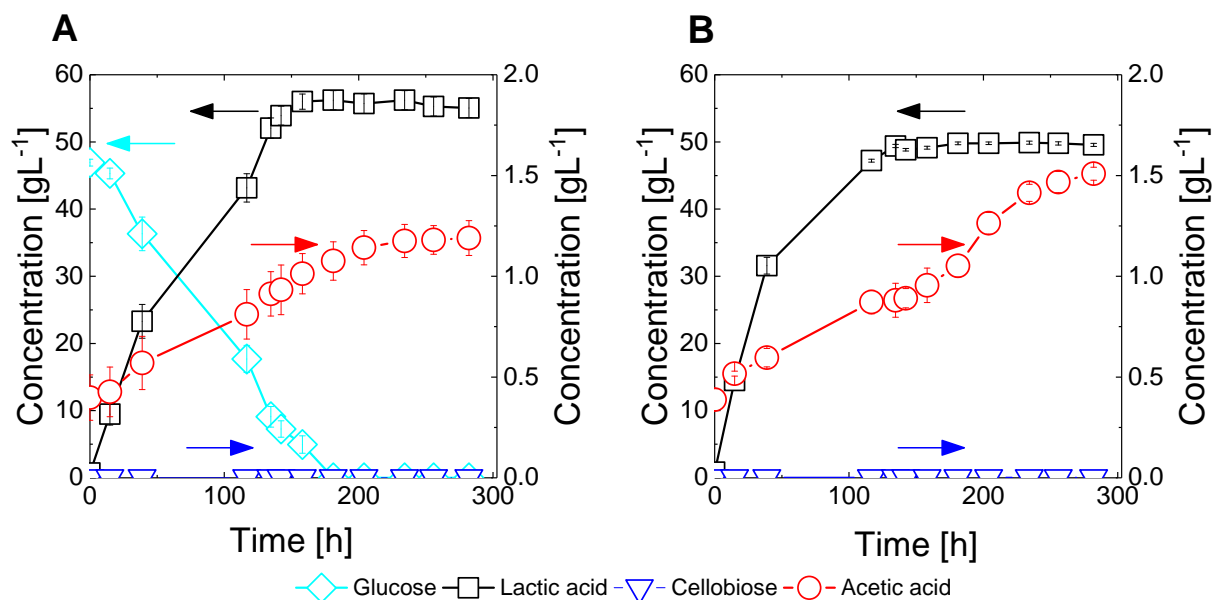


Figure B.4: Axenic cultivation of *L. pentosus* on glucose and in a SSF process on microcrystalline cellulose. (A) 55.5 gL⁻¹ glucose and (B) 5.00 % (w/w) Avicel with 15 FPU per g of cellulose Accellerase© 1500 purchased from DuPont (Wilmington, United States of America).

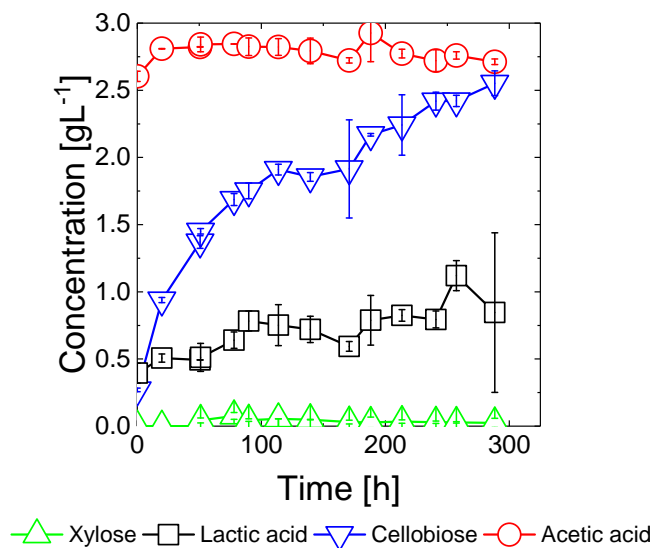


Figure B.5: Consolidated bioprocessing of whole slurry one-stage pretreated beech wood using *T. reesei* and *L. pentosus*. The solid loading was 3.86 % (w/w). Error bars represent standard deviation from two independent experiments.

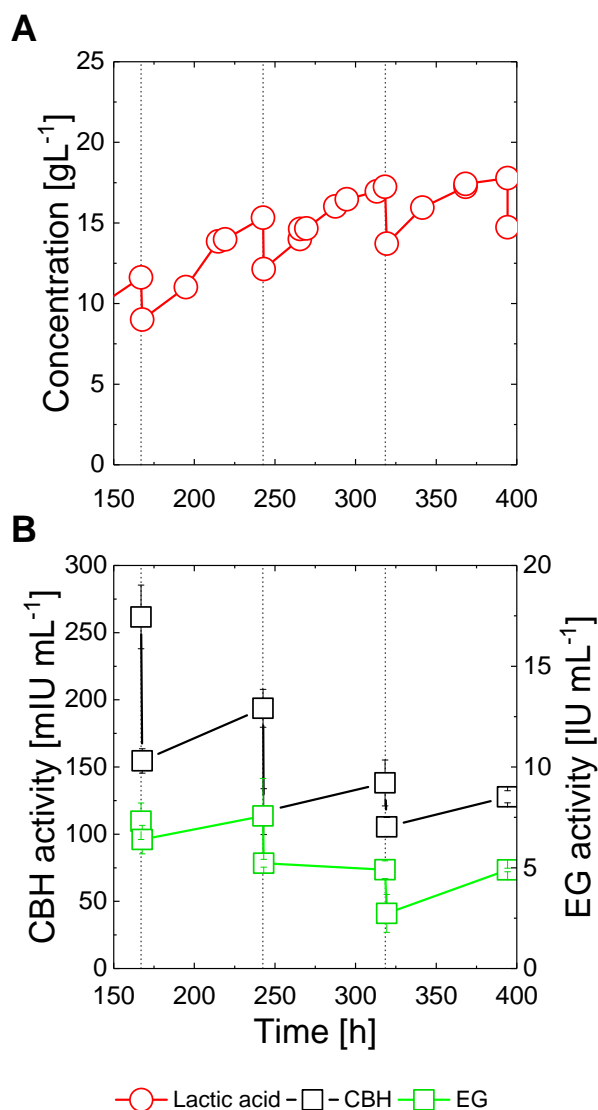


Figure B.6: **Semi-continuous CBP of microcrystalline cellulose to lactic acid using *T. reesei* and *L. pentosus*.** After a batch phase of 160 hours every 72 hours one quarter of the fermentation slurry was removed and replaced with fresh Mandel's medium containing 35 g L^{-1} Avicel. **(A)** shows the lactic acid concentration and **(B)** the activity of cellobiohydrolase (CBH) and endoglucanase (EG). Although the dilution rate was set too high for the release rate of CBH and EG which resulted in a decrease of the activity, the increase of the activity between the replacements indicates the feasibility of the reuse of the fungal biofilm.

APPENDIX C

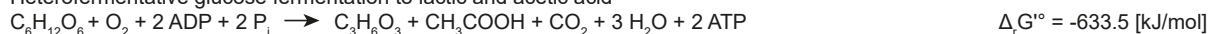
Supplementary for chapter 4: Butyric acid and propionic acid

Lactobacillus pentosus and *Lactobacillus brevis*:

Homofermentative glucose fermentation to lactic acid



Heterofermentative glucose fermentation to lactic and acetic acid

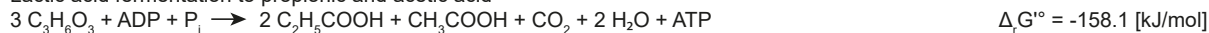


Heterofermentative pentose fermentation to lactic and acetic acid



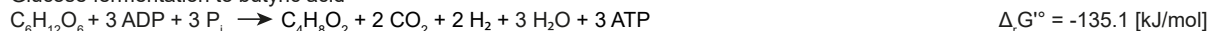
Veillonella criceti:

Lactic acid fermentation to propionic and acetic acid

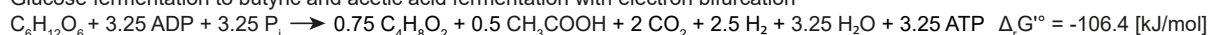


Clostridium tyrobutyricum:

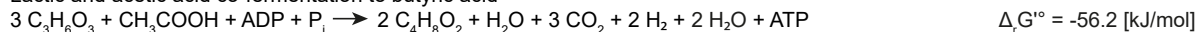
Glucose fermentation to butyric acid



Glucose fermentation to butyric and acetic acid fermentation with electron bifurcation



Lactic and acetic acid co-fermentation to butyric acid



Acetobacterium woodii:

Homofermentative lactic acid fermentation to acetic acid

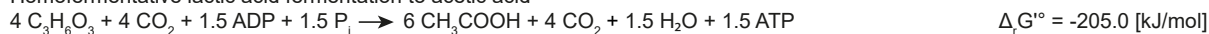


Figure C.1: Caption next page.

Figure C.1: **Overview of metabolic pathways of *L. pentosus*, *L. brevis*, *V. criceti*, *C. tyrobutyricum* and *A. woodii*.** *Lactobacillus pentosus* assimilates hexoses through the Embden-Meyerhof-Parnas pathway (1 mol glucose to 2 mol lactate) and pentoses through the phosphoketolase (PK) pathway (1 mol xylose to 1 mol lactic acid and 1 mol acetic acid). *Lactobacillus brevis* assimilates both hexoses (1 mol glucose to 1 mol lactic acid, 1 mol of acetic acid and 1 mol of carbon dioxide) and pentoses through the PK pathway. *Veillonella criceti* assimilates lactic acid to propionic and acetic acid. *Clostridium tyrobutyricum* can assimilate glucose to butyric acid and carbon dioxide. If *C. tyrobutyricum* co-produces butyric and acetic acid from glucose using electron bifurcation, the energy gain is with 3.25 mol ATP per mol glucose higher in comparison to sole butyric acid formation (3.0 mol ATP per mol glucose). *C. tyrobutyricum* assimilates 3 mol lactate and 1 mol of acetate to 2 mol butyric acid with carbon dioxide and hydrogen formation. *Acetobacterium woodii* can utilize 4 mol lactate and 4 mol carbon dioxide to produce 6 mol acetate and 4 mol carbon dioxide. $\Delta_r G'^{\circ}$ values indicating the Gibbs free energy change in the forward direction at neutral pH and standard state conditions, which were obtained from the eQuilibrator website [226].

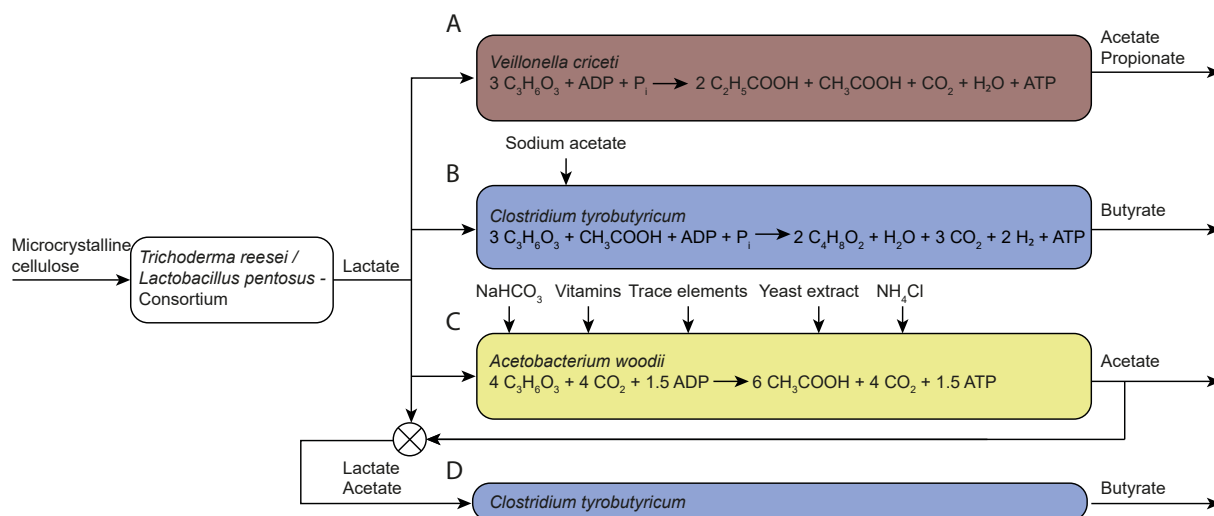


Figure C.2: **Schematic representation of the process flow for the subsequent secondary fermentation of lactate to acetate, propionate and butyrate, respectively.** In a consolidated bioprocess, microcrystalline cellulose was converted by *T. reesei* and *L. pentosus* to a model lactate broth. The model lactate broth was subsequently fermented in (A) to acetate and propionate by *V. criceti*. *V. criceti* is known for its high nutrient requirements [103,170], but we could show, that it is still active on Mandel's medium containing only 1.0 gL^{-1} complex media components. We found that the fermentation time was prolonged by a factor of about three without further supplementation of complex nutrients, while the yields remained the same (Tab. C.4). Therefore, we used Mandel's medium in the CBP experiments with *V. criceti* (section 4.3.3 and 4.3.4). (B) The model lactate broth was used for the subsequent secondary fermentation to butyrate by *C. tyrobutyricum* using sodium acetate as supplement. In order to avoid this supplementation of non-lignocellulosic acetic acid (Fig. 4.6A-E) or glucose (Fig. 4.6F-J), the homoacetogene *A. woodii* was implemented, which converted a part of the produced lactic acid to acetic acid without carbon loss (C). Since *A. woodii* showed no metabolic activity neither on Mandel's medium (data not shown), nor on lactic acid broth, we screened different media supplementations (results shown in table C.3). We blended the acetic acid broth produced with the CBP lactate broth to obtain a lactic to acetic acid ratio of 4.50 gg^{-1} (D). Using this mixture, we produced 12.2 gL^{-1} butyric acid after 135.2 hours (0.41 g butyric acid per g fermentable sugars, selectivity 97.6 %). The subsequent production of butyric acid using *A. woodii* and *C. tyrobutyricum* was successful and external acetic acid sources were omitted. However, more pH control agents were required compared to a consolidated bioprocess (Fig. 4.7E).

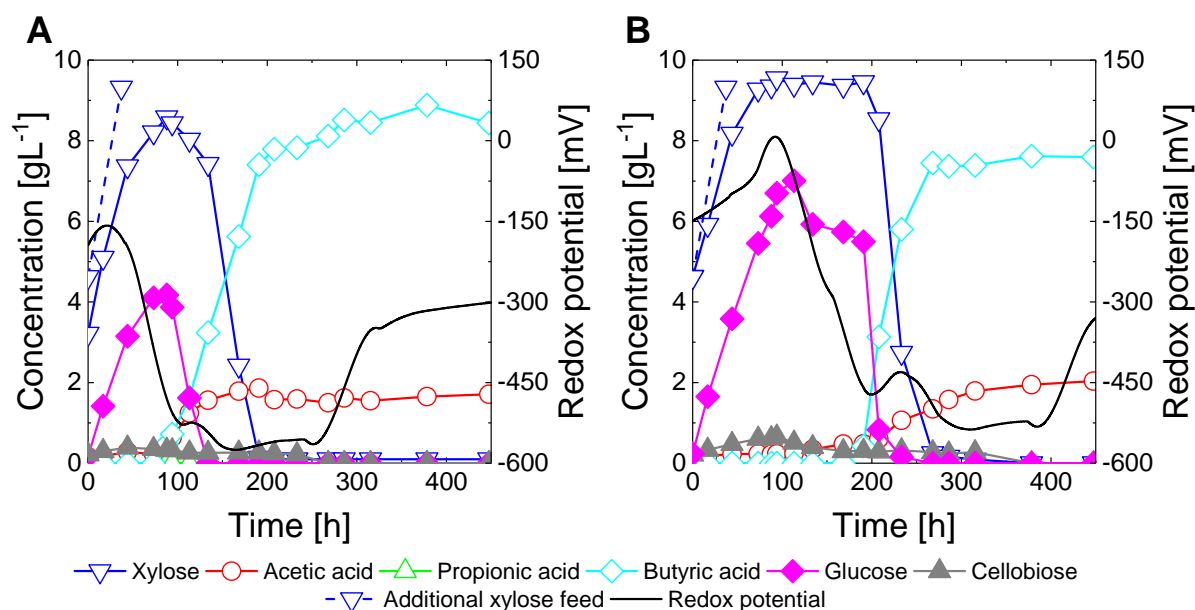


Figure C.3: **SSF of microcrystalline cellulose and xylose using *C. tyrobutyricum* in a fed-batch experiment.** 17.5 g L^{-1} Avicel, 4.7 g L^{-1} xylose and cellulase (15 FPU per gram of cellulose, Accellerase ©1500 DuPont (Wilmington, United States of America) was introduced in one portion. Xylose was fed at a constant rate to an accumulated concentration of 9.32 g L^{-1} in 37.8 hours (dashed blue line). The temperature was set to 30 °C, the pH to 6.0 and the culture was continuously sparged with nitrogen, until *C. tyrobutyricum* showed metabolic activity (A) 200 hours, (B) 250 hours). The reactor volume was 2.7 liter. The final butyric acid to acetic acid ratio was 4.33 ± 0.60 . (A) and (B) represent two duplicates of two independent experiments.

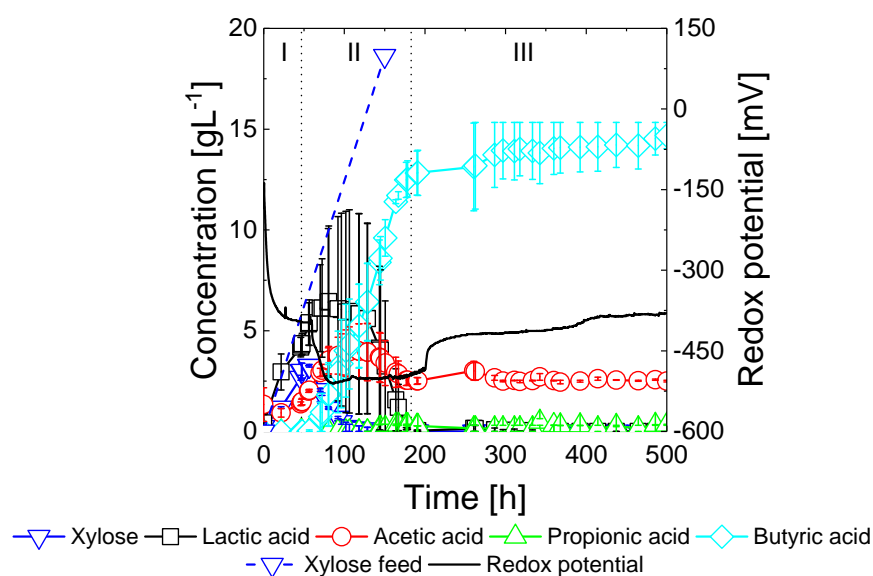


Figure C.4: Fed-batch experiment for CBP of microcrystalline cellulose and xylose to butyric acid, using *T. reesei*, *L. pentosus*, *L. brevis* and *C. tyrobutyricum*. 35 gL⁻¹ Avicel was introduced in one portion and xylose (dashed blue line) was fed at a constant rate to an accumulated concentration of 18.64 gL⁻¹ in 150 hours. The low OTR (0.34 h⁻¹) approach was used (mono-lumen tubing 1.58 mm×3.18 mm×0.80 mm). Error bars represent the standard deviation from two independent fed-batch experiments.

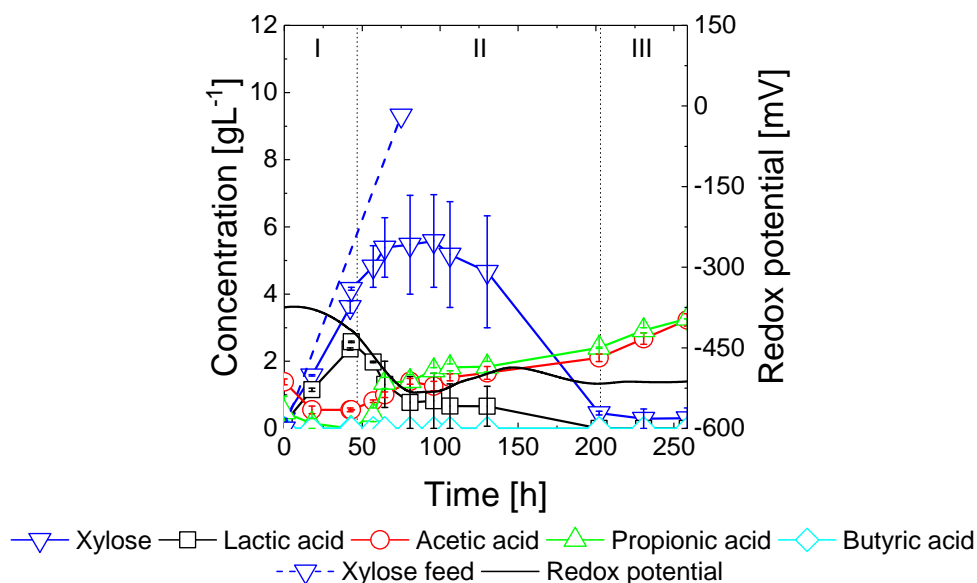


Figure C.5: Fed-batch experiment for CBP of microcrystalline cellulose and xylose to propionic and acetic acid using *T. reesei*, *L. pentosus* and *V. criceti*. 17.5 gL⁻¹ Avicel was introduced in one portion and xylose (dashed blue line) was fed at a constant rate to an accumulated concentration of 9.32 gL⁻¹ in 75 hours in the low OTR approach with a k_{La} of 0.34 h⁻¹ (mono-lumen tubing 1.58 mm×3.18 mm×0.80 mm). Error bars represent the standard deviation from two independent fed-batch experiments.

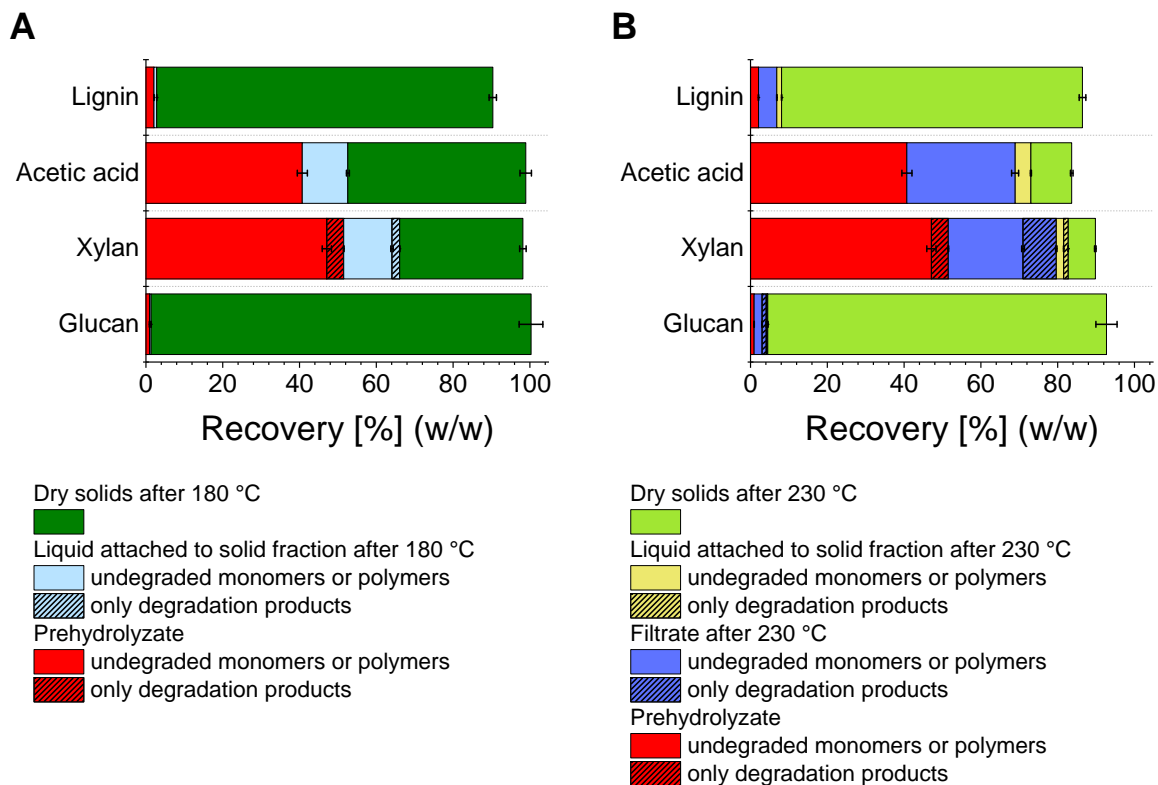


Figure C.6: **Steam pretreatment of beech wood: Recovery of lignin, acetic acid, xylan and glucan after the first stage at 180 °C and the second stage at 230 °C. (A) 180 °C and (B) 230 °C.** The recovery is quantified as a mass percent of input (raw) biomass. Detected degradation products were expressed as glucan or xylan using the following pathways: formic acid is the degradation product of furfural (hydrolytic fission of the aldehyde group [227,228]), which itself is the degradation product of xylose. Hydroxymethyl furfural is the degradation product of glucose.

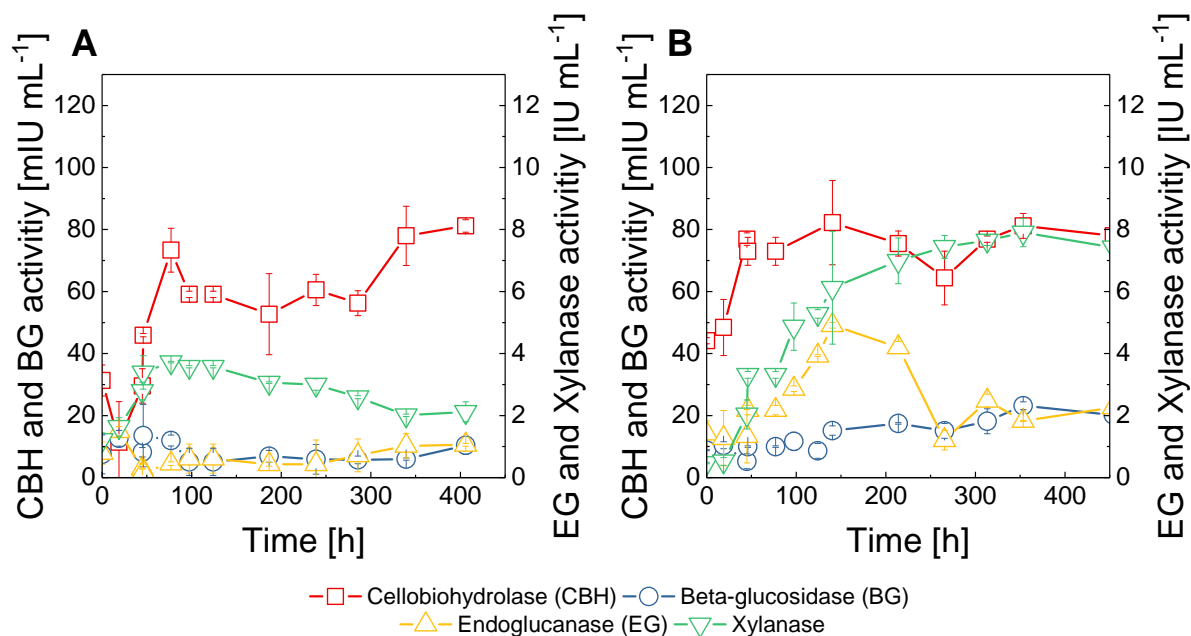


Figure C.7: Activity of cellobiohydrolase (CBH), beta-glucosidase (BG), endoglucanase (EG) and xylanase in the supernatant of the fermentation slurry during various stages of the CBP of pretreated beech wood to butyric acid or propionic acid and acetic acid. (A) CBP using *T. reesei*, *L. pentosus* and *C. tyrobutyricum* as shown in Fig. 4.9B. (B) CBP using *T. reesei*, *L. pentosus* and *V. criceti* as shown in Fig. 4.9C. Error bars represent the standard deviation from duplicate assays.

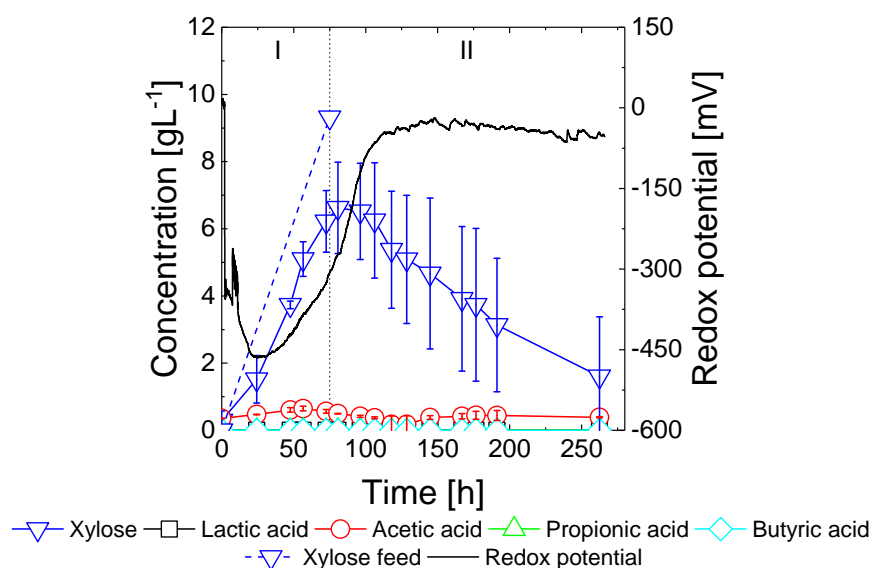


Figure C.8: **CBP for direct production of butyric acid from microcrystalline cellulose and xylose using a co-culture of *T. reesei* and *C. tyrobutyricum*.** In the high OTR approach (3.24 h^{-1}), *C. tyrobutyricum* was inoculated at time zero, 48 hours after *T. reesei*. In phase I, a linear xylose feed was applied to an accumulated concentration of 9.32 gL^{-1} . The redox potential dropped temporarily due to the presence of reducing agents from the pre-culture of *C. tyrobutyricum*, but increased rapidly to a level unsuitable for the cultivation of the obligate anaerobe *C. tyrobutyricum*, which therefore exhibited only temporary metabolic activity.

Table C.1: CBP of different substrates in fed-batch mode using *T. reesei*, different lactic acid bacteria and *C. tyrobutyricum*.

Microbial consortium	Fig.	OTR	Substrate	Ferm. time ¹ [h]	Acetic acid ¹ [gL ⁻¹]	Propionic acid ¹ [gL ⁻¹]	Butyric acid [gL ⁻¹]	Total carboxylic acids ¹ [gL ⁻¹]	Butyric acid yield [gg ⁻¹ ferment. sugars]	Product selectivity ² [%]	Carbox. acids yield [gg ⁻¹ ferment. sugars]
<i>T. reesei</i> , <i>L. pentosus</i> , <i>C. tyrobutyricum</i>	4.5A	high	1.75 % (w/w) Avicel + 9.32 gL ⁻¹ xylose ³	166.92	0.3±0.1	0.0±0.0	4.1±0.8	4.4±0.8	0.14±0.03	93.1±0.8	0.15±0.03
	4.5B	high	1.75 % (w/w) Avicel + 9.32 gL ⁻¹ xylose + 2 gL ⁻¹ acetic acid ³	216.92	3.1±0.1	0.0±0.0	10.7±0.2	13.8±0.2	0.37±0.01	77.6±0.3	0.41±0.01 ⁴
	4.5D	low	1.75 % (w/w) Avicel + 9.32 gL ⁻¹ xylose ³	371.67	0.4±0.1	0.0±0.0	10.2±0.5	10.5±0.5	0.35±0.02	96.7±0.1	0.37±0.02
<i>T. reesei</i> , <i>L. pentosus</i> , <i>L. brevis</i> , <i>C. tyrobutyricum</i>	4.5C	high	1.75 % (w/w) Avicel + 9.32 gL ⁻¹ xylose ³	202.00	2.7±0.1	0.0±0.0	9.5±0.3	12.2±0.3	0.33±0.01	77.9±10.3	0.42±0.01
	C.4	low	3.50 % (w/w) Avicel + 18.64 gL ⁻¹ xylose ⁵	500.00	2.5±0.1	0.3±0.0	14.7±0.7	17.6±0.6	0.26±0.01	83.6±0.7	0.31±0.01

Continued on next page.

¹At highest butyric acid concentration.²Percent (w/w) of butyric acid from total carboxylic acids.³Xylose or xylose/acetic acid fed at a constant rate over 75 hours.⁴Fed acetic acid subtracted.⁵Xylose fed at a constant feeding rate over 150 hours.

Table C.1: CBP of different substrates in fed-batch mode by *T. reesei*, different LAB and *C. tyrobutyricum* (continued).

Microbial consortium	Fig.	OTR	Substrate	Ferm. time ¹	Acetic acid ¹	Propionic acid ¹	Butyric acid	Total carboxylic acids ¹	Butyric acid yield [gg ⁻¹ ferment. sugars]	Product selectivity ² [%]	Carbox. acids yield [gg ⁻¹ ferment. sugars]
				[h]	[gL ⁻¹]	[gL ⁻¹]	[gL ⁻¹]	[gL ⁻¹]			
<i>T. reesei</i> , <i>L. pentosus</i> , <i>C. tyrobutyricum</i>	4.9B	low	3 % (w/w) pretreated beech wood with prehydrolyzate ⁶	765.00	0.7±0.1	0.2±0.1	9.5±0.2	10.4±0.1	0.38±0.01	91.5±0.8	0.42±0.01
<i>C. tyrobutyricum</i> SSF, 15 FPU, Accellerase®, 1500/g cellulose	C.3	-	1.75 % (w/w) Avicel + 9.32 gL ⁻¹ xylose ⁷	447.5	1.9±0.2	0.0±0.0	8.0±0.4	9.9±0.3	0.28±0.01	81.0±2.1	0.34±0.01

⁶Prehydrolyzate fed at a constant feeding rate over 200 hours.⁷Avicel and 4.7 gL⁻¹ xylose introduced at the beginning and the remaining xylose fed at a constant rate over 37.2 hours.

Table C.2: CBP of different substrates in fed-batch mode using *T. reesei*, *L. pentosus* and *V. criceti*.

Microbial consortium	Fig.	OTR	Substrate		Ferm. time	Acetic acid	Propionic acid	Total carboxylic acids	Acetic acid yield	Propionic acid yield	Carbox. acids yield
					[h]	[gL ⁻¹]	[gL ⁻¹]	[gL ⁻¹]	[gg ⁻¹ ferment. sugars]	[gg ⁻¹ ferment. sugars]	[gg ⁻¹ ferment. sugars]
<i>T. reesei</i> , <i>L. pentosus</i> , <i>V. criceti</i>	C.5	low	1.75 % (w/w) Avicel + 9.32 gL ⁻¹ xylose ¹		371.67	4.5±0.2	4.4±0.2	8.9±0.1	0.16±0.01	0.15±0.01	0.31±0.01
	4.8B	low	3.50 % (w/w) Avicel + 18.64 gL ⁻¹ xylose ²		342.50	13.7±0.3	9.3±0.2	23.0±0.1	0.24±0.01	0.16±0.01	0.40±0.01
	4.9C	low	3 % (w/w) pretreated beech wood with prehydrolyzate ³		406.00	6.7±0.2	5.6±0.1	12.4±0.1	0.27±0.01	0.35±0.02	0.50±0.01

¹Xylose fed at a constant rate over 75 hours.²Xylose fed at a constant rate over 150 hours.³Prehydrolyzate fed at a constant feeding rate over 200 hours.

Table C.3: **Cultivations of *A. woodii* on CBP lactate broths for various media supplements.** Lactate broth (273 mM lactic acid), NaHCO₃ (10 gL⁻¹), Na₂CO₃ (0.25 mL 5 % (w/v) per 10 mL of medium), vitamin mix (0.1 mL per 10 mL of medium), trace elements mix (0.2 mL per 10 mL of medium). A '+' indicates supplementation. *A. woodii* was cultivation at 30 °C for 217.8 hours under anoxic conditions. We found that the supplementation of various vitamins and high bicarbonate concentrations were essential for metabolic activity. When a mixture of trace elements was added in addition to the essential supplements, we reached a conversion of 22.9 gL⁻¹ lactic acid to 21.3 gL⁻¹ acetic acid after 150.5 hours (92 % of the theoretical yield).

	Lactate broth	NaHCO ₃	Na ₂ CO ₃	Vitamin mix- ture	Trace mix- ture	Lactic acid utilized [mM]	Acetic acid produced [mM]
CBP lactate broth from Avicel	+	-	-	-	-	34.0±9.1	46.0±11.1
	+	+	-	-	-	116.9±10.4	137.4±8.5
	+	+	+	-	-	75.4±15.6	95.1±13.2
	+	-	-	+	-	28.3±27.9	35.9±30.8
	+	+	-	+	-	127.0±21.0	142.6±16.9
	+	+	+	+	-	97.9±25.8	115.0±28.2
	+	-	-	-	+	15.3±1.6	24.3±1.5
	+	+	-	-	+	130.4±30.1	145.7±32.3
	+	+	+	-	+	105.7±22.7	123.8±29.3
	+	-	-	+	+	2.1±2.0	8.7±1.4
	+	+	-	+	+	159.5±5.9	190.1±1.6
	+	+	+	+	+	256.2±46.4	299.0±50.1
CBP lactate broth from steam- pretreated beech wood	+	+	+	+	+	-	-

Table C.4: Cultivations of *V. criceti* on CBP lactate broths for various media supplements. *V. criceti* is known for its high nutrient requirements, such as yeast extract and peptone. Since these complex nutrients are expensive and hamper a potential industrial application for the production of bulk chemicals, we tested if *V. criceti* grew on Mandels medium with only 0.75 gL^{-1} peptone and 0.25 gL^{-1} yeast extract as complex components. Metabolic activity could be measured (data not shown). The projected integration of the obligate anaerobe in the consortium would result in a nutritional competition. We added complex media components to the CBP lactate broth and tested their effect on the metabolic activity of *V. criceti*. The bacterium *V. criceti* grew on the lactate broth and converted $22.7 \pm 0.4 \text{ gL}^{-1}$ lactic acid to $9.2 \pm 0.2 \text{ gL}^{-1}$ propionic acid and $6.3 \pm 0.2 \text{ gL}^{-1}$ acetic acid after 222.3 hours. Nevertheless, a beneficial impact of the supplementation, especially of trypticase peptone, was observed, reducing the fermentation time from 222.3 to 72.1 hours. Concentrations used: lactate broth, 274 mM ; trypticase peptone, 5 gL^{-1} ; yeast extract, 3 gL^{-1} . A '+' indicates supplementation. For all experiments, 0.75 gL^{-1} sodium thioglycolate was added. All cultivations were performed at 37°C under anoxic conditions.

	Lactate broth	Trypticase peptone	Yeast extract	Lactic acid utilized [mM]	Acetic acid produced [mM]	Propionic acid produced [mM]
72.1 hours	+	-	-	175.0 ± 67.8	44.8 ± 31.3	70.0 ± 33.0
	+	+	-	253.6 ± 2.1	88.3 ± 2.0	115.0 ± 3.8
	+	-	+	174.9 ± 4.9	46.8 ± 4.8	64.8 ± 1.2
	+	+	+	266.1 ± 6.1	98.6 ± 4.3	124.7 ± 0.1
222.3 hours	+	-	-	252.1 ± 4.8	79.9 ± 1.0	121.2 ± 2.9
	+	+	-	253.6 ± 2.1	86.2 ± 1.2	122.8 ± 3.3
	+	-	+	222.8 ± 3.3	71.2 ± 2.1	121.3 ± 6.3
	+	+	+	266.1 ± 6.1	93.0 ± 0.3	129.2 ± 2.5

Table C.5: Theoretical yields of fermentation via lactate platform compared to alternative direct sugar fermentation routes for selected target products. Shown are the yields for conversion of glucose, xylose, acetic acid and steam-pretreated beech wood (a mixture of the three former compounds). The routes are described in tables C.6 and C.7.

Route	Target product	$\gamma_{P/Glu}$ [gg ⁻¹]		$\gamma_{P/Xyl}$ [gg ⁻¹]		$\gamma_{P/AA}$ [gg ⁻¹]		$\gamma_{P/(Glu+Xyl+AA)}$ [gg ⁻¹]	
		LA platform	Alternative platform	LA platform	Alternative platform	LA platform	Alternative platform	LA platform	Alternative platform
1	Acetic acid	1.00	0.67	1.00	0.67	1.00	1.00	1.00	0.69
2	Acetic acid	0.22	0.22	0.53	0.53	1.00	1.00	0.35	0.35
	Propionic acid	0.55	0.55	0.33	0.33	0.00	0.00	0.46	0.46
3	Acetic acid	0.00	0.00	0.27	0.00	1.00	1.00	0.00	0.07
	Butyric acid	0.53	0.49	0.39	0.49	0.00	0.00	0.52	0.45
4	Polyhydroxy-butyric acid	0.52	0.48	0.51	0.48	0.48	0.48	0.51	0.48
5	Hexanoic acid	0.43	0.43	0.39	0.39	0.00	0.00	0.47	0.47
6	Tripalmitin	0.27	0.27	0.27	0.27	0.27	0.27	0.27	0.27
7	Acetic acid	0.00	0.00	0.00	0.00	1.00	1.00	0.00	0.07
	Ethanol	0.77	0.51	0.77	0.51	0.77	0.00	0.77	0.48
8	Acetic acid	0.00	0.00	0.27	0.00	1.00	1.00	0.00	0.07
	Butanol	0.45	0.41	0.33	0.41	0.00	0.00	0.44	0.38
9	Acetic acid	0.33	0.33	0.60	0.33	1.00	1.00	0.45	0.38
	1,2-Propanediol	0.42	0.42	0.25	0.42	0.00	0.00	0.35	0.39
10	Acetic acid	0.33	unknown	0.60	unknown	1.00	unknown	0.45	unknown
	Propionic acid	0.21	unknown	0.12	unknown	0.00	unknown	0.17	unknown
	Propanol	0.17	unknown	0.10	unknown	0.00	unknown	0.14	unknown

Table C.6: Overview of microorganisms and pathways used for the calculation of the theoretical yield of the lactate platform and conventional production routes using glucose as substrate.

Route	Microbial pathways: (A) lactate platform, (B) conventional approach	Microorganism(s)	Ref.
1A	I) Glucose \rightarrow 2 Lactic acid	I) <i>L. pentosus</i>	
	II) 2 Lactic acid \rightarrow 3 Acetic acid	II) <i>A. woodii</i>	
	I-II): Glucose \rightarrow 3 Acetic acid		
1B	I) Glucose \rightarrow 2 EtOH + 2 CO ₂	I) <i>S. cerevisiae</i>	
	II) 2 EtOH + 2 O ₂ \rightarrow 2 Acetic acid + 2 H ₂ O	II) <i>Gluconobacter oxydans</i>	
	I-II): Glucose + 2 O₂ \rightarrow 2 Acetic acid + 2 CO₂ + 2 H₂O		
2A	I) 1.5 Glucose \rightarrow 3 Lactic acid	I) <i>L. pentosus</i>	
	II) 3 Lactic acid \rightarrow 2 Propionic acid + Acetic acid + CO ₂ + H ₂ O	II) <i>V. criceti</i>	
	I-II): 1.5 Glucose \rightarrow 2 Propionic acid + Acetic acid + CO₂ + H₂O		
2B	1.5 Glucose \rightarrow 2 Propionic acid + Acetic acid + CO₂ + H₂O	<i>Propionibacterium</i> spp.	
3A	I) 11 Glucose \rightarrow 22 Lactic acid	I) <i>L. pentosus</i>	
	II) 4 Lactic acid \rightarrow 6 Acetic acid	II) <i>A. woodii</i>	
	III) 18 Lactic acid + 6 Acetic acid \rightarrow 12 Butyric acid + 18 CO ₂ + 12 H ₂ + 6 H ₂ O	III) <i>C. tyrobutyricum</i>	
	I-III): 11 Glucose \rightarrow 12 Butyric acid + 18 CO₂ + 12 H₂ + 6 H₂O		
3B	Glucose \rightarrow Butyric acid + 2 CO₂ + 2 H₂	<i>C. tyrobutyricum</i>	
4A	I) 11 Glucose \rightarrow 22 Lactic acid	I) <i>L. pentosus</i>	
	II) 4 Lactic acid \rightarrow 6 Acetic acid	II) <i>A. woodii</i>	
	III) 18 Lactic acid + 6 Acetic acid \rightarrow 12 Butyric acid + 18 CO ₂ + 12 H ₂ + 6 H ₂ O	III) <i>C. tyrobutyricum</i>	
	IV) 12 Butyric acid + 6 O ₂ + 12 H ₂ O \rightarrow 12 Polyhydroxybutyrate + 24 H ₂ O	IV) <i>Rhodospirillum rubrum</i>	[229]
	I-IV): 11 Glucose + 6 O₂ + 12 H₂O \rightarrow 12 Polyhydroxybutyrate + 18 CO₂ + 12 H₂ + 30 H₂O		
4B	Glucose + 1.5 O₂ \rightarrow Polyhydroxybutyrate + 2 CO₂ + 3 H₂O	<i>Rhodospirillum rubrum</i>	[229]
Continued on next page.			

Table C.6: Overview of microorganisms and pathways used for the calculation of the theoretical yield of the lactate platform and conventional production routes using glucose as substrate (continued).

Route	Microbial pathways: (A) lactate platform, (B) conventional approach	Microorganism(s)	Ref.
5A	I) 3 Glucose \rightarrow 6 Lactic acid II) 6 Lactic acid \rightarrow 2 Hexanoic acid + 6 CO ₂ + 2 H ₂ O + 4 H ₂ I-II): 3 Glucose \rightarrow 2 Hexanoic acid + 6 CO₂ + 2 H₂O + 4 H₂	I) <i>L. pentosus</i> II) <i>M. elsdenii</i>	
5B	3 Glucose \rightarrow 2 Hexanoic acid + 6 CO₂ + 2 H₂O + 4 H₂	<i>M. elsdenii</i>	[230]
6A	I) 16.33 Glucose \rightarrow 32.67 Lactic acid II) 32.67 Lactic acid \rightarrow 49 Acetic acid III) 49 Acetic acid + 13.5 O ₂ \rightarrow C ₅₁ H ₉₈ O ₆ + 47 CO ₂ ¹ I-III): 16.33 Glucose + 13.5 O₂ \rightarrow C₅₁H₉₈O₆ + 47 CO₂	I) <i>L. pentosus</i> II) <i>A. woodii</i> III) <i>Yarrowia lipolytica</i>	[231,232]
6B	16.33 Glucose + 13.5 O₂ \rightarrow C₅₁H₉₈O₆ + 47 CO₂¹	<i>Yarrowia lipolytica</i>	
7A	I) Glucose \rightarrow 2 Lactic acid II) 2 Lactic acid \rightarrow 3 Acetic acid III) 3 Acetic acid + 6 CO + 3 H ₂ O \rightarrow 3 EtOH + 6 CO ₂ I-III): Glucose + 6 CO + 3 H₂O \rightarrow 3 EtOH + 6 CO₂	I) <i>L. pentosus</i> II) <i>A. woodii</i> III) <i>P. furiosus</i> ²	[207]
7B	Glucose \rightarrow 2 EtOH + 2 CO₂	<i>S. cerevisiae</i>	
8A	I) 11 Glucose \rightarrow 22 Lactic acid II) 4 Lactic acid \rightarrow 6 Acetic acid III) 12 Lactic acid + 6 Acetic acid \rightarrow 12 Butyric acid + 18 CO ₂ + 12 H ₂ + 6 H ₂ O IV) 12 Butyric acid + 24 CO + 12 H ₂ O \rightarrow 12 n-Butanol + 24 CO ₂ I-IV): 11 Glucose + 24 CO + 12 H₂O \rightarrow 12 n-Butanol + 42 CO₂ + 12 H₂ + 6 H₂O	I) <i>L. pentosus</i> II) <i>A. woodii</i> III) <i>C. tyrobutyricum</i> IV) <i>P. furiosus</i> ²	[207]
8B	Glucose \rightarrow n-Butanol + 2 CO₂ + H₂O	<i>C. acetobutyricum</i>	
Continued on next page.			

¹Tripalmitin used as model lipid.²*P. furiosus* engineered.

Table C.6: Overview of microorganisms and pathways used for the calculation of the theoretical yield of the lactate platform and conventional production routes using glucose as substrate (continued).

Route	Microbial pathways: (A) lactate platform, (B) conventional approach	Microorganism(s)	Ref.
9A	I) Glucose \rightarrow 2 Lactic acid	I) <i>L. pentosus</i>	[233]
	II) 2 Lactic acid \rightarrow 1,2-Propanediol + Acetic acid + CO ₂	II) <i>Lactobacillus buchneri</i>	
	I-II): Glucose \rightarrow 1,2-Propanediol + Acetic acid + CO₂		
9B	Glucose \rightarrow 1,2-Propanediol + Acetic acid + CO₂	<i>C. thermosaccharolyticum</i>	[234]
10A	I) Glucose \rightarrow 2 Lactic acid	I) <i>L. pentosus</i>	[233]
	II) 2 Lactic acid \rightarrow 1,2-Propanediol + Acetic acid + CO ₂	II) <i>L. bucheri</i>	
	III) 1,2-Propanediol \rightarrow 0.5 1-Propanol + 0.5 Propionic acid + 0.5 H ₂ O	III) <i>Lactobacillus diolivorans</i>	[235]
	I-III): Glucose \rightarrow 0.5 1-Propanol + 0.5 Propionic acid + Acetic acid + 0.5 H₂O + CO₂		
10B	unknown		

Table C.7: Overview of microorganisms and pathways used for the calculation of the theoretical yield of the lactate platform and conventional production routes using xylose as substrate.

Route	Microbial pathways: (A) lactate platform, (B) conventional approach	Microorganism(s)	Ref.
1A	I) Xylose \rightarrow Lactic acid + Acetic acid	I) <i>L. pentosus</i>	
	II) Lactic acid \rightarrow 1.5 Acetic acid	II) <i>A. woodii</i>	
	I-II): Xylose \rightarrow 2.5 Acetic acid		
1B	I) 3 Xylose \rightarrow 5 EtOH + 5 CO ₂	I) <i>Pichia stipitis</i>	
	II) 5 EtOH + 5 O ₂ \rightarrow 5 Acetic acid + 5 H ₂ O	II) <i>G. oxydans</i>	
	I-II): 3 Xylose + 5 O₂ \rightarrow 5 Acetic acid + 5 H₂O		
2A	I) 3 Xylose \rightarrow 3 Lactic acid + 3 Acetic acid	I) <i>L. pentosus</i>	
	II) 3 Lactic acid \rightarrow 2 Propionic acid + Acetic acid + CO ₂ + H ₂ O	II) <i>V. criceti</i>	
	I-II): 3 Xylose \rightarrow 2 Propionic acid + 4 Acetic acid + CO₂ + H₂O		
2B	3 Xylose \rightarrow 2 Propionic acid + 4 Acetic acid + CO₂ + H₂O	<i>Propionibacterium</i> spp.	
3A	I) 3 Xylose \rightarrow 3 Lactic acid + 3 Acetic acid	I) <i>L. pentosus</i>	
	II) 3 Lactic acid + Acetic acid \rightarrow 2 Butyric acid + 3 CO ₂ + 2 H ₂ + H ₂ O	II) <i>C. tyrobutyricum</i>	
	I-II): 3 Xylose \rightarrow 2 Butyric acid + 2 Acetic acid + 3 CO₂ + 2 H₂ + H₂O		
3B	3 Xylose \rightarrow 2.5 Butyric acid + 5 CO₂ + 5 H₂	<i>C. tyrobutyricum</i>	
4A	I) 3 Xylose \rightarrow 3 Lactic acid + 3 Acetic acid	I) <i>L. pentosus</i>	[229]
	II) 3 Lactic acid + Acetic acid \rightarrow 2 Butyric acid + 3 CO ₂ + 2 H ₂ + H ₂ O	II) <i>C. tyrobutyricum</i>	
	III) 2 Butyric acid + O ₂ + 2 H ₂ O \rightarrow 2 Polyhydroxybutyrate + 4 H ₂ O	III) <i>R. rubrum</i>	
	IV) 2 Acetic acid + O ₂ \rightarrow 0.667 Polyhydroxybutyrate + 1.33 CO ₂ + 2 H ₂ O	IV) <i>R. rubrum</i>	
	I-IV): 3 Xylose + 2 O₂ + 2 H₂O \rightarrow 2.667 Polyhydroxybutyrate + 4.33 CO₂ + 2 H₂ + 7 H₂O		
4B	1.2 Xylose + 1.5 O₂ \rightarrow Polyhydroxybutyrate + 2 CO₂ + 3 H₂O	<i>Burkholderia sacchari</i>	[236]
Continued on next page.			

Table C.7: Overview of microorganisms and pathways used for the calculation of the theoretical yield of the lactate platform and conventional production routes using xylose as substrate (continued).

Route	Microbial pathways: (A) lactate platform, (B) conventional approach	Microorganism(s)	Ref.
5A	I) 2 Xylose \rightarrow 2 Lactic acid + 2 Acetic acid II) Lactic acid + Acetic acid \rightarrow Butyric acid + H ₂ O + CO ₂ III) Lactic acid + Butyric acid \rightarrow Hexanoic acid + H ₂ O + CO ₂ I-III): 2 Xylose \rightarrow Hexanoic acid + Acetic acid + 2 H ₂ O + 2 CO ₂	I) <i>L. pentosus</i> II) <i>M. elsdenii</i> III) <i>M. elsdenii</i>	
5B	2 Xylose \rightarrow Hexanoic acid + Acetic acid + 2 H ₂ O + 2 CO ₂	<i>M. elsdenii</i>	
6A	I) 19.6 Xylose \rightarrow 19.6 Lactic acid + 19.6 Acetic acid II) 19.6 Lactic acid \rightarrow 29.4 Acetic acid III) 49 Acetic acid + 13.5 O ₂ \rightarrow C ₅₁ H ₉₈ O ₆ + 47 CO ₂ I-III): 19.6 Xylose + 13.5 O ₂ \rightarrow C ₅₁ H ₉₈ O ₆ + 47 CO ₂ ¹	I) <i>L. pentosus</i> II) <i>A. woodii</i> III) e.g. <i>Y. lipolytica</i>	[231,232]
6B	19.6 Xylose + 13.5 O ₂ \rightarrow C ₅₁ H ₉₈ O ₆ + 47 CO ₂ ¹	<i>Y. lipolytica</i>	
7A	I) 2 Xylose \rightarrow 2 Lactic acid + 2 Acetic acid II) 2 Lactic acid \rightarrow 3 Acetic acid III) 5 Acetic acid + 10 CO + 5 H ₂ O \rightarrow 5 EtOH + 10 CO ₂ ² I-III): 2 Xylose + 10 CO + 5 H ₂ O \rightarrow 5 EtOH + 10 CO ₂	I) <i>L. pentosus</i> II) <i>A. woodii</i> III) <i>P. furiosus</i>	[207]
7B	3 Xylose \rightarrow 5 EtOH + 5 CO ₂ ²	<i>S. cerevisiae</i>	
8A	I) 3 Xylose \rightarrow 3 Lactic acid + 3 Acetic acid II) 3 Lactic acid + Acetic acid \rightarrow 2 Butyric acid + 3 CO ₂ + 2 H ₂ + H ₂ O III) 2 Butyric acid + 4 CO + 2 H ₂ O \rightarrow 2 n-Butanol + 4 CO ₂ I-III): 3 Xylose + 4 CO + 2 H ₂ O \rightarrow 2 n-Butanol + 2 Acetic acid + 7 CO ₂ + 2 H ₂ + H ₂ O	I) <i>L. pentosus</i> II) <i>C. tyrobutyricum</i> III) <i>P. furiosus</i>	[207]
8B	1.2 Xylose \rightarrow n-Butanol + 2 CO ₂ + H ₂ O	<i>C. acetobutyricum</i>	
Continued on next page.			

¹Tripalmitin used as model lipid.

²*P. furiosus* engineered.

Table C.7: Overview of microorganisms and pathways used for the calculation of the theoretical yield of the lactate platform and conventional production routes using xylose as substrate (continued).

Route	Microbial pathways: (A) lactate platform, (B) conventional approach	Microorganism(s)	Ref.
9A	I) 2 Xylose \rightarrow 2 Lactic acid + 2 Acetic acid	I) <i>L. pentosus</i>	[233]
	II) 2 Lactic acid \rightarrow 1,2-Propanediol + Acetic acid + CO ₂	II) <i>L. buchneri</i>	
	I-II): 2 Xylose \rightarrow 1,2-Propanediol + 3 Acetic acid + CO₂		
9B	1.2 Xylose \rightarrow 1,2-Propanediol + Acetic acid + CO₂	<i>C. thermosaccharolyticum</i>	[234]
10A	I) 2 Xylose \rightarrow 2 Lactic acid + 2 Acetic acid	I) <i>L. pentosus</i>	[233]
	II) 2 Lactic acid \rightarrow 1,2-Propanediol + Acetic acid + CO ₂	II) <i>L. bucheri</i>	
	III) 1,2-Propanediol \rightarrow 0.5 1-Propanol + 0.5 Propionic acid + 0.5 H ₂ O	III) <i>L. diolivorans</i>	[235]
	I-III): 2 Xylose \rightarrow 0.5 1-Propanol + 0.5 Propionic acid + 3 Acetic acid + 0.5 H₂O + CO₂		
10B	unknown		

APPENDIX D

References

- [1] Intergovernmental Panel on Climate Change (IPCC). *Special Report on Global Warming of 1.5 °C*. Tech. rep., Incheon, South Korea [2018].
- [2] J. Blunden, D. S. Arndt and G. Hartfield. *State of the Climate in 2017*. Bulletin of the American Meteorological Society, 99(8):1–310 [2018]. doi: 10.1175/2018BAMSStateoftheClimate.1.
- [3] P. Tans and R. Keeling. *Trends in Atmospheric Carbon Dioxide*. NOAA/ESRL (www.esrl.noaa.gov/gmd/ccgg/trends/) and Scripps Institution of Oceanography (www.scrippsco2.ucsd.edu/), accessed on 2018-12-16. [2018].
- [4] D. W. Keith, G. Holmes, D. St. Angelo *et al.* *A Process for Capturing CO₂ from the Atmosphere*. Joule, 2(8):1573–1594 [2018]. doi: 10.1016/J.JOULE.2018.05.006.
- [5] M. R. Ghaffariyan, M. Brown, M. Acuna *et al.* *An international review of the most productive and cost effective forest biomass recovery technologies and supply chains*. Renewable and Sustainable Energy Reviews, 74:145–158 [2017]. doi: 10.1016/j.rser.2017.02.014.
- [6] R. D. Perlack, L. L. Wright, A. F. Turhollow *et al.* *Biomass as feedstock for a bioenergy and bioproducts industry: the technical feasibility of a billion-ton annual supply*. Tech. rep., United States Department of Energy, Oak Ridge, United States of America [2005]. doi: 10.2172/885984.
- [7] R. D. Perlack, L. M. Eaton, A. F. Turhollow *et al.* *U.S. Billion-ton Update: Biomass Supply for a Bioenergy and Bioproducts Industry*. Tech. rep., United States Department of Energy, Oak Ridge, United States of America [2011]. doi: 10.1089/ind.2011.7.375.

-
- [8] V. Burg, G. Bowman, M. Erni *et al.* *Analyzing the potential of domestic biomass resources for the energy transition in Switzerland*. *Biomass and Bioenergy*, 111:60–69 [2018]. doi: 10.1016/j.biombioe.2018.02.007.
- [9] B. Kamm and M. Kamm. *Principles of biorefineries*. *Applied Microbiology and Biotechnology*, 64(2):137–145 [2004]. doi: 10.1007/s00253-003-1537-7.
- [10] S. Brethauer and M. H. Studer. *Consolidated bioprocessing of lignocellulose by a microbial consortium*. *Energy and Environmental Science*, 7(4):1446–1453 [2014]. doi: 10.1039/c3ee41753k.
- [11] J. H. Yeap, F. Héroguel, R. L. Shahab *et al.* *Selectivity Control during the Single-Step Conversion of Aliphatic Carboxylic Acids to Linear Olefins*. *ACS Catalysis*, 8(11):10769–10773 [2018]. doi: 10.1021/acscatal.8b03370.
- [12] D. C. Elliott. *Catalytic hydrothermal gasification of biomass*. *Biofuels, Bioproducts and Biorefining*, 2(3):254–265 [2008]. doi: 10.1002/bbb.74.
- [13] D. Mohan, C. U. Pittman and P. H. Steele. *Pyrolysis of wood/biomass for bio-oil: A critical review*. *Energy and Fuels*, 20(3):848–889 [2006]. doi: 10.1021/ef0502397.
- [14] R. van Ree and A. van Zeeland. *IEA Bioenergy Task42 Biorefinining*. Tech. rep., Wageningen, Netherlands [2014]. doi: 10.1016/S0961-9534(07)00064-5.
- [15] O. Thees, V. Burg, M. Erni *et al.* *Biomassenpotenziale der Schweiz für die energetische Nutzung, Ergebnisse des Schweizerischen Energiekompetenzzentrums SCCER BIOSWEET*. Tech. rep., Eidg. Forschungsanstalt für Wald, Schnee und Landschaft (WSL) [2017]. doi: 10.16904/18.
- [16] Bundesamt für Energie (BFE). *Schweizerische Gesamtenergiestatistik 2017*. Tech. rep., Ittigen, Switzerland [2017].
- [17] M. Studer and P. Poldervaart. *Neue Wege zur holzbasierten Bioraffinerie, Thematische Synthese im Rahmen des Nationalen Forschungsprogramms NFP66 "Ressource Holz"*. Tech. rep., Swiss National Science Foundation, Bern, Switzerland [2017].
- [18] S. Ladanai and J. Vinterbäck. *Global Potential of Sustainable Biomass*. Tech. rep., Swedish University of Agricultural Sciences, Uppsala, Sweden [2009].
- [19] B. Yang and C. E. Wyman. *Pretreatment: the key to unlocking low-cost cellulosic ethanol*. *Biofuels, Bioproducts and Biorefining*, 2(1):26–40 [2008]. doi: 10.1002/bbb.49.
- [20] K. Kucharska, P. Rybarczyk, I. Hołowacz *et al.* *Pretreatment of lignocellulosic materials as substrates for fermentation processes*. *Molecules*, 23(11):2937–2969 [2018]. doi: 10.3390/molecules23112937.

- [21] S. Brethauer and M. H. Studer. *Biochemical Conversion Processes of Lignocellulosic Biomass to Fuels and Chemicals – A Review*. CHIMIA International Journal for Chemistry, 69(10):572–581 [2015]. doi: 10.2533/chimia.2015.572.
- [22] Z. Barta, K. Kovacs, K. Reczey *et al.* *Process design and economics of on-site cellulase production on various carbon sources in a softwood-based ethanol plant*. Enzyme Research, 2010 [2010]. doi: 10.4061/2010/734182.
- [23] L. R. Lynd, W. H. Van Zyl, J. E. McBride *et al.* *Consolidated bioprocessing of cellulosic biomass: An update*. Current Opinion in Biotechnology, 16(5):577–583 [2005]. doi: 10.1016/j.copbio.2005.08.009.
- [24] L. R. Lynd, P. J. Weimer, W. H. van Zyl *et al.* *Microbial Cellulose Utilization: Fundamentals and Biotechnology*. Microbiology and Molecular Biology Reviews, 66(3):506–577 [2002]. doi: 10.1128/MMBR.66.3.506-577.2002.
- [25] T. Stevanovic. *Chemical Composition and Properties of Wood*. John Wiley & Sons, Inc., Hoboken, United States of America [2016]. doi: 10.1002/9781118773727.ch3.
- [26] E. Sjöström. *Wood Polysaccharides*. In *Wood chemistry: fundamentals and applications*, pp. 51–70. Academic Press, San Diego [1993]. doi: 10.1016/B978-0-08-092589-9.50007-3.
- [27] B. Rozmysłowicz, J. H. Yeap, A. M. I. Elkhaiary *et al.* *Catalytic valorization of the acetate fraction of biomass to aromatics and its integration into the carboxylate platform*. submitted to Green Chemistry.
- [28] L. R. Lynd and H. E. Grethlein. *Hydrolysis of dilute acid pretreated mixed hardwood and purified microcrystalline cellulose by cell-free broth from Clostridium thermocellum*. Biotechnology and Bioengineering, 29(1):92–100 [1987]. doi: 10.1002/bit.260290114.
- [29] J. M. D. Paye, A. Guseva, S. K. Hammer *et al.* *Biological lignocellulose solubilization: comparative evaluation of biocatalysts and enhancement via cotreatment*. Biotechnology for Biofuels, 9(1):8 [2016]. doi: 10.1186/s13068-015-0412-y.
- [30] J. S. Van Dyk and B. I. Pletschke. *A review of lignocellulose bioconversion using enzymatic hydrolysis and synergistic cooperation between enzymes—Factors affecting enzymes, conversion and synergy*. Biotechnology Advances, 30(6):1458–1480 [2012]. doi: 10.1016/j.biotechadv.2012.03.002.
- [31] S. D. Mansfield, C. Mooney and J. N. Saddler. *Substrate and enzyme characteristics that limit cellulose hydrolysis*. Biotechnology Progress, 15(5):804–816 [1999]. doi: 10.1021/bp9900864.

- [32] L. da Costa Sousa, S. P. Chundawat, V. Balan *et al.* 'Cradle-to-grave' assessment of existing lignocellulose pretreatment technologies. *Current Opinion in Biotechnology*, 20(3):339–347 [2009]. doi: 10.1016/j.copbio.2009.05.003.
- [33] L. J. Jönsson, B. Alriksson and N.-O. Nilvebrant. *Bioconversion of lignocellulose: inhibitors and detoxification*. *Biotechnology for Biofuels*, 6(1):16 [2013]. doi: 10.1186/1754-6834-6-16.
- [34] A. Aden, M. Ruth, K. Ibsen *et al.* *Lignocellulosic Biomass to Ethanol Process Design and Economics Utilizing Co-Current Dilute Acid Prehydrolysis and Enzymatic Hydrolysis for Corn Stover*. Tech. rep., Nation Renewable Energy Laboratory, Colorado, United States of America [2002].
- [35] D. Humbird, R. David, L. Tao *et al.* *Process Design and Economics for Biochemical Conversion of Lignocellulosic Biomass to Ethanol*. Tech. rep., NREL/TP-5100-47764, Colorado, United States of America [2011].
- [36] P. Alvira, E. Tomás-Pejó, M. Ballesteros *et al.* *Pretreatment technologies for an efficient bioethanol production process based on enzymatic hydrolysis: A review*. *Bioresource Technology*, 101(13):4851–4861 [2010]. doi: 10.1016/j.biortech.2009.11.093.
- [37] T. Pielhop, J. Amgarten, P. R. von Rohr *et al.* *Steam explosion pretreatment of softwood: the effect of the explosive decompression on enzymatic digestibility*. *Biotechnology for Biofuels*, 9(1):152 [2016]. doi: 10.1186/s13068-016-0567-1.
- [38] A. K. Kumar and S. Sharma. *Recent updates on different methods of pretreatment of lignocellulosic feedstocks: a review*. *Bioresources and Bioprocessing*, 4(1):7 [2017]. doi: 10.1186/s40643-017-0137-9.
- [39] N. Mosier, C. Wyman, B. Dale *et al.* *Features of promising technologies for pretreatment of lignocellulosic biomass*. *Bioresource Technology*, 96(6):673–86 [2005]. doi: 10.1016/j.biortech.2004.06.025.
- [40] L. Zhu, J. P. O'Dwyer, V. S. Chang *et al.* *Structural features affecting biomass enzymatic digestibility*. *Bioresource Technology*, 99(9):3817–3828 [2008]. doi: 10.1016/j.biortech.2007.07.033.
- [41] C. A. Mooney, S. D. Mansfield, M. G. Touhy *et al.* *The effect of initial pore volume and lignin content on the enzymatic hydrolysis of softwoods*. *Bioresource Technology*, 64(2):113–119 [1998].
- [42] T. K. Kirk and D. Cullen. *Enzymology and Molecular Genetics of Wood Degradation Enzymology and Molecular Genetics of Wood Degradation by White-Rot Fungi*. In *Environmentally Friendly Technologies for the Pulp and Paper Industry*, pp. 273–307. John Wiley & Sons, Inc., Hoboken, United States of America [1998].

- [43] Á. T. Martínez, M. Speranza, F. J. Ruiz-Dueñas *et al.* *Biodegradation of lignocellulosics: microbial, chemical, and enzymatic aspects of the fungal attack of lignin*. *International Microbiology*, 8(3):195–204 [2005].
- [44] M. Ballesteros, A. D. Moreno, D. Ibarra *et al.* *A review of biological delignification and detoxification methods for lignocellulosic bioethanol production*. *Critical Reviews in Biotechnology*, 35(3):342–354 [2015]. doi: 10.3109/07388551.2013.878896.
- [45] M. L. Balch, E. K. Holwerda, M. F. Davis *et al.* *Lignocellulose fermentation and residual solids characterization for senescent switchgrass fermentation by *Clostridium thermocellum* in the presence and absence of continuous in situ ball-milling*. *Energy and Environmental Science*, 10(5):1252–1261 [2017]. doi: 10.1039/C6EE03748H.
- [46] J. C. Liao, L. Mi, S. Pontrelli *et al.* *Fuelling the future: microbial engineering for the production of sustainable biofuels*. *Nature Reviews Microbiology*, 14(5):288–304 [2016]. doi: 10.1038/nrmicro.2016.32.
- [47] R. R. Singhanian, A. K. Patel, R. K. Sukumaran *et al.* *Role and significance of beta-glucosidases in the hydrolysis of cellulose for bioethanol production*. *Bioresource Technology*, 127(8):500–507 [2013]. doi: 10.1016/j.biortech.2012.09.012.
- [48] H. Teugjas and P. Våljamäe. *Product inhibition of cellulases studied with ¹⁴C-labeled cellulose substrates*. *Biotechnology for Biofuels*, 6(1):104 [2013]. doi: 10.1186/1754-6834-6-104.
- [49] R. R. Singhanian, A. K. Patel, R. K. Sukumaran *et al.* *Role and significance of beta-glucosidases in the hydrolysis of cellulose for bioethanol production*. *Bioresource Technology*, 127:500–507 [2013]. doi: 10.1016/j.biortech.2012.09.012.
- [50] J. van den Brink and R. P. de Vries. *Fungal enzyme sets for plant polysaccharide degradation*. *Applied Microbiology and Biotechnology*, 91(6):1477–1492 [2011]. doi: 10.1007/s00253-011-3473-2.
- [51] S. M. Cragg, G. T. Beckham, N. C. Bruce *et al.* *Lignocellulose degradation mechanisms across the Tree of Life*. *Current Opinion in Chemical Biology*, 29:108–119 [2015]. doi: 10.1016/j.cbpa.2015.10.018.
- [52] R. Peterson and H. Nevalainen. *Trichoderma reesei RUT-C30 - Thirty years of strain improvement*. *Microbiology*, 158(1):58–68 [2012]. doi: 10.1099/mic.0.054031-0.
- [53] M. Mandels and E. T. Reese. *Induction of cellulase in *Trichoderma viride* as influenced by carbon sources and metals*. *Journal of Bacteriology*, 73(2):269–278 [1956].

- [54] B. S. Montenecourt and D. E. Eveleigh. *Semiquantitative Plate Assay for Determination of Cellulase Production by Trichoderma viridel*. Applied and Environmental Microbiology, 33(1):178–183 [1977].
- [55] B. S. Montenecourt and D. E. Eveleigh. *Preparation of Mutants of Trichoderma reesei with Enhanced Cellulase Production*. Applied and Environmental Microbiology, 34(6):777–782 [1977].
- [56] B. S. Montenecourt and D. E. Eveleigh. *Selective Screening Methods for the Isolation of High Yielding Cellulase Mutants of Trichoderma reesei*. In *Hydrolysis of Celullose: Mechanism of Enzymatic and Acid Catalysis*, pp. 289–301 [1979]. doi: 10.1021/ba-1979-0181.ch014.
- [57] S. K. Tangnu, H. W. Blanch and C. R. Wilke. *Enhanced production of cellulase, hemicellulase, and beta-glucosidase by Trichoderma reesei (RUT-C-30)*. Biotechnology and Bioengineering, 23(8):1837–1849 [1981]. doi: 10.1002/bit.260230811.
- [58] M. Wang and X. Lu. *Exploring the synergy between cellobiose dehydrogenase from Phanerochaete chrysosporium and cellulase from Trichoderma reesei*. Frontiers in Microbiology, 7:620 [2016]. doi: 10.3389/fmicb.2016.00620.
- [59] C.-w. C. Hsieh, D. Cannella, H. Jørgensen et al. *Cellulase Inhibition by High Concentrations of Monosaccharides*. Journal of Agricultural and Food Chemistry, 62(17):3800–3805 [2014]. doi: 10.1021/jf5012962.
- [60] Z. Xiao, X. Zhang, D. J. Gregg et al. *Effects of Sugar Inhibition on Cellulases and β -Glucosidase During Enzymatic Hydrolysis of Softwood Substrates*. Applied Biochemistry and Biotechnology, 115(1-3):1115–1126 [2004]. doi: 10.1385/ABAB:115:1-3:1115.
- [61] Y. Lu, Y.-H. P. Zhang and L. R. Lynd. *Enzyme-microbe synergy during cellulose hydrolysis by Clostridium thermocellum*. Proceedings of the National Academy of Sciences of the United States of America, 103(44):16165–16169 [2006]. doi: 10.1073/pnas.0605381103.
- [62] J. B. Kristensen, C. Felby and H. Jørgensen. *Yield-determining factors in high-solids enzymatic hydrolysis of lignocellulose*. Biotechnology for Biofuels, 2(1):11 [2009]. doi: 10.1186/1754-6834-2-11.
- [63] K. M. Roberts, D. M. Lavenson, E. J. Tozzi et al. *The effects of water interactions in cellulose suspensions on mass transfer and saccharification efficiency at high solids loadings*. Cellulose, 18(3):759–773 [2011]. doi: 10.1007/s10570-011-9509-z.
- [64] B. Hahn-Hägerdal, K. Karhumaa, M. Jeppsson et al. *Metabolic Engineering for Pentose Utilization in Saccharomyces cerevisiae*. In *Biofuels*, pp. 147–177. Springer Berlin Heidelberg, Berlin, Heidelberg [2007]. doi: 10.1007/10_2007_062.

- [65] K. Olofsson, M. Bertilsson and G. Lidén. *A short review on SSF – an interesting process option for ethanol production from lignocellulosic feedstocks*. *Biotechnology for Biofuels*, 1(1):7 [2008]. doi: 10.1186/1754-6834-1-7.
- [66] M. Takagi. *Inhibition of cellulase by fermentation products*. *Biotechnology and Bioengineering*, 26(12):1506–1507 [1984]. doi: 10.1002/bit.260261216.
- [67] L. R. Lynd, M. S. Laser, D. Bransby *et al.* *How biotech can transform biofuels*. *Nature Biotechnology*, 26(2):169–172 [2008]. doi: 10.1038/nbt0208-169.
- [68] D. G. Olson, J. E. McBride, a. Joe Shaw *et al.* *Recent progress in consolidated bioprocessing*. *Current Opinion in Biotechnology*, 23(3):396–405 [2012]. doi: 10.1016/j.copbio.2011.11.026.
- [69] R. den Haan, E. van Rensburg, S. H. Rose *et al.* *Progress and challenges in the engineering of non-cellulolytic microorganisms for consolidated bioprocessing*. *Current Opinion in Biotechnology*, 33:32–38 [2015]. doi: 10.1016/j.copbio.2014.10.003.
- [70] S. G. Hays, W. G. Patrick, M. Ziesack *et al.* *Better together: Engineering and application of microbial symbioses*. *Current Opinion in Biotechnology*, 36:40–49 [2015]. doi: 10.1016/j.copbio.2015.08.008.
- [71] X. N. Peng, S. P. Gilmore and M. A. O'Malley. *Microbial communities for bioprocessing: lessons learned from nature*. *Current Opinion in Chemical Engineering*, 14:103–109 [2016]. doi: 10.1016/j.coche.2016.09.003.
- [72] M. Wagner, A. Loy, R. Nogueira *et al.* *Microbial community composition and function in wastewater treatment plants*. *Antonie van Leeuwenhoek*, 81(1):665–680 [2002]. doi: 10.1023/A:1020586312170.
- [73] R. Xu, K. Zhang, P. Liu *et al.* *A critical review on the interaction of substrate nutrient balance and microbial community structure and function in anaerobic co-digestion*. *Bioresource Technology*, 247:1119–1127 [2018]. doi: 10.1016/j.biortech.2017.09.095.
- [74] B. E. Wolfe and R. J. Dutton. *Fermented foods as experimentally tractable microbial ecosystems*. *Cell*, 161(1):49–55 [2015]. doi: 10.1016/j.cell.2015.02.034.
- [75] E. Lhomme, C. Urien, J. Legrand *et al.* *Sourdough microbial community dynamics: An analysis during French organic bread-making processes*. *Food Microbiology*, 53:41–50 [2016]. doi: 10.1016/j.fm.2014.11.014.
- [76] A. L. Teoh, G. Heard and J. Cox. *Yeast ecology of Kombucha fermentation*. *International Journal of Food Microbiology*, 95(2):119–126 [2004]. doi: 10.1016/j.ijfoodmicro.2003.12.020.

- [77] P. J. Weimer, J. B. Russell and R. E. Muck. *Lessons from the cow: What the ruminant animal can teach us about consolidated bioprocessing of cellulosic biomass*. *Bioresource Technology*, 100(21):5323–5331 [2009]. doi: 10.1016/j.biortech.2009.04.075.
- [78] J. B. Russell. *Rumen Microbiology and Its Role in Animal Nutrition*. United States Department of Agriculture, Ithaca, United States of America [2002].
- [79] S. Taco Vasquez, J. Dunkleman, S. K. Chaudhuri *et al.* *Biomass conversion to hydrocarbon fuels using the MixAlco™ process at a pilot-plant scale*. *Biomass and Bioenergy*, 62:138–148 [2014]. doi: 10.1016/j.biombioe.2014.01.005.
- [80] M. T. Holtzapple and C. B. Granda. *Carboxylate platform: The MixAlco process part 1: Comparison of three biomass conversion platforms*. *Applied Biochemistry and Biotechnology*, 156(1):95–106 [2009]. doi: 10.1007/s12010-008-8466-y.
- [81] M. T. Agler, C. M. Spirito, J. G. Usack *et al.* *Chain elongation with reactor microbiomes: upgrading dilute ethanol to medium-chain carboxylates*. *Energy and Environmental Science*, 5(8):8189–8192 [2012]. doi: 10.1039/c2ee22101b.
- [82] L. Xu and U. Tschirner. *Improved ethanol production from various carbohydrates through anaerobic thermophilic co-culture*. *Bioresource Technology*, 102(21):10065–10071 [2011]. doi: 10.1016/j.biortech.2011.08.067.
- [83] T. R. Zuroff, S. Barri Xiques and W. R. Curtis. *Consortia-mediated bioprocessing of cellulose to ethanol with a symbiotic Clostridium phytofermentans/yeast co-culture*. *Biotechnology for Biofuels*, 6(1):59 [2013]. doi: 10.1186/1754-6834-6-59.
- [84] J. J. Minty, M. E. Singer, S. A. Scholz *et al.* *Design and characterization of synthetic fungal-bacterial consortia for direct production of isobutanol from cellulosic biomass*. *Proceedings of the National Academy of Sciences of the United States of America*, 110(36):14592–14597 [2013]. doi: 10.1073/pnas.1218447110.
- [85] Z. Wen, M. Wu, Y. Lin *et al.* *Artificial symbiosis for acetone-butanol-ethanol (ABE) fermentation from alkali extracted deshelled corn cobs by co-culture of Clostridium beijerinckii and Clostridium cellulovorans*. *Microbial Cell Factories*, 13(1):92 [2014]. doi: 10.1186/s12934-014-0092-5.
- [86] N. I. Johns, T. Blazejewski, A. L. Gomes *et al.* *Principles for designing synthetic microbial communities*. *Current Opinion in Microbiology*, 31:146–153 [2016]. doi: 10.1016/j.mib.2016.03.010.
- [87] K. Zhou, K. Qiao, S. Edgar *et al.* *Distributing a metabolic pathway among a microbial consortium enhances production of natural products*. *Nature Biotechnology*, 33(4):377–383 [2015]. doi: 10.1038/nbt.3095.

- [88] S. B. Said and D. Or. *Synthetic microbial ecology: Engineering habitats for modular consortia*. *Frontiers in Microbiology*, 8:1125 [2017]. doi: 10.3389/fmicb.2017.01125.
- [89] K. Faust and J. Raes. *Microbial interactions: from networks to models*. *Nature Reviews Microbiology*, 10(8):538–550 [2012]. doi: 10.1038/nrmicro2832.
- [90] W. Z. Lidicker. *A Clarification of Interactions in Ecological Systems*. *BioScience*, 29(8):475–477 [1979]. doi: 10.2307/1307540.
- [91] T. P. Curtis, W. T. Sloan and J. W. Scannell. *Estimating prokaryotic diversity and its limits*. *Proceedings of the National Academy of Sciences of the United States of America*, 99(16):10494–10499 [2002]. doi: 10.1073/pnas.142680199.
- [92] B. Görke and J. Stülke. *Carbon catabolite repression in bacteria: Many ways to make the most out of nutrients*. *Nature Reviews Microbiology*, 6(8):613–624 [2008]. doi: 10.1038/nrmicro1932.
- [93] N. Fu, P. Peiris, J. Markham *et al.* *A novel co-culture process with *Zymomonas mobilis* and *Pichia stipitis* for efficient ethanol production on glucose/xylose mixtures*. *Enzyme and Microbial Technology*, 45(3):210–217 [2009]. doi: 10.1016/j.enzmictec.2009.04.006.
- [94] H. Zhang, B. Pereira, Z. Li *et al.* *Engineering *Escherichia coli* coculture systems for the production of biochemical products*. *Proceedings of the National Academy of Sciences of the United States of America*, 112(27):8266–8271 [2015]. doi: 10.1073/pnas.1506781112.
- [95] T. Xia, M. A. Eiteman and E. Altman. *Simultaneous utilization of glucose, xylose and arabinose in the presence of acetate by a consortium of *Escherichia coli* strains*. *Microbial Cell Factories*, 11(1):77 [2012]. doi: 10.1186/1475-2859-11-77.
- [96] M. A. Eiteman, S. A. Lee and E. Altman. *A co-fermentation strategy to consume sugar mixtures effectively*. *Journal of Biological Engineering*, 2(1):3 [2008]. doi: 10.1186/1754-1611-2-3.
- [97] M. Ghoul, A. S. Griffin and S. A. West. *Toward an evolutionary definition of cheating*. *Evolution*, 68(2):318–331 [2013]. doi: 10.1111/evo.12266.
- [98] J. Gore, H. Youk and A. van Oudenaarden. *Snowdrift game dynamics and facultative cheating in yeast*. *Nature*, 459(7244):253–256 [2009]. doi: 10.1038/nature07921.
- [99] V. A. Portnoy, M. J. Herrgård and B. Ø. Palsson. *Aerobic fermentation of D-glucose by an evolved cytochrome oxidase-deficient *Escherichia coli* strain*. *Applied and Environmental Microbiology*, 74(24):7561–7569 [2008]. doi: 10.1128/AEM.00880-08.
- [100] H. J. Kim, J. Q. Boedicker, J. W. Choi *et al.* *Defined spatial structure stabilizes a synthetic multispecies bacterial community*. *Proceedings of the National Academy of Sciences of the United States of America*, 105(47):18188–18193 [2008]. doi: 10.1073/pnas.0807935105.

- [101] M. Ohno, I. Okano, T.-o. Watsuji *et al.* *Establishing the Independent Culture of a Strictly Symbiotic Bacterium Symbiobacterium thermophilum from Its Supporting Bacillus Strain*. *Bioscience, Biotechnology, and Biochemistry*, 63(6):1083–1090 [1999]. doi: 10.1271/bbb.63.1083.
- [102] K. Ueda, H. Saka, I. Yoshiyuki *et al.* *Development of a membrane dialysis bioreactor and its application to a large-scale culture of a symbiotic bacterium, Symbiobacterium thermophilum*. *Applied Microbiology and Biotechnology*, 60(3):300–305 [2002]. doi: 10.1007/s00253-002-1117-2.
- [103] D. Dietz, W. Sabra and A. P. Zeng. *Co-cultivation of Lactobacillus zeae and Veillonella criceti for the production of propionic acid*. *AMB Express*, 3(1):29 [2013]. doi: 10.1186/2191-0855-3-29.
- [104] L. Hall-Stoodley, J. W. Costerton and P. Stoodley. *Bacterial biofilms: from the natural environment to infectious diseases*. *Nature Reviews Microbiology*, 2:95–108 [2004]. doi: 10.1038/nrmicro821.
- [105] K. K. Jefferson. *What drives bacteria to produce a biofilm?* *FEMS Microbiology Letters*, 236(2):163–173 [2004]. doi: 10.1016/j.femsle.2004.06.005.
- [106] H. C. Flemming and J. Wingender. *The biofilm matrix*. *Nature Reviews Microbiology*, 8(9):623–633 [2010]. doi: 10.1038/nrmicro2415.
- [107] T. Bjarnsholt. *The role of bacterial biofilms in chronic infections*. *APMIS Supplementum*, 121(136):1–54 [2013]. doi: 10.1111/apm.12099.
- [108] P. Stoodley, K. Sauer, D. G. Davies *et al.* *Biofilms as complex differentiated communities*. *Annual Review of Microbiology*, 56(1):187–209 [2002]. doi: 10.1146/annurev.micro.56.012302.160705.
- [109] O. E. Petrova and K. Sauer. *Escaping the biofilm in more than one way: Desorption, detachment or dispersion*. *Current Opinion in Microbiology*, 30:67–78 [2016]. doi: 10.1016/j.mib.2016.01.004.
- [110] P. S. Stewart and M. J. Franklin. *Physiological heterogeneity in biofilms*. *Nature Reviews Microbiology*, 6(3):199–210 [2008]. doi: 10.1038/nrmicro1838.
- [111] M. Berlanga and R. Guerrero. *Living together in biofilms: The microbial cell factory and its biotechnological implications*. *Microbial Cell Factories*, 15(1):165 [2016]. doi: 10.1186/s12934-016-0569-5.
- [112] M. Burmølle, D. Ren, T. Bjarnsholt *et al.* *Interactions in multispecies biofilms: do they actually matter?* *Trends in Microbiology*, 22(2):84–91 [2014]. doi: 10.1016/j.tim.2013.12.004.
- [113] T. K. Wood, S. J. Knabel and B. W. Kwan. *Bacterial persister cell formation and dormancy*. *Applied and Environmental Microbiology*, 79(23):7116–7121 [2013]. doi: 10.1128/AEM.02636-13.

- [114] M. A. Abdel-Rahman, Y. Tashiro and K. Sonomoto. *Recent advances in lactic acid production by microbial fermentation processes*. *Biotechnology Advances*, 31(6):877–902 [2013]. doi: 10.1016/j.biotechadv.2013.04.002.
- [115] C. C. Geddes, I. U. Nieves and L. O. Ingram. *Advances in ethanol production*. *Current Opinion in Biotechnology*, 22(3):312–319 [2011]. doi: 10.1016/j.copbio.2011.04.012.
- [116] H. Kawaguchi, T. Hasunuma, C. Ogino *et al.* *Bioprocessing of bio-based chemicals produced from lignocellulosic feedstocks*. *Current Opinion in Biotechnology*, 42:30–39 [2016]. doi: 10.1016/j.copbio.2016.02.031.
- [117] C. M. Agapakis, P. M. Boyle and P. A. Silver. *Natural strategies for the spatial optimization of metabolism in synthetic biology*. *Nature Chemical Biology*, 8(6):527–535 [2012]. doi: 10.1038/nchembio.975.
- [118] C. D. Nadell, K. Drescher and K. R. Foster. *Spatial structure, cooperation and competition in biofilms*. *Nature Reviews Microbiology*, 14(9):589–600 [2016]. doi: 10.1038/nrmicro.2016.84.
- [119] M. A. Abdel-Rahman and K. Sonomoto. *Opportunities to overcome the current limitations and challenges for efficient microbial production of optically pure lactic acid*. *Journal of Biotechnology*, 236:176–192 [2016]. doi: 10.1016/j.jbiotec.2016.08.008.
- [120] F. Cui, Y. Li and C. Wan. *Lactic acid production from corn stover using mixed cultures of *Lactobacillus rhamnosus* and *Lactobacillus brevis**. *Bioresource Technology*, 102(2):1831–1836 [2011]. doi: 10.1016/j.biortech.2010.09.063.
- [121] M. S. Ou, L. O. Ingram and K. T. Shanmugam. *L(+)-Lactic acid production from non-food carbohydrates by thermotolerant *Bacillus coagulans**. *Journal of Industrial Microbiology and Biotechnology*, 38(5):599–605 [2011]. doi: 10.1007/s10295-010-0796-4.
- [122] A. Romaní, R. Yáñez, G. Garrote *et al.* *SSF production of lactic acid from cellulosic biosludges*. *Bioresource Technology*, 99(10):4247–4254 [2008]. doi: 10.1016/j.biortech.2007.08.051.
- [123] E. C. van der Pol, G. Eggink and R. A. Weusthuis. *Production of L(+)-lactic acid from acid pretreated sugarcane bagasse using *Bacillus coagulans* DSM2314 in a simultaneous saccharification and fermentation strategy*. *Biotechnology for Biofuels*, 9(1):248 [2016]. doi: 10.1186/s13068-016-0646-3.
- [124] R. H. W. Maas, R. R. Bakker, M. L. A. Jansen *et al.* *Lactic acid production from lime-treated wheat straw by *Bacillus coagulans*: Neutralization of acid by fed-batch addition of alkaline substrate*. *Applied Microbiology and Biotechnology*, 78(5):751–758 [2008]. doi: 10.1007/s00253-008-1361-1.

- [125] X. Tian, N. Zhang, Y. Yang *et al.* *The effect of redox environment on l-lactic acid production by Lactobacillus paracasei - A proof by genetically encoded in vivo NADH biosensor.* *Process Biochemistry*, 50(12):2029–2034 [2015]. doi: 10.1016/j.procbio.2015.10.001.
- [126] A. Sharma, R. Tewari, S. S. Rana *et al.* *Cellulases: Classification, Methods of Determination and Industrial Applications.* *Applied Biochemistry and Biotechnology*, 179(8):1346–1380 [2016]. doi: 10.1007/s12010-016-2070-3.
- [127] J. L. Rahikainen, J. D. Evans, S. Mikander *et al.* *Cellulase-lignin interactions—The role of carbohydrate-binding module and pH in non-productive binding.* *Enzyme and Microbial Technology*, 53(5):315–321 [2013]. doi: 10.1016/j.enzmictec.2013.07.003.
- [128] M. A. Abdel-Rahman, Y. Tashiro, T. Zendo *et al.* *Efficient homofermentative L-(+)-Lactic acid production from xylose by a novel lactic acid bacterium, Enterococcus mundtii QU 25.* *Applied and Environmental Microbiology*, 77(5):1892–1895 [2011]. doi: 10.1128/AEM.02076-10.
- [129] K. Mahr, W. Hillen and F. Titgemeyer. *Carbon catabolite repression in Lactobacillus pentosus: analysis of the ccpA region.* *Applied and Environmental Microbiology*, 66(1):277–283 [2000]. doi: 10.1128/AEM.66.1.277-283.2000.
- [130] B. C. Lokman, M. Heerikhuisen, R. J. Leer *et al.* *Regulation of expression of the Lactobacillus pentosus xylAB operon.* *Journal of Bacteriology*, 179(17):5391–5397 [1997]. doi: 10.1128/jb.179.17.5391-5397.1997.
- [131] E. Jourdier, L. Poughon, C. Larroche *et al.* *Comprehensive Study and Modeling of Acetic Acid Effect on Trichoderma reesei Growth.* *Industrial Biotechnology*, 9(3):132–138 [2013]. doi: 10.1089/ind.2013.0002.
- [132] K. Z. Coyte, J. Schluter and K. R. Foster. *The ecology of the microbiome: Networks, competition, and stability.* *Science*, 350(6261):663–666 [2015]. doi: 10.1126/science.aad2602.
- [133] L. J. Jönsson and C. Martín. *Pretreatment of lignocellulose: Formation of inhibitory by-products and strategies for minimizing their effects.* *Bioresource Technology*, 199:103–112 [2016]. doi: 10.1016/j.biortech.2015.10.009.
- [134] G. Stephanopoulos. *Challenges in Engineering Microbes for Biofuels Production.* *Science*, 315(5813):801–804 [2007]. doi: 10.1126/science.1139612.
- [135] H. Michlmayr, J. Hell, C. Lorenz *et al.* *Arabinoxylan Oligosaccharide Hydrolysis by Family 43 and 51 Glycosidases from Lactobacillus brevis DSM 20054.* *Applied and Environmental Microbiology*, 79(21):6747–6754 [2013]. doi: 10.1128/AEM.02130-13.

- [136] E. Palmqvist, B. Hahn-Hägerdal, Z. Szengyel *et al.* *Simultaneous detoxification and enzyme production of hemicellulose hydrolysates obtained after steam pretreatment.* *Enzyme and Microbial Technology*, 20(4):286–293 [1997]. doi: 10.1016/S0141-0229(96)00130-5.
- [137] J. Jalak, M. Kurasin, H. Teugjas *et al.* *Endo-exo Synergism in Cellulose Hydrolysis Revisited.* *Journal of Biological Chemistry*, 287(34):28802–28815 [2012]. doi: 10.1074/jbc.M112.381624.
- [138] H. Michlmayr and W. Kneifel. *β -Glucosidase activities of lactic acid bacteria: mechanisms, impact on fermented food and human health.* *FEMS Microbiology Letters*, 352(1):1–10 [2014]. doi: 10.1111/1574-6968.12348.
- [139] A. Mougi. *The roles of amensalistic and commensalistic interactions in large ecological network stability.* *Scientific Reports*, 6:29929 [2016]. doi: 10.1038/srep29929.
- [140] M. T. Agler, B. A. Wrenn, S. H. Zinder *et al.* *Waste to bioproduct conversion with undefined mixed cultures: The carboxylate platform.* *Trends in Biotechnology*, 29(2):70–78 [2011]. doi: 10.1016/j.tibtech.2010.11.006.
- [141] R. Tsoi, F. Wu, C. Zhang *et al.* *Metabolic division of labor in microbial systems.* *Proceedings of the National Academy of Sciences of the United States of America*, 115(10):2526–2531 [2018]. doi: 10.1073/pnas.1716888115.
- [142] D. Dugar and G. Stephanopoulos. *Relative potential of biosynthetic pathways for biofuels and bio-based products.* *Nature Biotechnology*, 29(12):1074–1078 [2011]. doi: 10.1038/nbt.2055.
- [143] B. W. Biggs, B. De Paepe, C. N. S. Santos *et al.* *Multivariate modular metabolic engineering for pathway and strain optimization.* *Current Opinion in Biotechnology*, 29(1):156–162 [2014]. doi: 10.1016/j.copbio.2014.05.005.
- [144] A. Gupta, I. M. Reizman, C. R. Reisch *et al.* *Dynamic regulation of metabolic flux in engineered bacteria using a pathway-independent quorum-sensing circuit.* *Nature Biotechnology*, 35(3):273–279 [2017]. doi: 10.1038/nbt.3796.
- [145] P. P. Peralta-Yahya, F. Zhang, S. B. Del Cardayre *et al.* *Microbial engineering for the production of advanced biofuels.* *Nature*, 488(7411):320–328 [2012]. doi: 10.1038/nature11478.
- [146] L. Goers, P. Freemont and K. M. Polizzi. *Co-culture systems and technologies: taking synthetic biology to the next level.* *Journal of The Royal Society Interface*, 11(96):20140065 [2014]. doi: 10.1098/rsif.2014.0065.
- [147] S. R. Lindemann, H. C. Bernstein, H.-S. Song *et al.* *Engineering microbial consortia for controllable outputs.* *The ISME Journal*, 10(9):2077–2084 [2016]. doi: 10.1038/ismej.2016.26.

- [148] Y. Liu, M. Ding, W. Ling *et al.* *A three-species microbial consortium for power generation.* Energy and Environmental Science, 10(7):1600–1609 [2017]. doi: 10.1039/C6EE03705D.
- [149] H. von Canstein, S. Kelly, Y. Li *et al.* *Species diversity improves the efficiency of mercury-reducing biofilms under changing environmental conditions.* Applied and Environmental Microbiology, 68(6):2829–2837 [2002]. doi: 10.1128/AEM.68.6.2829-2837.2002.
- [150] J. L. R. Gallego, M. J. Garcia-Martinez, J. F. Llamas *et al.* *Biodegradation of oil tank bottom sludge using microbial consortia.* Biodegradation, 18(3):269–281 [2007]. doi: 10.1007/s10532-006-9061-y.
- [151] S. Kato, S. Haruta, Z. J. Cui *et al.* *Stable coexistence of five bacterial strains as a cellulose-degrading community.* Applied and Environmental Microbiology, 71(11):7099–7106 [2005]. doi: 10.1128/AEM.71.11.7099-7106.2005.
- [152] L. Ma, X. Wang, J. Tao *et al.* *Bioleaching of the mixed oxide-sulfide copper ore by artificial indigenous and exogenous microbial community.* Hydrometallurgy, 169:41–46 [2017]. doi: 10.1016/j.hydromet.2016.12.007.
- [153] S. Pawelczyk, W.-R. Abraham, H. Harms *et al.* *Community-based degradation of 4-chorosalicylate tracked on the single cell level.* Journal of Microbiological Methods, 75(1):117–126 [2008]. doi: 10.1016/j.mimet.2008.05.018.
- [154] M. Schwering, J. Song, M. Louie *et al.* *Multi-species biofilms defined from drinking water microorganisms provide increased protection against chlorine disinfection.* Biofouling, 29(8):917–928 [2013]. doi: 10.1080/08927014.2013.816298.
- [155] E. O. Petrof, G. B. Gloor, S. J. Vanner *et al.* *Stool substitute transplant therapy for the eradication of Clostridium difficile infection: 'RePOOPulating' the gut.* Microbiome, 1(1):3 [2013]. doi: 10.1186/2049-2618-1-3.
- [156] B. Allen, J. Gore and M. A. Nowak. *Spatial dilemmas of diffusible public goods.* eLife, 2:e01169 [2013]. doi: 10.7554/eLife.01169.
- [157] Á. T. Kovács. *Impact of spatial distribution on the development of mutualism in microbes.* Frontiers in Microbiology, 5:649 [2014]. doi: 10.3389/fmicb.2014.00649.
- [158] R. L. Shahab, J. S. Luterbacher, S. Brethauer *et al.* *Consolidated bioprocessing of lignocellulosic biomass to lactic acid by a synthetic fungal-bacterial consortium.* Biotechnology and Bioengineering, 115(5):1207–1215 [2018]. doi: 10.1002/bit.26541.
- [159] J. B. Xavier and K. R. Foster. *Cooperation and conflict in microbial biofilms.* Proceedings of the National Academy of Sciences of the United States of America, 104(3):876–881 [2007]. doi: 10.1073/pnas.0607651104.

- [160] V. Huchet, D. Thuault and C. M. Bourgeois. *The stereoselectivity of the use of lactic acid by Clostridium tyrobutyricum*. Food Microbiology, 14(3):227–230 [1997].
- [161] G. M. Kim, Byung Hong and Gadd. *Anaerobic fermentation*. In *Bacterial physiology and metabolism*, pp. 252–297. Cambridge University Press [2008].
- [162] C. Nowak, B. Beer, A. Pick *et al.* *A water-forming NADH oxidase from Lactobacillus pentosus suitable for the regeneration of synthetic biomimetic cofactors*. Frontiers in Microbiology, 6:957 [2015]. doi: 10.3389/fmicb.2015.00957.
- [163] B. Ai, X. Chi, J. Meng *et al.* *Consolidated Bioprocessing for Butyric Acid Production from Rice Straw with Undefined Mixed Culture*. Frontiers in Microbiology, 7:1648 [2016]. doi: 10.3389/fmicb.2016.01648.
- [164] X. Chi, J. Li, X. Wang *et al.* *Hyper-production of butyric acid from delignified rice straw by a novel consolidated bioprocess*. Bioresource Technology, 254:115–120 [2018]. doi: 10.1016/j.biortech.2018.01.042.
- [165] K. Merklein, S. S. Fong and Y. Deng. *Production of butyric acid by a cellulolytic actinobacterium Thermobifida fusca on cellulose*. Biochemical Engineering Journal, 90:239–244 [2014]. doi: 10.1016/j.bej.2014.06.012.
- [166] Y. Suo, M. Ren, X. Yang *et al.* *Metabolic engineering of Clostridium tyrobutyricum for enhanced butyric acid production with high butyrate/acetate ratio*. Applied Microbiology and Biotechnology, 102(10):4511–4522 [2018]. doi: 10.1007/s00253-018-8954-0.
- [167] M. Saini, Z. W. Wang, C.-J. Chiang *et al.* *Metabolic Engineering of Escherichia coli for Production of Butyric Acid*. Journal of Agricultural and Food Chemistry, 62(19):4342–4348 [2014]. doi: 10.1021/jf500355p.
- [168] Y. Suo, H. Fu, M. Ren *et al.* *Butyric acid production from lignocellulosic biomass hydrolysates by engineered Clostridium tyrobutyricum overexpressing Class I heat shock protein GroESL*. Bioresource Technology, 250:691–698 [2018]. doi: 10.1016/j.biortech.2017.11.059.
- [169] M. Kim, K. Y. Kim, K. M. Lee *et al.* *Butyric acid production from softwood hydrolysate by acetate-consuming Clostridium sp. S1 with high butyric acid yield and selectivity*. Bioresource Technology, 218:1208–1214 [2016]. doi: 10.1016/j.biortech.2016.07.073.
- [170] T. D. Mays, L. V. Holdeman, W. E. C. Moore *et al.* *Taxonomy of the Genus Veillonella Prévot*. International Journal of Systematic Bacteriology, 32(1):28–36 [1982]. doi: 10.1099/00207713-32-1-28.
- [171] A. Endo and L. M. Dicks. *Physiology of the LAB*. In *Lactic acid bacteria: biodiversity and taxonomy*, pp. 13–30. John Wiley & Sons, Inc., Hoboken, United States of America [2014].

- [172] C. Dellomonaco, J. M. Clomburg, E. N. Miller *et al.* *Engineered reversal of the β -oxidation cycle for the synthesis of fuels and chemicals.* *Nature*, 476(7360):355–359 [2011]. doi: 10.1038/nature10333.
- [173] J. Wu, X. Zhang, X. Xia *et al.* *A systematic optimization of medium chain fatty acid biosynthesis via the reverse beta-oxidation cycle in Escherichia coli.* *Metabolic Engineering*, 41:115–124 [2017]. doi: 10.1016/j.ymben.2017.03.012.
- [174] H. Seedorf, W. F. Fricke, B. Veith *et al.* *The genome of Clostridium kluyveri, a strict anaerobe with unique metabolic features.* *Proceedings of the National Academy of Sciences of the United States of America*, 105(6):2128–2133 [2008]. doi: 10.1073/pnas.0711093105.
- [175] P. J. Weimer and D. M. Stevenson. *Isolation, characterization, and quantification of Clostridium kluyveri from the bovine rumen.* *Applied Microbiology and Biotechnology*, 94(2):461–466 [2012]. doi: 10.1007/s00253-011-3751-z.
- [176] R. J. Wallace, L. C. Chaudhary, E. Miyagawa *et al.* *Metabolic properties of Eubacterium pyruvativorans, a ruminal 'hyper-ammonia-producing' anaerobe with metabolic properties analogous to those of Clostridium kluyveri.* *Microbiology*, 150(9):2921–2930 [2004]. doi: 10.1099/mic.0.27190-0.
- [177] S. R. Elsdén, F. M. Gilchrist, D. Lewis *et al.* *Properties of a fatty acid forming organism isolated from the rumen of sheep.* *Journal of Bacteriology*, 72(5):681–689 [1956].
- [178] A. Ohnishi. *Megasphaera as Lactate-Utilizing Hydrogen-Producing Bacteria.* In *Microbial Factories*, pp. 47–71. Springer India, New Delhi, India [2015]. doi: 10.1007/978-81-322-2598-0_4.
- [179] E. R. Marella, C. Holkenbrink, V. Siewers *et al.* *Engineering microbial fatty acid metabolism for biofuels and biochemicals.* *Current Opinion in Biotechnology*, 50:39–46 [2018]. doi: 10.1016/j.copbio.2017.10.002.
- [180] J. P. Torella, T. J. Ford, S. N. Kim *et al.* *Tailored fatty acid synthesis via dynamic control of fatty acid elongation.* *Proceedings of the National Academy of Sciences of the United States of America*, 110(28):11290–11295 [2013]. doi: 10.1073/pnas.1307129110.
- [181] L. A. Kucek, J. Xu, M. Nguyen *et al.* *Waste conversion into n-caprylate and n-caproate: Resource recovery from wine lees using anaerobic reactor microbiomes and in-line extraction.* *Frontiers in Microbiology*, 7:1892 [2016]. doi: 10.3389/fmicb.2016.01892.
- [182] K. Brenner, L. You and F. H. Arnold. *Engineering microbial consortia: a new frontier in synthetic biology.* *Trends in Biotechnology*, 26(9):483–489 [2008]. doi: 10.1016/j.tibtech.2008.05.004.

- [183] O. Ponomarova and K. R. Patil. *Metabolic interactions in microbial communities: Untangling the Gordian knot*. *Current Opinion in Microbiology*, 27:37–44 [2015]. doi: 10.1016/j.mib.2015.06.014.
- [184] B. Rezaia, N. Cicek and J. A. Oleszkiewicz. *Kinetics of hydrogen-dependent denitrification under varying pH and temperature conditions*. *Biotechnology and Bioengineering*, 92(7):900–906 [2005]. doi: 10.1002/bit.20664.
- [185] C.-C. Wang, L.-W. Zhu, H.-M. Li *et al.* *Performance analyses of a neutralizing agent combination strategy for the production of succinic acid by Actinobacillus succinogenes ATCC 55618*. *Bioprocess and Biosystems Engineering*, 35(4):659–664 [2012]. doi: 10.1007/s00449-011-0644-6.
- [186] M. Marounek, K. Fliegrova and S. Bartos. *Metabolism and some characteristics of ruminal strains of Megasphaera elsdenii*. *Applied and Environmental Microbiology*, 55(6):1570–1573 [1989].
- [187] X. Zhu, Y. Zhou, Y. Wang *et al.* *Production of high-concentration n-caproic acid from lactate through fermentation using a newly isolated Ruminococcaceae bacterium CPB6*. *Biotechnology for Biofuels*, 10(1):102 [2017]. doi: 10.1186/s13068-017-0788-y.
- [188] R. Prabhu, E. Altman and M. A. Eitemana. *Lactate and acrylate metabolism by Megasphaera elsdenii under batch and steady-state conditions*. *Applied and Environmental Microbiology*, 78(24):8564–8570 [2012]. doi: 10.1128/AEM.02443-12.
- [189] C. H. Martin, H. Dhamankar, H. C. Tseng *et al.* *A platform pathway for production of 3-hydroxyacids provides a biosynthetic route to 3-hydroxy- γ -butyrolactone*. *Nature Communications*, 4:1414–1419 [2013]. doi: 10.1038/ncomms2418.
- [190] S. B. Jeon, O. Choi, Y. Um *et al.* *Production of medium-chain carboxylic acids by Megasphaera sp. MH with supplemental electron acceptors*. *Biotechnology for Biofuels*, 9(1):129 [2016]. doi: 10.1186/s13068-016-0549-3.
- [191] A. R. Volker, D. S. Gogerty, C. Bartholomay *et al.* *Fermentative production of short-chain fatty acids in Escherichia coli*. *Microbiology*, 160(7):1513–1522 [2014]. doi: 10.1099/mic.0.078329-0.
- [192] T. Hino, K. Miyazaki and S. Kuroda. *Role of extracellular acetate in the fermentation of glucose by a ruminal bacterium, Megasphaera elsdenii*. *The Journal of General and Applied Microbiology*, 37(1):121–129 [1991]. doi: 10.2323/jgam.37.121.
- [193] W. H. van Zyl, L. R. Lynd, R. den Haan *et al.* *Consolidated Bioprocessing for Bioethanol Production Using Saccharomyces cerevisiae*. In *Biofuels*, pp. 205–235. Springer Berlin Heidelberg, Berlin, Heidelberg [2007]. doi: 10.1007/10_2007_061.

- [194] P. Christakopoulos, B. J. Macris and D. Kekos. *Direct fermentation of cellulose to ethanol by *Fusarium oxysporum**. *Enzyme and Microbial Technology*, 11(4):236–239 [1989]. doi: 10.1016/0141-0229(89)90098-7.
- [195] D. Aaron, S. A. Tripathi, T. F. Barrett *et al.* *High Ethanol Titrers from Cellulose by Using Metabolically Engineered Thermophilic, Anaerobic Microbes*. *Applied and Environmental Microbiology*, 77(23):8288–8294 [2011]. doi: 10.1128/AEM.00646-11.
- [196] L. Tian, B. Papanek, D. G. Olson *et al.* *Simultaneous achievement of high ethanol yield and titer in *Clostridium thermocellum**. *Biotechnology for Biofuels*, 9(1):116 [2016]. doi: 10.1186/s13068-016-0528-8.
- [197] S. A. Rounds, F. D. Wilde and G. F. Ritz. *Dissolved oxygen (ver. 3.0)*. In *U.S. Geological Survey Techniques of Water-Resources Investigations, book 9*. U.S. Geological Survey, Reston, United States of America [2013].
- [198] M. M. M. Bisschops, T. Vos, R. Martínez-moreno *et al.* *Oxygen availability strongly affects chronological lifespan and thermotolerance in batch cultures of *Saccharomyces cerevisiae**. *Microbial Cell*, 2(11):429–444 [2015]. doi: 10.15698/mic2015.11.238.
- [199] H. G. Crabtree. *Observations on the carbohydrate metabolism of tumours*. *Biochemical Journal*, 23(3):536–545 [1929]. doi: 10.1042/bj0230536.
- [200] K. D. Jones and D. S. Kompala. *Cybernetic model of the growth dynamics of *Saccharomyces cerevisiae* in batch and continuous cultures*. *Journal of Biotechnology*, 71:105–131 [1999]. doi: 10.1016/S0168-1656(99)00017-6.
- [201] C. Verduyn, T. P. L. Zomerdijk, J. P. van Dijken *et al.* *Continuous measurement of ethanol production by aerobic yeast suspensions with an enzyme electrode*. *Applied Microbiology and Biotechnology*, 19(3):181–185 [1984]. doi: 10.1007/BF00256451.
- [202] A. Hagman and J. Piškur. *A study on the fundamental mechanism and the evolutionary driving forces behind aerobic fermentation in yeast*. *PLOS ONE*, 10:1–24 [2015]. doi: 10.1371/journal.pone.0116942.
- [203] L. M. Raamsdonk, B. Teusink, D. Broadhurst *et al.* *A functional genomics strategy that uses metabolome data to reveal the phenotype of silent mutations*. *Nature Biotechnology*, 19:45–50 [2001]. doi: 10.1038/83496.
- [204] C. Xiros and M. H. Studer. *A Multispecies Fungal Biofilm Approach to Enhance the Cellulolytic Efficiency of Membrane Reactors for Consolidated Bioprocessing of Plant Biomass*. *Frontiers in Microbiology*, 8:1930 [2017]. doi: 10.3389/fmicb.2017.01930.

- [205] R. L. Shahab and M. H.-P. Studer. *A method for the microbial production of short chain fatty acids and lipids*. Patent appl., DE 10 2018 206 987.5 [2018].
- [206] H. D. Baehr and S. Kabelac. *Thermodynamik*. Berlin, Heidelberg, Germany [2012]. doi: 10.1007/978-3-642-24161-1.
- [207] M. Basen, G. J. Schut, D. M. Nguyen *et al.* *Single gene insertion drives bioalcohol production by a thermophilic archaeon*. *Proceedings of the National Academy of Sciences of the United States of America*, 111(49):17618–17623 [2014]. doi: 10.1073/pnas.1413789111.
- [208] P. J. Anderson, K. McNeil and K. Watson. *High-Efficiency Carbohydrate Fermentation to Ethanol at Temperatures above 40°C by Kluyveromyces marxianus var. marxianus Isolated from Sugar Mills*. *Applied and Environmental Microbiology*, 51(6):1314–1320 [1986].
- [209] L. Xu, P. J. Weathers, X. R. Xiong *et al.* *Microalgal bioreactors: Challenges and opportunities*. *Engineering in Life Sciences*, 9(3):178–189 [2009]. doi: 10.1002/elsc.200800111.
- [210] O. Perez-Garcia and Y. Bashan. *Microalgal Heterotrophic and Mixotrophic Culturing for Bio-refining: From Metabolic Routes to Techno-economics*. In *Algal Biorefineries*, pp. 61–131. Springer International Publishing, Heidelberg, Germany [2015]. doi: 10.1007/978-3-319-20200-6_3.
- [211] P. S. Schulze, L. A. Barreira, H. G. Pereira *et al.* *Light emitting diodes (LEDs) applied to microalgal production*. *Trends in Biotechnology*, 32(8):422–430 [2014]. doi: 10.1016/j.tibtech.2014.06.001.
- [212] W. Blanken, M. Cuaresma, R. H. Wijffels *et al.* *Cultivation of microalgae on artificial light comes at a cost*. *Algal Research*, 2(4):333–340 [2013]. doi: 10.1016/j.algal.2013.09.004.
- [213] B. L. Marrone, R. E. Lacey, D. B. Anderson *et al.* *Review of the harvesting and extraction program within the National Alliance for Advanced Biofuels and Bioproducts*. *Algal Research*, 33:470–485 [2017]. doi: 10.1016/j.algal.2017.07.015.
- [214] R. Davis, A. Aden and P. T. Pienkos. *Techno-economic analysis of autotrophic microalgae for fuel production*. *Applied Energy*, 88(10):3524–3531 [2011]. doi: 10.1016/j.apenergy.2011.04.018.
- [215] M. Gross, W. Henry, C. Michael *et al.* *Development of a rotating algal biofilm growth system for attached microalgae growth with in situ biomass harvest*. *Bioresource Technology*, 150:195–201 [2013]. doi: 10.1016/j.biortech.2013.10.016.
- [216] Cree Inc. *Datasheet of Cree XLamp XHP 70.2 LEDs*. Tech. rep., Durham, United States of America [2017].

- [217] O. Blifernez-Klassen, V. Klassen, A. Doebbe *et al.* *Cellulose degradation and assimilation by the unicellular phototrophic eukaryote Chlamydomonas reinhardtii*. *Nature Communications*, 3:1214 [2012]. doi: 10.1038/ncomms2210.
- [218] R. Sager and S. Granick. *Nutritional studies with Chlamydomonas reinhardtii*. *Annals of the New York Academy of Sciences*, 56(5):831–838 [1953]. doi: 10.1111/j.1749-6632.1953.tb30261.x.
- [219] A. Doebbe, J. Rupprecht, J. Beckmann *et al.* *Functional integration of the HUP1 hexose symporter gene into the genome of C. reinhardtii: Impacts on biological H₂ production*. *Journal of Biotechnology*, 131(1):27–33 [2007]. doi: 10.1016/j.jbiotec.2007.05.017.
- [220] O. Björkman and B. Demmig. *Photon yield of O₂ evolution and chlorophyll fluorescence characteristics at 77 K among vascular plants of diverse origins*. *Planta*, 170(4):489–504 [1987]. doi: 10.1007/BF00402983.
- [221] W. P. Inskeep and P. R. Bloom. *Extinction Coefficients of Chlorophyll a and b in N,N-Dimethylformamide and 80% Acetone*. *Plant Physiology*, 77(2):483–485 [1985].
- [222] A. R. Wellburn. *The Spectral Determination of Chlorophylls a and b, as well as Total Carotenoids, Using Various Solvents with Spectrophotometers of Different Resolution*. *Journal of Plant Physiology*, 144(3):307–313 [1994]. doi: 10.1016/S0176-1617(11)81192-2.
- [223] Y. di Chen, S. H. Ho, D. Nagarajan *et al.* *Waste biorefineries — integrating anaerobic digestion and microalgae cultivation for bioenergy production*. *Current Opinion in Biotechnology*, 50:101–110 [2018]. doi: 10.1016/j.copbio.2017.11.017.
- [224] G. L. Miller. *Use of Dinitrosalicylic Acid Reagent for Determination of Reducing Sugar*. *Analytical Chemistry*, 31(3):426–428 [1959]. doi: 10.1021/ac60147a030.
- [225] A. Sluiter, B. Hames, R. Ruiz *et al.* *Laboratory Analytical Procedure (LAP). Determination of Structural Carbohydrates and Lignin in Biomass*. Tech. rep., NREL, Colorado, United States of America [2008].
- [226] A. Flamholz, E. Noor, A. Bar-Even *et al.* *eQuilibrator - the biochemical thermodynamics calculator*. *Nucleic Acids Research*, 40(1):770–775 [2012]. doi: 10.1093/nar/gkr874.
- [227] D. L. Williams and A. P. Dunlop. *Kinetics of Furfural Destruction in Acidic Aqueous Media*. *Industrial and Engineering Chemistry*, 40(2):239–241 [1948]. doi: 10.1021/ie50458a012.
- [228] W. Hongsiri, B. Danon and W. De Jong. *Kinetic study on the dilute acidic dehydration of pentoses toward furfural in seawater*. *Industrial and Engineering Chemistry Research*, 53(13):5455–5463 [2014]. doi: 10.1021/ie404374y.

- [229] T. Yamane. *Yield of poly-D(-)-3-hydroxybutyrate from various carbon sources: A theoretical study*. Biotechnology and Bioengineering, 41(1):165–170 [1993]. doi: 10.1002/bit.260410122.
- [230] R. S. Nelson, D. J. Peterson, E. M. Karp *et al.* *Mixed Carboxylic Acid Production by *Megasphaera elsdenii* from Glucose and Lignocellulosic Hydrolysate*. Fermentation, 3(1):10 [2017]. doi: 10.3390/fermentation3010010.
- [231] J. van Milgen. *Modeling Biochemical Aspects of Energy Metabolism in Mammals*. The Journal of Nutrition, 132(10):3195–3202 [2002]. doi: 10.1093/jn/131.10.3195.
- [232] G. Stephanopoulos. *Bioprocess and microbe engineering for total carbon utilization in biofuel production*. Patent appl., US 2011/0177564 [2011].
- [233] S. J. W. H. Oude Elferink, J. Krooneman, J. C. Gottschal *et al.* *Anaerobic Conversion of Lactic Acid to Acetic Acid and 1,2-Propanediol by *Lactobacillus buchneri**. Applied and Environmental Microbiology, 67(1):125–132 [2001]. doi: 10.1128/AEM.67.1.125.
- [234] D. C. Cameron and C. L. Cooney. *A Novel Fermentation: The Production of R(-)-1,2-Propanediol and Acetol by *Clostridium thermosaccharolyticum**. Nature Biotechnology, 4(7):651–654 [1986]. doi: 10.1038/nbt0786-651.
- [235] J. Krooneman, F. Faber, A. C. Alderkamp *et al.* **Lactobacillus diolivorans* sp. nov., a 1,2-propanediol-degrading bacterium isolated from aerobically stable maize silage*. International Journal of Systematic and Evolutionary Microbiology, 52(2):639–646 [2002]. doi: 10.1099/00207713-52-2-639.
- [236] L. F. Silva, M. K. Taciro, M. E. Michelin Ramos *et al.* *Poly-3-hydroxybutyrate (P3HB) production by bacteria from xylose, glucose and sugarcane bagasse hydrolysate*. Journal of Industrial Microbiology and Biotechnology, 31(6):245–254 [2004]. doi: 10.1007/s10295-004-0136-7.

APPENDIX E

List of publications

Publications

- under review** *The lactate platform – a consortium based consolidated bioprocessing strategy for the yield-optimized production of volatile fatty acids from lignocellulose*
R. L. Shahab, S. Brethauer, M. Davey, J. S. Luterbacher, A. Smith, S. Vignolini, M. H. Studer
Nature Biotechnology
- under review** *Catalytic valorization of the acetate fraction of biomass to aromatics and its integration into the carboxylate platform*
B. Rozmysłowicz, J. H. Yeap, A. M. I. Elkhaiary, M. Talebi Amiri, R. L. Shahab, Y. M. Questell-Santiago, C. Xiros, M. H. Studer, J. S. Luterbacher
Green Chemistry
- 2019** *A cellulolytic fungal biofilm enhances the consolidated bioconversion of cellulose to short chain fatty acids by the rumen microbiome*
C. Xiros, R. L. Shahab, M. H. Studer
Applied Microbiology and Biotechnology. doi: 10.1007/s00253-019-09706-1

- 2018** *Selectivity control during the single-step conversion of aliphatic carboxylic acids to linear olefins*
J. H. Yeap, F. Héroguel, R. L. Shahab, B. Rozmysłowicz, M. H. Studer, J. S. Luterbacher
ACS Catalysis, 8(11):10769-10773 [2018]. doi: 10.1021/acscatal.8b03370.
- 2018** *Consolidated bioprocessing of lignocellulosic biomass to lactic acid by a synthetic fungal-bacterial consortium*
R. L. Shahab, J. S. Luterbacher, S. Brethauer and M. H. Studer
Biotechnology and Bioengineering 115(5):1207-1215 [2018]. doi: 10.1002/bit.26541.
- 2017** *Enhanced simultaneous saccharification and fermentation of pretreated beech wood by in situ treatment with the white rot fungus Irpex lacteus in a membrane aerated biofilm reactor*
S. Brethauer, R. L. Shahab and M. H. Studer
Bioresource Technology 237:135-138 [2017]. doi: 10.1016/j.biortech.2017.03.050.
- 2015** *Microbial life on green biomass and their use for production of platform chemicals*
P. Schönicke, R. Shahab, R. Hamann and B. Kamm
Chapter in Microorganisms in Biorefineries, Microbiology Monographs, Springer-Verlag Berlin Heidelberg, 26:21-49 [2015]

Patents

- 2018** *A method for the microbial production of short chain fatty acids and lipids*
R. L. Shahab, M. H. Studer
DE 10 2018 206 987.5 [2018]
- 2014** *Apparatus and method for providing energy in biological system*
R. Shahab
DE 10 2014 213 346 [2014]

Conference contributions

- 06/2017** **BioTech2017**, Prague, Czech Republic
Consolidated production of volatile fatty acids from plant biomass using defined and natural microbial consortia
C. Xiros, R. Shahab, M. Studer
- 05/2017** **39th Symposium on Biotechnology**, San Francisco, United States of America
Consolidated bioprocessing of lactic acid from cellulosic biomass by a synthetic fungal-bacterial consortium
R. Shahab, M. Studer
- 04/2014** **36th Symposium on Biotechnology**, Clearwater Beach, United States of America
Continuous consolidated bioprocessing of lignocellulose to ethanol or organic acids in a multi-species biofilm membrane reactor
R. Shahab, S. Brethauer, M. Studer
- 02/2013** **PLANT 2030 Status Seminar 2013**, Potsdam, Germany
Tree for joules: improving eucalypt and poplar properties for bioenergy
R. Shahab, P. Schönicke, B. Kamm

Grants and honours

- 09/2018** Mobility grant from Swiss-European Mobility Programme
- 07/2018** Mobility grant from Swiss National Science Foundation
- 05/2018** Mobility grant from Swiss-European Mobility Programme
- 08/2014** Funding of project *Procedure for the direct utilization of electrical energy in biological systems*
Idea contest *New products for a biobased economy* from German Federal Ministry of Education and Research
- 10/2014** Honour from the Association of German Engineers

APPENDIX F

Curriculum vitae

Name Robert Lawrence Shahab
Date of birth 12th December 1987
Nationality German

Education

02/2015 - 04/2019 Doctoral student

École Polytechnique Fédérale de Lausanne, Laboratory of Sustainable and Catalytic Processing and Bern University of Applied Sciences, Laboratory of Biofuels and Biochemicals

PhD thesis *Labor division in engineered cross-kingdom consortia: Consolidated bioprocessing of lignocellulosic biomass to carboxylic acids*
Prof. Dr. Jeremy Luterbacher, Dr. Michael Studer

10/2008 - 10/2013 Diploma student (Biotechnology, Dipl.-Ing.)

Technical University Berlin

Specialization *Bioprocess engineering/genetics*

Diploma thesis *Direct fermentation of lignocellulose to alternative chemicals using the multi-species biofilm membrane reactor*

Swiss Federal Institute of Technology Zurich, Institute for Process Engineering

Prof. Dr. Philipp Rudolf von Rohr

Semester thesis *Investigations of the human malic enzyme 2 as G-quadruplex-binding protein*
Technical University Berlin, Department of Applied Biochemistry
Prof. Dr. Jens Kurreck

06/2000 - 06/2007 High school student (Abitur)
Gustav-Heinemann-Oberschule, Berlin

Professional experience

05/2018 - 03/2019 Visiting doctoral student
University of Cambridge, Department of Plant Sciences
Research topic *Towards consolidated bioprocessing of lignocellulose to lipids: Engineering of bioreactor for niche differentiation, characterization of microalgal-fungal biofilm*
Prof. Dr. Alison Smith

08/2014 - 02/2015 Researcher
Technical University Berlin, Department of Bioprocess Engineering
Research topic *Conception and development of a process for the direct usage of electric energy in biological systems*
Prof. Dr. Peter Neubauer

11/2013 - 06/2014 Research assistant
Bern University of Applied Sciences, Lab. of Biofuels and Biochemicals
Research topic *Scale-up and process development of continuous production of ethanol*
Dr. Michael Studer

01/2013 - 03/2013 Intern
Research Institute of Bioactive Polymer Systems, Teltow
Research topic *Process development of simultaneous saccharification and fermentation of lignocellulose to ethanol with online gas analytics*
Prof. Dr. Birgit Kamm

05/2011 - 04/2013 Student assistant
Technical University Berlin, Department of Applied Biochemistry
Practical courses *Organisation and supervision: Biochemistry I and II*
Prof. Dr. Jens Kurreck

06/2010 - 09/2010 Intern
Technical University Berlin, Institute for Biological Chemistry
Research topic *Genetic engineering of E. coli and purification of recombinant protein*
Prof. Dr. Roderich Süßmuth

